Optimization of Microelectrolysis Treatment to Remove Arsenic from Landfill Gas Condensate and Correlations between Changes of Redox Potential and Arsenic Removal

Ivette Andrea Del Carmen Pinochet Troncoso

A thesis

submitted in partial fulfillment of the

requirements for the degree of

Master of Science in Civil Engineering

University of Washington

2023

Committee:

Gregory Korshin

Jessica Ray

Program Authorized to Offer Degree:

Civil and Environmental Engineering

© Copyright 2023

Ivette Andrea Del Carmen Pinochet Troncoso

University of Washington

Abstract

Optimization of Microelectrolysis Treatment to Remove Arsenic from Landfill Gas Condensate and Correlations between Changes of Redox Potential and Arsenic Removal

Ivette Andrea Del Carmen Pinochet Troncoso

Chair of the Supervisory Committee

Gregory Korshin

Department of Civil and Environmental Engineering

This thesis is focused on the optimization of the microelectrolysis (ME) process for removing arsenic from landfill gas (LFG) condensate. The ME process utilizes redox and adsorption processes that take place at the interface of zero-valent iron and activated carbon.

Multiple optimization experiments were conducted in this study to minimize treatment time and resources while maximizing arsenic removal.

The study found that minimizing the ingress of atmospheric oxygen to the reactor, and that using mechanical mixing in a batch conical bottom reactor is the optimal configuration for the treatment. The results also showed that granular activated carbon (GAC) and zero valent iron (ZVI) are highly effective at removing arsenic from the LFG condensate when used in sufficiently high dosages. Multiple batches of LFG condensate can be treated using the same amount of the combined ZVI/GAC active media. Additionally, the study found that a more

acidic environment (e.g., pH 3) can enhance the efficiency of contaminant removal, and that a treatment duration of 30 minutes is typically sufficient to achieve >90% As removal.

Results of this study suggest that future research should further explore a detailed correlation between the redox potential measured in the ME reactors and the As removal efficiency. It is also necessary to find the optimal mixing parameters to achieve a good balance of both active media particle suspension in the reactor and catalytic interactions between ZVI and GAC, and to determine the maximum number of solid reuse cycles that ZVI and GAC can withstand.

Table of Contents

Acknowledgment ..... **iv**

List of abbreviations ..... **vi**

List of figures ..... **vii**

List of tables ..... **xix**

1. Executive Summary **1**

2. Literature review **4**

2.1. Geogenic and anthropogenic sources of arsenic 4
2.2. Arsenic chemistry and occurrence 6
2.3. Geogenic and anthropogenic sources of antimony 9
2.4. Landfill gas condensate 10
2.5. Arsenic and antimony in landfills 12
2.6. Treatment of arsenic and antimony in the industry 15
2.7. Outline of the Results of Prior Research of Arsenic Removal from Landfill Gas condensate 18
2.8. Goals of the study 21

3. Experimental reactors for microelectrolysis treatment **22**

3.1. Equipment and materials 23
3.1.1. Personal protection equipment (PPE) 23
3.1.2. Column reactors 23
3.1.3. Experiments equipment and materials 24
3.2. Reagents 25
3.2.1. Zero valent iron gain size determination 26
3.2.2. Activated carbon gain size determination 28
3.3. Gas condensate samples 29
3.4. Analytical instruments 31
3.4.1. ICP-MS 31

4. Optimization and scaling of the microelectrolysis process results 32

4.1. Prevention of ingress of atmospheric oxygen in ME reactors 34

4.2. Gas flow rates and injection modes 39

4.3. Effects of carrier gas recirculation on As removal in ME reactors 43

4.4. Effects of variation of ZVI activation, ZVI/AC weight ratios, and active media dosing and particle sizes on As removal 49

4.4.1. Effects of ZVI activation 49

4.4.2. Effects of ZVI/PAC weight ratio 52

4.4.3. Effects of ZVI/PAC particle size 53

4.4.4. Effects of ZVI/PAC doses 56

4.5. Repeated sample loading cycles (active media reuse) 61

4.6. Effects of mechanical mixing on As removal in ME operations 70

4.6.1. Mechanical mixing with gas flow versus recirculation of gas with no mixing 71

4.6.2. Mixing modes: continuous versus intermittent 72

4.6.3. Effects of pH on As removal in the case of mechanical mixing 74

4.6.4. As removal using mechanical mixing and varying active media dosage 76

4.6.5. As removal in the presence of mechanical mixing: comparison of the data for different landfill gas condensate samples 77

4.6.6. As removal in the presence of mechanical mixing: effects of active media particle size 79

4.6.7. As removal in the presence of mechanical mixing: Effects of repeated sample loading cycles (active media reuse) 82

4.7. Effects of temperature variations on As and Sb removal in ME reactors 95

4.8. Effects of reactor headspace on As/Sb removal in ME reactors 97

5. Arsenic mass balance experiments 107

6. Examination of changes of redox potential during ME treatment 117

6.1. Regressions between As/Sb concentrations and redox potential changes 121

6.2. Quantile Regressions and a Probabilistic Approach 125

7. Conclusions and future work 132

7.1. ME optimization conclusions 132

7.2. Mass balance conclusions 137

7.3. Redox potential and As/Sb removal correlation conclusions 138
7.4. Recommendations for future work: Engineering aspects of ME treatment 140
8. References 142
9. Appendices 146
9.1. Additional Tables 146
9.2. P&ID of the treatment process 152

Acknowledgment

I extend my sincere appreciation to all those who supported me throughout my academic journey. First and foremost, I am deeply grateful to my mother Deidamia for her constant presence in my education. She has been my rock, instilling in me the values of perseverance, hard work, compassion, and love that have helped me pursue my career and navigate life's challenges.

To my beloved husband Ian, whose tireless support has been my guiding light throughout this journey, I cannot thank you enough. Your unwavering love and companionship have made me a better person, and I cherish every precious moment by your side.

I also thank my dear brother, Christian, a passionate mathematician whose guidance and encouragement ignited my love for engineering. To my father Hugo for being a great example and motivator in my education, and to my mother-in-law, Nolda, for always providing a word of encouragement and caring, I express my gratitude.

To my close friends in Seattle, and my acapella friends, thank you for the humor and inspiring conversations that cheered me up when everything seemed harder than expected. And to my dearest Chilean friends, I want to extend my heartfelt thanks for always been there for me when I needed them. Your friendship and constant presence have been a source of comfort and strength.

I express my heartfelt thanks to Dr. Gregory Korshin, who gave me the opportunity to work alongside him on this outstanding project. His guidance, experience, and wisdom were instrumental in my academic journey, and I will never forget his passion for teaching and his compassionate care for his students. Dr. Jessica Ray, thank you for being a part of my committee, providing feedback on my work and for being a great professor.

I extend my appreciation to the managers, engineers, and other professionals of King County Solid Waste Division for their great knowledge, experience, and enthusiastic assistance throughout the project. To the team at King County Solid Waste Division who funded this study, thank you for your invaluable collaboration and advice.

I am also grateful to the University of Washington for accepting me into this program and providing a quality education, and with all the people in the Department of Civil and Environmental Engineering who helped create a friendly environment for me to work in. I am especially grateful to Sam Walters, who trained me on all the lab work, Dr. Chenyang Zhang, whose advice was always invaluable, and to Annapaola Panico and Geneva Schlepp, who provided their brilliant minds and hard work to the project.

I would also like to thank my other lab mates Aminda Cheney-Irgens, Dr. Po-An Chen, Dr. Domenico Giaquinto, Dr. Yaswanth Penke, Chloe Tang, Elaine Guo, and Wanyu Mao for their companionship and advice whenever I needed it. The diversity of experience and backgrounds that my fellow researchers brought to the project was vital, and I am grateful for the friendships we have formed.

Finally, to my classmates and friends at UW, and particularly to Zach Brodkey, whose work in our data analysis project provided invaluable progress in my thesis, I thank you for your unwavering support and friendship.

List of abbreviations

As -Arsenic

ASARCO - American smelting and refining corporation

BC – 3 L column reactor

CDF - Cumulative distribution function

CHRLF - Cedar Hills regional landfill

CR – 700 mL column reactor

EPA - Environmental Protection Agency

GAC - Granular Activated Carbon

LFG - Landfill Gas

LPM - Liters per minute

ME - Micro Electrolysis

MWD - Microwave Digestion

PAC - Powder Activated Carbon

PDF - Probability distribution function

ppb - parts per billion

ppm - parts per million

SR - Sampling Round

Sb - Antimony

ZVI - Zero Valent Iron

List of figures

Figure 1 - Various sources of arsenic into paddy field (Sahoo et al., 2013)..... 6
Figure 2 - Eh-pH diagram for aqueous arsenic species in the system (Smedley et al., 2002)..... 7
Figure 3 - Speciation of arsenite and arsenate as a function of pH..... 8
Figure 4 - Basic elements of the simplified sequence of biogeochemical reactions of arsenic involved in the generation of methylated As solutes and arsines (Korshin lecture 2021)..... 8
Figure 5 – General elements of the landfill water cycle (Adapted from Introduction to Solid Waste Management, 2021) 11
Figure 6 - Two types of laboratory scale ME reactors: 500 mL reactor (top), 3 L reactor (bottom) 22
Figure 7 - ZVI sieve results: mass fractions associated with different ranges of ZVI particle diameters. 27
Figure 8 - ZVI sieve results: estimates of the total surface area and its fractions associated with different ZVI particle diameters..... 28
Figure 9 - GAC sieve results: mass fractions associated with different ranges of GAC particle diameters. 29
Figure 10 - 500 mL column reactor used for ME experiments at the beginning of phase III 33
Figure 11 (As) - Comparison of 500 mL volume ME reactor treatment results for oxygen exposure: open reactor versus reactor insulated from atmosphere by connecting it to $KMnO_4$ and Na_2SO_3 for gas capture. Active media used: PAC and ZVI LC plus fine. Initial As concentration: 8.1 ppm 35
Figure 12 (Sb) - Comparison of 500 mL volume ME reactor treatment results for oxygen exposure: open reactor versus reactor insulated from atmosphere by connecting it to $KMnO_4$ and Na_2SO_3 for gas capture. Active media used: PAC and ZVI LC plus fine. Initial Sb concentration: 0.4 ppm. 35
Figure 13. Comparison of redox potential changes versus treatment time in a 500 mL volume ME reactor: open reactor versus reactor insulated from atmosphere by connecting it to $KMnO_4$ and Na_2SO_3 for gas capture. Active media used: PAC and ZVI LC plus fine 37
Figure 14 (As) - Comparison of ME treatment results in the presence and absence of 0.00075 M Na_2SO_3. 500 mL ME reactor, SR12 LFG condensate, 3 g/L of PAC and ZVI LC plus fine 38
Figure 15 (Sb) - Comparison of ME treatment results in the presence and absence of 0.00075 M Na_2SO_3. 500 mL ME reactor, SR12 LFG condensate, 3 g/L of PAC and ZVI LC plus fine 38

Figure 16 (As) - Comparison of ME treatment results for gas flow rates variations: 0.2, 0.4, and 0.6 LPM of CO_2 injection in a 500 mL ME reactor to treat SR12 LFG condensate using 3 g/L PAC and ZVI LC plus fine 40
Figure 17 (Sb) - Comparison of ME treatment results for gas flow rates variations: 0.2, 0.4, and 0.6 LPM of CO_2 injection in a 500 mL ME reactor to treat SR12 LFG condensate using 3 g/L PAC and ZVI LC plus fine 41
Figure 18 (As) - Comparison of ME treatment results for gas flow variations: continuous versus intermittent CO_2 injection in a 500 mL ME reactor to treat SR12 LFG condensate using 3 g/L PAC and ZVI LC plus fine and a CO_2 flow rate of 0.6 LPM. Initial As concentration: 6.5 ppm..... 42
Figure 19 (Sb) - Comparison of ME treatment results for gas flow variations: continuous versus intermittent CO_2 injection in a 500 mL ME reactor to treat SR12 LFG condensate using 3 g/L PAC and ZVI LC plus fine and a CO_2 flow rate of 0.6 LPM. Initial Sb concentration: 0.7 ppm..... 42
Figure 20 (As) - Comparison of ME treatment results for gas recirculation mode variations: ME reactor using 20 g/L of PAC and ZVI LC plus fine to treat 500 mL of SR15 LFG condensate with 0.6 LPM CO_2 . Initial As concentration: 9.3 ppm 44
Figure 21 (Sb) - Comparison of ME treatment results for gas recirculation mode variations: ME reactor using 20 g/L of PAC and ZVI LC plus fine to treat 500 mL of SR15 LFG condensate with 0.6 LPM CO_2. Initial Sb concentration: 0.8 ppm..... 44
Figure 22 (As) - Comparison of ME treatment results for gas recirculation mode variations: ME reactor using 20 g/L of PAC/GAC and ZVI LC plus fine/ ZVI LC plus to treat 500 mL of SR15 LFG condensate with 0.6 LPM CO_2..... 46
Figure 23 (Sb) - Comparison of ME treatment results for gas recirculation mode variations: ME reactor using 20 g/L of PAC/GAC and ZVI LC plus fine/ ZVI LC plus to treat 500 mL of SR15 LFG condensate with 0.6 LPM CO_2..... 46
Figure 24 (As) - Comparison of ME treatment results for gas recirculation mode variations: ME reactor using 20 g/L of PAC and ZVI LC plus fine to treat 3 L of SR15 LFG condensate with 2 and 3 LPM CO_2..... 47
Figure 25 (Sb) - Comparison of ME treatment results for gas recirculation mode variations: ME reactor using 20 g/L of PAC and ZVI LC plus fine to treat 3 L of SR15 LFG condensate with 2 and 3 LPM CO_2..... 48

Figure 26 (As) - Comparison of ME treatment results for ZVI activation modes variations at different pH: rinsed strainer activation versus no activation at pH 3, 3.5, and 4 in a 500 mL ME reactor to treat SR12 LFG condensate using 3 g/L PAC and ZVI LC plus fine..... 50
Figure 27 (Sb) - Comparison of ME treatment results for ZVI activation modes variations at different pH: rinsed strainer activation versus no activation at pH 3, 3.5, and 4 in a 500 mL ME reactor to treat SR12 LFG condensate using 3 g/L PAC and ZVI LC plus fine..... 51
Figure 28 (As) - Comparison of ME treatment results for PAC/ZVI weight ratio variations: 0:1, 1:1, 1:2, 1:3, and 1:4 added to a 500 mL ME reactor to treat SR12 LFG condensate using 3 g/L PAC and ZVI LC plus fine and CO_2 flow rate of 0.6 LPM. Initial As concentration: 6.5 ppm... 52
Figure 29 (Sb) - Comparison of ME treatment results for PAC/ZVI weight ratio variations: 0:1, 1:1, 1:2, 1:3, and 1:4 added to a 500 mL ME reactor to treat SR12 LFG condensate using 3 g/L PAC and ZVI LC plus fine and CO_2 flow rate of 0.6 LPM. Initial Sb concentration: 0.7 ppm... 53
Figure 30 (As) - Comparison of ME treatment results for active media particle size variations: PAC/GAC variations, and ZVI LC plus / ZVI LC plus fine variations, added to a 500 mL ME reactor to treat SR12 LFG condensate using 3 g/L of active media and CO_2 flow rate of 0.6 LPM 54
Figure 31 (Sb) - Comparison of ME treatment results for active media particle size variations: PAC/GAC variations, and ZVI LC plus / ZVI LC plus fine variations, added to a 500 mL ME reactor to treat SR12 LFG condensate using 3 g/L of active media and CO_2 flow rate of 0.6 LPM 55
Figure 32 (As) - Comparison of ME treatment results for active media dosing variations: ME reactor using from 1 to 40 g/L of PAC and ZVI LC plus fine to treat 500 mL of SR12 LFG condensate. Initial As concentration: 6.5 ppm..... 56
Figure 33 (Sb) - Comparison of ME treatment results for active media dosing variations: ME reactor using from 1 to 40 g/L of PAC and ZVI LC plus fine to treat 500 mL of SR12 LFG condensate. Initial Sb concentration: 0.7 ppm..... 57
Figure 34 (As) - Comparison of ME treatment results for active media dosing variations: ME reactor using from 3 to 40 g/L of PAC and ZVI LC plus fine to treat 500 mL of SR13 LFG condensate. Initial As concentration: 8.1 ppm..... 57

Figure 35 (Sb) - Comparison of ME treatment results for active media dosing variations: ME reactor using from 3 to 40 g/L of PAC and ZVI LC plus fine to treat 500 mL of SR13 LFG condensate. Initial Sb concentration: 0.4 ppm 58
Figure 36 (As) - Comparison of ME treatment results for active media dosing variations: ME reactor using from 3 to 40 g/L of PAC and ZVI LC plus fine to treat 500 mL of SR14 LFG condensate. Initial As concentration: 200 ppm 58
Figure 37 (Sb) - Comparison of ME treatment results for active media dosing variations: ME reactor using from 3 to 40 g/L of PAC and ZVI LC plus fine to treat 500 mL of SR14 LFG condensate. Initial Sb concentration: 9.7 ppm 59
Figure 38 (As) - Comparison of ME treatment results for active media dosing variations: ME reactor using from 3 to 20 g/L of GAC and ZVI LC plus to treat 500 mL of SR12 and SR15 LFG condensate. Initial As concentration: 6.5 ppm 60
Figure 39 (Sb) - Comparison of ME treatment results for active media dosing variations: ME reactor using from 3 to 20 g/L of GAC and ZVI LC plus to treat 500 mL of SR12 and SR15 LFG condensate. Initial Sb concentration: 0.7 ppm 60
Figure 40 (As) - Comparison of ME treatment results for repeated sample loading cycles: 3 cycles using 10 g/L of PAC and ZVI LC plus fine to treat 3 loads of 500 mL SR15 LFG condensate with 0.6 LPM CO_2 62
Figure 41 (Sb) - Comparison of ME treatment results for repeated sample loading cycles: 3 cycles using 10 g/L of PAC and ZVI LC plus fine to treat 3 loads of 500 mL SR15 LFG condensate with 0.6 LPM CO_2 62
Figure 42 (As) - Comparison of ME treatment results for repeated sample loading cycles: 3 cycles using 20 g/L of PAC and ZVI LC plus fine to treat 3 loads of 500 mL SR15 LFG condensate with 0.6 LPM CO_2 63
Figure 43 (Sb) - Comparison of ME treatment results for repeated sample loading cycles: 3 cycles using 20 g/L of PAC and ZVI LC plus fine to treat 3 loads of 500 mL SR15 LFG condensate with 0.6 LPM CO_2 63
Figure 44 (As) - Comparison of ME treatment results for repeated sample loading cycles: 3 cycles using 6.6 g/L of ZVI LC plus fine only, to treat 3 loads of 500 mL SR15 LFG condensate with 0.6 LPM of continuous CO_2 65

Figure 45 (Sb) - Comparison of ME treatment results for repeated sample loading cycles: 3 cycles using 6.6 g/L of ZVI LC plus fine only, to treat 3 loads of 500 mL SR15 LFG condensate with 0.6 LPM of continuous CO_2 65
Figure 46 (As) - Comparison of ME treatment results for repeated sample loading cycles: 3 cycles using 13.3 g/L of ZVI LC plus fine only, to treat 3 loads of 500 mL SR15 LFG condensate with 0.6 LPM of continuous CO_2 66
Figure 47 (Sb) - Comparison of ME treatment results for repeated sample loading cycles: 3 cycles using 13.3 g/L of ZVI LC plus fine only, to treat 3 loads of 500 mL SR15 LFG condensate with 0.6 LPM of continuous CO_2 66
Figure 48 (As) - Comparison of ME treatment results for repeated sample loading cycles: 5 cycles using 20 g/L of PAC and ZVI LC plus fine to treat 5 loads of 500 mL SR15 LFG condensate with 0.6 LPM of intermittent CO_2 (30 seconds on, 5 minutes off) 68
Figure 49 (Sb) - Comparison of ME treatment results for repeated sample loading cycles: 5 cycles using 20 g/L of PAC and ZVI LC plus fine to treat 5 loads of 500 mL SR15 LFG condensate with 0.6 LPM of intermittent CO_2 (30 seconds on, 5 minutes off) 68
Figure 50 (As) - Comparison of ME treatment results for repeated sample loading cycles: 5 cycles using 20 g/L of PAC and ZVI LC plus fine to treat 5 loads of 500 mL SR13 LFG condensate with 0.6 LPM of intermittent CO_2 (30 seconds on, 5 minutes off) 69
Figure 51 (Sb) - Comparison of ME treatment results for repeated sample loading cycles: 5 cycles using 20 g/L of PAC and ZVI LC plus fine to treat 5 loads of 500 mL SR13 LFG condensate with 0.6 LPM of intermittent CO_2 (30 seconds on, 5 minutes off) 69
Figure 52 (As) - Comparison of ME treatment results for CO_2 recirculation with and without mechanical mixing: ME reactor using 20 g/L of PAC and ZVI LC plus fine to treat 2 L of SR16 LFG condensate. Initial As concentration: 25 ppm 71
Figure 53 (Sb) - Comparison of ME treatment results for CO_2 recirculation with and without mechanical mixing: ME reactor using 20 g/L of PAC and ZVI LC plus fine to treat 2 L of SR16 LFG condensate. Initial Sb concentration: 1.2 ppm 72
Figure 54 (As) - Comparison of ME treatment results for mechanical mixing mode variations: ME reactor using 20 g/L of PAC and ZVI LC plus fine to treat 2 L of SR16 LFG condensate with continuous and intermittent mixing 73

Figure 55 (Sb) - Comparison of ME treatment results for mechanical mixing mode variations: ME reactor using 20 g/L of PAC and ZVI LC plus fine to treat 2 L of SR16 LFG condensate with continuous and intermittent mixing 73
Figure 56 (As) - Comparison of ME treatment results for mechanical mixing with pH variations: ME reactor using 20 g/L of PAC and ZVI LC plus fine to treat 2 L of SR16 LFG condensate for pH 3, 4.5 and 7 (not controlled). Initial As concentration: 25 ppm 75
Figure 57 (Sb) - Comparison of ME treatment results for mechanical mixing with pH variations: ME reactor using 20 g/L of PAC and ZVI LC plus fine to treat 2 L of SR16 LFG condensate for pH 3, 4.5 and 7 (not controlled). Initial Sb concentration: 1.2 ppm 75
Figure 58 (As) - Comparison of ME treatment results for mechanical mixing with active media dosage variations: ME reactor using PAC and ZVI LC plus fine to treat 2 L of SR16 LFG condensate for active media dosing of 7, 14, and 20 g/L. Initial As concentration: 25 ppm 76
Figure 59 (Sb) - Comparison of ME treatment results for mechanical mixing with active media dosage variations: ME reactor using PAC and ZVI LC plus fine to treat 2 L of SR16 LFG condensate for active media dosing of 7, 14, and 20 g/L. Initial Sb concentration: 1.2 ppm..... 77
Figure 60 (As) - Comparison of ME treatment results for mechanical mixing with sample variations: ME reactor using 20 g/L of PAC and ZVI LC plus fine to treat 2 L of SR13, SR14, SR15, and SR16 LFG condensate. Initial As concentrations: SR13=8.1 ppm, SR14 =200 ppm, SR15=9.3 ppm, SR16=25 ppm 78
Figure 61 (Sb) - Comparison of ME treatment results for mechanical mixing with sample variations: ME reactor using 20 g/L of PAC and ZVI LC plus fine to treat 2 L of SR13, SR14, SR15, and SR16 LFG condensate. Initial Sb concentrations: SR13=0.4 ppm, SR14 =9.7 ppm, SR15=0.8 ppm, SR16=1.2 ppm 79
Figure 62 (As) - Comparison of ME treatment results for mechanical mixing with active media particle size variations: ME reactor using 20 and 50 g/L of active media to treat 2 L of SR16 LFG condensate, at pH 3 and with continuous mixing 80
Figure 63 (Sb) - Comparison of ME treatment results for mechanical mixing with active media particle size variations: ME reactor using 20 and 50 g/L of active media to treat 2 L of SR16 LFG condensate 81

Figure 64 (As) – ME treatment results for repeated sample loading cycles in the presence of continuous mechanical mixing: 4 cycles using 50 g/L of GAC and ZVI LC plus to treat 4 loads of 500 mL SR16 LFG condensate. Initial As concentration: 25 ppm 82
Figure 65 (Sb) – ME treatment results for repeated sample loading cycles in the presence of continuous mechanical mixing: 4 cycles using 50 g/L of GAC and ZVI LC plus to treat 4 loads of 500 mL SR16 LFG condensate. Initial Sb concentration: 1.2 ppm 83
Figure 66 (As) – Comparison of ME treatment results for repeated influent loading cycles: 4 cycles using 50 g/L of GAC and ZVI LC plus and adding 10 g/L of fresh active media per cycle to treat 4 loads of 500 mL SR16 LFG condensate using continuous mechanical mixing. Initial As concentration: 25 ppm..... 83
Figure 67 (Sb) – Comparison of ME treatment results for repeated influent loading cycles: 4 cycles using 50 g/L of GAC and ZVI LC plus and adding 10 g/L per cycle to treat 4 loads of 500 mL SR16 LFG condensate using continuous mixing. Initial Sb concentration: 1.2 ppm 84
Figure 68 (As) - Comparison of ME treatment results for repeated sample loading cycles: 10 cycles using 50 g/L of GAC and ZVI LC plus to treat 10 loads of 500 mL SR16 LFG condensate..... 85
Figure 69 – As removal efficiency for repeated sample loading cycles: 10 cycles using 50 g/L of GAC and ZVI LC plus to treat 10 loads of 500 mL SR16 LFG condensate 86
Figure 70 (Sb) - Comparison of ME treatment results for repeated sample loading cycles: 10 cycles using 50 g/L of GAC and ZVI LC plus to treat 10 loads of 500 mL SR16 LFG condensate..... 86
Figure 71 – Sb removal efficiency for repeated sample loading cycles: 10 cycles using 50 g/L of GAC and ZVI LC plus to treat 10 loads of 500 mL SR16 LFG condensate 87
Figure 72 (As) - Comparison of ME treatment results for repeated sample loading cycles: 10 cycles using 50 g/L of GAC and ZVI LC plus and adding 1 g/L per cycle to treat 10 loads of 500 mL SR16 LFG condensate 87
Figure 73 - As removal efficiency for repeated sample loading cycles: 10 cycles using 50 g/L of GAC and ZVI LC plus and adding 1 g/L per cycle to treat 10 loads of 500 mL SR16 LFG condensate..... 88
Figure 74 (Sb) - Comparison of ME treatment results for repeated sample loading cycles: 10 cycles using 50 g/L of GAC and ZVI LC plus and adding 1 g/L per cycle to treat 10 loads of 500 mL SR16 LFG condensate 88

Figure 75 - Sb removal efficiency for repeated sample loading cycles: 10 cycles using 50 g/L of GAC and ZVI LC plus and adding 1 g/L per cycle to treat 10 loads of 500 mL SR16 LFG condensate 89
Figure 76 (As) - Comparison of ME treatment results for repeated sample loading cycles: 5 cycles using 50 g/L of GAC and ZVI LC plus and adding 1 g/L per cycle to treat 10 loads of 500 mL SR16 LFG condensate using an intermittent mixing configuration (2.5 minutes on - 5 minutes off) 90
Figure 77 - As removal efficiency for repeated sample loading cycles: 5 cycles using 50 g/L of GAC and ZVI LC plus and adding 1 g/L per cycle to treat 10 loads of 500 mL SR16 LFG condensate using an intermittent mixing configuration (2.5 minutes on - 5 minutes off)..... 91
Figure 78 (Sb) - Comparison of ME treatment results for repeated sample loading cycles: 5 cycles using 50 g/L of GAC and ZVI LC plus and adding 1 g/L per cycle to treat 10 loads of 500 mL SR16 LFG condensate using an intermittent mixing configuration (2.5 minutes on - 5 minutes off) 91
Figure 79 - Sb removal efficiency for repeated sample loading cycles: 5 cycles using 50 g/L of GAC and ZVI LC plus and adding 1 g/L per cycle to treat 10 loads of 500 mL SR16 LFG condensate using an intermittent mixing configuration (2.5 minutes on - 5 minutes off)..... 92
Figure 80 (As) - Comparison of ME treatment results for repeated sample loading cycles: 3 cycles using 33.3 g/L of ZVI LC plus only, to treat 3 loads of 500 mL SR16 LFG condensate using continuous mixing..... 93
Figure 81 – As removal efficiency for repeated sample loading cycles: 3 cycles using 33.3 g/L of ZVI LC plus only, to treat 3 loads of 500 mL SR16 LFG condensate using continuous mixing. 94
Figure 82 (Sb) - Comparison of ME treatment results for repeated sample loading cycles: 3 cycles using 33.3 g/L of ZVI LC plus only, to treat 3 loads of 500 mL SR16 LFG condensate using continuous mixing..... 94
Figure 83 -Sb removal efficiency for repeated sample loading cycles: 3 cycles using 33.3 g/L of ZVI LC plus only, to treat 3 loads of 500 mL SR16 LFG condensate using continuous mixing. 95
Figure 84 (As) - Comparison of ME treatment at varying temperatures: ME reactor at 6, 20, and 34 Celsius degrees using 50 g/L of GAC and ZVI LC plus, to treat 2 L of SR16 LFG condensate using continuous mixing. Initial As concentration: 25 ppm 96

Figure 85 (Sb) - Comparison of ME treatment at varying temperatures: ME reactor at 6, 20, and 34 Celsius degrees using 50 g/L of GAC and ZVI LC plus, to treat 2 L of SR16 LFG condensate using continuous mixing. Initial Sb concentration: 1.2 ppm 97
Figure 86 (As) - Comparison of ME treatment results for reactor headspace variations: ME reactor using 50 g/L of GAC and ZVI LC plus, to treat 3 L, 2 L, 1 L, 500 mL, and 250 mL of SR14 LFG condensate using continuous mixing 98
Figure 87 - As removal efficiency for different headspace in the reactor: ME reactor using 50 g/L of GAC and ZVI LC plus, to treat 3 L, 2 L, 1 L, 500 mL, and 250 mL of SR14 LFG condensate using continuous mixing 99
Figure 88 – As removal efficiency and headspace percentage in the reactor relation: ME reactor using 50 g/L of GAC and ZVI LC plus, to treat 3 L, 2 L, 1 L, 500 mL, and 250 mL of SR14 LFG condensate using continuous mixing 99
Figure 89 (Sb) - Comparison of ME treatment results for reactor headspace variations: ME reactor using 50 g/L of GAC and ZVI LC plus, to treat 3 L, 2 L, 1 L, 500 mL, and 250 mL of SR14 LFG condensate using continuous mixing 100
Figure 90 - Sb removal efficiency for different headspace in the reactor: ME reactor using 50 g/L of GAC and ZVI LC plus, to treat 3 L, 2 L, 1 L, 500 mL, and 250 mL of SR14 LFG condensate using continuous mixing 100
Figure 91 - Sb removal efficiency and headspace percentage in the reactor relation: ME reactor using 50 g/L of GAC and ZVI LC plus, to treat 3 L, 2 L, 1 L, 500 mL, and 250 mL of SR14 LFG condensate using continuous mixing 101
Figure 92 (As) - Comparison of ME treatment results for reactor headspace variations: ME reactor using 50 g/L of GAC and ZVI LC plus, to treat 3 L, 2 L, 1 L, 500 mL, and 250 mL of SR17 LFG condensate using continuous mixing and CO_2 flushing at the beginning of the experiment 102
Figure 93 - As removal efficiency for different headspace in the reactor: ME reactor using 50 g/L of GAC and ZVI LC plus, to treat 3 L, 2 L, 1 L, 500 mL, and 250 mL of SR17 LFG condensate using continuous mixing and CO_2 flushing at the beginning of the experiment 103
Figure 94 - As removal efficiency and headspace percentage in the reactor relation: ME reactor using 50 g/L of GAC and ZVI LC plus, to treat 3 L, 2 L, 1 L, 500 mL, and 250 mL of SR17 LFG condensate using continuous mixing and CO_2 flushing at the beginning of the experiment 103

Figure 95 (Sb) - Comparison of ME treatment results for reactor headspace variations: ME reactor using 50 g/L of GAC and ZVI LC plus, to treat 3 L, 2 L, 1 L, 500 mL, and 250 mL of SR17 LFG condensate using continuous mixing and CO_2 flushing at the beginning of the experiment 104
Figure 96 - Sb removal efficiency for different headspace in the reactor: ME reactor using 50 g/L of GAC and ZVI LC plus, to treat 3 L, 2 L, 1 L, 500 mL, and 250 mL of SR17 LFG condensate using continuous mixing and CO_2 flushing at the beginning of the experiment 104
Figure 97 - Sb removal efficiency and headspace percentage in the reactor relation: ME reactor using 50 g/L of GAC and ZVI LC plus, to treat 3 L, 2 L, 1 L, 500 mL, and 250 mL of SR17 LFG condensate using continuous mixing and CO_2 flushing at the beginning of the experiment 105
Figure 98 (As) - Release profile from spent PAC / ZVI LC plus fine active media suspended in 100 mL of 0.1 M NaOH agitated up to 24 hours: ME treatments using 2 L of SR16 in a column reactor, with 20 g/L PAC and ZVI LC plus fine, continuous mixing, and pH and 7 (not controlled) 108
Figure 99 (As) - Release profile from spent PAC / ZVI LC plus fine active media suspended in 100 mL of 0.1 M NaOH agitated up to 24 hours: ME treatments using 2 L of SR16 in a column reactor, pH 3, continuous mixing, and active media dosing of 7 and 14 g/L 108
Figure 100 - Mass balance experiment results: Spent wet active media recovered from ME treatment suspended in 100 mL of 1 M NaOH. Experiment details: 2 L of SR16 treated with 20 g/L PAC- ZVI LC plus, and pH 3 (For As initial and final concentrations in the ME process, see Figure 54)..... 110
Figure 101 - Mass balance experiment results: Spent wet active media recovered from ME treatment suspended in 100 mL of 1 M NaOH, 0.1 M NaOH and passing 1 M NaOH over the spent active media. Experiment details: 200 mL of SR16 treated in a beaker with 20 g/L PAC- ZVI LC plus fine, pH 3, and continuous mixing 111
Figure 102 - Mass balance experiment results: Spent active media recovered from ME treatment suspended in 10 mL of concentrated HNO_3 and HCl and exposed to microwave digestion (MWD). Experiment details: Headspace experiments for SR14 treated with 50 g/L GAC- ZVI LC plus, pH 3, and continuous mixing (As removal results in Figure 86)..... 113
Figure 103 - Mass balance experiment results: Spent active media recovered from ME treatment suspended in 10 mL of concentrated HCl and exposed to microwave digestion. Experiment details: Headspace experiments for 3 L and 2 L of SR17 treated with 50 g/L GAC- ZVI LC plus, pH 3,

continuous mixing, and CO_2 flushing at the beginning to push out the oxygen in the reactor (As removal results in Figure 92) 115
Figure 104 - Logarithm of As and Sb concentrations vs. redox potential scatter plots obtained from multiple ME treatment experiments developed with different samples and operational conditions 118
Figure 105 - Logarithm of As and Sb concentrations in SR12 vs. redox potential scatter plots obtained from multiple ME treatment experiments developed with different samples and operational conditions 119
Figure 106 - Logarithm of As and Sb concentrations in SR13 vs. redox potential scatter plots obtained from multiple ME treatment experiments developed with different samples and operational conditions 119
Figure 107 - Logarithm of As and Sb concentrations in SR14 vs. redox potential scatter plots obtained from multiple ME treatment experiments developed with different samples and operational conditions 120
Figure 108 Logarithm of As and Sb concentrations in SR15 vs. redox potential scatter obtained from multiple ME treatment experiments developed with different samples and operational conditions 120
Figure 109 - SR12 and SR14 linear regressions and residuals results obtained from multiple ME treatment experiments developed with different samples and operational conditions 122
Figure 110 - SR14 segmented linear regressions and residuals results obtained from multiple ME treatment experiments developed with different samples and operational conditions: Log As concentrations 124
Figure 111 - SR14 segmented linear regressions and residuals results obtained from multiple ME treatment experiments developed with different samples and operational conditions: Log Sb concentrations 124
Figure 112 - SR12 Quantile Regressions of logarithms of As and Sb concentrations with split-sample analysis obtained from multiple ME treatment experiments developed with different samples and operational conditions 126
Figure 113 - SR14 Quantile regressions of logarithms of As and Sb concentrations with split-sample analysis obtained from multiple ME treatment experiments developed with different samples and operational conditions 126

Figure 114 - SR12 segmented quantile regressions of logarithms of As and Sb obtained from multiple ME treatment experiments developed with different samples and operational conditions 128
Figure 115 – Probability density function and heatmap of log10 As concentration in μg/L across 200 mV redox intervals obtained from multiple ME treatment experiments developed with different samples and operational conditions. Sample used for this analysis: SR12, SR13 and SR15 129

List of tables

Table 1 - Reagents used for ME experiments 26
Table 2 - Sieve numbers used to characterize the diameter of ZVI 26
Table 3 - Summary of the sample collection dates and arsenic concentration 30
Table 4 - Mass balance experiment results: Spent wet active media recovered from ME treatment suspended in 100 mL of 1 M NaOH. Experiment details: 2 L of SR16 treated with 20 g/L PAC-ZVI LC plus fine (1:2), and pH 3 (Experiment results: Figure 54, Mass balance chart: Figure 100) 146
Table 5 - Mass balance experiment results: Spent wet active media recovered from ME treatment suspended in 100 mL of 1 M NaOH. Experiment details: 200 mL of SR16 treated in a beaker with 20 g/L PAC- ZVI LC plus, pH 3, and continuous mixing (Mass balance chart: Figure 101) 147
Table 6 - Mass balance experiment results: Spent active media recovered from ME treatment suspended in 10 mL of concentrated HNO_3 and exposed to microwave digestion. Experiment details: Headspace experiments for SR14 treated with 50 g/L GAC- ZVI LC plus, pH 3, and continuous mixing (Experiment results: Figure 86, Mass balance chart: Figure 102) 148
Table 7 - Mass balance experiment results: Spent active media recovered from ME treatment suspended in 10 mL of concentrated HCl and exposed to microwave digestion. Experiment details: Headspace experiments for SR14 treated with 50 g/L GAC- ZVI LC plus, pH 3, and continuous mixing (Experiment results: Figure 86, Mass balance chart: Figure 102)..... 149
Table 8 - Mass balance experiment results: Spent active media recovered from ME treatment suspended in 10 mL of concentrated HCl and exposed to microwave digestion. Experiment details: Headspace experiments for SR17, with 50 g/L GAC- ZVI LC plus, pH 3, continuous mixing, and CO_2 flushing at the beginning (Experiment results: Figure 92, Mass balance chart: Figure 103) 150
Table 9 - Mass balance experiment results: Spent active media recovered from ME treatment dried and suspended in 10 mL of concentrated HCl and exposed to microwave digestion. Experiment details: Headspace experiments for SR17 treated with 50 g/L GAC- ZVI LC plus, pH 3, continuous mixing, and CO_2 flushing at the beginning to push out the oxygen in the reactor (Experiment results: Figure 92, Mass balance chart: Figure 103 151

1. Executive Summary

The Cedar Hills Regional Landfill (CHRLF) is the only active landfill in King County, Washington state. The landfill, operated by King County Solid Waste Division, spans 920 acres in Maple Valley, approximately 20 miles southeast of Seattle, and receives more than 800,000 tons of solid waste annually (kingcounty.gov, 2023).

At the CHRLF site, the active fill area is currently limited to Area 8 while Area 9 is reserved for future use. Each area uses a layer-by-layer filling process, followed by compaction and soil capping. The final cap consists of multiple layers of soil, screening material, clay, geomembrane, sand, and grass (Rifkin, 2021).

When solid waste is deposited in the landfill, it generates water due to microbiological processes that degrade the deposited waste. Rainwater that infiltrates open areas of solid waste deposition combines with the infiltrated rainwater to generate landfill leachate that must be treated and prevented from leaching into the groundwater. The microbiological processes also generate LFG which contains a high fraction of water vapor which upon cooling in LFG collection pipework forms LFG condensate. LFG at CHRLF is collected and used by a third party to generate bioenergy.

On June 23rd, 2015, a King County Industrial Waste sample detected an arsenic exceedance at CHRLF. The maximum daily load for arsenic, which has been established for CHRLF operations, is 0.27 pounds per day, with an instantaneous limit of 4.0 mg/L. Since February 2016, violations of the arsenic maximum daily load have been frequent, with levels reaching as high as 1.4 pounds per day in 2019 (Rifkin, 2021).

The provenance of elevated levels of arsenic in the landfill has been attributed to the occurrence of this element in the cover soils and, more importantly, waste material deposited in the landfill. Arsenic is known to be able to undergo volatilization driven by the reducing conditions within the active areas of the landfill, and the subsequent disposal of arsenic-containing spent landfill gas treatment solids back into the landfill, creates a dynamic feedback loop. As a result, the concentration of arsenic in the leachate and gas condensate at CHRLF has increased over time.

In light of these circumstances, CHRLF has requested the University of Washington to develop a cost-effective treatment process to remove arsenic from landfill gas condensate. The project started in 2019, and over the course of the project, an innovative process called Microelectrolysis (ME) has been developed, tested, and chosen for practical implementation at CHRLF site.

The ME process involves an electrochemical reaction that occurs at the interface between zero-valent iron (ZVI) and activated carbon (AC), which serves as active media for the treatment process. During the reaction, the AC enhances the electrochemical oxidation (corrosion) of ZVI. This process helps convert arsenic into more readily extractable species by reducing them to species that can be adsorbed by the iron-carbon combination. More details of the Microelectrolysis treatment process are explained in the following chapters.

During the initial phases of the project, the team worked to determine the efficiency of different processes to treat the CHRLF leachates and landfill gas condensates with the main goal of removing arsenic. The experiments showed that the treatment that utilized zero valence iron/activated carbon combinations (so called microelectrolysis approach) resulted in reasonably high levels (>80%) of the removal of arsenic. More details of these results are in Malik 2020, Rifkin 2021, Cheney-Irgens 2022, and Walters, 2022.

Once the ME treatment was selected as the best option to pursue, the team worked on determining the best type, size, and shape of the ME process reactor. More details on the experiments and results can be found in Cheney-Irgens 2022, and Walters, 2022.

As a continuation of Cheney-Irgens, and Walters's works, this thesis in focused on performing extensive ME experiments whose main objective is to optimize the process and close the mass balance for arsenic for ME treatment in a fluidized-bed column reactor.

Throughout the research, a variety of operational variables were examined to identify the optimal treatment for the landfill gas condensate. The process was optimized to a point where it needs only 30 minutes treatment, with minimal CO_2 gas required and only the presence of active media and acid to facilitate the reaction. Experiment results indicate that activated carbon and zero valent iron are highly effective at retaining the majority of arsenic, and that multiple loads of LFG condensate can be treated using the same amount of combined active media, ranging from 20 to 50 g/L.

Based on the results of this study, recommendations for future work are to standardize certain process parameters in preparation for the pilot plant construction, such as identifying the most effective mixing configuration and mode for the ME reactors, determining the correlation between active media fluidization versus arsenic removal, selecting the optimal active media particle size and ratio between AC and ZVI, their recycling and regeneration, finding a detailed correlation between the redox potential data and the arsenic removal efficiency that facilitates arsenic removal monitoring during the process, evaluating the optimal energy consumption and other operational parameters for the system, among other activities detailed in the next chapters.

2. Literature review

2.1. Geogenic and anthropogenic sources of arsenic

Arsenic (As) is a highly hazardous element that poses significant risks to human health and the environment. It originates from both anthropogenic and geogenic sources, and the US Environmental Protection Agency (EPA) has classified it as a group A human carcinogen. Exposure to arsenic can result in severe health effects, including various cancers such as skin, lung, bladder, liver, and kidney cancer, as well as numerous cardiovascular, neurological, hematological, renal, and respiratory diseases (Sahoo et al., 2013).

Arsenic is ubiquitous in the environment, occurring naturally in the atmosphere, soil and rocks, natural waters, and living organisms. Its mobilization is facilitated by various natural processes, such as weathering, biological activity, and volcanic emissions, as well as by a range of anthropogenic activities. Although most environmental arsenic issues result from As mobilization under natural conditions, human activities have had a significant impact on the levels of arsenic in the environment. These activities include mining, combustion of fossil fuels, use of arsenical pesticides, herbicides, crop desiccants, and as an additive in livestock feed (Smedley et al., 2002).

The presence, mobility, and speciation of arsenic in natural systems can be attributed to several factors. Groundwater often has the highest concentrations and widest range of arsenic levels due to the presence of numerous As-rich minerals that interact with water with resultant As release and accumulation in the case of favorable physical and geochemical conditions for arsenic mobilization in aquifers.

Other geogenic inputs such as wind erosion, volcanic emissions, low-temperature volatilization from soils, marine aerosols, and pollution contribute to the occurrence of arsenic in the atmosphere,

which is then deposited back to the earth's surface through wet and dry deposition. Arsenic occurs in over 200 minerals, albeit many of these minerals are relatively rare in the natural environment. The highest concentrations of arsenic minerals are found in in association with transition metals, Cd, Pb, Ag, Au, Sb, P, W, and Mo. Arsenopyrite, FeAsS, is the most abundant arsenic ore mineral, typically forming under high-temperature conditions in the earth's crust, but recent reports have shown its presence in sediments through microbial precipitation.

Another As pyrite, arsenian pyrite, $Fe(S,As)_2$, is likely the most important source of arsenic in ore zones. Arsenic is also found in varying concentrations in other common rock-forming minerals, with the highest concentrations occurring in sulfide minerals such as pyrite, chalcopyrite, galena, and marcasite (Smedley et al., 2002).

In addition to sulfide minerals, high concentrations of arsenic have been found in oxide minerals and hydrous metal oxides, either as part of the mineral structure or as sorbed species. Fe oxides can contain arsenic concentrations that reach weight percent values. Although arsenic concentrations in phosphate minerals vary greatly, with apatite containing up to 1000 mg/kg, phosphate minerals are much less abundant than oxide minerals and contribute relatively little to the overall arsenic concentration in most sediments (Smedley et al., 2002).

Smelter operations and fossil-fuel combustion are the most significant anthropogenic sources of arsenic, contributing around 70% of the global atmospheric arsenic flux, which amounts to approximately 18,800 tons per year. Although the impact of these sources on airborne arsenic is widely accepted, its influence on the overall arsenic cycle has not been well established. Baseline concentrations of arsenic in rural rainfall and snow are typically less than 0.03 mg/L. However, areas affected by smelter operations, coal burning, and volcanic emissions generally have higher airborne As concentrations. Rainfall potentially affected by smelting and coal burning can have

arsenic concentrations of around 0.5 mg/L, but a concentration as high as 16 mg/L was found in rainfall collected 35 km downwind of a copper smelter in Seattle (Smedley et al., 2002). Figure 1 shows a list of geogenic and anthropogenic arsenic sources.

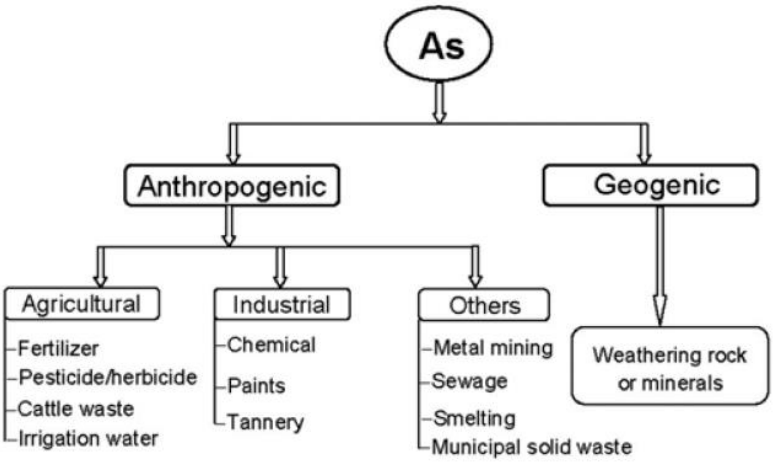

Figure 1 - Various sources of arsenic into paddy field (Sahoo et al., 2013)

2.2. Arsenic chemistry and occurrence

Arsenic is unique among heavy metals and metalloids due to its sensitivity to mobilization at typical groundwater pH values and the complexity of its species formed under both oxidizing and reducing conditions. It occurs in the environment in inorganic form such as oxyanions of trivalent arsenite [As (III)] or pentavalent arsenate [As (V)] while organic forms of As are typically produced via biological activity.

Oxyanions of As (V) tend to become less strongly sorbed as pH increases, which results in high concentrations of As to persist in solution even at near-neutral pH values. This makes As(V) and other oxyanion-forming elements such as antimony, selenium, molybdenum, chromium, and uranium, among others, to be common trace contaminants in groundwaters, with arsenic being particularly problematic due to the combination of its toxicity and mobility over a wide range of redox conditions (Smedley et al., 2002).

At equilibrium, the speciation of As(V) and As(III) oxyanions is controlled by redox potential and pH. At low pH (less than about pH 6.9), $H_2AsO_4^-$ prevails under oxidizing conditions, whereas at higher pH, $HAsO_4^{-2}$ becomes dominant (pKa_1=2.20, pKa_2=6.97, and pKa_3=11.53) (Raven et al., 1998). Under reducing conditions with a pH less than about pH 9.2, the uncharged arsenite species H_3AsO_3 predominates, while extremely acidic and alkaline conditions may contain H_3AsO_4 and AsO_4^{-3}, respectively (pKa_1=9.22, pKa_2=12.13, and pKa_3=13.4) (Raven et al., 1998).

If reduced S is present in sufficiently high concentrations, formations of dissolved As-sulfide solutes and solids may be significant. Reducing, acidic conditions promote the precipitation of orpiment (As_2S_3), realgar (AsS), or other sulfide minerals, for instance iron sulfides, which contain coprecipitated arsenic (Smedley et al., 2002).

The distribution of the species as a function of pH, and a Eh-pH diagram of arsenic speciation can be found in Figure 2 and Figure 3.

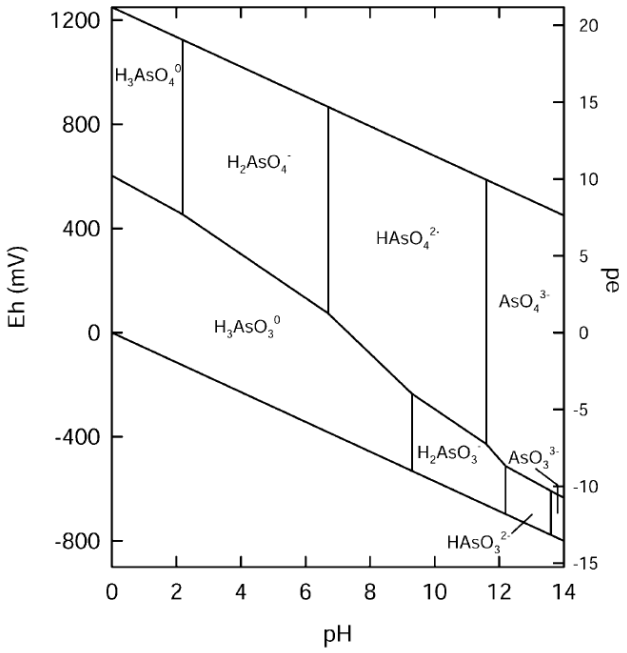

Figure 2 - Eh-pH diagram for aqueous arsenic species in the system (Smedley et al., 2002)

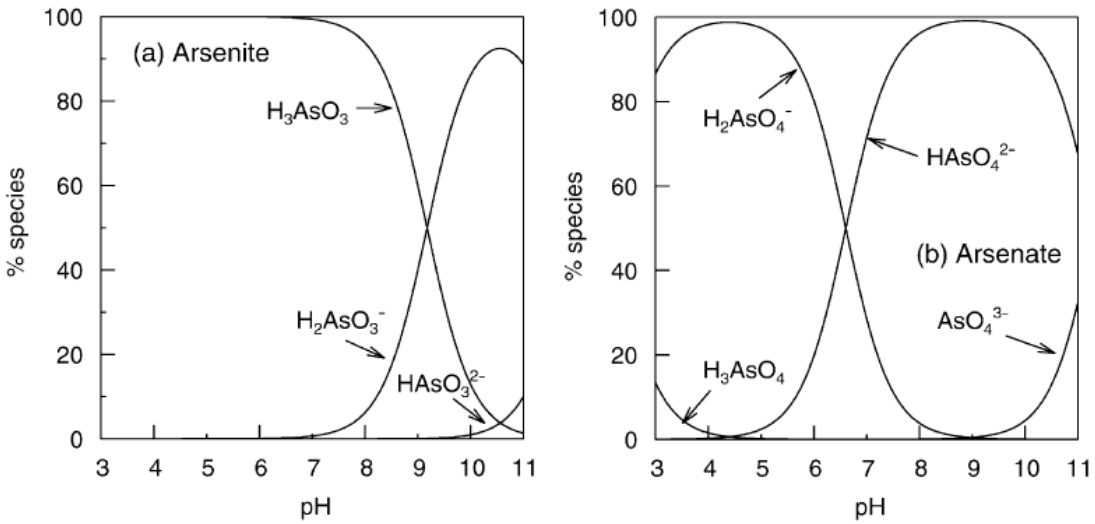

Figure 3 - Speciation of arsenite and arsenate as a function of pH

Figure 4 presents a simplified scheme of the biogeochemical processes that cause changes of As speciation and formation of As volatiles (arsines), solutes, and solid phases. The various forms of arsenic considered in this overview include arsine AsH_3, its methylated forms, arsenous acid, dimethylarsinic acid, trimethyl arsine gas, and others.

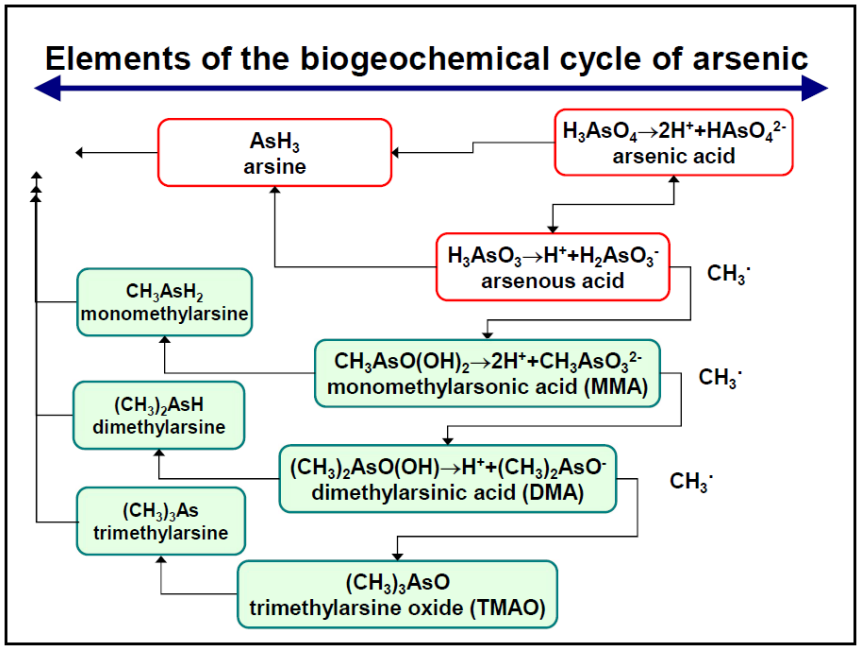

Figure 4 - Basic elements of the simplified sequence of biogeochemical reactions of arsenic involved in the generation of methylated As solutes and arsines (Korshin lecture 2021)

The toxicity and mobility of arsenic species are highly dependent on their chemical forms. Inorganic arsenic species are more toxic but less mobile than methylated arsenic species. Conversely, organic arsenic species with more complex structures, such as arsenobetaine and arsenosugars, are generally considered to be much less toxic. As a result, for effective risk assessment, it is more useful to identify the specific relevant arsenic species rather than determining total arsenic concentrations (Huang et al., 2009) although due to the complexities of As speciation analyses, total As concentrations are regulated in practice.

2.3. Geogenic and anthropogenic sources of antimony

Due to the presence of many similarities between the environmental chemistries of arsenic and antimony, consistent attention was paid in this study to comparisons of the removal of both elements from landfill gas condensate.

Antimony is an element that is widely found in the earth's crust. It has been designated as a probable human carcinogen by the International Agency for Research on Cancer (IARC) and as a priority pollutant by the US EPA (De Oliveira et al., 2022).

Antimony has a global reserve of 1.9 million tons. Most of the Sb production, approximately 80%, is concentrated in China, Russia, and Bolivia (Bolan et al., 2022). Antimony has a wide range of industrial applications. Elemental antimony can be used to produce semiconductors, infrared detectors, and diodes, while its alloyed form is used to manufacture lead storage batteries, solder, sheet and pipe metal, bearings, castings, and pewter, among others. Antimony oxide finds applications in fire-retardant formulations for plastics, rubbers, textiles, paper, and paints, while antimony trisulfide is utilized in the production of explosives, pigments, antimony salts, and ruby glass. Medicinally, antimony compounds have been used since the 14^{th} century for the treatment

of leishmaniasis and schistosomiasis, two parasitic diseases (Huang et al., 2009) (Sundar et al., 2010).

Sb is released into soil and aquatic environments from various sources, including the weathering of sulfide ores, leaching from mining wastes, and anthropogenic activities such as smelting, metallurgical operations, and shooting (Bolan et al., 2022).

Sb compounds can be released into the environment through volcanic eruptions, forest fires, sea spray and others. Sb substances can also be introduced into the environment through human activities. The concentration of antimony in the air is relatively low, typically ranging from a few nanograms per cubic meter (ng/m^3) to about 170 ng/m^3. In aquatic systems, antimony is usually found in its pentavalent state, but can exist in the trivalent state under certain conditions or due to human activities. The average concentration of antimony in soil is around 0.48 parts per million (ppm), with levels ranging from less than 1 to 8.8 ppm.

The general population is typically exposed to low levels of antimony, with an estimated intake of around 5 μg/day from food and water. However, exposure to higher levels of antimony can occur through occupational exposure or when it is used as a therapy, as discussed in more detail in the review article by Sundar et al., 2010.

2.4. Landfill gas condensate

Waste management (WM) is a demanding undertaking in all countries, with important implications for human health, environmental preservation, sustainability, and a circular economy (Vaverková, 2019). One of the most widely employed methods of disposal of municipal solid waste is landfilling (Brown et al., 1994). The most common type of landfill receives a mixture of municipal, commercial, and mixed industrial waste (Huang, 2009).

Landfilling is defined as the disposal, compression, and isolation of waste at an appropriate site (Vaverková, 2019). When the solid waste is deposited in the landfill, it interacts with the water cycle by rainwater infiltration, evaporation, and leaching into the groundwater. Figure 5 shows the water cycle in landfills.

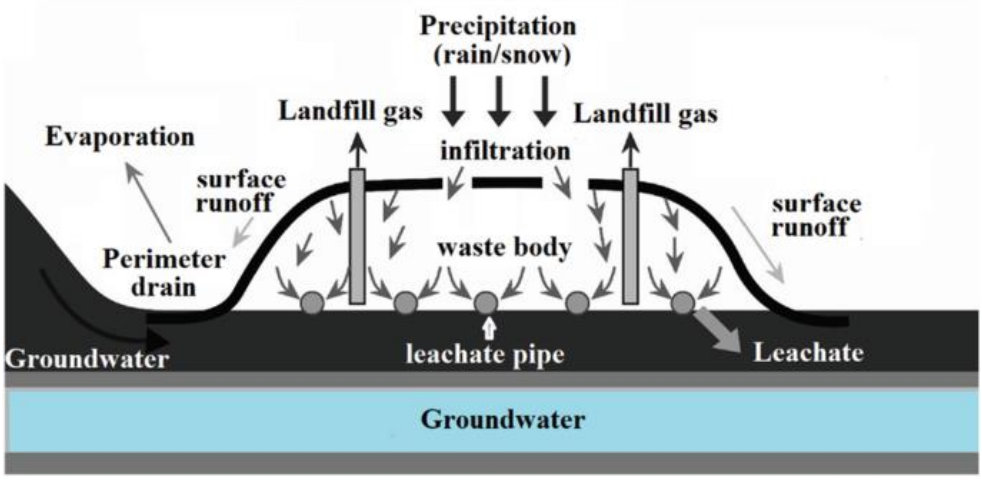

Figure 5 – General elements of the landfill water cycle (Adapted from Introduction to Solid Waste Management, 2021)

Landfill gas condensate is a liquid that is produced during the collection of LFG from landfills. The production of condensate can occur through natural or artificial cooling of the gas, or through physical processes such as volume expansion. The composition of LFG condensate is primarily water and a wide range of organic compounds, notably volatile organic contaminants (VOC) that condense simultaneously with the formation of water condensate. However, these organic compounds are often not soluble and/or miscible in water, frequently resulting in the separation of the condensate into two distinct phases: a watery (aqueous) phase and a floating organic (largely hydrocarbon, with significant presence of halogen-containing solvents) phase. This hydrocarbon/solvent phase can make up to five percent of the total condensate volume (Briggs, 1988). According to Zhao (2012), the presence of the hydrocarbon/solvent phase is a significant contributor to the overall emission of greenhouse gases into the atmosphere from landfills.

The greenhouse gas effects of LFG are primarily associated with the generation of methane formed as a result of microbiological degradation of solid wastes. Specifically, the release of methane (35-65%) and carbon dioxide (15-50%) from landfills contributes significantly to global warming (Konkol, 2022). The high concentration of methane and lower levels of other hydrocarbons in LFG also makes it an attractive source of energy. In fact, many landfills today are taking advantage of this by selling their methane-rich LFG to energy producers, allowing for energy generation while simultaneously reducing greenhouse gas emissions.

Purified LFG with enriched hydrocarbon concentration gas is called biogas. As a renewable biofuel, biogas has garnered interest in replacing fossil fuels. Furthermore, the prevention of methane ingress in the atmosphere can significantly reduce the global warming potential (GWP) of these gases, as the GWP of methane is 25 to 30 times that of carbon dioxide (Zhao et al., 2013).

LFG can be purified, making it suitable for combustion systems, engines, and turbines. The purification process involves the removal of water and other vapors through natural or artificial cooling or physical processes such as volume expansion, where different boiling points and critical pressure points are utilized. The liquid collected during this process is known as condensate or gas-derived liquids. However, this condensate requires treatment before discharge to a publicly owned treatment works r the environment as it contains pollutant compounds such as benzene, toluene, phenol, and other organic compounds (Zhao et al., 2013).

2.5. Arsenic and antimony in landfills

Landfills are potential sources of environmental pollution through the generation of landfill leachate, fugitive gas emissions and LFG condensates, which are typically mixed with the other leachate streams (Huang et al., 2009). The leachate and condensate formation are mediated by

physical, chemical, and microbial processes within the waste body that transfer pollutants to the percolating and evaporated water. These pollutants can be broadly classified into four groups, namely dissolved organic matter, inorganic macro-components, heavy metals, and xenobiotic organic compounds.

The presence of arsenic in landfills is a major concern due to its potential toxicity and the high concentrations found in landfill leachates. Historically, arsenic was used as a preservative to produce treated wood, and its presence in commercial products, such as seafood, wood, and electronic components, could increase arsenic concentrations in the landfill body and/or landfill leachate (De Oliveira et al., 2022).

Recent studies have indicated that elevated As concentrations in the groundwater beneath municipal solid waste landfills are favored by anoxic conditions, which result in the reductive release of As from underlying soil layers (Intrakamhaeng et al., 2020; Wang et al., 2012).

In Washington state, it is noteworthy that the concentration of arsenic in precipitation may exceed normal levels. A study conducted in the 1970s investigated the presence of arsenic in filtered rain samples collected near the outlet of Lake Washington in Seattle. To account for significant seasonal variations in rainfall, the mean As concentrations for each month were multiplied by the average monthly rainfall observed over the past 62 years. The findings revealed an average arsenic concentration of 16 ppb in the collected rainfall (Smedley et al., 2002).

These exceptionally high arsenic levels can be attributed to the emissions of very fine arsenic-rich stack dust, with a diameter of approximately 1 μm, originating from the ASARCO Smelter, a copper operation active for almost 100 years in Tacoma, Washington (Crecelius et al., 1975).

Moreover, the arsenic levels in rainwater in Seattle, located 35 km downwind of the smelter, were significantly higher compared to rainwater collected near the Washington coast, situated 100 km upwind of the smelter (0.4 ppb), as well as rainwater collected in Japan (1.6 ppb) (Crecelius et al., 1975).

Overall, the As concentrations in landfill leachates reported in a past study are of 10 to 1000 μg/L (Huang et al., 2009), and the presence of high levels of reactive sulfur compounds in landfill gas (H_2S, CH_3SH, $(CH_3)_2S$, CS_2, and $(CH_3)_2S_2$) is likely to result in the domination of As-S compounds in landfill gas condensates (Chen, Korshin et al., 2023).

In the case of antimony, over 40,000 tons are used annually in consumer goods. After their use, most of these products end up in landfills. (De Oliveira et al., 2022). In municipal solid waste, antimony is commonly found in the plastic fraction of electronic devices, including e-waste or waste electrical and electronic equipment, with reported concentrations ranging from 0.09-0.17% and 0.17-2.0% in e-waste and e-waste plastics, respectively (Intrakamhaeng et al., 2020).

In a study of trace metal presence in 22 municipal solid waste categories, Sb concentrations from 1.3 to 21,000 mg/kg were measured in different waste components, with polyethylene terephthalate (PET) plastics identified as the most significant sources of Sb (De Oliveira et al., 2022).

According to De Oliveira et al. (2022) and other sources, arsenic (As) and antimony (Sb) can volatilize under anaerobic conditions typical for landfills. As and Sb volatiles formed in these conditions include relevant inorganic forms (arsine (AsH_3) or stibine (SbH_3)) and as methylated varieties (mono-, di-, or trimethylarsine/stibine). The volatilization is the result of microbially-mediated landfill processes, and the volatile species is subsequently transported from the landfill via landfill gas (LFG) (De Oliveira et al., 2022).

2.6. Treatment of arsenic and antimony in the industry

The importance of reducing anthropogenic methane emissions and promoting renewable energy sources highlights the significance of renewable natural gas generation as a global technology. Studies have indicated that LFG gas condensate, which is formed during the purification process, can contain exceptionally high arsenic concentrations of up to 18 mg/L (Zhao et al., 2013), and antimony concentrations of up to 1.2 mg/L.

While most municipal solid waste landfills usually flare their LFG, the latest trend in utilizing landfill gas for bioenergy production necessitates the purification and cleansing of the gas rather than its burning.

In the field of industrial arsenic and antimony removal, conventional physical-chemical methods such as precipitation, adsorption, ion exchange, and membrane technology have been widely employed. Specifically, the following section outlines some of the most common treatments:

1. **Chemical precipitation**: process in which a chemical reaction occurs between arsenic and some metal salts, sulfides, or sulfates, resulting in the formation of As-containing solids. These solids can then be physically separated from the influent through precipitation, followed by subsequent post-separation processing. One common example of solids formed through chemical precipitation is As(III) sulfide. This solid is produced through the following chemical reaction:

   $$2HAsO_2(aq) + 3H_2S(g) \rightarrow As_2S_3(s) + 4H_2O(aq)$$ (Nazari et al, 2017)

   This process, although effective, requires a large amount of chemicals and results in the production of high amounts of chemical sludge, which is difficult to treat or dispose of directly. While As(III) sulfide, and other As-containing solids like calcium arsenate, and ferric arsenate

were previously shown to be the most typical As-containing solids formed via precipitation performed for arsenic removal, research has demonstrated that these materials are unstable under reducing conditions (Shih, 2005). Consequently, direct disposal of these materials into uncontained tailings is inadvisable, as it may lead to the generation of leachate containing arsenic (Shih, 2005).

2. **Adsorption**: this process utilizes selective materials that have a strong affinity for dissolved arsenic. The adsorbents can be biological materials, mineral oxides, activated carbons, or polymer resins. The most commonly used adsorbent is activated carbon, due to its efficiency and low cost. The effectiveness of this method is dependent on the properties of the activated carbon, chemical properties of the adsorbate, temperature, pH, and ionic strength, among others (Mohan et al., 2007 and Shih, 2005). This process is an important part of the Microelectrolysis treatment, and of the experiments conducted for this thesis.
3. **Ion exchange**: this process consists in exchanging arsenic anions for chloride or other anions at active sites bound to resin. While some ion exchange processes are highly effective in removing arsenic from water, the disadvantage of this method is that it releases toxic chemical reagents used in the resin regeneration process into the environment (Shih, 2005).
4. **Membrane separation processes**: this technology removes arsenic and other dissolved species and microorganisms. While membrane treatment is effective, it also tends to be the most expensive process for removing contaminants due to the high pressure and energy required to operate it (Shih, 2005).
5. **Advanced oxidation processes (AOPs)**: these processes utilize in-situ generated hydroxyl or sulfate radicals for the degradation of contaminants (Babu, 2019). AOPs rely on oxidants such as chlorine, ozone, or permanganate, and are effective in oxidizing arsenite to arsenate for

arsenic treatment (Zaw, 2002). However, despite its effectiveness, AOP treatment typically requires combination with other processes to reduce arsenic concentrations and can present challenges in toxicity testing and the generation of toxic byproducts from naturally occurring organic matter (Babu, 2019; Zaw, 2002).

Although the techniques described above are commonly used, they have been associated with several problems such as generating substantial waste, incurring high operational costs, exhibiting suboptimal removal efficiencies, and producing residuals (Khodabakhshi et al., 2011 and Mohan et al., 2007). Consequently, there is an urgent need for the development of novel and sustainable approaches to alleviate the negative impacts of these traditional methods. Addressing this need, researchers at the University of Washington have developed a new, more efficient, and cost-effective method of arsenic removal based on an existing process called microelectrolysis (ME).

The mechanism associated with As removal during ME remains to be ascertained, but it is thought to involve electrochemical reactions that occur at the interface between zero-valent iron (ZVI) and activated carbon, either in powder form (PAC) or granular form (GAC), which serve as active media for the treatment process. During the reaction, the activated carbon (AC) enhances the electrochemical oxidation (corrosion) of ZVI. Together, they form numerous micro-galvanic cells, and simultaneous reduction reactions occur on the surfaces of the iron and activated carbon particles, leading to the formation of Fe(II) and Fe(III) ions, which can result in significant electron transport to suitable electron acceptors (Liu and Korshin et al., 2022). This process helps convert organic arsenic into a number of species (whose nature remains to be ascertained) that can be adsorbed by the iron-carbon combination (Ying et al., 2012). More detailed information on the hypothesized process can be found in Liu and Korshin et al., 2022.

The development of the ME treatment is a result of extensive research and experimentation conducted during the CHRLF project. Previous studies have revealed that the treatment efficacy of microelectrolysis in As removal is predominantly influenced by several factors such as solution pH, Fe/C ratio, reaction time, and aeration rate, including the presence of oxygen in the system (Cheng et al., 2007; Liu and Korshin, 2022). Further elaboration of the results of the prior research and optimization efforts carried out to enhance the ME process can be found in the next chapter.

2.7. Outline of the Results of Prior Research of Arsenic Removal from Landfill Gas condensate

During the initial phases of the project, the team worked to determine the efficiency of different processes to treat the CHRLF leachates and landfill gas condensates with the main goal of removing arsenic. The treatment methods tested included electrochemical pre-oxidation using PbO_2 electrodes, permanganate oxidation and adsorption via manganese dioxide, pre-treatment using ozonation, adsorption on manganese dioxide, coagulation with ferric chloride, adsorption on AC, reduction and adsorption using ZVI, and reduction and adsorption via ME. The experiments showed that while applications of oxidative/adsorption approaches were largely unsuccessful for arsenic removal, the treatment that utilized zero valence iron/activated carbon combinations (so called microelectrolysis approach) resulted in reasonably high levels (>80%) of the removal of arsenic. A more detailed description of these results is presented in Malik 2020, Rifkin 2021, and Cheney-Irgens 2022.

Once the microelectrolysis treatment was selected as the best option to pursue, the team worked on determining the type, size, and shape of the microelectrolysis process reactor.

Experiments were conducted on fluidized-bed columns reactors and fixed bed columns reactors to test different active media materials, bed layer heights, pH levels, and LFG condensate makeup. However, the fixed bed columns were found to be consistently obstructed hydraulically, leading to the cessation of these experiments. After several trials, it was determined that fluidized-bed reactors were the best configuration for carrying out the ME process.

After conducting initial ME batch column experiments using a flat-bottomed PVC column, alternative designs were evaluated to enhance the interaction between PAC and ZVI, which is crucial for removing arsenic and antimony. Among the designs explored were a 3D printed dome and a 3D printed funnel. Ultimately, the 3D printed funnel proved to be the most effective design for the bottom part of the column reactors.

Also, the research team worked on determining the best process operational variables to treat a limited amount (500 mL) of LFG condensate. The variables tested included empty bed contact time (EBCT) in the experiments with packed bed columns, active media dosage, operating pH, carrier gas type and flow, experiment run time, counterflow gas conditions, filtration methods, and variations in gas diffuser materials.

The prior research experiments determined the following operational variables as the optimal for the ME process:

- The employment of CO_2 as the carrier gas resulted in the highest rates of removal for arsenic and antimony (Malik, 2020, Cheney-Irgens, 2022, and Walters, 2022). These experiments were carried out using relatively small ZVI/PAC dosages.
- The pH of the solution tends to increase with treatment time. The findings indicated that utilizing LFG condensate at a controlled, low pH of 3 or 4 was more successful in removing

arsenic and antimony than treatment at a pH of 5 or 6 (Cheney-Irgens, 2022 and Walters, 2022).

- The role of activated carbon, specifically PAC, in the ME process is essential. When PAC was combined with zero valent iron, a significantly higher arsenic and antimony removal efficiency was achieved. Larger particle-sized ZVI materials exhibited a decreased ability to remove arsenic compared to more dispersed materials, presumably due to the smaller particle's larger surface area available for the reaction. A similar observation was made regarding the use of GAC and PAC (Malik, 2020 and Rifkin, 2021).
- Tests investigating the impact of the active media dose demonstrated that a dosage of 4 g/L of PAC and ZVI (ratio 1:2) was the most efficient. However, a higher dosage of active media resulted in quicker removal of arsenic and antimony (Walters, 2022).
- The use of inline filtration to remove the spent active media (ZVI/PAC) was found to be a more efficient method compared to filtering the samples after collection. During an 8-hour experiment, the use of inline filtration led to a higher removal rate of arsenic (Walters, 2022).

Finally, the research team also calculated the mass balance of arsenic and antimony. The findings indicated that extracting the arsenic retained by the Fe/C active media using nitric acid and sodium hydroxide resulted in frequently insignificant arsenic recoveries for the samples generated during the experiments with CO_2 flux. In contrast, the arsenic recovery for the experiments without CO_2 tended to be higher but still lower than 100%, ranging from 10% to 40%. Similar results were observed for antimony.

More details on the column reactor configurations and mass balance results can be found in Walters 2022, and Cheney-Irgens 2022.

2.8. Goals of the study

The goal of this thesis is to perform extensive microelectrolysis experiments whose main objective is to optimize and scale up the process and close the mass balance for arsenic for microelectrolysis treatment in a fluidized-bed column reactor, equipped with a funnel shape bottom part and multiple ports to allow the measurement of pH, and redox potential during the process.

Some of the most important ME operational variables that we explored in this study are:

- Isolating the reactor from the atmosphere to determine the correlation between the presence of oxygen in the ME reactor and the arsenic removal efficiency.
- Comparing the efficiency of using CO_2 versus stirring the reactor with a mechanical mixer.
- Studying the feasibility of using larger particle size of active media (GAC and ZVI LC plus) when variating active media dosage . The main goal of using larger particle size is to improve operability and evaluate the feasibility of reusing the active media in multiple LFG condensate loading cycles.
- Assessing the impact of pH on the reaction when using mechanical mixing during the ME process.
- Studying the effects of temperature on the ME process.

Another highly important objective is to continue examination of the mass balances in the ME process by tracking the concentrations of arsenic and antimony on the active media after treatment. The primary aim is to achieve a complete mass balance and determine the fraction of removed contaminants that remain in the active media and the fraction that is released to the atmosphere.

3. Experimental reactors for microelectrolysis treatment

ME reactors have been developed in the University of Washington laboratory using advanced technology equipment and have undergone continuous improvement over the past two years by multiple researchers involved in the project (Malik 2020, Rifkin 2021, Cheney-Irgens 2022, Walters 2022). Figure 6 shows photos of the setups of two of the current microelectrolysis treatment reactors employed.

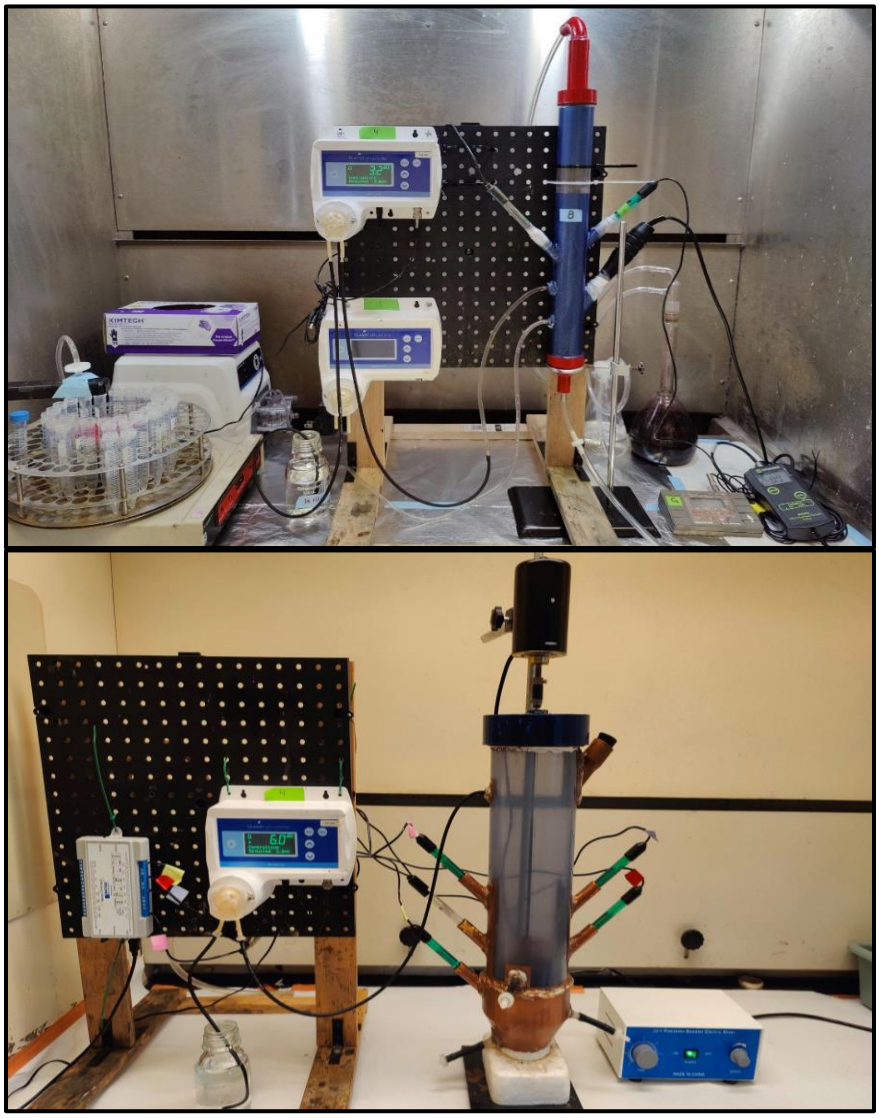

Figure 6 - Two types of laboratory scale ME reactors: 500 mL reactor (top), 3 L reactor (bottom)

Further details on the equipment, materials, and chemicals are provided in the next section.

3.1. Equipment and materials

The complexity of this novel process requires customized equipment, along with common laboratory machinery and accessories. The list of equipment and materials used for the experiments are following:

3.1.1. Personal protection equipment (PPE)

- Laboratory coats
- Safety goggles
- Carbon activated masks
- KN95 masks
- Safety nitrile gloves
- Sampling pants
- Sampling gloves

3.1.2. Column reactors

Fabrication of the microelectrolysis reactors requires both commercially available materials and tailor designed 3D pieces. All the materials used are listed below:

a) Materials:

- PVC columns
- Plastic barbed tube fittings
- MarineWeld adhesive
- Silicone 100% waterproof
- Spray on protective enamel
- Electric tools: 20V cordless drill, variable-speed Dremel
- Common tools: saw, hammer, screwdrivers, pliers, tweezers, and scissors.
- Regular and sealant tape
- Tygon® tubing
- Ender Pro 5 3D and Flashforge Adventurer 4 3D printers

    - The printers were used to fabricate selected components of ME reactors that would be difficult to make or order conventionally.
- Silk Polylactic Acid (PLA) 3D printing filament 1.75 mm

b) Instrumentation and sensors:

- Advanced electrochemistry multimeters
- Data acquisition kit
- ORP electrodes
- Dissolved oxygen meters
- pH meters
- pH controllers
- Gas flowmeters
- Digital timer outlets

c) Software:

- AutoCAD Autodesk student version

3.1.3. Experiments equipment and materials

a) Equipment:

- Electric mixer JJ-1, permanent magnet DC motor 60W
- Cartridge Filter
- Grooved sediment water filter cartridge
- Positive displacement pumps
- Air pumps
- Anton Paar Multiwave 3000 Microwave digestor
- Mettler Toledo Compact titrator G20
- Magnetic agitators
- Scale
- Voltage converter
- Autosampler

b) Materials:

- Glass beakers
- Glass bottles
- Plastic bottles
- Funnels
- Vacuum filters
- Pipettes
- One-way valves
- Rubber stoppers
- Grommets and washers

c) Consumables:

- MilliQ and DI water
- Filter papers and membranes
- Pipette tips
- Syringes
- Plastic weighing containers
- In-line filters (0.45 um)
- Disposable spatulas
- Glass beads
- Vacuum grease
- Disposable bags
- Disposable bottles
- Paper towels

3.2. Reagents

ME optimization research requires extensive experimentation. Table *1* shows the reagents used for the different configurations of the experiments.

Table 1 - Reagents used for ME experiments

Reagent	CAS Number	Supplier
LC Plus Fine (Zero Valence Iron)	7439-89-6	Hoganas
LC Plus (Zero Valence Iron)	7439-89-6	Hoganas
Powder Activated Carbon	7440-44-0	Fisher Chemical
Granular Activated Charcoal (12-40 mesh)	7440-44-0	Acros Organics
Sulfuric Acid	7664-93-9	VWR analytical
Hydrochloric Acid	7647-01-0	Supelco
Sodium Hydroxide	1310-73-2	Fisher Scientific
USP Grade Carbon Dioxide	124-38-9	Linde Gas
Potassium permanganate	7722-64-7	Fisher Chemical
Sodium sulfite	7757-83-7	Fisher Chemical
Nitric Acid, Trace Metal Grade	7697-37-2	Fisher Chemical
Arsenic (III)	ICP-151	Agilent
Antimony	ICP-033	Agilent
ICP-MS Yttrium standard	IMS-115	Ultra Scientific

3.2.1. Zero valent iron gain size determination

As the zero valent iron is a commercial product, an experiment to measure the distribution of ZVI particle diameters was conducted. Table *2* shows the sieve numbers used for the analysis.

Table 2 - Sieve numbers used to characterize the diameter of ZVI

Sieve number	Diam. min (mm)
16	1.18
20	0.85
40	0.4255
60	0.25
70	0.212
140	0.102

Sieve number	Diam. min (mm)
200	0.074
500	0.025

Figure 7 shows the mass of ZVI passing every sieve number and the corresponding distribution of ZVI masses.

Using the mass percentage per diameter, the total surface area for the two ZVI types that were most commonly used in this study was calculated. Figure 8 presents the results, which demonstrate that ZVI LC plus has an estimated surface area of approximately 40% compared to that of LC plus fine.

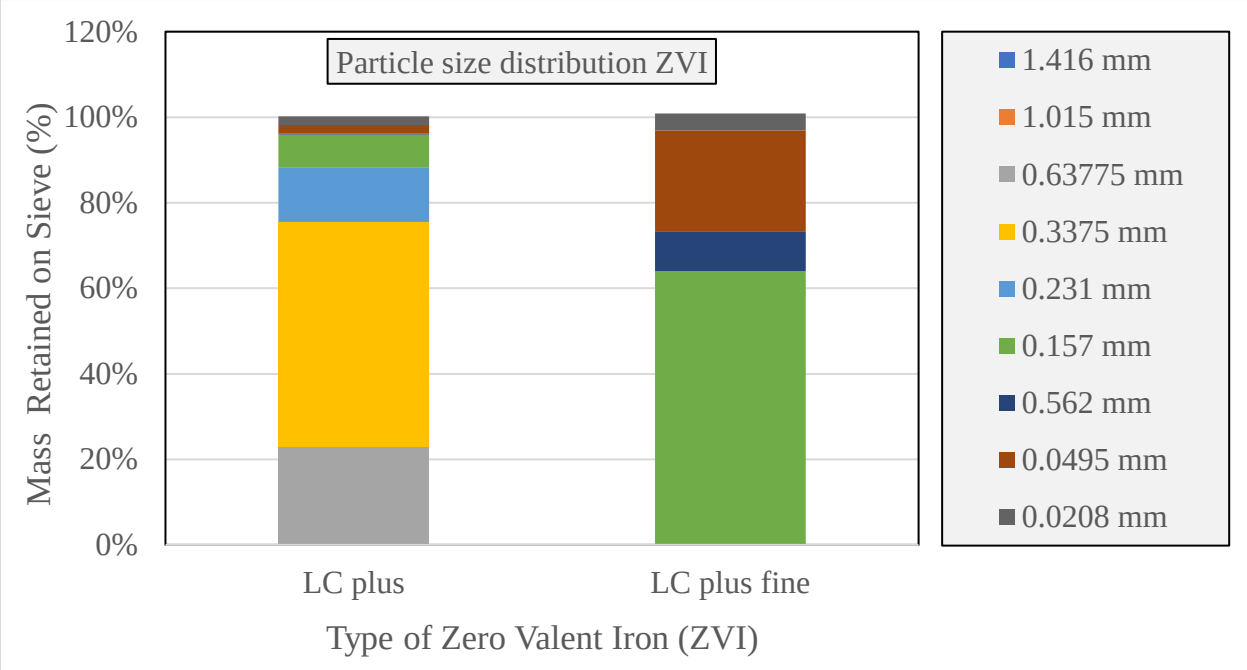

Figure 7 - ZVI sieve results: mass fractions associated with different ranges of ZVI particle diameters.

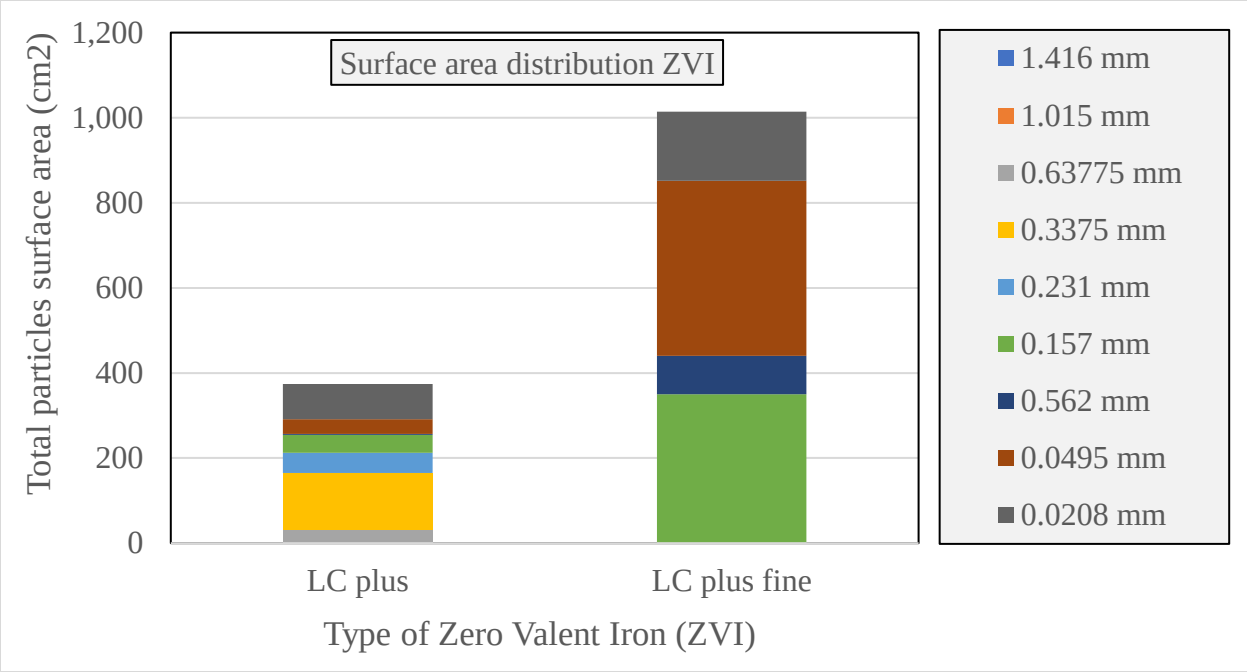

Figure 8 - ZVI sieve results: estimates of the total surface area and its fractions associated with different ZVI particle diameters.

These differences are expected to affect the outcomes of the ME experiments, as a larger surface area of ZVI generally leads to a more effective removal of arsenic and antimony. However, further analysis is required to establish a more precise relationship between the surface area of iron and the efficiency of removal.

3.2.2. Activated carbon gain size determination

Activated carbon particle size may also have an impact on the removal efficiency. The granular activated carbon particles sold commercially already have a mesh declared. However, an experiment to measure the distribution of particle diameters was conducted to confirm the particle size of the GAC used in the experiments. Table 2 shows the sieve numbers used for the analysis.

Figure 9 shows the mass of GAC passing through every sieve number and the corresponding distributions of the masses of GAC particles.

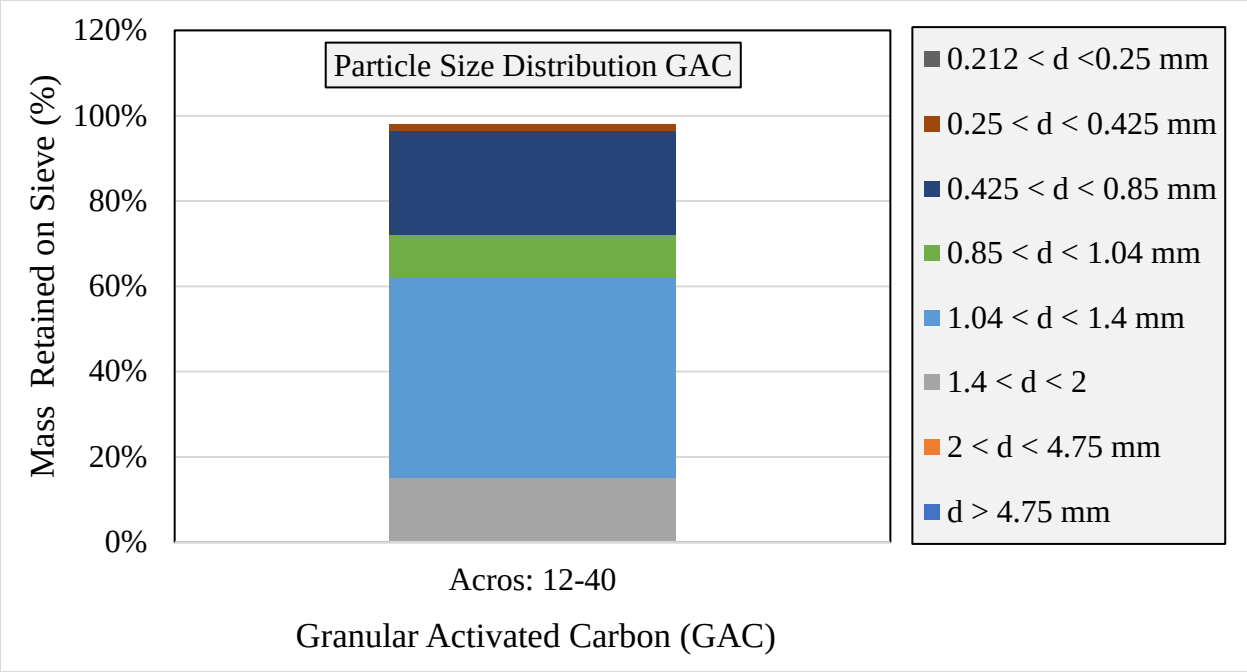

Figure 9 - GAC sieve results: mass fractions associated with different ranges of GAC particle diameters.

Additionally, the USP powder activated carbon has a 100% passing mass on the sieve 500, indicating that every PAC particle has a diameter smaller than 25 μm.

3.3. Gas condensate samples

A systematic sampling approach was employed to investigate the properties of the landfill gas condensate and address effects of changes of its composition. The condensate was collected at semi-regular intervals from a sampling point located at the CHRLF site. Each collection event was identified by the letters SR (which means Sampling Round), and a sequential number. All procured condensate samples exhibited variations in the concentration of arsenic and antimony. These differences underscore the importance of using multiple sampling rounds to gain a comprehensive understanding of the behavior and properties of landfill gas condensate and possible changes of its treatability, and to ensure an acceptably high arsenic removal.

Table 3 lists the samples used in the ME experiments described in this thesis.

Table 3 - Summary of the sample collection dates and arsenic concentration

Identifier	Sampling Date	Use Date	As Concentration (ppm)	Sb Concentration (ppm)
SR12	09/14/2021	Dec/2021 - Sept/2022	6.5	0.7
SR13	03/02/2022	Mar/2022 - Sept/2022	8.1	0.4
SR14	05/13/2022	May/2022 - Mar/2023	200	9.7
SR15	08/12/2022	Aug/2022 - Dec/2022	9.3	0.8
SR16	11/22/2023	Dec/2022 - Mar/2023	25	1.2
SR17	03/10/2023	March 2023 - Present	9.5	0.6

The sample collection process involved the visit to the landfill utility, where the sample containers were filled headspace-free from the condensate collection tank. The collected samples were stored in a cold room at a temperature of 4°C.

Prior to ME treatment and other relevant experiments, all the SRs except SR17, underwent two rounds of filtration using 1 μm cartridge filters. A peristaltic pump connected to each filter cartridge housing pumped LFG condensate through the filters connected in series. Filtration was deemed necessary due to the varying levels of suspended solids present in each SR. Despite the differing amounts of suspended solids present in the LFG condensate, the ME treatment was shown to effectively remove arsenic and antimony from all SRs, as discussed in more detail in the sections that follow. These data show that the presence of higher levels of suspended solids does not negatively impact the efficiency of the ME treatment.

3.4. Analytical instruments

3.4.1. ICP-MS

The Nanoscience Institute of the University of Washington owns and operates a Nexion 2000B ICP-MS that was used in this study for elemental analysis. This instrument aerosolizes liquid samples, transfers the atomized solution into a plasma torch with argon as a carrier gas, and quantifies element concentrations based on the counts of the mass ions with the corresponding masses for a given isotope.

To prepare LFG condensate samples taken prior to and after ME treatment, they had to be diluted with DI water and acidified with trace metal-grade nitric. Also, an aliquot from a 1 ppb stock solution of yttrium, which is used as an internal standard, was added. Depending on the expected concentration of the target elements, the samples were diluted from 50x times to 500x times.

To calibrate the ICP-MS for determinations of As and Sb concentrations, eight standards were prepared, with the concentrations of the target elements ranging from 1 ppb to 200 ppb. The analysis was deemed to be correct only when the calibration curve had an R^2 of >95% for both arsenic and antimony.

4. Optimization and scaling of the microelectrolysis process results

The previous phases of the project determined that microelectrolysis is the optimal process to remove arsenic and antimony from the landfill gas condensate. Initial experiments carried out earlier in the project used beakers of a limited size, typically below a volume of 100 mL. To achieve a closer approximation of the ME treatment to field conditions, the volume of LFG condensate treated was subsequently increased. To accomplish this, two ME reactors with a total volume of 500 mL and 3000 mL were designed and built.

The 500 mL column setup was configured to operate as a batch reactor. Its initial setup and ME treatment procedure were relatively more complicated (this was optimized later in this study, as explained in more detail further in this document).

The basic experimental setup included a 500 mL ME column reactor equipped with a gas diffuser installed in the bottom funnel of the reactor and used to provide CO_2 gas flow. The initial period of CO_2 sparging was to remove the dissolved oxygen which interferes with ME treatment. Then, a requisite aliquot of ZVI (Hoganas LC plus fine) was activated with 0.1 M hydrochloric acid and added to the reactor along with powder activated carbon (Fisher Chemical PAC). The dosage of active media used was 3 g/L with a ratio of 1:2 in mass between PAC and ZVI, respectively. After adding the active media, the column was capped, and its off-gas line was connected to a gas sparging bottle containing acidified permanganate or other strong oxidizers to capture arsenic volatiles. The experiment was performed for up to 8 hours, and solution aliquots were taken at equally distributed times to analyze the arsenic and antimony concentrations in the sample. Figure 10 shows the initial setup of the batch column.

Figure 10 - 500 mL column reactor used for ME experiments at the beginning of phase III

The optimization experiments included modifications in most of the operating parameters. The variations that were experimented with are as following:

- Prevention of ingress of atmospheric oxygen in ME reactors
- Gas flow rates and injection modes
- Effects of variation of active media activation, dosage, ratio, and particle size
- Effects of carrier gas recirculation
- Active media reuse: repeated sample loading cycles
- Effects of mechanical mixing
- Effects of temperature variations
- Effects of reactor headspace

One of the major aspects of ME treatment examined in the experiments was the repeatability of ME treatment results. The main finding was that ME performance is strongly impacted by the shape of the reactors and the ingress of atmospheric oxygen that interferes with ME treatment. To establish these points, multiple repeatability experiments were conducted, and modified column

reactors were designed and fabricated, with the ultimate goal to ensure that the treatment results be consistent under identical conditions.

4.1. Prevention of ingress of atmospheric oxygen in ME reactors

The first experiment was performed to compare the As removal in an open-air column reactor versus an isolated column reactor. As mentioned above, to provide isolation, the column reactor was capped, and its off-gas line connected to a gas sparging bottle containing 500 mL of 0.1 M potassium permanganate acidified to pH 1 with concentrated sulfuric acid. The primary objective of potassium permanganate was to oxidize any potential arsine gas that might escape the reactor, ensuring its confinement within the process and preventing it from being released outside of the system.

The potassium permanganate was subsequently connected to a gas sparging bottle containing 200 mL of 0.1 M sodium sulfite (Na_2SO_3). The primary aim of sodium sulfite, on the other hand, was to safeguard the system by inhibiting the entry of Oxygen. Figure 11 and Figure 12 show one of the many results regarding reactor isolation obtained from in these experiments.

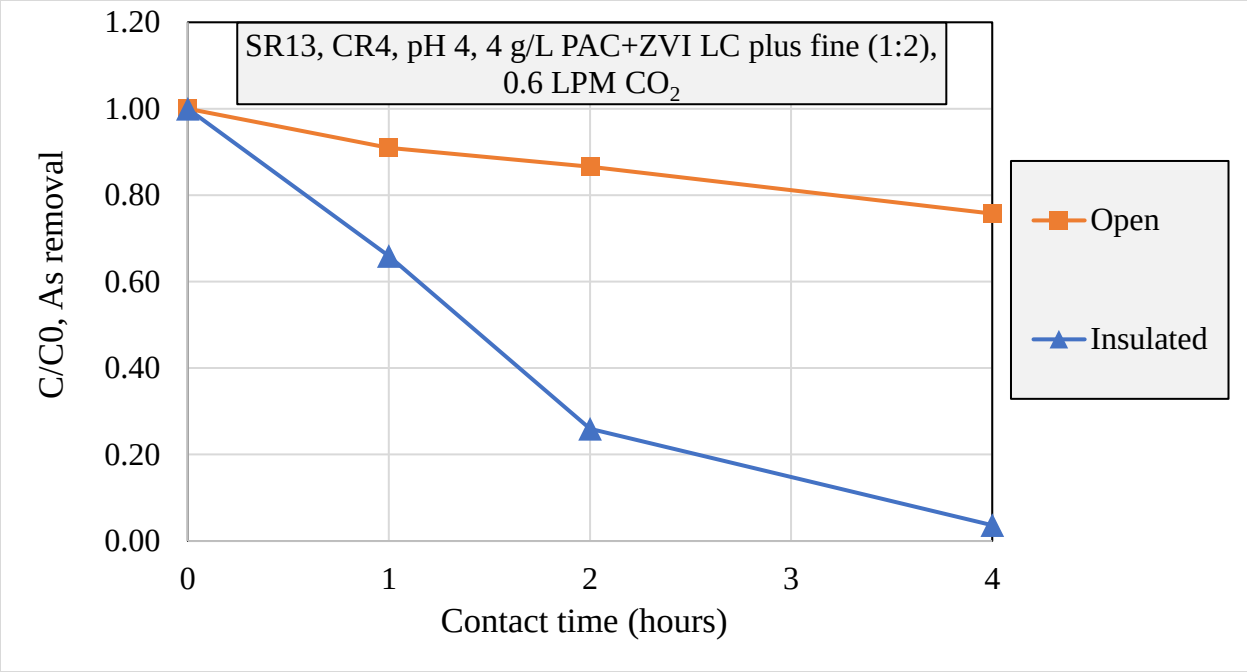

Figure 11 (As) - Comparison of 500 mL volume ME reactor treatment results for oxygen exposure: open reactor versus reactor insulated from atmosphere by connecting it to $KMnO_4$ and Na_2SO_3 for gas capture. Active media used: PAC and ZVI LC plus fine. Initial As concentration: 8.1 ppm

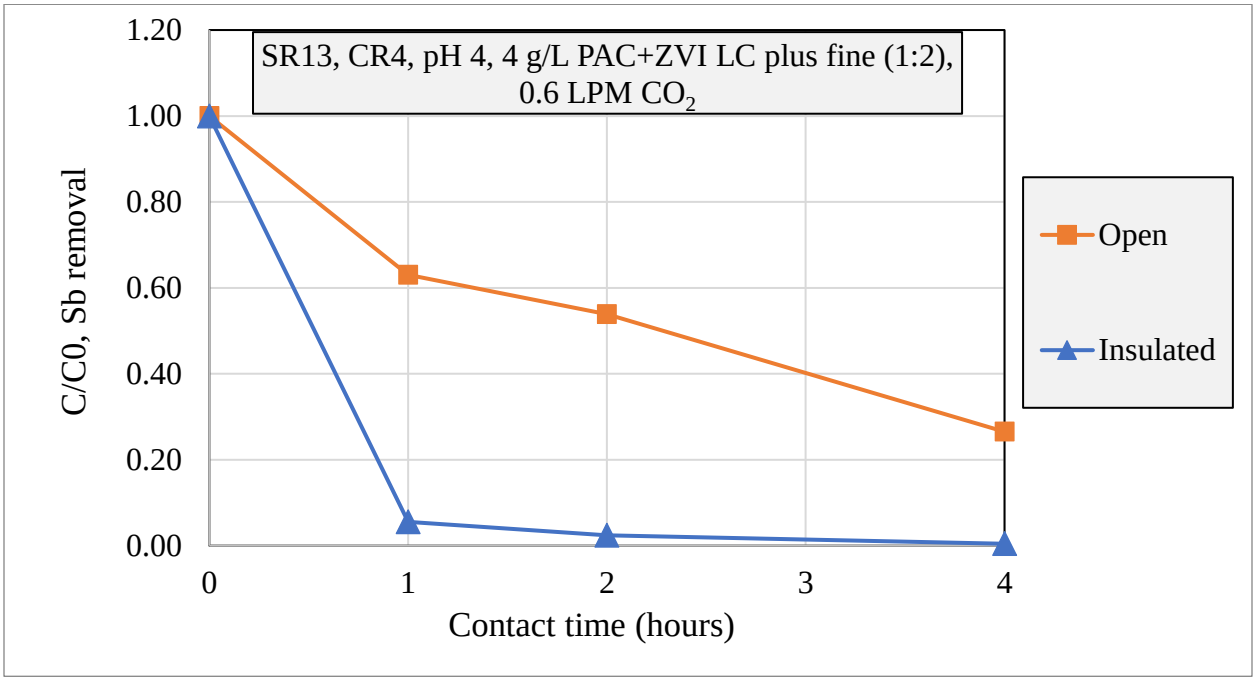

Figure 12 (Sb) - Comparison of 500 mL volume ME reactor treatment results for oxygen exposure: open reactor versus reactor insulated from atmosphere by connecting it to $KMnO_4$ and Na_2SO_3 for gas capture. Active media used: PAC and ZVI LC plus fine. Initial Sb concentration: 0.4 ppm

As shown in the plots, after four hours, the reactor exposed to the air achieved only 24% efficacy in the removal of arsenic. Conversely, use of the reactor connected to potassium permanganate and sodium sulfite resulted in >95% removal rate. Regarding antimony, the reactor exposed to open air reached a 73% removal rate, while the insulated reactor achieved over 99% removal.

To understand the impact of atmospheric oxygen on the ME process, a study was conducted to examine the redox potential levels in the LFG condensate during treatment. Oxygen acts as an oxidizing agent by accepting electrons, and as its concentration decreases in a solution, the redox potential also decreases. The primary objectives of this investigation were to establish a correlation between the presence of oxygen within the reactor (as indicated by the redox potential value) and the removal of arsenic and antimony from the LFG condensate.

To this end, measurements of redox potential using commercially available redox potential probes were incorporated in the ME experimental procedures. The redox potential results versus time profiles are shown in Figure 13.

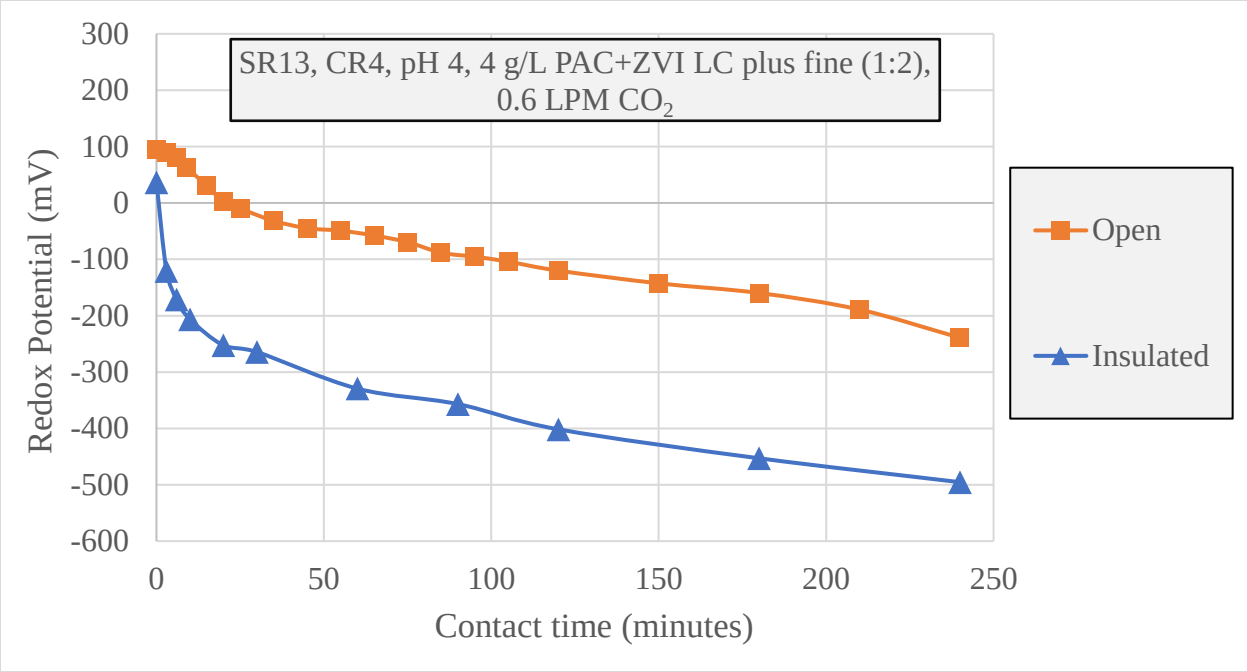

Figure 13. Comparison of redox potential changes versus treatment time in a 500 mL volume ME reactor: open reactor versus reactor insulated from atmosphere by connecting it to $KMnO_4$ and Na_2SO_3 for gas capture. Active media used: PAC and ZVI LC plus fine

The findings presented in Figure 13 demonstrate that the insulated column reactor attains lower redox potentials compared to the open-to-air column reactor. These outcomes may be linked to the arsenic and antimony removal efficiencies illustrated in Figure 11 and Figure 12. The correlation between these variables was deeply studied for multiple ME optimization experiments and will be further explored in the chapter 6 of this thesis.

Another experiment performed to decrease the dissolved oxygen in the reaction was performed by adding a dose of 0.00075 M sodium sulfite along with the reagents to the ME column reactor, along with 500 mL of sample SR12. The results of the experiment are following:

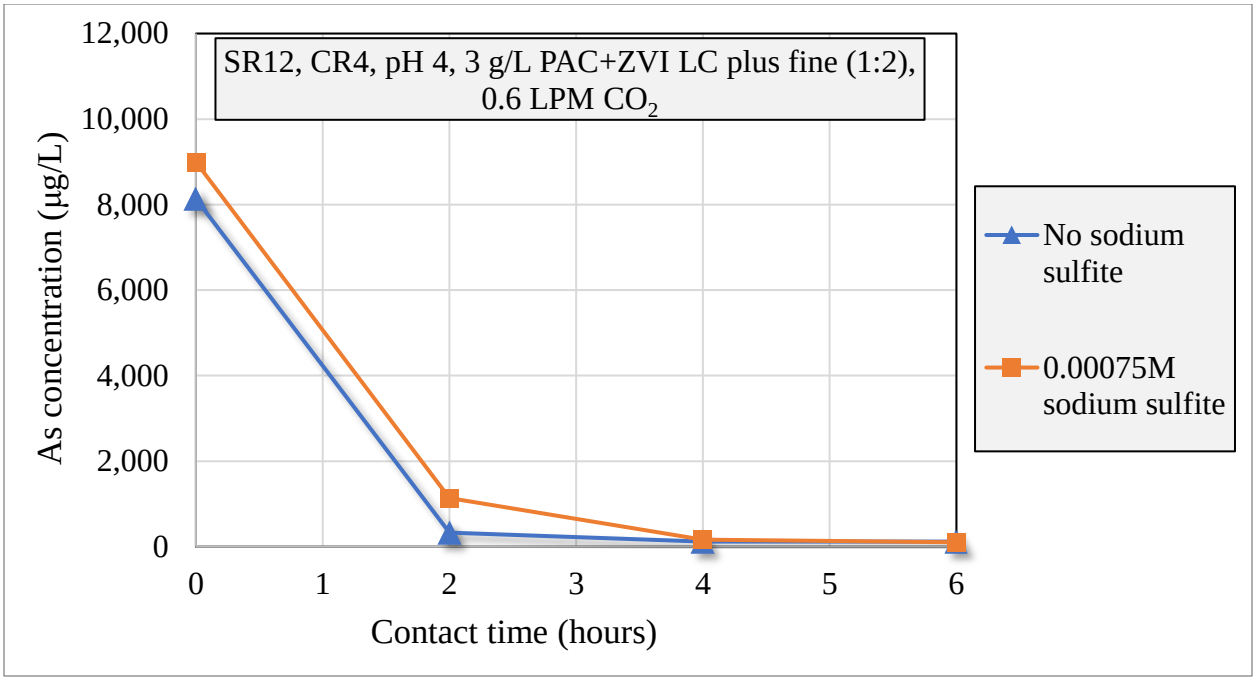

Figure 14 (As) - Comparison of ME treatment results in the presence and absence of 0.00075 M Na_2SO_3. 500 mL ME reactor, SR12 LFG condensate, 3 g/L of PAC and ZVI LC plus fine

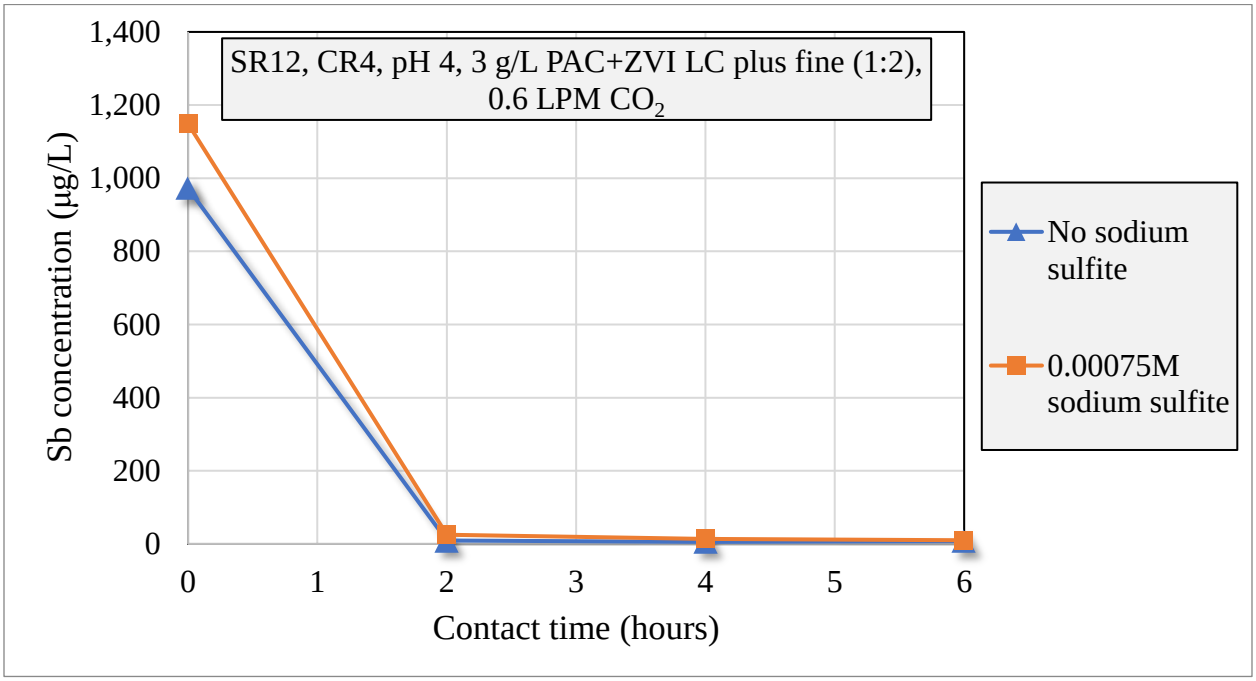

Figure 15 (Sb) - Comparison of ME treatment results in the presence and absence of 0.00075 M Na_2SO_3. 500 mL ME reactor, SR12 LFG condensate, 3 g/L of PAC and ZVI LC plus fine

As shown in Figure 14 and Figure 15Figure 15, the introduction of a reducing reagent (sulfite) had no discernible impact on the efficiency of As/Sb removal. For all further experiments, no Na_2SO_3 was added to the column reactor.

4.2. Gas flow rates and injection modes

The utilization of gas flows in ME treatment poses significant challenges due to increased operational complexity, safety aspects and additional costs. Prior experiments carried out in this project showed that presence of a gas flow through the ME reactor resulted in a notable improvement in the removal of As and Sb. In study, this point was elaborated further to explore in more detail effects of gas flows and compare their efficiency and overall necessity with the corresponding ME data obtained using only mechanical agitation of the solution being treated in an ME reactor.

The introduction of the carrier gas into the reactor was achieved via a gas diffuser positioned in the bottom of the reactor, with the bubbles serving the dual purpose of transporting the arsine and antimony volatiles, if such are formed, and facilitating the mixing of reagents necessary for the microelectrolysis reaction. Prior to this thesis, previous experiments have demonstrated that the use of carbon dioxide as a process gas results in superior results compared to that of other inert gases, such as nitrogen gas. Detailed information on these experiments is presented in the theses of Sam Walters (Walters, 2022) and Aminda Cheney-Irgens (Cheney-Irgens, 2022).

As part of the efforts to optimize the process, this thesis reports experiments that were focused on determining the optimal CO_2 flow rate and mode of application. The initial experiment involved an assessment of the efficacy of arsenic and antimony removal at various CO_2 flow rates. Four

different flow rates were employed: 0.2 LPM, 0.4 LPM, 0.6 LPM, and 1 LPM. The results of this experiment are depicted in Figure 16 and Figure 17.

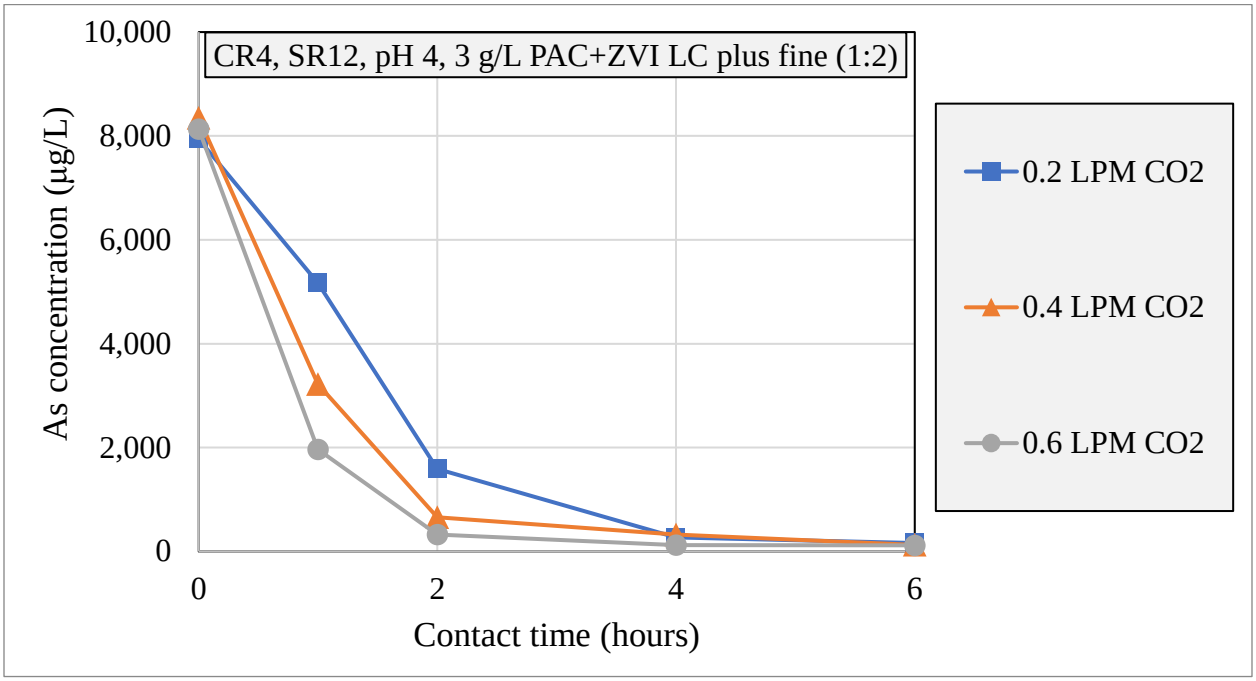

Figure 16 (As) - Comparison of ME treatment results for gas flow rates variations: 0.2, 0.4, and 0.6 LPM of CO_2 injection in a 500 mL ME reactor to treat SR12 LFG condensate using 3 g/L PAC and ZVI LC plus fine

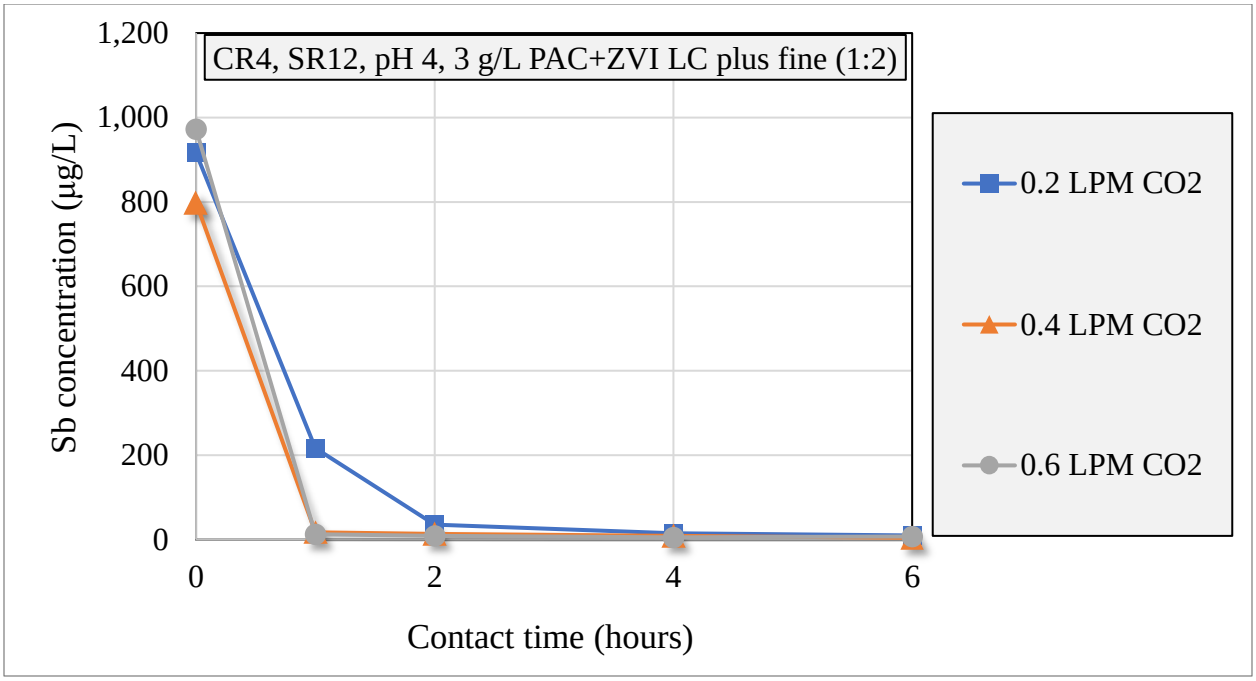

Figure 17 (Sb) - Comparison of ME treatment results for gas flow rates variations: 0.2, 0.4, and 0.6 LPM of CO_2 injection in a 500 mL ME reactor to treat SR12 LFG condensate using 3 g/L PAC and ZVI LC plus fine

The results illustrated in Figure 16 and Figure 17 indicate that all CO_2 flow rates achieved >98% removal of arsenic and antimony after a period of six hours. Differences between the various flow rates were discernible only during the initial four hours of treatment. Based on these findings, a flow rate of 0.6 LPM was chosen as the standard carrier gas flow for 500 mL ME reactors in further optimization and related experiments.

An additional crucial aspect of the process optimization was the evaluation of gas injection modes. In the subsequent experiments, a gas flow rate of 0.6 LPM was established, and various intermittent gas modes were examined. The intermittent modes analyzed are following:

1) Continuous CO_2 flow.
2) 60 minutes of continuous CO_2 flow, and 60 minutes of no CO_2 flow (60'on-60'off).
3) 30 minutes of continuous CO_2 flow, and 90 minutes of no CO_2 flow (30'on-90'off).
4) 15 minutes of continuous CO_2 flow, and 105 minutes of no CO_2 flow (15'on-105'off).

The results of these experiments are illustrated in Figure 18 and Figure 19.

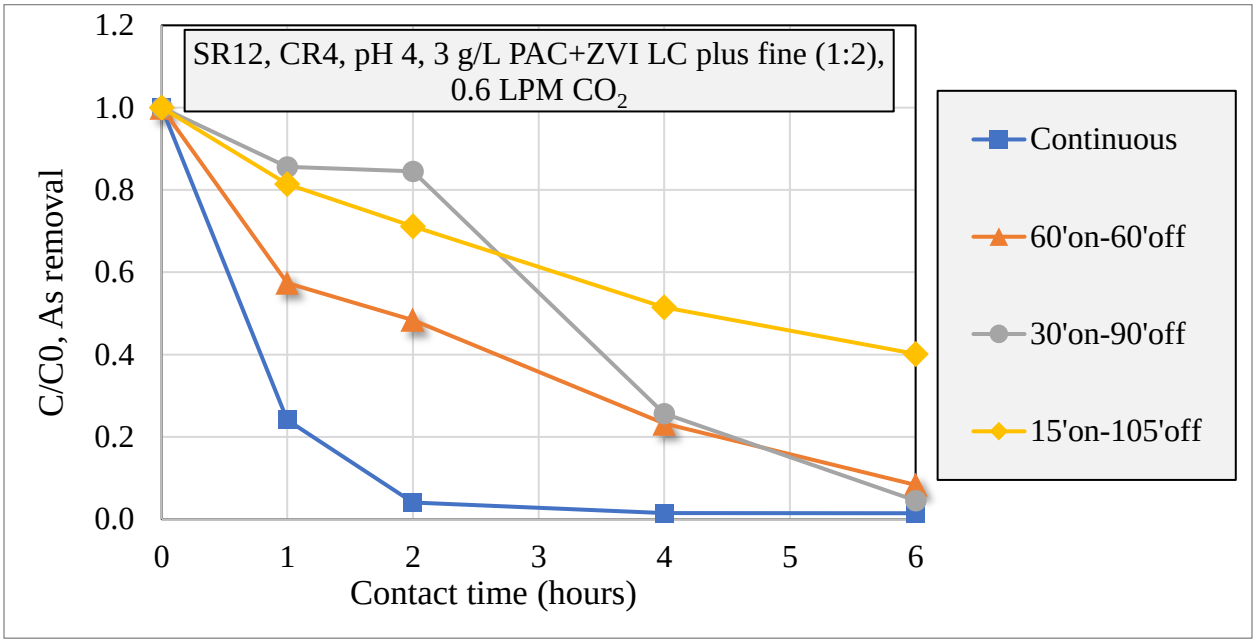

Figure 18 (As) - Comparison of ME treatment results for gas flow variations: continuous versus intermittent CO_2 injection in a 500 mL ME reactor to treat SR12 LFG condensate using 3 g/L PAC and ZVI LC plus fine and a CO_2 flow rate of 0.6 LPM. Initial As concentration: 6.5 ppm

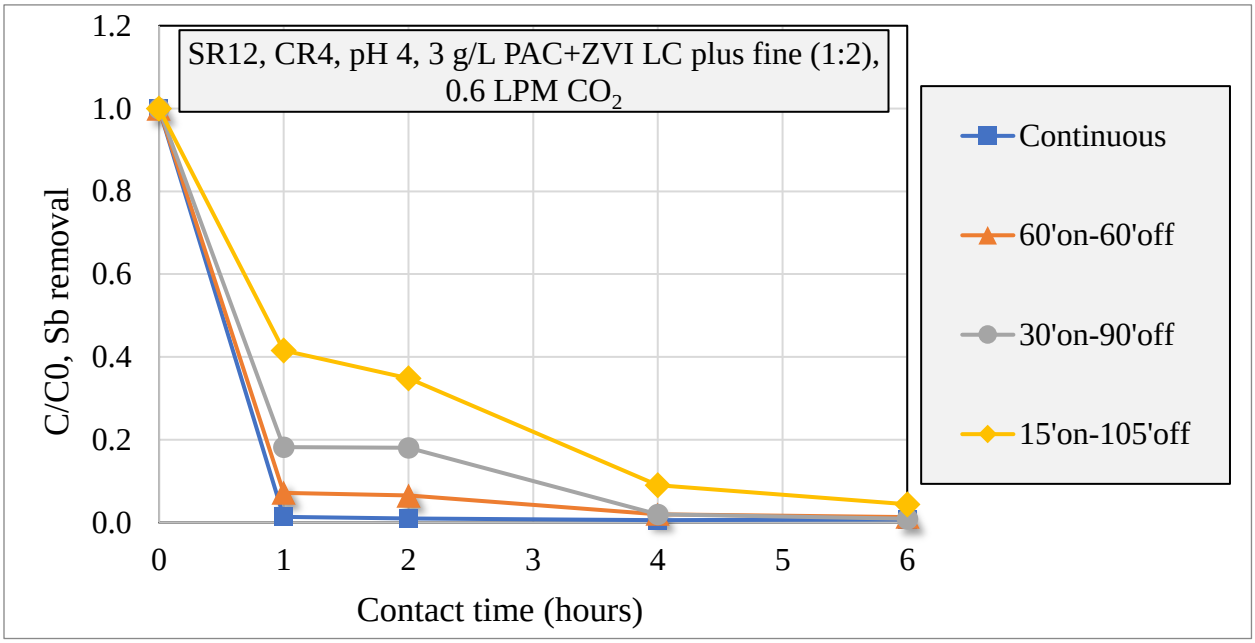

Figure 19 (Sb) - Comparison of ME treatment results for gas flow variations: continuous versus intermittent CO_2 injection in a 500 mL ME reactor to treat SR12 LFG condensate using 3 g/L PAC and ZVI LC plus fine and a CO_2 flow rate of 0.6 LPM. Initial Sb concentration: 0.7 ppm

The results illustrated in Figure 18 and Figure 19 indicate that the presence of the continuous CO_2 flow resulted in the removal of >99% of arsenic and antimony after six hours while intermittent CO_2 flows exhibited > 90% efficiency for 60'on-60'off and 30'on-90'off, and 60% efficiency for 15'on-15'off. Regarding antimony removal, all CO_2 injection modes resulted in >95% efficiency after six hours. These results suggest that intermittent flow may be a viable option for long treatment processes, if CO_2 carrier gas is used in the ME process and the contact time is sufficiently long. Further experiments using intermittent gas flow modalities were performed in different conditions, and the results are shown in the subsequent chapters of this thesis. However, for consistency considerations, continuous CO_2 flow (typically 0.6 LPM for a 500 mL reactor and increased proportionally when larger reactors were used) was used in the column reactor optimization experiments performed in this study.

4.3. Effects of carrier gas recirculation on As removal in ME reactors

Experimental results obtained in prior experiments may be interpreted to indicate that the emission of arsine volatiles may represent an important aspect of the microelectrolysis process, as CO_2 gas can displace these volatiles from the system. To prevent the loss of As volatiles and minimize gas consumption requirements, a potential strategy involves purging the system with CO_2 for a determined duration, followed by recirculating all the gas produced using an air pump, and directing it back to the reactor through its diffuser. The experiments were carried out at pH 3, utilizing small size particle active media. The recirculation modalities analyzed are following:

1) 30 minutes of continuous CO_2 flow, no gas recirculation.
2) 3 minutes of continuous CO_2 flow (10% of the original time), plus 27 minutes of gas recirculation (no CO_2 flow).
3) 30 minutes of gas recirculation (no CO_2 flow).

The results obtained in these experiments are presented below:

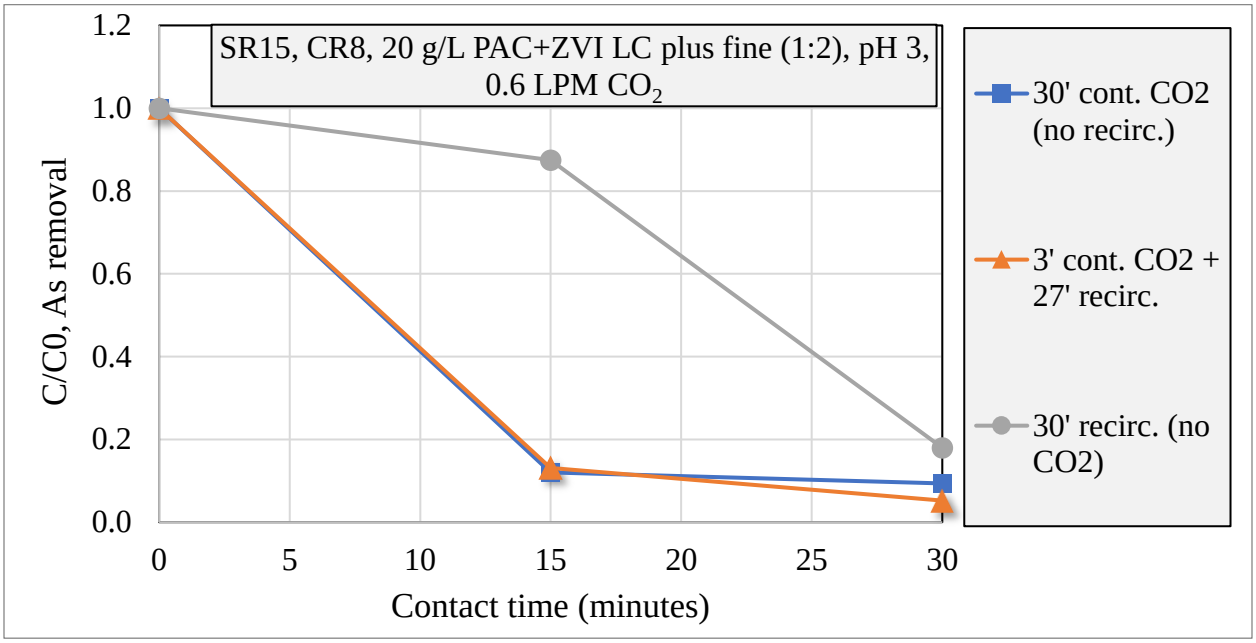

Figure 20 (As) - Comparison of ME treatment results for gas recirculation mode variations: ME reactor using 20 g/L of PAC and ZVI LC plus fine to treat 500 mL of SR15 LFG condensate with 0.6 LPM CO_2 . Initial As concentration: 9.3 ppm

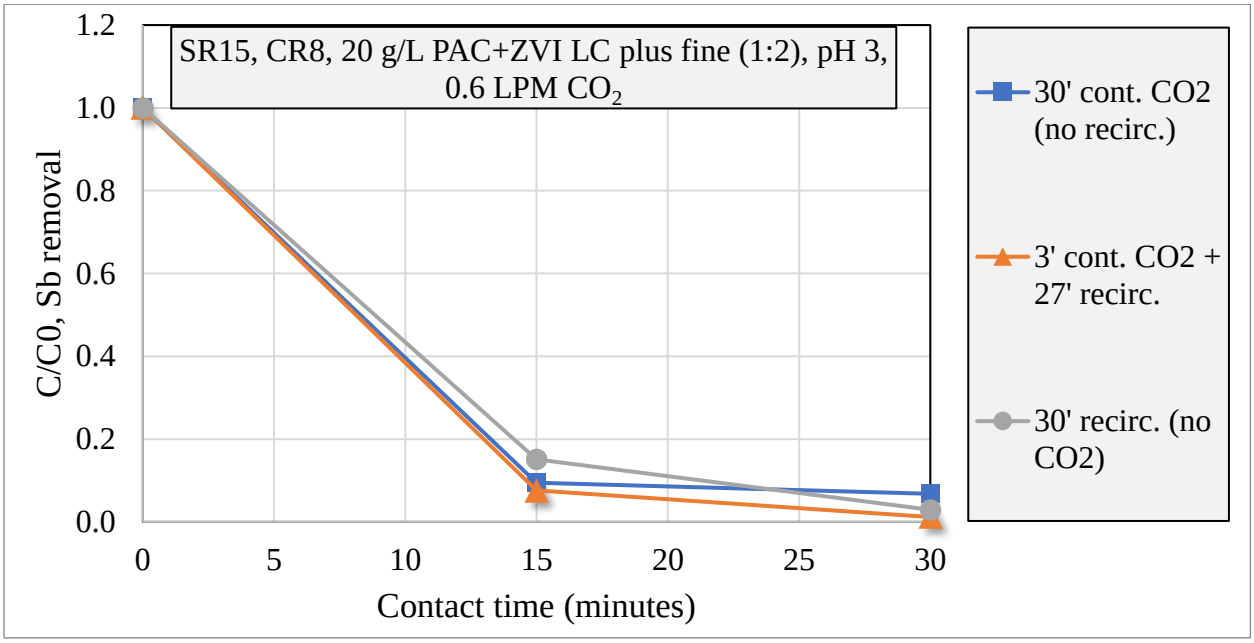

Figure 21 (Sb) - Comparison of ME treatment results for gas recirculation mode variations: ME reactor using 20 g/L of PAC and ZVI LC plus fine to treat 500 mL of SR15 LFG condensate with 0.6 LPM CO_2. Initial Sb concentration: 0.8 ppm

The plots demonstrate that flushing the system with CO_2 for a period of three minutes (10% of the original time) and subsequently recirculating the generated gas yield results are equivalent to those obtained using continuous CO_2 flow throughout the entire treatment duration. This finding is particularly noteworthy since it has the potential to minimize the use of CO_2 while also preventing As volatiles from escaping the system. Conversely, solely recirculating the gas yields comparable outcomes after 30 minutes, albeit at a slower rate compared to using CO_2.

In a further experiment, gas recirculation was performed utilizing active media of larger particle size (GAC and ZVI LC plus), and the results were compared to those obtained using smaller particle size (PAC and ZVI LC plus fine). The experiments were performed with the minimum flow of CO_2 possible due to the client requirement. The recirculation modalities analyzed are following:

1) PAC and ZVI LC plus fine with 30 seconds of continuous CO_2 flow, plus 29.5 minutes of gas recirculation (no CO_2 flow).
2) GAC and ZVI LC plus with 30 seconds of continuous CO_2 flow, plus 29.5 minutes of gas recirculation (no CO_2 flow).
3) GAC and ZVI LC plus with 30 minutes of continuous CO_2 flow, no gas recirculation.

The outcomes are presented below:

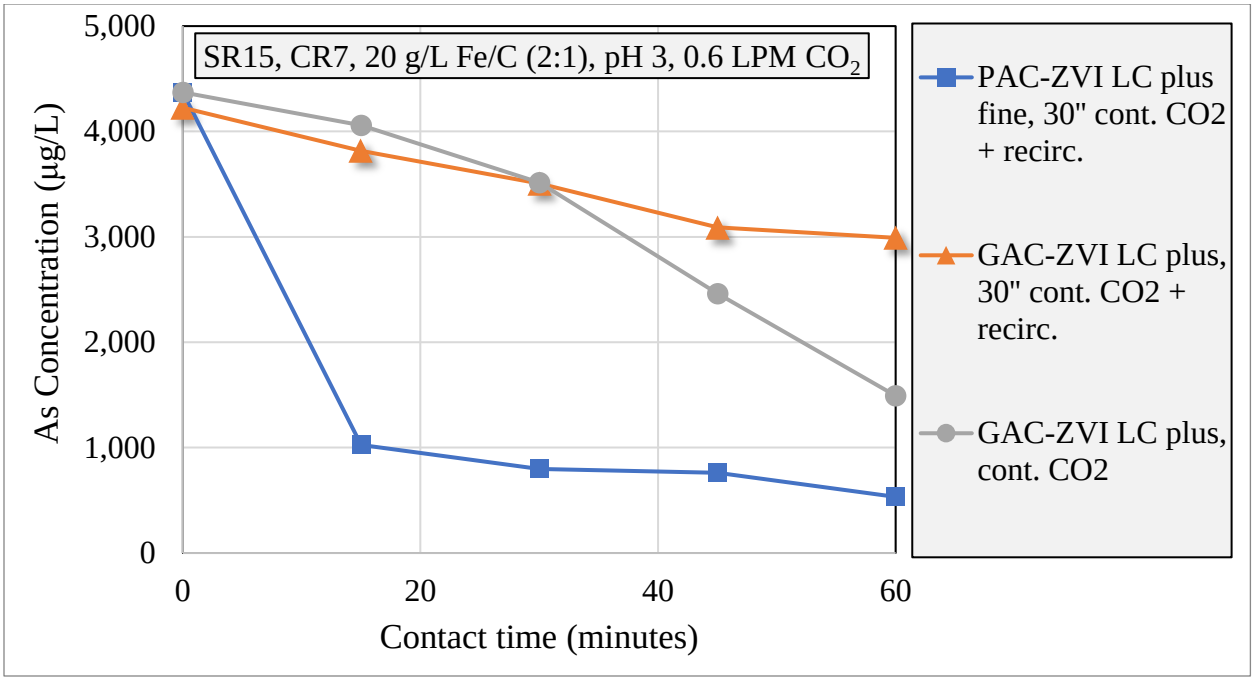

Figure 22 (As) - Comparison of ME treatment results for gas recirculation mode variations: ME reactor using 20 g/L of PAC/GAC and ZVI LC plus fine/ ZVI LC plus to treat 500 mL of SR15 LFG condensate with 0.6 LPM CO_2

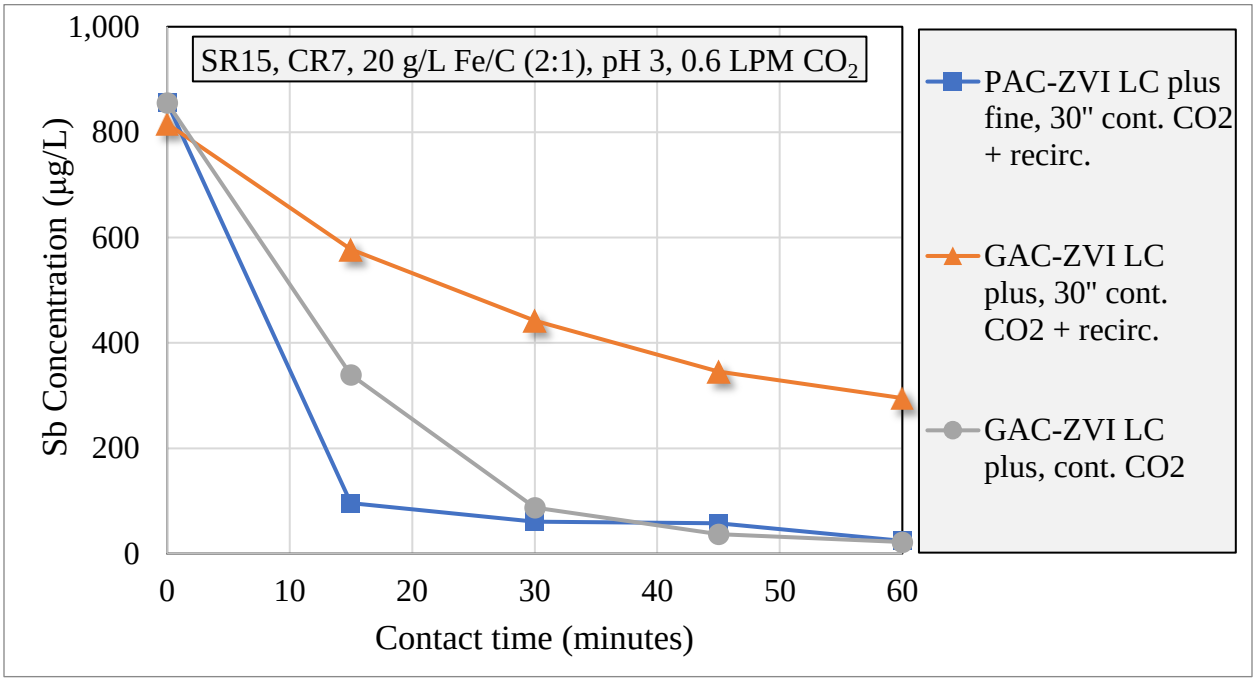

Figure 23 (Sb) - Comparison of ME treatment results for gas recirculation mode variations: ME reactor using 20 g/L of PAC/GAC and ZVI LC plus fine/ ZVI LC plus to treat 500 mL of SR15 LFG condensate with 0.6 LPM CO_2

Finally, the same gas recirculation experiments were conducted in the 3 L size batch column reactor. The findings are presented below.

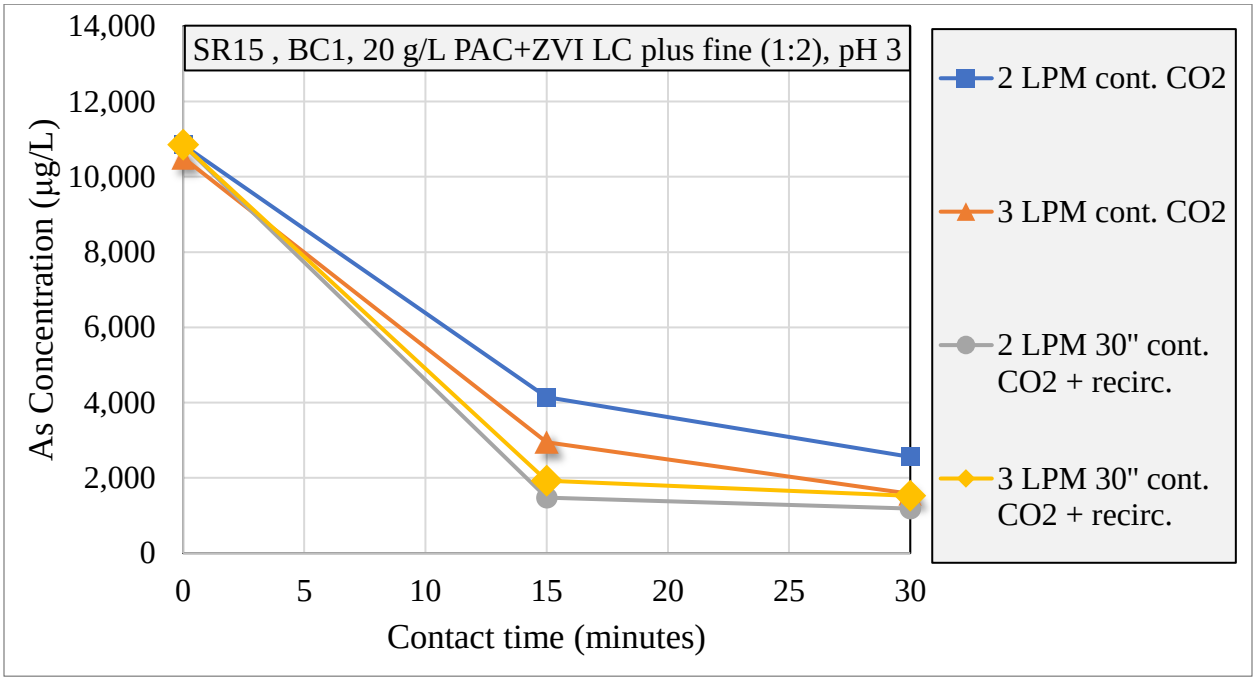

Figure 24 (As) - Comparison of ME treatment results for gas recirculation mode variations: ME reactor using 20 g/L of PAC and ZVI LC plus fine to treat 3 L of SR15 LFG condensate with 2 and 3 LPM CO_2

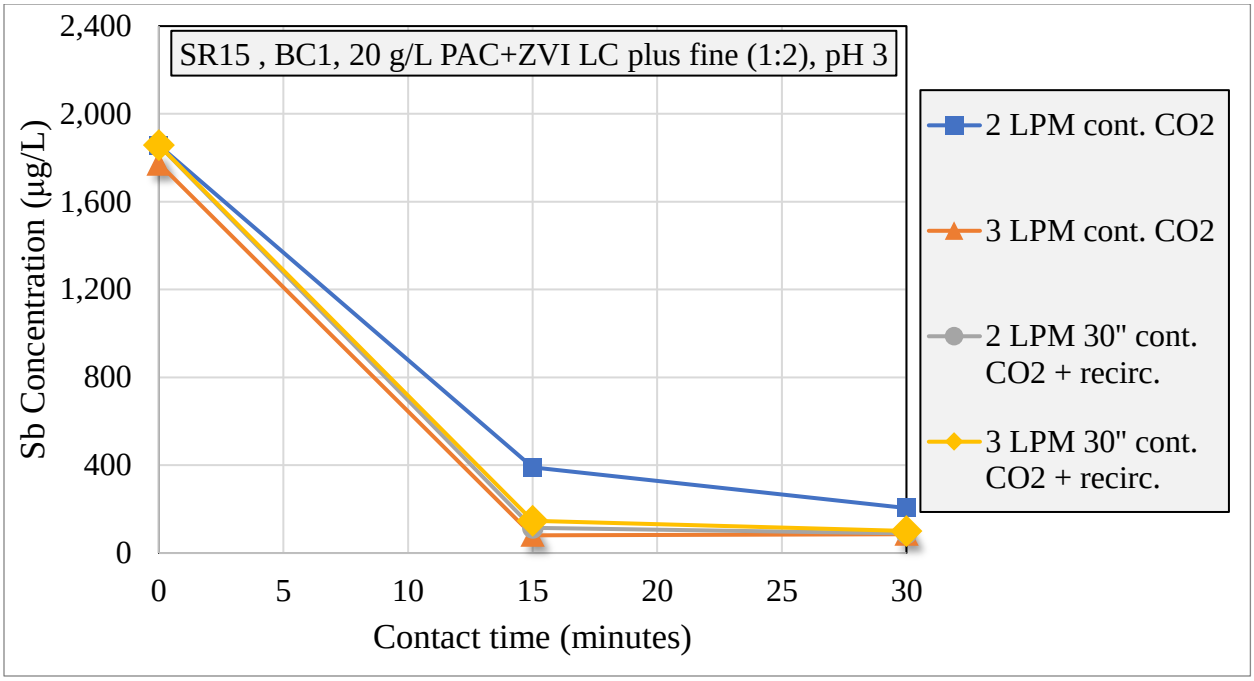

Figure 25 (Sb) - Comparison of ME treatment results for gas recirculation mode variations: ME reactor using 20 g/L of PAC and ZVI LC plus fine to treat 3 L of SR15 LFG condensate with 2 and 3 LPM CO_2

The plots presented above indicate that all the tested modes of CO_2 carrier gas recirculation exhibit comparable removal efficiency for both arsenic and antimony. Notably, the gas recirculation experiments resulted in over 75% removal of arsenic after 30 minutes of treatment, and >89% removal of antimony. These outcomes suggest that gas recirculation should be prioritized over continuous CO_2, enabling operational cost optimization, and simplifying the process. Additionally, there is no need to employ potassium permanganate or sodium sulfite after the reactor to capture arsine volatiles, if they are formed, since the mode of gas recirculation in ME treatment eliminates this requirement.

4.4. Effects of variation of ZVI activation, ZVI/AC weight ratios, and active media dosing and particle sizes on As removal

The utilization of reagents during the treatment process can constitute a considerable proportion of the operational and capital expenses of a plant. The storage and handling of active media (PAC or GAC, and ZVI) can affect the design and size of the equipment, further increasing capital costs. Thus, it is important to determine the best possible combination of active media particle size, proportions of weights of ZVI and activated carbon, dosages, and activation method. This thesis examined these factors to achieve the most efficient and cost-effective arsenic-antimony removal process.

4.4.1. Effects of ZVI activation

The initial experiment aimed to assess the effectiveness of ZVI activation and comparing it with no ZVI activation prior to the introduction of the ZVI phase in the reactor. The methods tested were as follows:

1. The ZVI was placed in a stainless-steel strainer and rinsed for 1 minute with 0.1 M HCl. Then, the wet ZVI was rinsed with 0.001 M HCl for 1 minute. The ZVI was then drained and then added when still wet to the sample in the column reactor. This method was tested using pH 4 during the reaction.
2. No activation method was used, and dry ZVI was added directly to the column reactor. This method was tested using three different pH during the reaction.

The hypothesis was that if the surface scales impeding ZVI activity are eliminated outside the reactor (ex-situ activation), oxygen can oxidize the surface while ZVI is being transferred into the reactor. This situation can be detrimental to the process, as it would result in a reduced amount of

available ZVI to interact with the arsenic compounds. The theory to prove is that activating ZVI in situ would be the best approach to prevent its oxidation. The study yielded the following results:

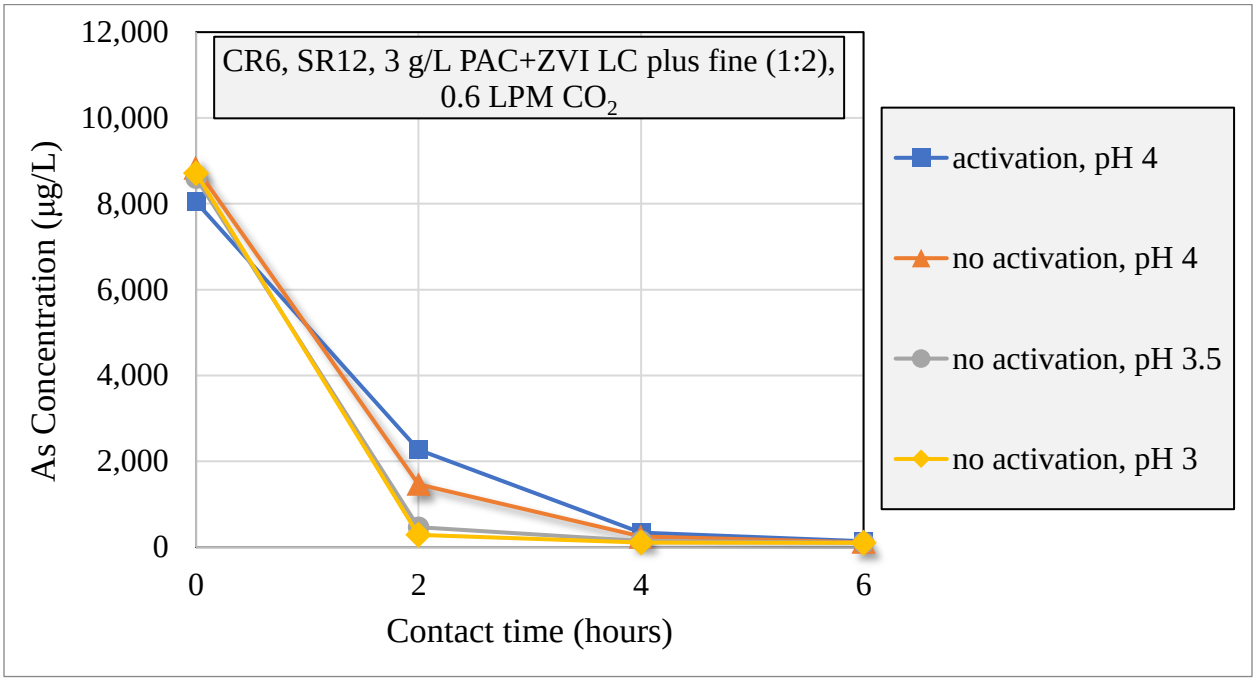

Figure 26 (As) - Comparison of ME treatment results for ZVI activation modes variations at different pH: rinsed strainer activation versus no activation at pH 3, 3.5, and 4 in a 500 mL ME reactor to treat SR12 LFG condensate using 3 g/L PAC and ZVI LC plus fine

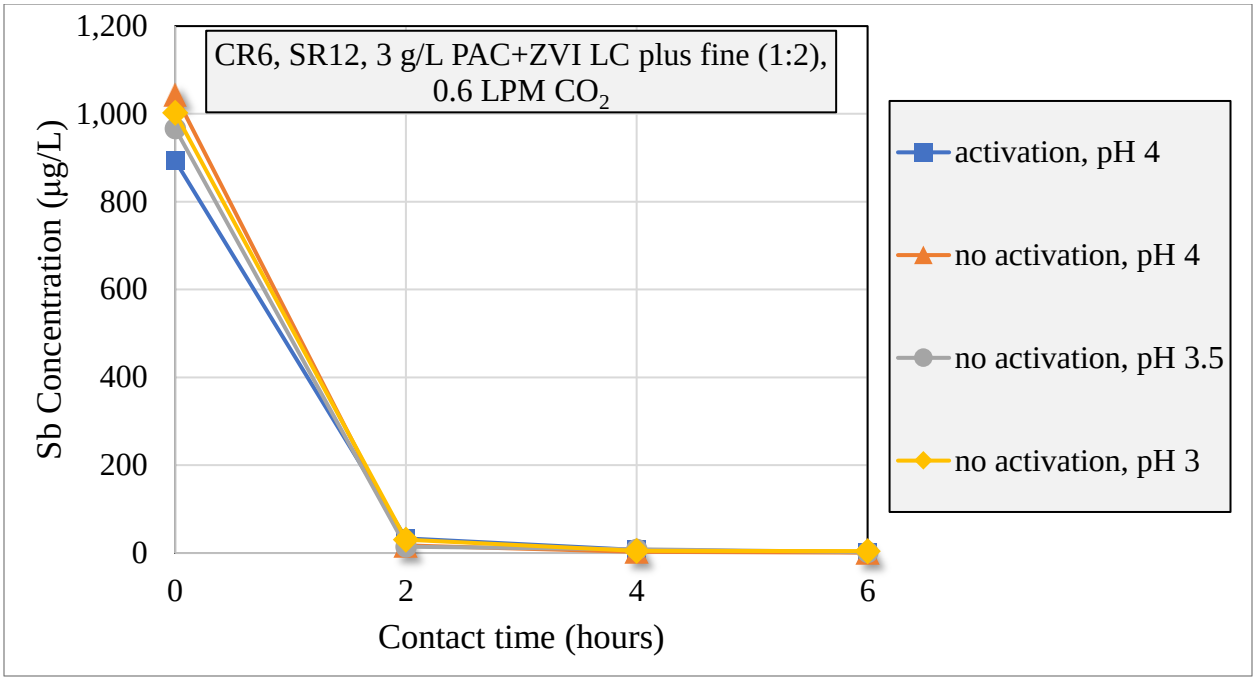

Figure 27 (Sb) - Comparison of ME treatment results for ZVI activation modes variations at different pH: rinsed strainer activation versus no activation at pH 3, 3.5, and 4 in a 500 mL ME reactor to treat SR12 LFG condensate using 3 g/L PAC and ZVI LC plus fine

The results indicate that non-activated ZVI demonstrated equal or superior performance in the removal of arsenic and antimony compared to activated ZVI under the same experimental conditions. This observation highlights that when ZVI is activated in situ, the oxidation of ZVI can be effectively prevented during the process, leading to the formation of a greater number of As and Sb complexes within the column reactor. These results are significant in elucidating that the activation of ZVI can occur in situ within the column before the subsequent ME reactions take place.

The findings also suggest that a more acidic environment can enhance, although not prominently, the efficiency of contaminant removal, as the ZVI self-activates within the reactor. The elimination of the activation process can significantly streamline operations and reduce both capital and

operational costs. As a result, subsequent experiments were carried out using non-activated ZVI that underwent activation in situ, once introduced in the ME reactor.

4.4.2. Effects of ZVI/PAC weight ratio

To investigate the impact of the ratio of weight of ZVI/activated carbon media, an experiment was conducted using a dosage of 3 g/L of PAC and ZVI LC plus fine. The experiment evaluated various ratios between the two materials, including an absence of PAC (i.e., only ZVI) at a ratio of 0:1. The study yielded the following results:

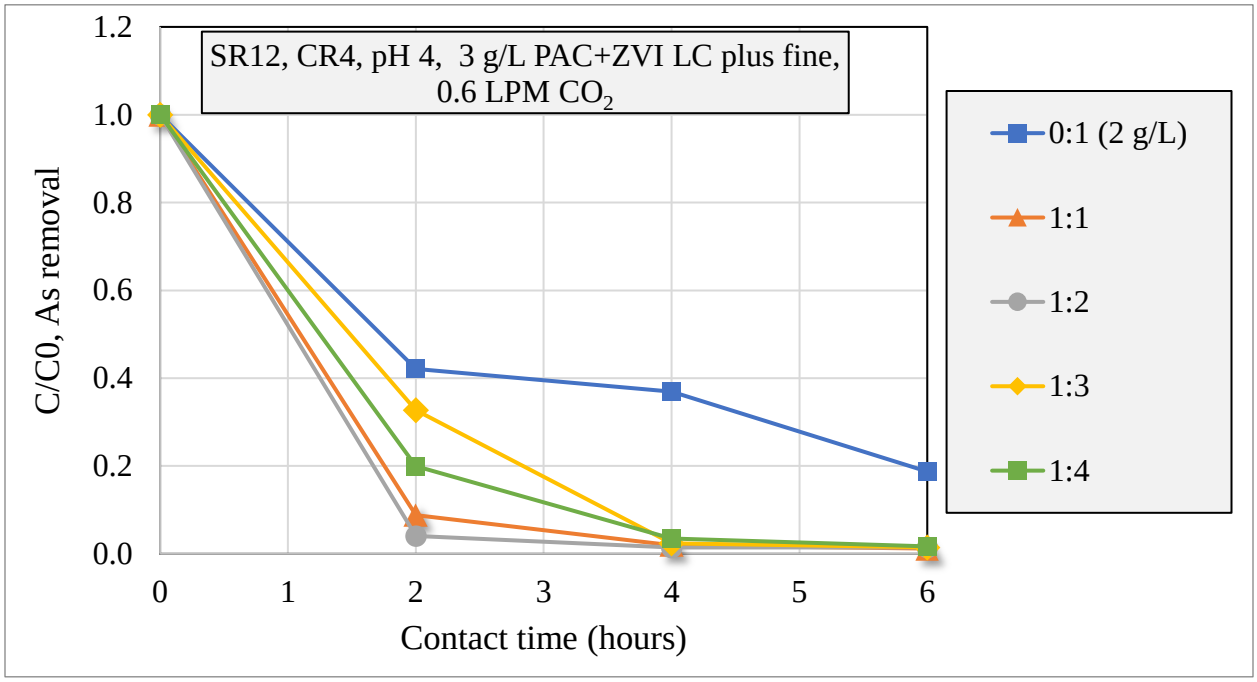

Figure 28 (As) - Comparison of ME treatment results for PAC/ZVI weight ratio variations: 0:1, 1:1, 1:2, 1:3, and 1:4 added to a 500 mL ME reactor to treat SR12 LFG condensate using 3 g/L PAC and ZVI LC plus fine and CO_2 flow rate of 0.6 LPM. Initial As concentration: 6.5 ppm

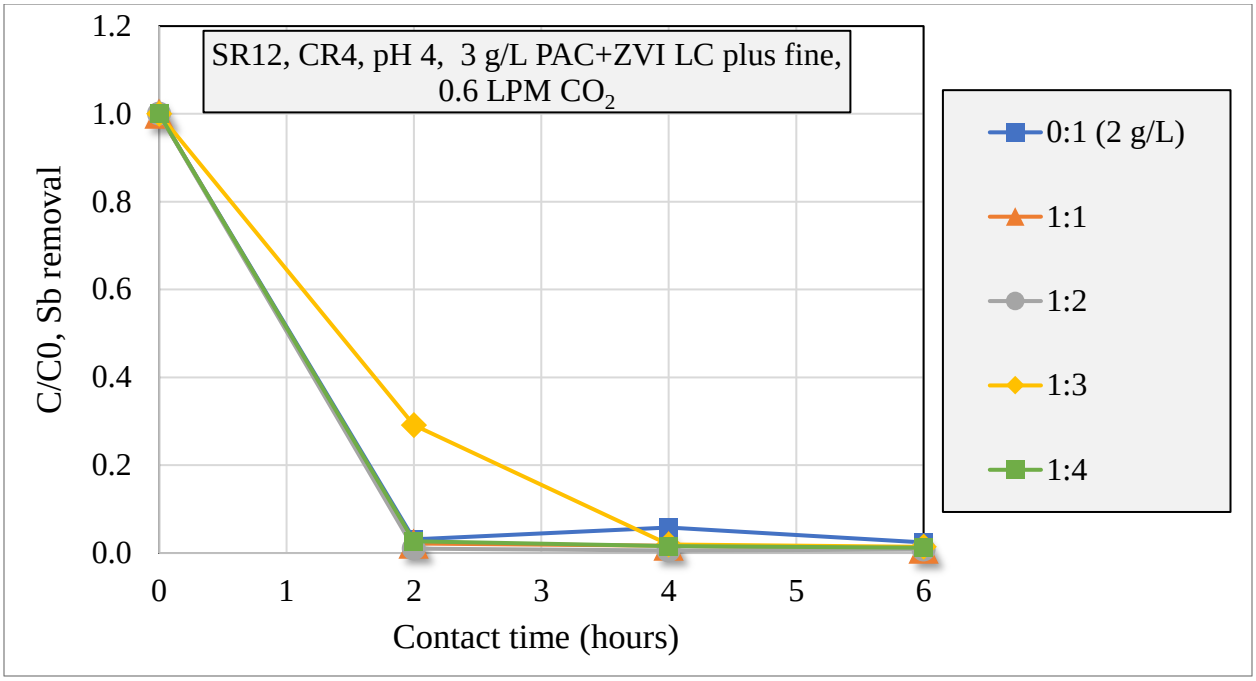

Figure 29 (Sb) - Comparison of ME treatment results for PAC/ZVI weight ratio variations: 0:1, 1:1, 1:2, 1:3, and 1:4 added to a 500 mL ME reactor to treat SR12 LFG condensate using 3 g/L PAC and ZVI LC plus fine and CO_2 flow rate of 0.6 LPM. Initial Sb concentration: 0.7 ppm

The results demonstrate that the combination of PAC and ZVI always exhibited greater removal efficiency of arsenic than using ZVI only. The performance of all other ratios analyzed was found to be relatively similar, with a slightly better performance for PAC: ZVI LC plus fine weight ratios of 1:1 and 1:2. Considering operational convenience, further experiments were conducted using a ratio of 1:2 for the PAC to ZVI combination.

4.4.3. Effects of ZVI/PAC particle size

The particle size of the active media is a crucial factor in the operational convenience of any treatment processes. Smaller particles may be more challenging to separate from the sample, leading to increased expenses for filtration or sedimentation after treatment. Additionally, small particles can generate more particulates during transport and may adhere more readily to equipment and instruments, resulting in additional operational complications. Therefore, it is

essential to examine the efficacy of larger particle sizes for active media in water treatment. In the next set of experiments, the effects of varying active media particle sizes on the microelectrolysis treatment performance were evaluated. For the study, the following particle sizes were used (mesh distribution in chapter 3.2.1):

- Powdered activated carbon – PAC: smaller AC particle size used (mesh>500, diameter<50 µm).
- Granular activated carbon 12-40 mesh - GAC: larger AC particle size used (diameter between ~638 and ~1,700 µm, as shown in Figure *9*).
- ZVI LC plus fine: smaller ZVI particle size used (64% of the particles have mesh 140, diameter ~ 157 µm, as shown in Figure *7*).
- ZVI LC plus: larger ZVI particle size used (53% of the particles have mesh 60, diameter ~ 338 µm, as shown in Figure *7*).

The study yielded the following results:

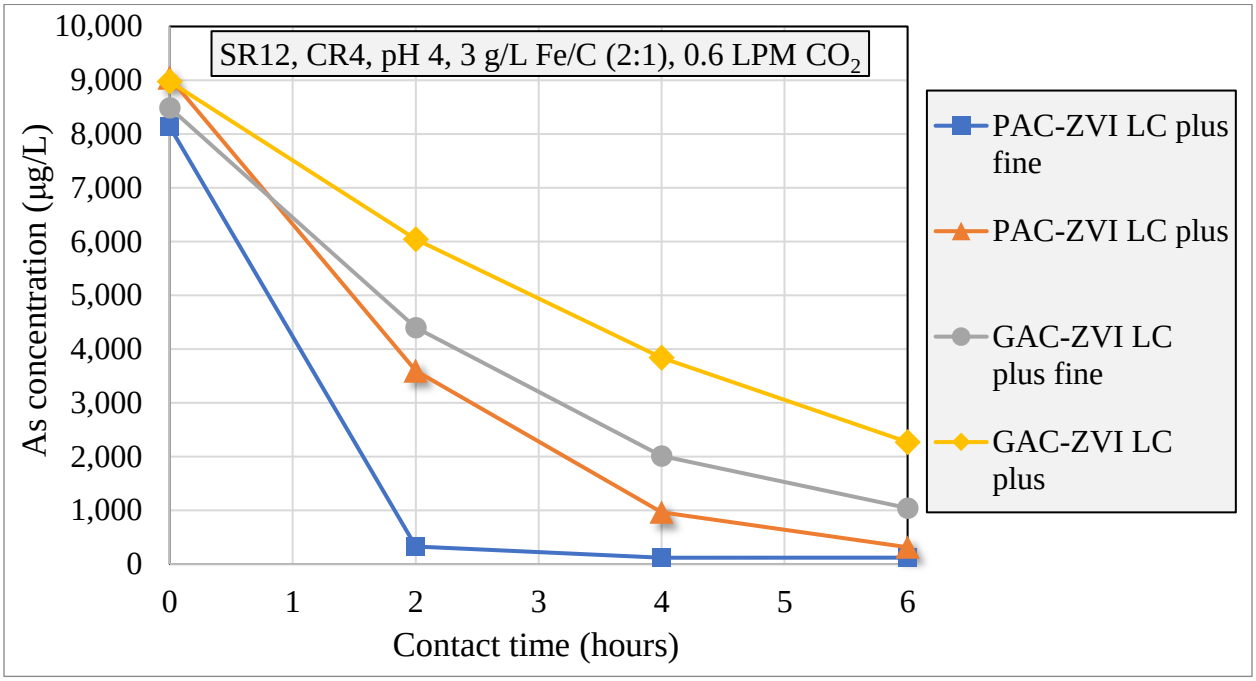

Figure 30 (As) - Comparison of ME treatment results for active media particle size variations: PAC/GAC variations, and ZVI LC plus / ZVI LC plus fine variations, added to a 500 mL ME reactor to treat SR12 LFG condensate using 3 g/L of active media and CO_2 flow rate of 0.6 LPM

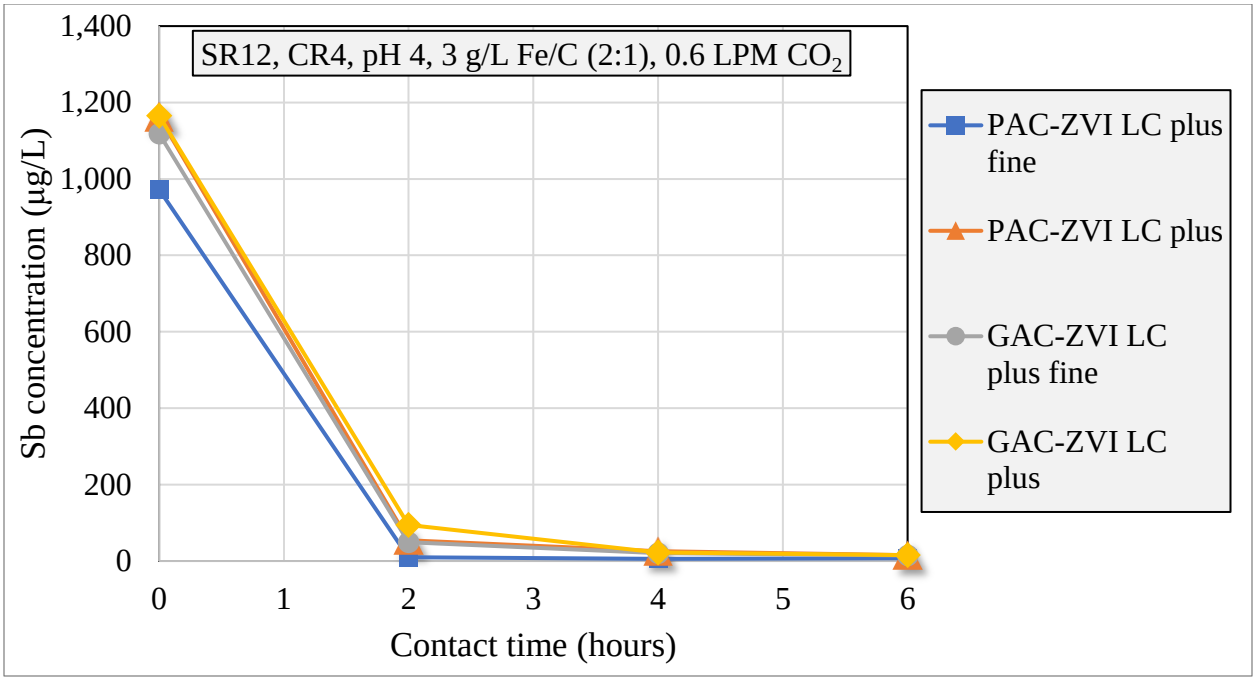

Figure 31 (Sb) - Comparison of ME treatment results for active media particle size variations: PAC/GAC variations, and ZVI LC plus / ZVI LC plus fine variations, added to a 500 mL ME reactor to treat SR12 LFG condensate using 3 g/L of active media and CO_2 flow rate of 0.6 LPM

The experimental results shown above indicate that, as expected, smaller particles of the active media demonstrate superior removal efficiency for arsenic compared to larger particles. However, larger particle sizes still exhibited significant removal efficiency, with up to 75% removal efficiency for arsenic and 99% removal efficiency for antimony. These findings are highly encouraging, particularly given the low amount of active media used in the experiments. Nonetheless, additional experiments with larger amounts of active media are necessary to further evaluate the use of larger size.

Based on the prior findings, several experiments were conducted utilizing higher doses of both small and large particle active media.

4.4.4. Effects of ZVI/PAC doses

The initial set of experiments involved the comparison of different dosages of small size particle active media with various landfill condensate samples. The main goal of bringing the dosage analysis back was to decrease the treating times, and to ensure the As removal of SR14, a high initial As concentration sample round.

The primary objective of reintroducing the dosage analysis in this thesis research was to reduce the treatment duration while ensuring effective removal of arsenic from all available sample rounds, including SR14, a sample with a high initial concentration of arsenic. These comparisons were performed over a shorter period of time, taking into account the remarkable arsenic and antimony removal efficiencies achieved. The results of these experiments are presented below.

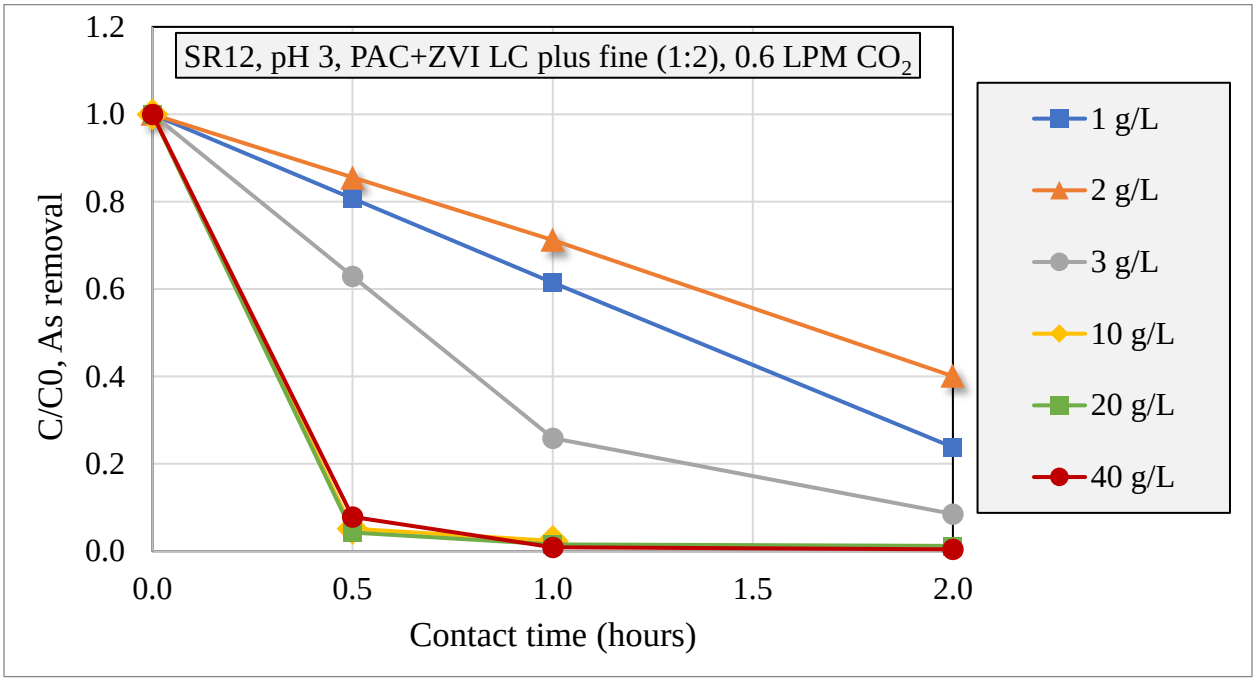

Figure 32 (As) - Comparison of ME treatment results for active media dosing variations: ME reactor using from 1 to 40 g/L of PAC and ZVI LC plus fine to treat 500 mL of SR12 LFG condensate. Initial As concentration: 6.5 ppm

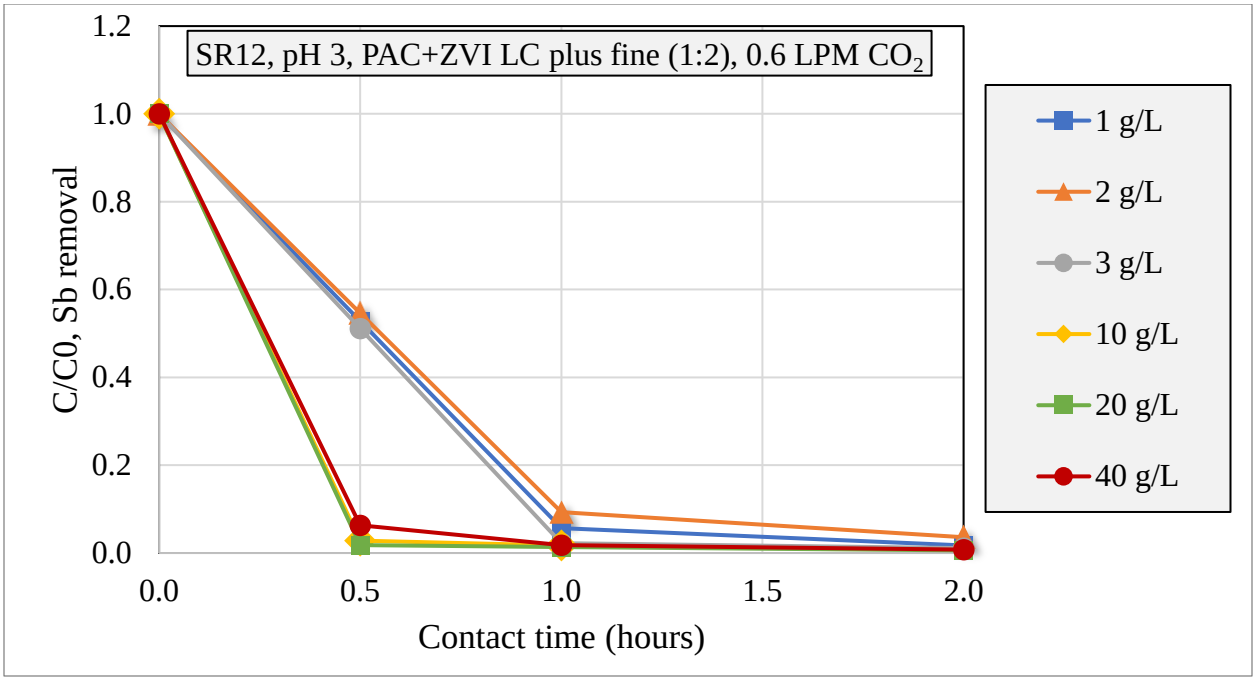

Figure 33 (Sb) - Comparison of ME treatment results for active media dosing variations: ME reactor using from 1 to 40 g/L of PAC and ZVI LC plus fine to treat 500 mL of SR12 LFG condensate. Initial Sb concentration: 0.7 ppm

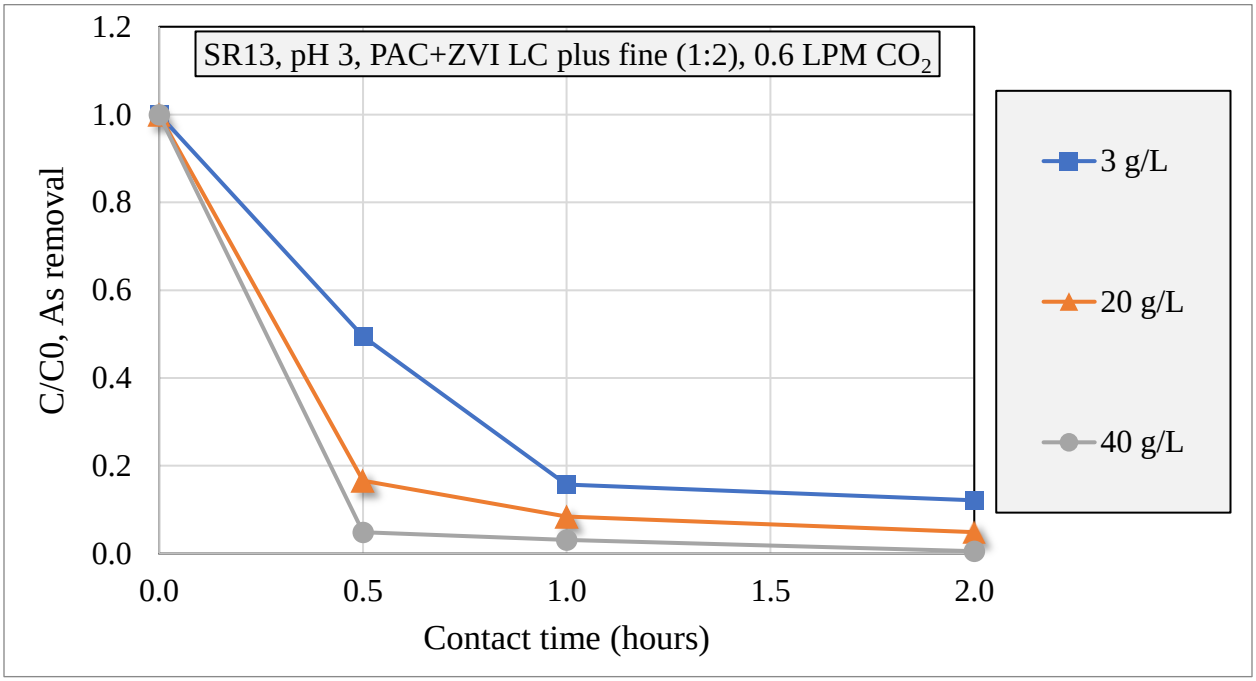

Figure 34 (As) - Comparison of ME treatment results for active media dosing variations: ME reactor using from 3 to 40 g/L of PAC and ZVI LC plus fine to treat 500 mL of SR13 LFG condensate. Initial As concentration: 8.1 ppm

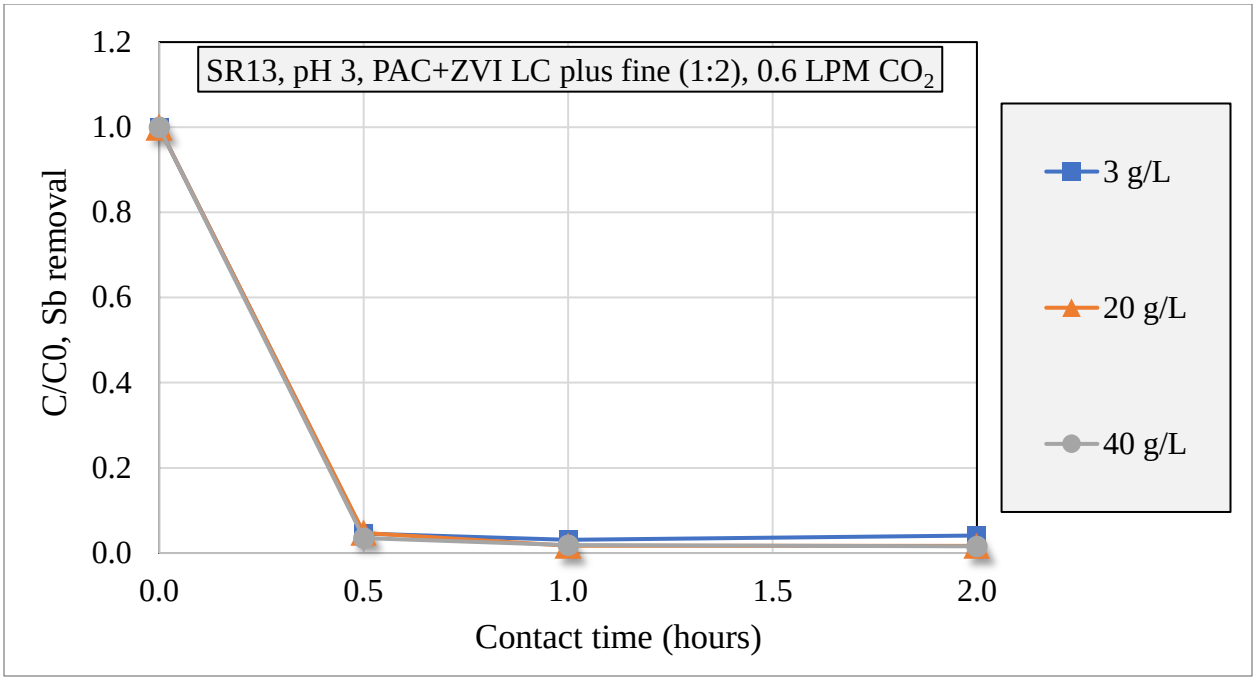

Figure 35 (Sb) - Comparison of ME treatment results for active media dosing variations: ME reactor using from 3 to 40 g/L of PAC and ZVI LC plus fine to treat 500 mL of SR13 LFG condensate. Initial Sb concentration: 0.4 ppm

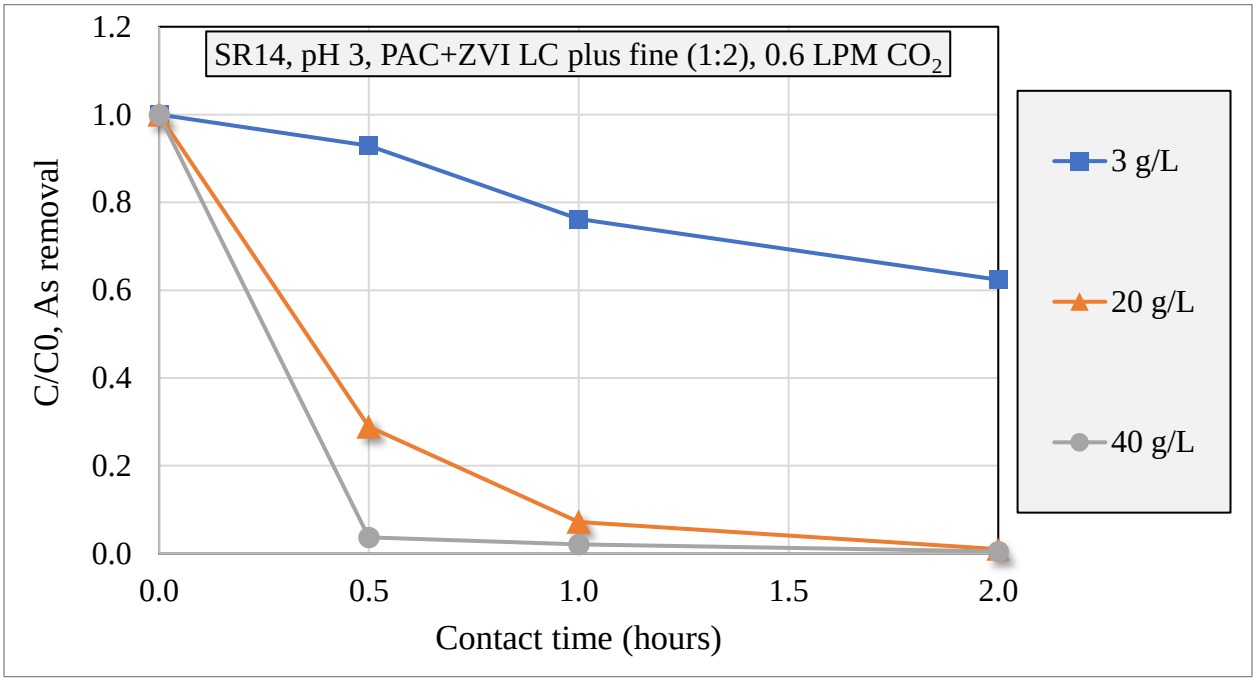

Figure 36 (As) - Comparison of ME treatment results for active media dosing variations: ME reactor using from 3 to 40 g/L of PAC and ZVI LC plus fine to treat 500 mL of SR14 LFG condensate. Initial As concentration: 200 ppm

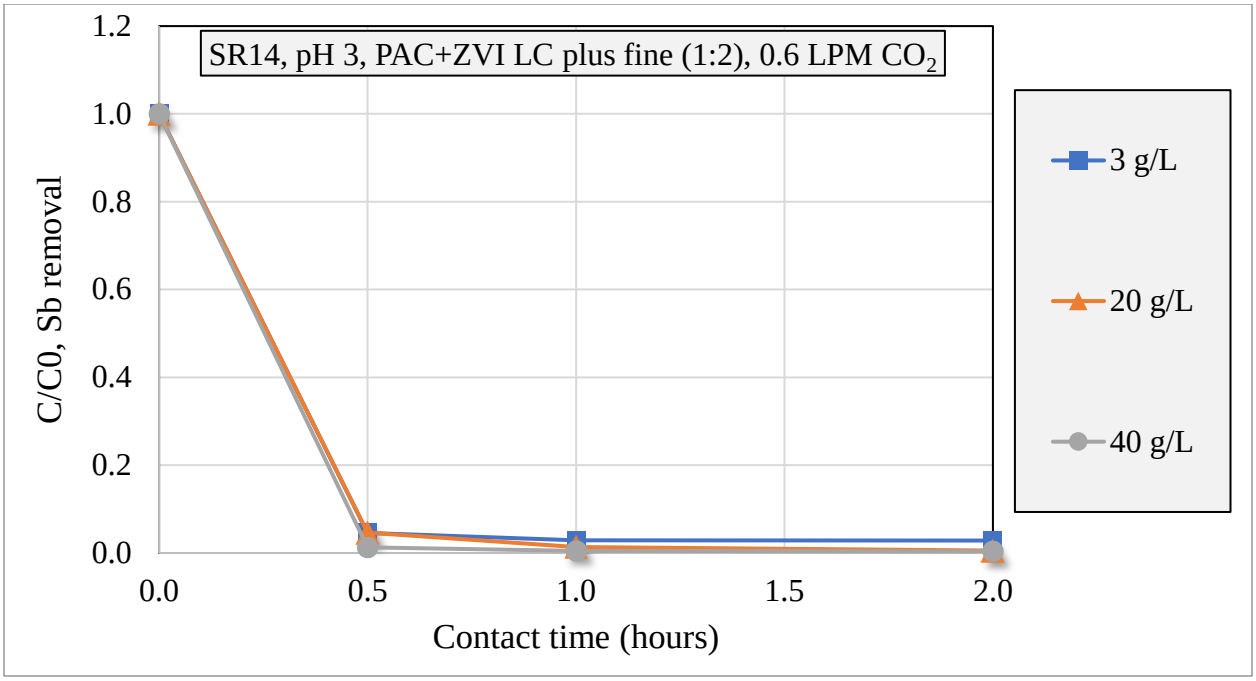

Figure 37 (Sb) - Comparison of ME treatment results for active media dosing variations: ME reactor using from 3 to 40 g/L of PAC and ZVI LC plus fine to treat 500 mL of SR14 LFG condensate. Initial Sb concentration: 9.7 ppm

The plots presented above demonstrate that an increase in the active media doses results in a corresponding enhancement in arsenic and antimony removal efficiency. Notably, for active media dosages exceeding 10 g/L, the removal efficiency is markedly high within the initial 30 minutes. This outcome is significant as it translates to substantial gas and energy savings by reducing the treatment time from six hours to 30 or 60 minutes. In addition, even for the sample SR14, which exhibits extremely high initial concentrations of arsenic and antimony, a active media dosage of 20 g/L proves effective within one hour Based on these findings, all subsequent experiments employed a active media dosage of 10 g/L or higher.

Building on prior findings, experiments were conducted utilizing higher dosages of large particle size active media (ZVI LC plus and GAC). The resulting outcomes are presented and compared below:

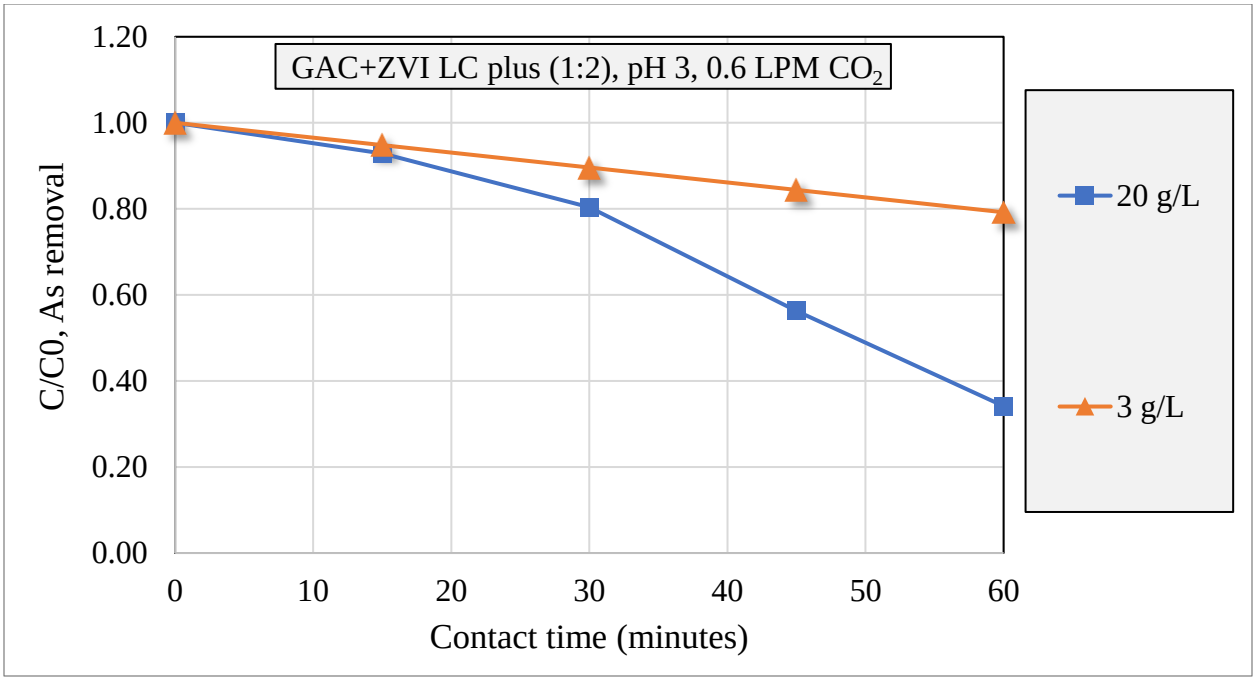

Figure 38 (As) - Comparison of ME treatment results for active media dosing variations: ME reactor using from 3 to 20 g/L of GAC and ZVI LC plus to treat 500 mL of SR12 and SR15 LFG condensate. Initial As concentration: 6.5 ppm

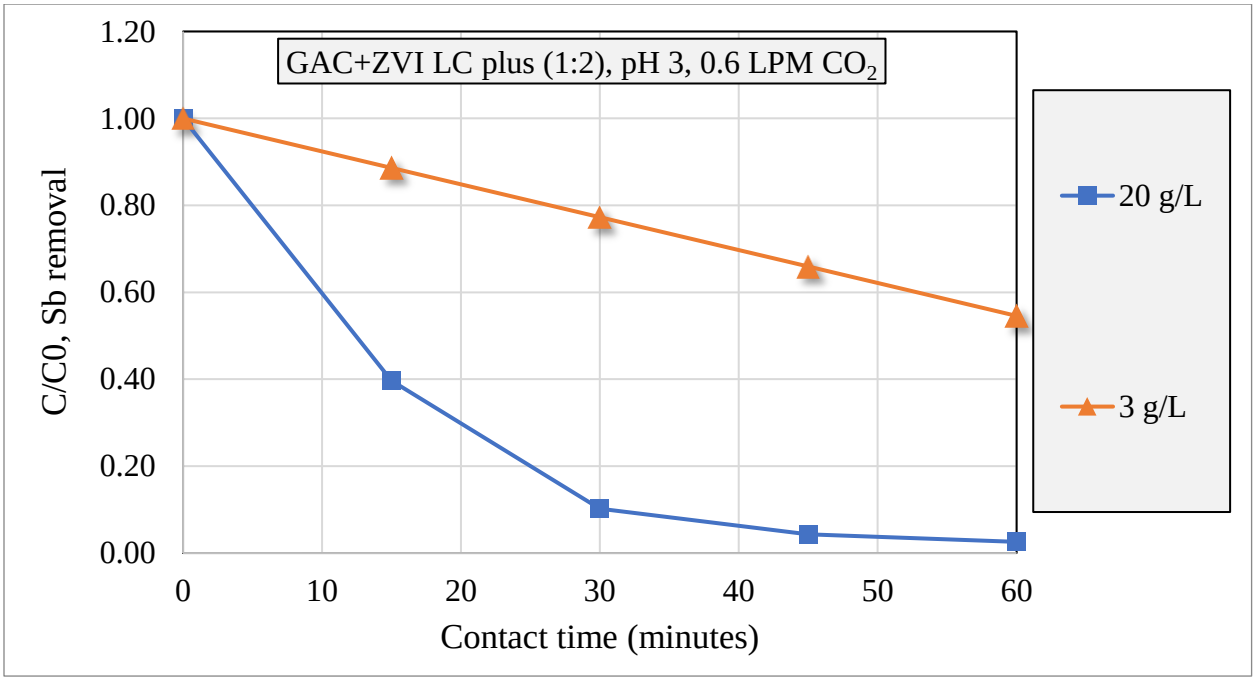

Figure 39 (Sb) - Comparison of ME treatment results for active media dosing variations: ME reactor using from 3 to 20 g/L of GAC and ZVI LC plus to treat 500 mL of SR12 and SR15 LFG condensate. Initial Sb concentration: 0.7 ppm

The results suggest that using 20 g/L of active media with a larger particle size (GAC and ZVI LC plus) instead of 3 g/L leads to significantly improved and rapid removal of arsenic and antimony. Arsenic removal increased from 20% to 65%, and antimony removal from 45% to 97%. These outcomes demonstrate a substantial advancement in the efficacy of the treatment process. The results suggest that the total surface area of the active media plays a significant role in the As/Sb removal process. However, further analysis considering different total surface areas will be conducted in future studies.

4.5. Repeated sample loading cycles (active media reuse)

When utilizing a higher dosage of active media for the reaction, additional optimization may be required to avoid generating excessive solid waste. One option that should be investigated is the reutilization of the active media to treat several sequential batches of the LFG condensate.

The process used on the experiments described below involves allowing the system to decant for ten minutes following treatment, removing the treated effluent, and adding new sample while retaining the used active media in the reactor's volume. The initial set of experiments utilized two of the three higher dosages of active media that achieved faster As/Sb removal: 10 and 20 g/L of PAC and ZVI LC plus fine and three consecutive loading cycles. The results of these measurements are presented below:

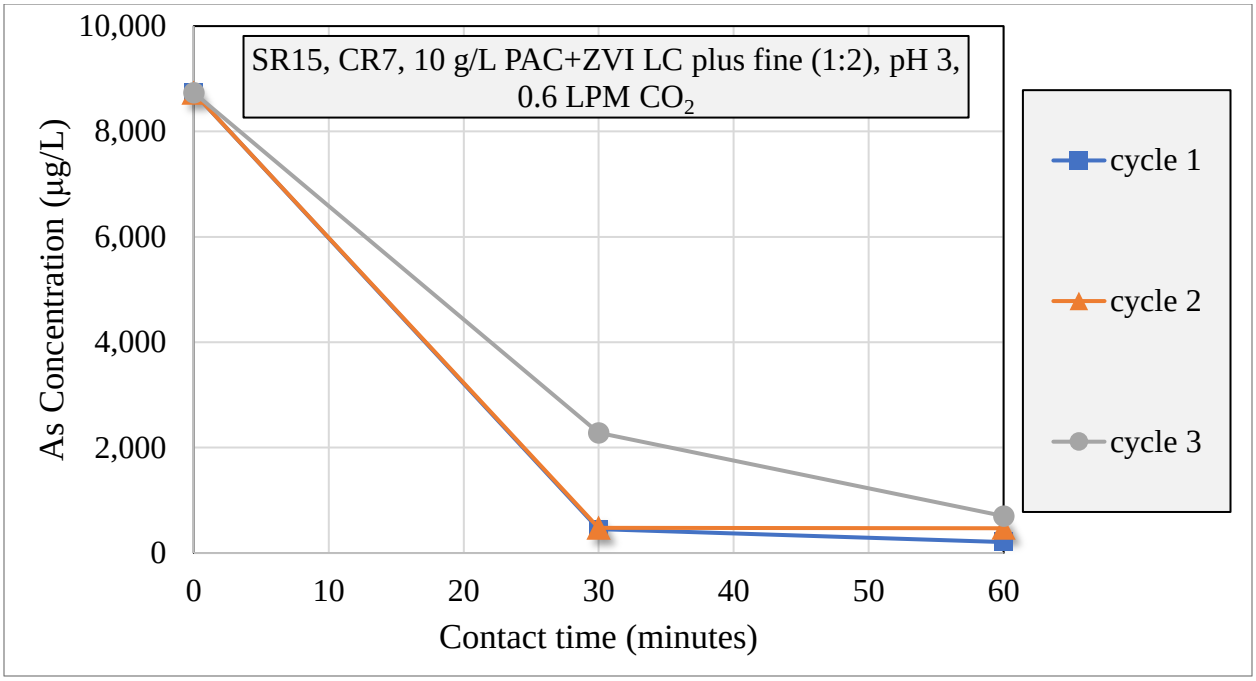

Figure 40 (As) - Comparison of ME treatment results for repeated sample loading cycles: 3 cycles using 10 g/L of PAC and ZVI LC plus fine to treat 3 loads of 500 mL SR15 LFG condensate with 0.6 LPM CO_2

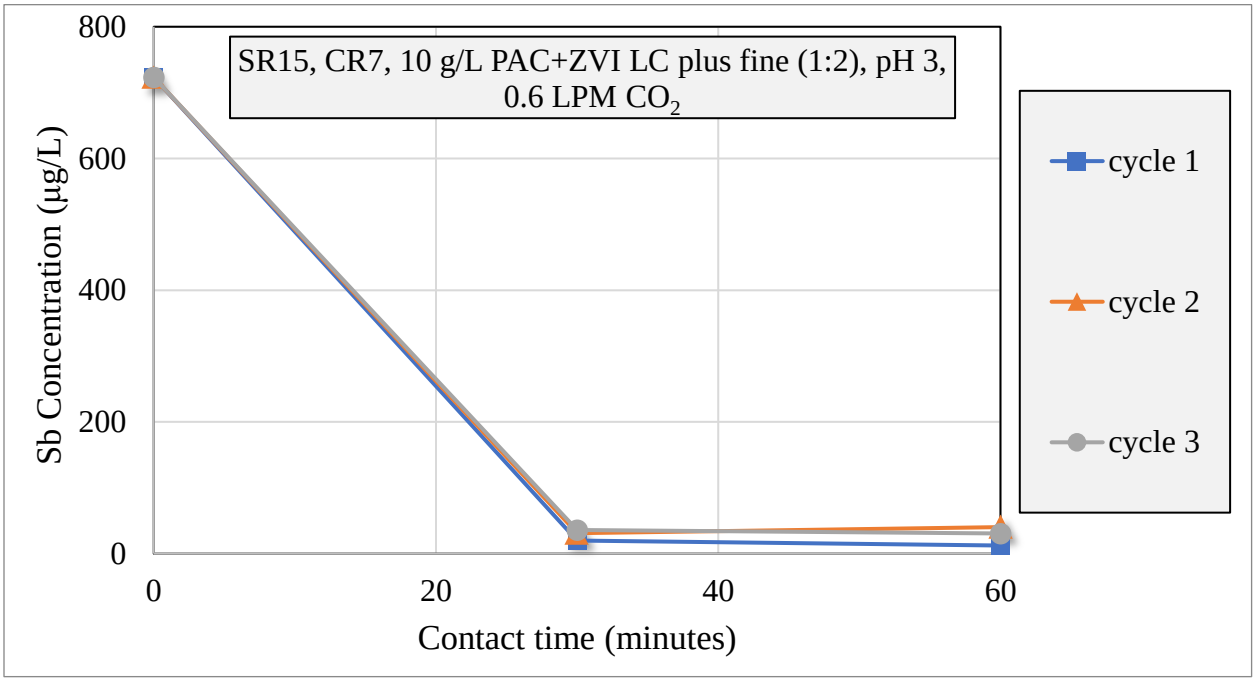

Figure 41 (Sb) - Comparison of ME treatment results for repeated sample loading cycles: 3 cycles using 10 g/L of PAC and ZVI LC plus fine to treat 3 loads of 500 mL SR15 LFG condensate with 0.6 LPM CO_2

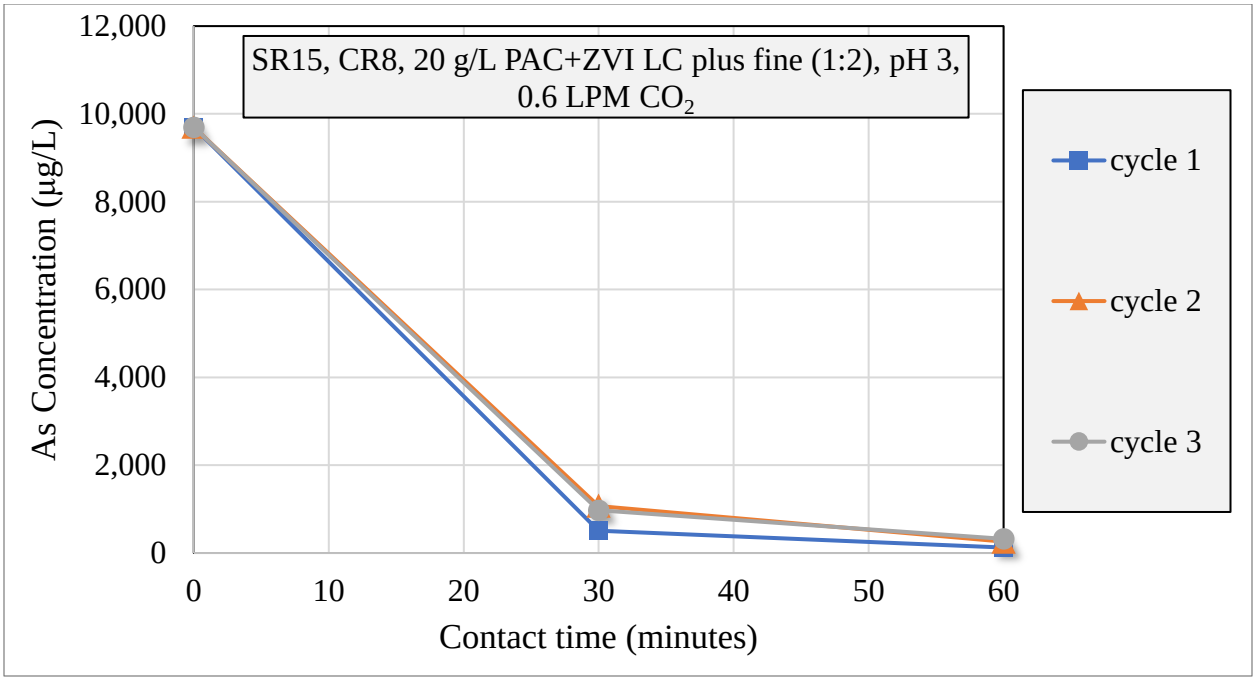

Figure 42 (As) - Comparison of ME treatment results for repeated sample loading cycles: 3 cycles using 20 g/L of PAC and ZVI LC plus fine to treat 3 loads of 500 mL SR15 LFG condensate with 0.6 LPM CO_2

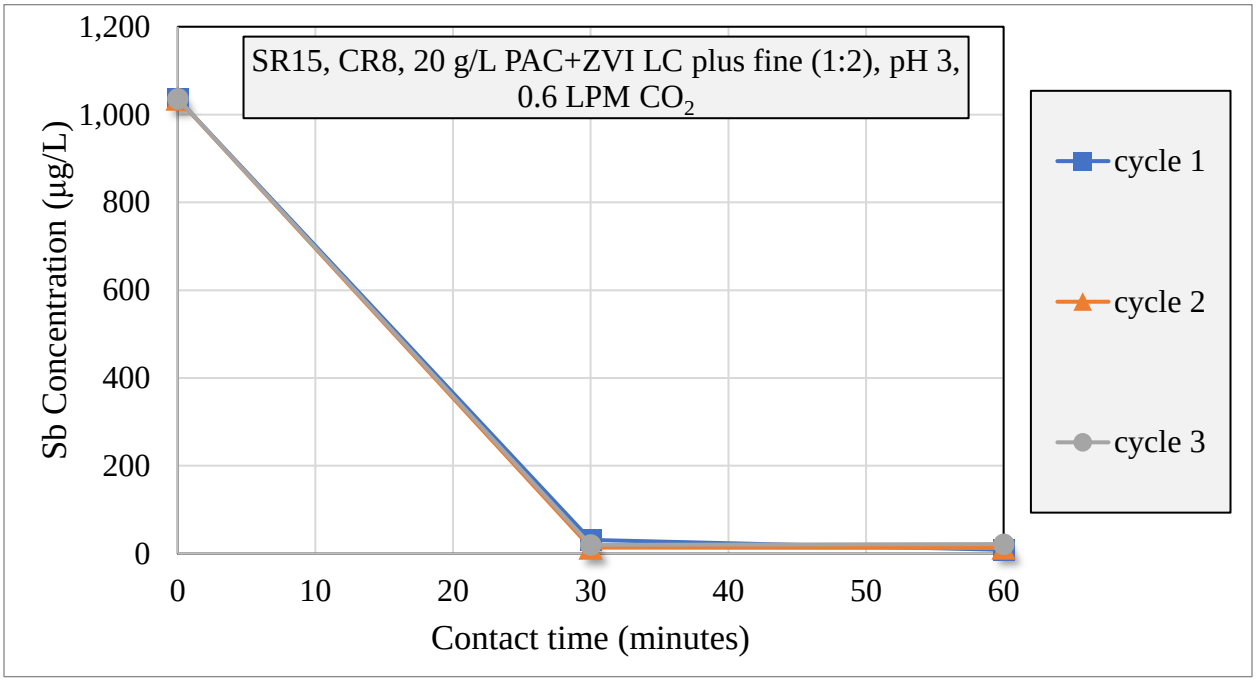

Figure 43 (Sb) - Comparison of ME treatment results for repeated sample loading cycles: 3 cycles using 20 g/L of PAC and ZVI LC plus fine to treat 3 loads of 500 mL SR15 LFG condensate with 0.6 LPM CO_2

For the 10 and 20 g/L dosages, the experiments utilizing three cycles effectively removed both arsenic and antimony. Specifically, removal of arsenic exceeded 92% in both cases, while removal of antimony exceeded 94%. The data of the experiments on active media reutilization are quite promising as they suggest the potential to reduce operational costs and enhance the process's operability.

The successful removal of As/Sb achieved in the three cycles through the reuse of high dosages of active media (ZVI and PAC) raises the possibility of using solely ZVI at higher dosages and cycling it. This line of experimentation is prompted by the promising results obtained in Figure 28 and Figure 29, where 2 g/L of ZVI alone achieved more than 60% removal within a 2-hour timeframe. If successful, these results would present an excellent opportunity to eliminate powdered activated carbon from the process, which could simplify the treatment process and potentially reduce operational and capital costs. The findings are illustrated below.

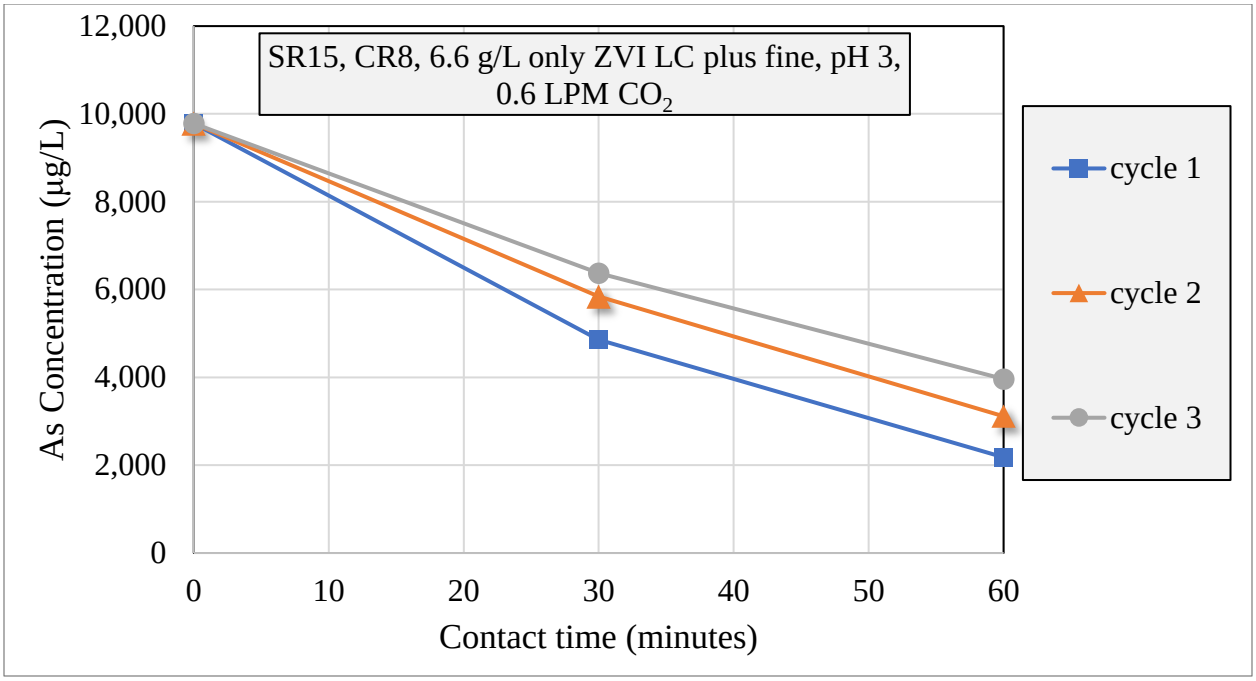

Figure 44 (As) - Comparison of ME treatment results for repeated sample loading cycles: 3 cycles using 6.6 g/L of ZVI LC plus fine only, to treat 3 loads of 500 mL SR15 LFG condensate with 0.6 LPM of continuous CO_2

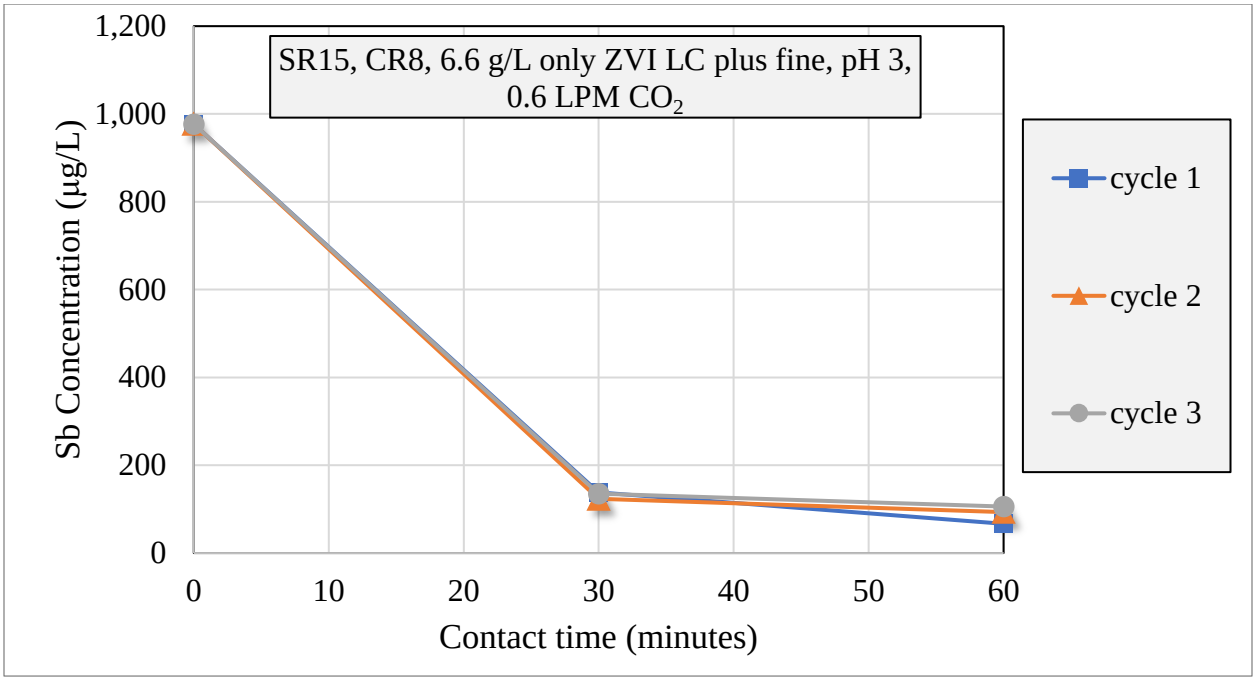

Figure 45 (Sb) - Comparison of ME treatment results for repeated sample loading cycles: 3 cycles using 6.6 g/L of ZVI LC plus fine only, to treat 3 loads of 500 mL SR15 LFG condensate with 0.6 LPM of continuous CO_2

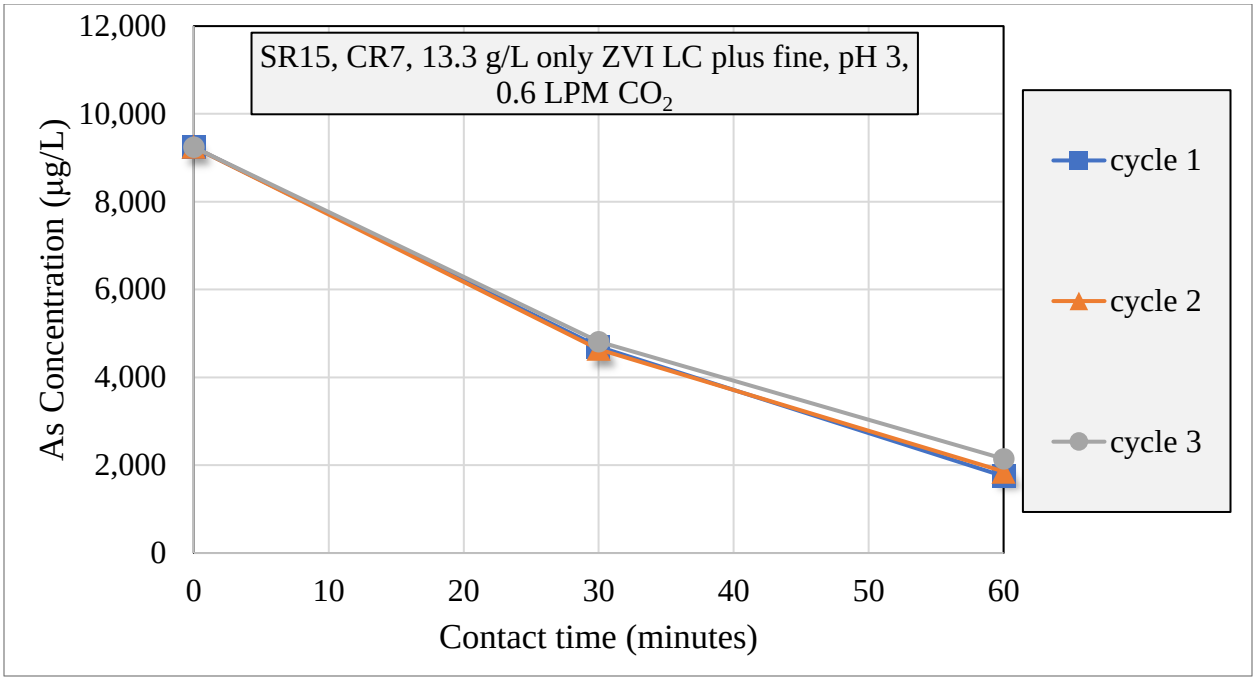

Figure 46 (As) - Comparison of ME treatment results for repeated sample loading cycles: 3 cycles using 13.3 g/L of ZVI LC plus fine only, to treat 3 loads of 500 mL SR15 LFG condensate with 0.6 LPM of continuous CO_2

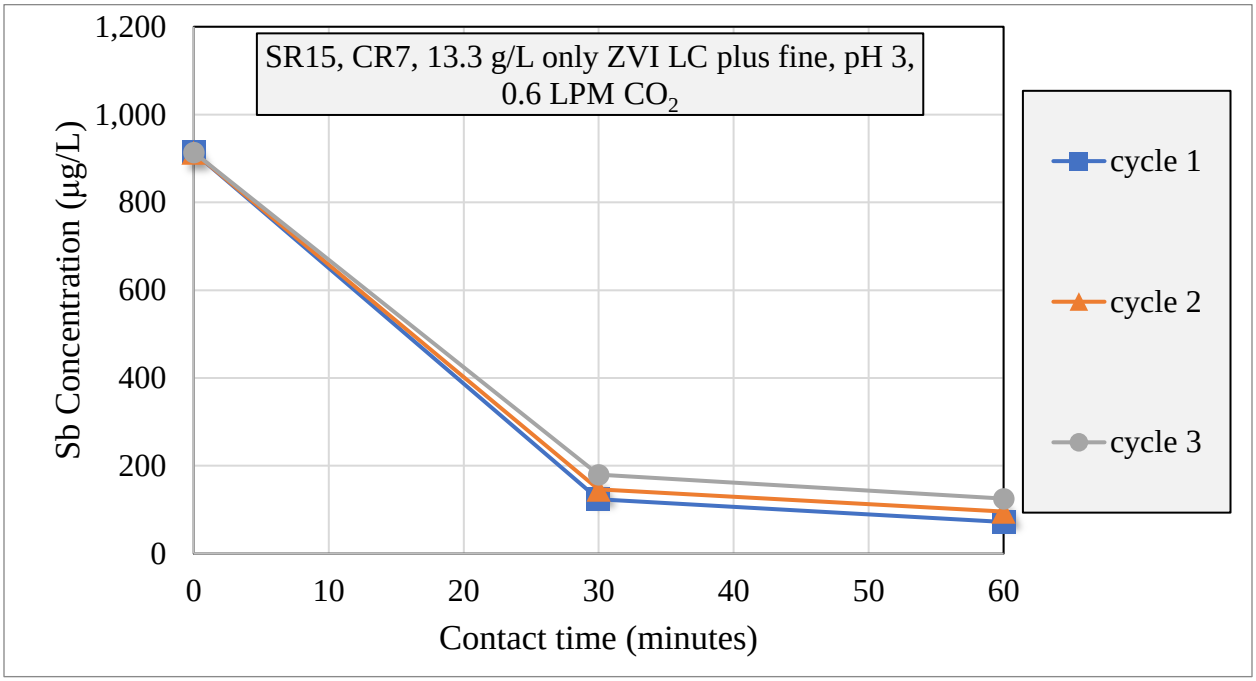

Figure 47 (Sb) - Comparison of ME treatment results for repeated sample loading cycles: 3 cycles using 13.3 g/L of ZVI LC plus fine only, to treat 3 loads of 500 mL SR15 LFG condensate with 0.6 LPM of continuous CO_2

The findings using a higher dosage of ZVI are encouraging, with arsenic removal efficiency reaching up to 77% in the third cycle. Future studies should explore the use of larger-sized ZVI particles with more than three cycles. The potential elimination of activated carbon from the system may enhance its overall operability. However, the use of ZVI only instead of mixed ZVI/activated carbon media requires longer contact times. Future work will address the benefits and drawbacks of these options in more detail.

The results above show that even if the active media cycling using solely ZVI was promising, the removal of As was faster when using together ZVI and PAC.

The outcomes of the cycling performed with ZVI and PAC also prompted further experimentation involving more than three cycles of using the same batch of active media. At the next step, five cycles were carried out using different samples (SR15 and SR13), intermittent CO_2 flow, and only 30 minutes of cycling time, as the previous results showed high As/Sb removal efficiency within the first 30 minutes of treatment.

The main goal of the next cycles is to assess the feasibility of reusing active media when using intermittent CO_2, and testing LFG condensate with different initial concentrations. The results of these experiments are shown below:

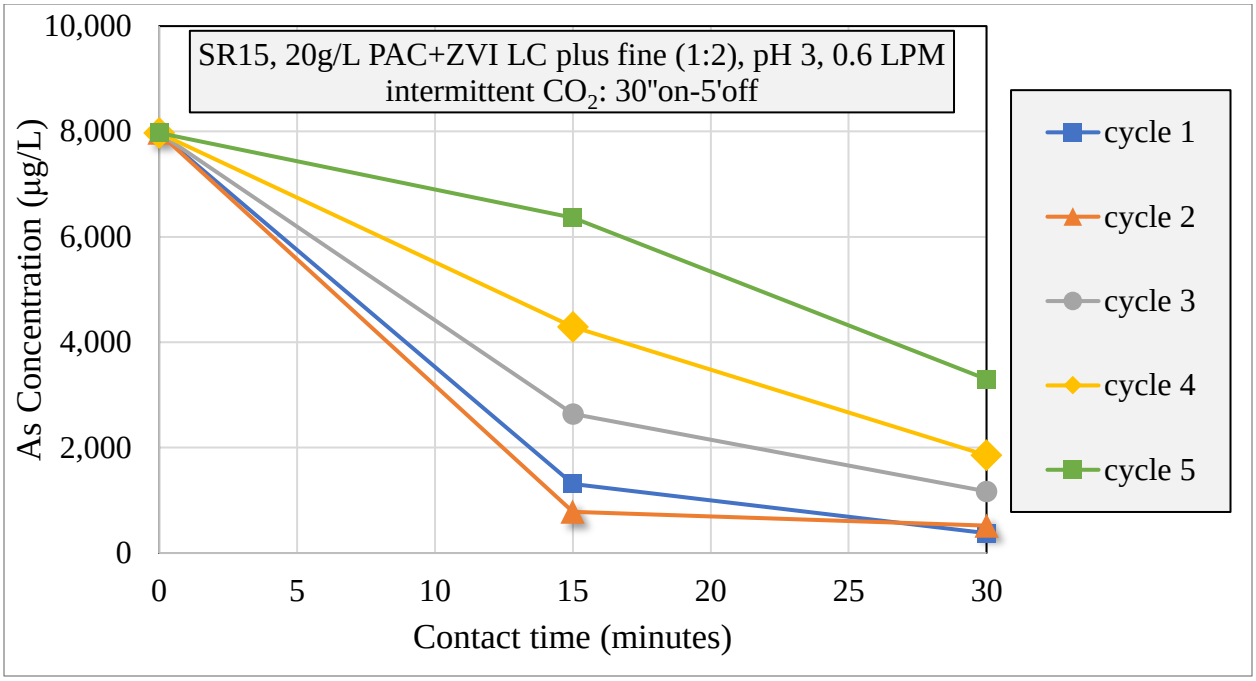

Figure 48 (As) - Comparison of ME treatment results for repeated sample loading cycles: 5 cycles using 20 g/L of PAC and ZVI LC plus fine to treat 5 loads of 500 mL SR15 LFG condensate with 0.6 LPM of intermittent CO_2 (30 seconds on, 5 minutes off)

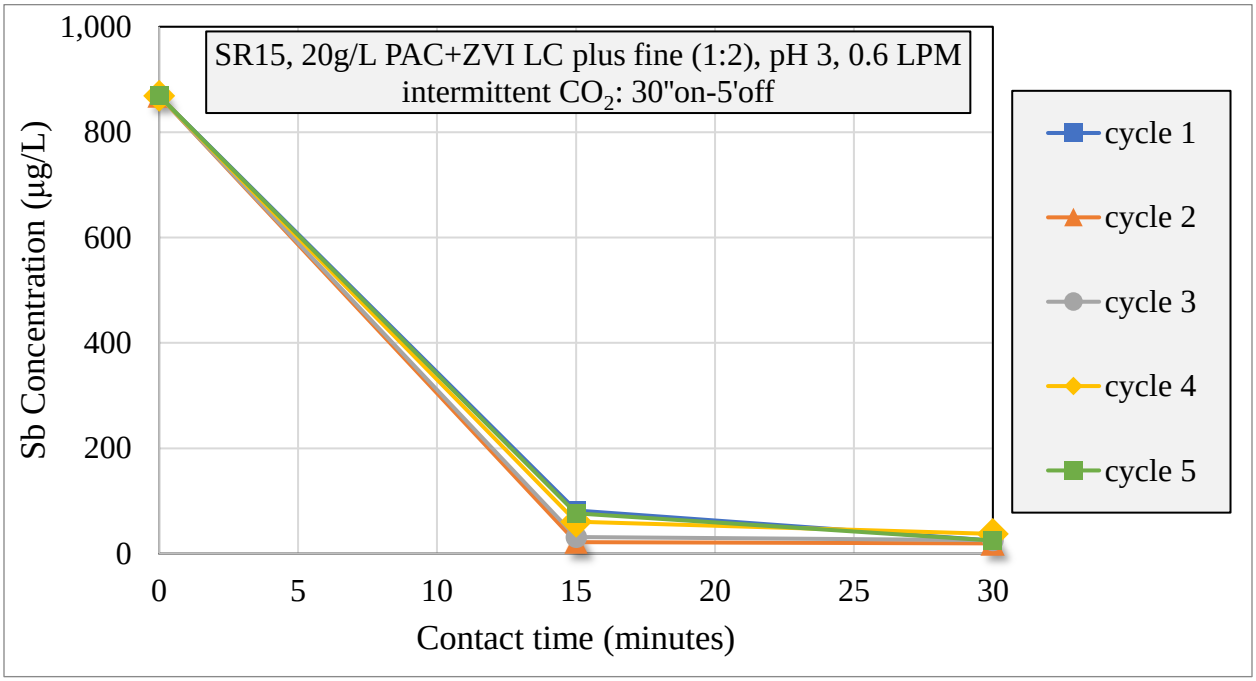

Figure 49 (Sb) - Comparison of ME treatment results for repeated sample loading cycles: 5 cycles using 20 g/L of PAC and ZVI LC plus fine to treat 5 loads of 500 mL SR15 LFG condensate with 0.6 LPM of intermittent CO_2 (30 seconds on, 5 minutes off)

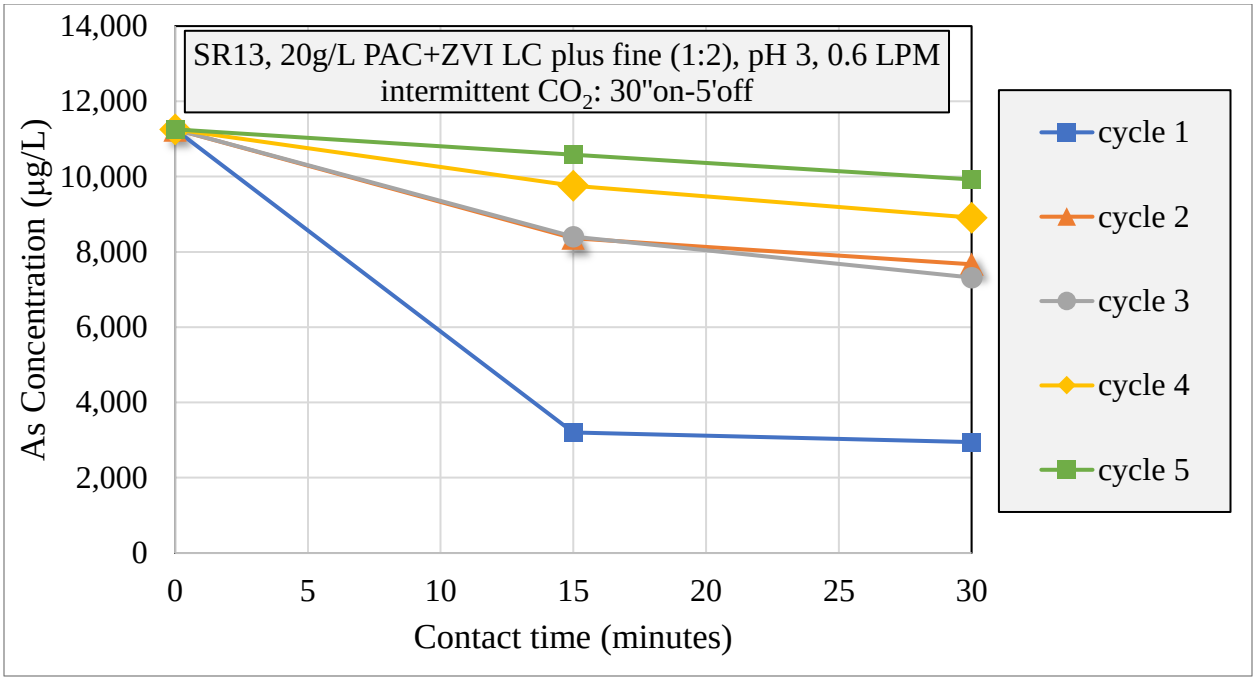

Figure 50 (As) - Comparison of ME treatment results for repeated sample loading cycles: 5 cycles using 20 g/L of PAC and ZVI LC plus fine to treat 5 loads of 500 mL SR13 LFG condensate with 0.6 LPM of intermittent CO_2 (30 seconds on, 5 minutes off)

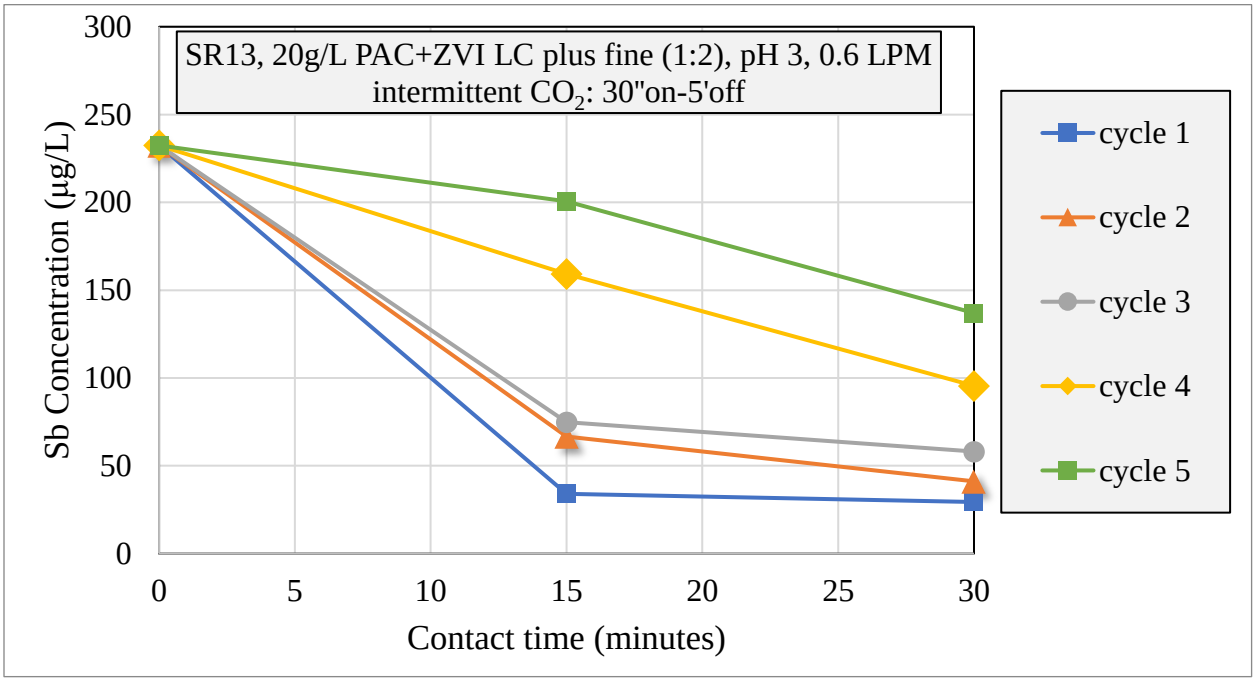

Figure 51 (Sb) - Comparison of ME treatment results for repeated sample loading cycles: 5 cycles using 20 g/L of PAC and ZVI LC plus fine to treat 5 loads of 500 mL SR13 LFG condensate with 0.6 LPM of intermittent CO_2 (30 seconds on, 5 minutes off)

In the case of SR15, the initial three cycles exhibited >85% removal of arsenic within 30 minutes. However, cycles 4 and 5 demonstrated 77% and 59% arsenic removal, respectively. In contrast, for antimony, all five cycles showed excellent performance, with >96% removal achieved in each cycle.

Conversely, SR13 manifested only 74% arsenic removal in the first cycle, and <30% removal in the subsequent cycles. Additionally, even for antimony, the cycles did not display satisfactory performance. The outcomes suggest that for determined LFG condensate sample, such as SR13, more extended cycle times, a greater dosage of reagents, or continuous CO_2 flow are necessary to achieve better results. Further investigations will be carried out to optimize the cycling process in future experiments.

4.6. Effects of mechanical mixing on As removal in ME operations

One of the fundamental roles of CO_2 gas is to facilitate the interaction between active media and contaminants, promoting the occurrence of the electrochemical reactions that cause the removal of arsenic. In an attempt to reduce the reliance on gas flow-induced mixing in ME reactors, an alternative approach involving using an overhead mechanical mixer installed in an isolated batch column reactor was explored.

Mechanical mixing experiments were conducted initially in the presence of CO_2 carrier gas flow, followed by the subsequent removal of gas from the system. A wide range of ME treatment experiments using mechanical mixing were carried out. These experiments evaluated the effects of variations in pH, sample, active media dosing and particle size, and the reuse of active media. The experiments are described below.

4.6.1. Mechanical mixing with gas flow versus recirculation of gas with no mixing

In this experiment, a comparison was made between two modes of CO_2 injection into a system. The first mode involved the simultaneous use of mechanical mixing and gas recirculation, while the second setup involved only gas recirculation without any mixing. The CO_2 was injected into the system for a duration of 30 seconds, after which the gas was recirculated with an air pump for a period of 60 minutes. The results of the experiments are presented below.

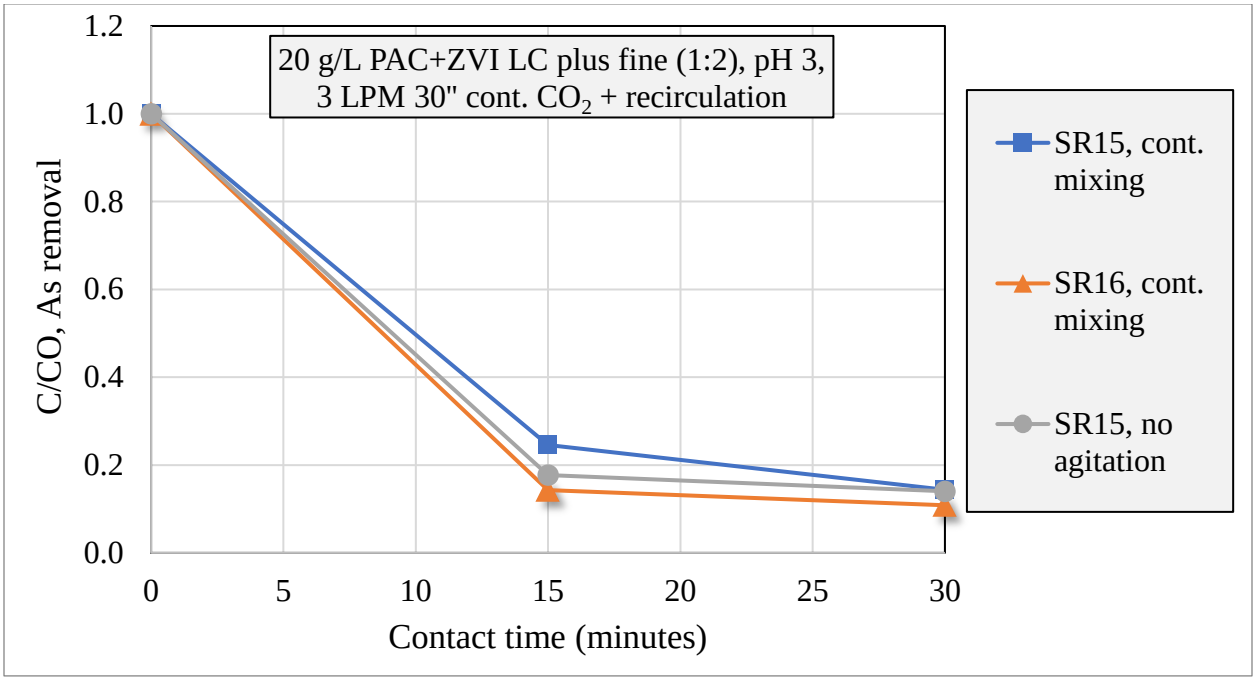

Figure 52 (As) - Comparison of ME treatment results for CO_2 recirculation with and without mechanical mixing: ME reactor using 20 g/L of PAC and ZVI LC plus fine to treat 2 L of SR16 LFG condensate. Initial As concentration: 25 ppm

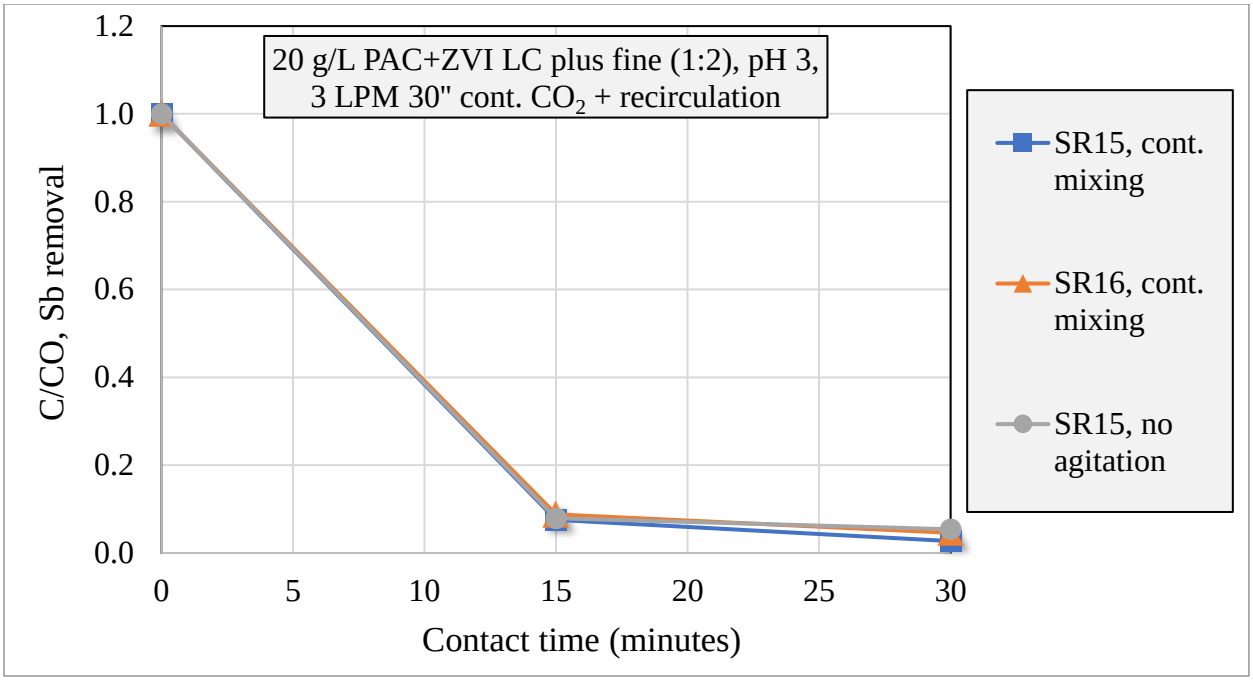

Figure 53 (Sb) - Comparison of ME treatment results for CO_2 recirculation with and without mechanical mixing: ME reactor using 20 g/L of PAC and ZVI LC plus fine to treat 2 L of SR16 LFG condensate. Initial Sb concentration: 1.2 ppm

The plotted data reveals that samples SR15 and SR16 exhibited similar results when mechanical mixing with gas recirculation was compared to the use of only CO_2 gas recirculation. In both cases, all arsenic removal efficiencies were greater than 85%, and all antimony removal efficiencies were greater than 94% within a 30-minute timeframe. This finding suggested that experiments should be conducted using mechanical mixing only, without the presence of recirculated CO_2 carrier gas.

4.6.2. Mixing modes: continuous versus intermittent

In light of the high removal efficiency achieved in the previous experiments, further experiments were conducted using only mechanical mixing. Specifically, a comparison was made between continuous and intermittent mixing modes. The results of these experiments are presented below:

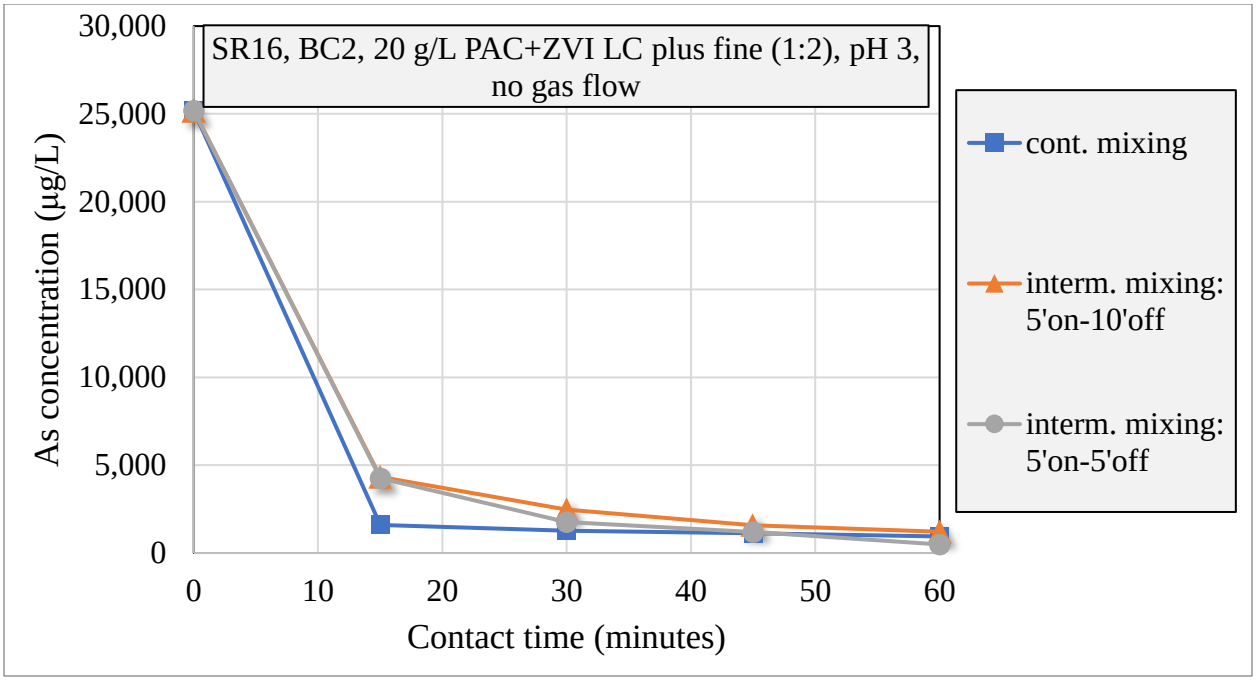

Figure 54 (As) - Comparison of ME treatment results for mechanical mixing mode variations: ME reactor using 20 g/L of PAC and ZVI LC plus fine to treat 2 L of SR16 LFG condensate with continuous and intermittent mixing

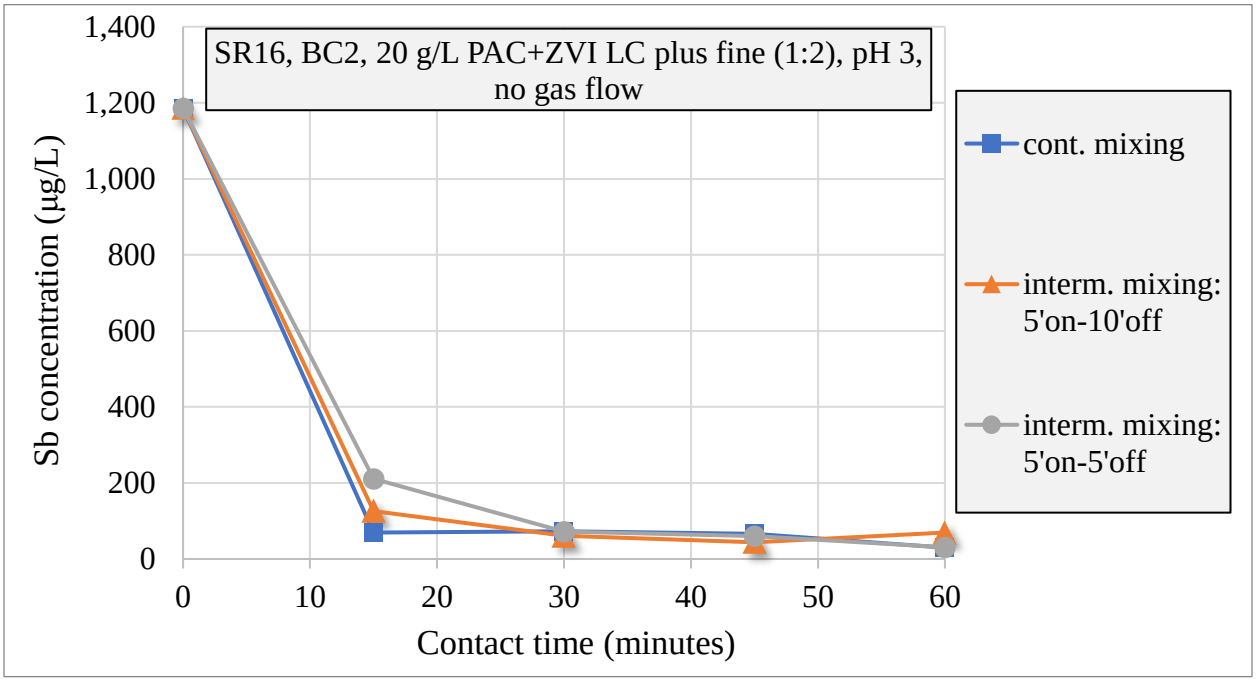

Figure 55 (Sb) - Comparison of ME treatment results for mechanical mixing mode variations: ME reactor using 20 g/L of PAC and ZVI LC plus fine to treat 2 L of SR16 LFG condensate with continuous and intermittent mixing

The experimental results shown above indicate that all three mixing modes performed similarly, with arsenic and antimony removal efficiencies consistently exceeding 90% for all experiments within a 30-minute timeframe. This finding suggests that optimizing the mixing modes could result in significant energy savings and reduced operational costs. Additionally, the experiments suggest that a treatment duration of 30 minutes is sufficient, as the As/Sb removal efficiency achieved within this period is excellent.

4.6.3. Effects of pH on As removal in the case of mechanical mixing

To optimize the amount of reagents used in the process, additional experiments were conducted to compare the removal of As at different pH values. Based on previous experiments results (Figure 26 and Figure 27), the ME process performs more effectively at lower pH. However, pH 4 still had an acceptable As/Sb removal when using CO_2. Considering these results, the experiments with mechanical mixing (no CO_2) were performed with the typical pH value of 3, a pH value of 4.5, and with no pH control. The experiment without pH control started with an initial pH of 6.5 and increased to 7 when the active media was added. The results of these experiments are presented below.

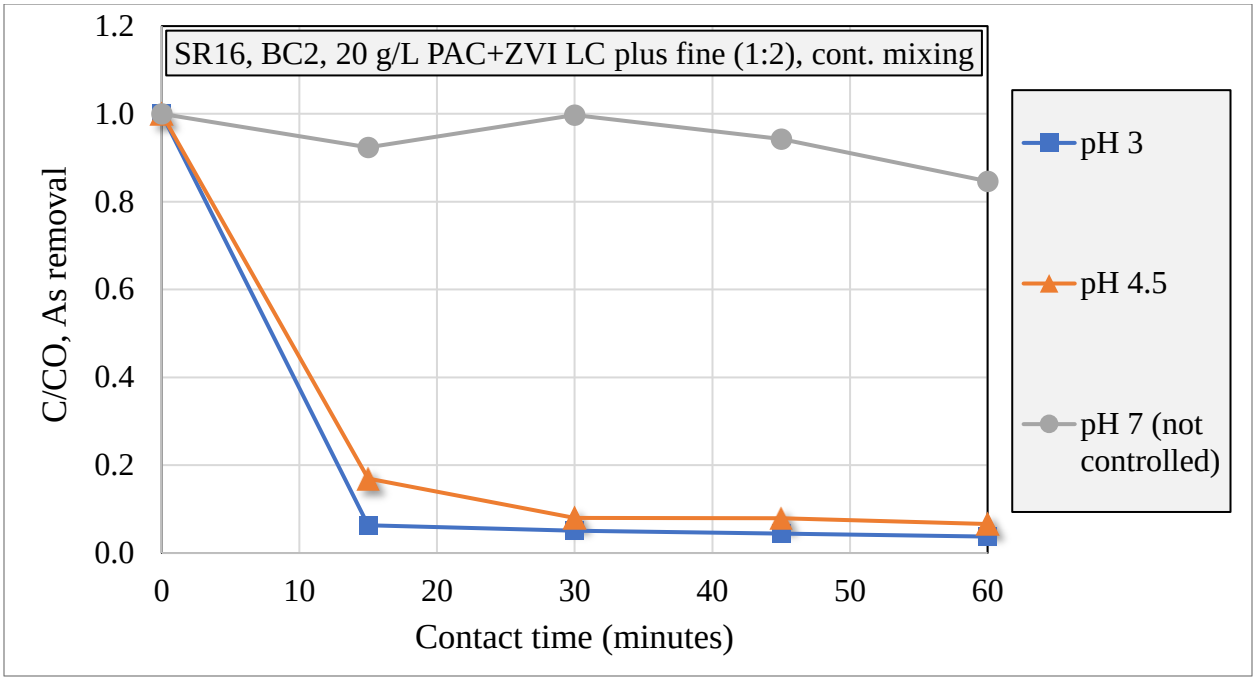

Figure 56 (As) - Comparison of ME treatment results for mechanical mixing with pH variations: ME reactor using 20 g/L of PAC and ZVI LC plus fine to treat 2 L of SR16 LFG condensate for pH 3, 4.5 and 7 (not controlled). Initial As concentration: 25 ppm

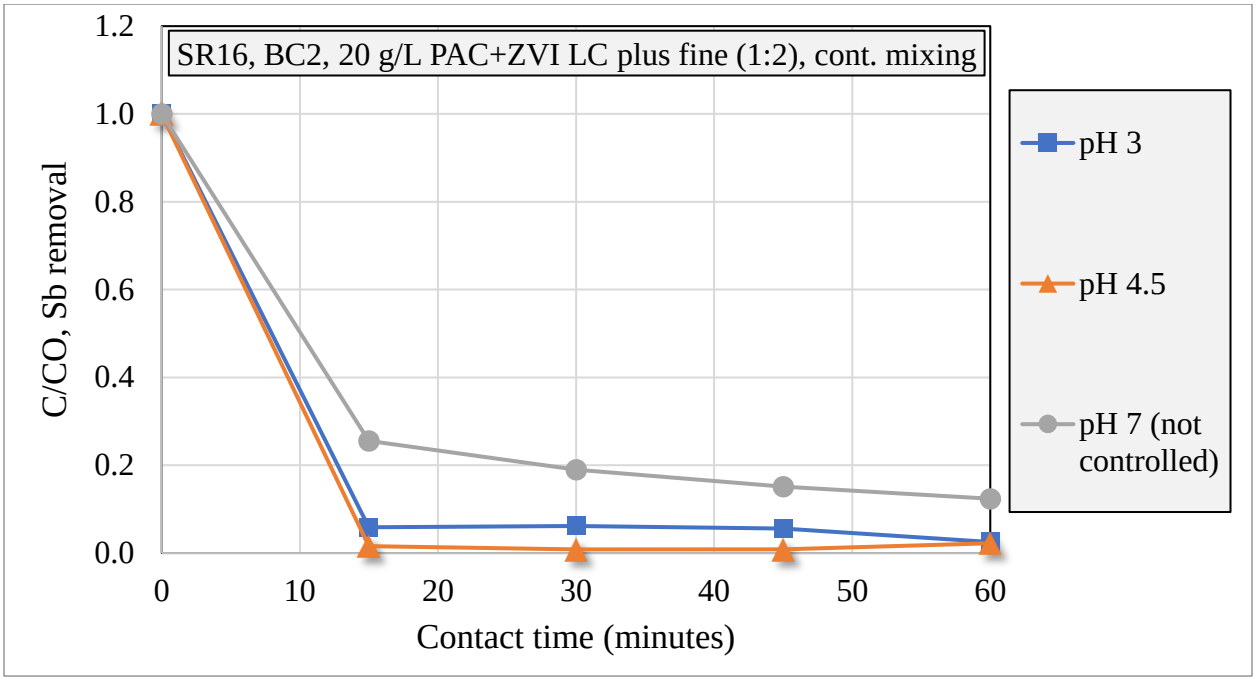

Figure 57 (Sb) - Comparison of ME treatment results for mechanical mixing with pH variations: ME reactor using 20 g/L of PAC and ZVI LC plus fine to treat 2 L of SR16 LFG condensate for pH 3, 4.5 and 7 (not controlled). Initial Sb concentration: 1.2 ppm

Based on the results, it is apparent that the efficacy of removing arsenic and antimony is comparable at pH 3 and pH 4.5, whereas the absence of pH control leads to minimal removal of arsenic. The results demonstrate the ME processes in the presence of mechanical agitation may carried out at pHs above 3, for instance at pH 4.5 thus requiring less acid resulting in lower operational expenses. However, results of these experiments needed to be confirmed and expanded in further measurements.

4.6.4. As removal using mechanical mixing and varying active media dosage

The dosage of active media can also be optimized since the standard experiments were conducted using 20 g/L of PAC and ZVI LC plus fine. In order to reduce the dosage required for the removal of arsenic and antimony, experiments were conducted and tested using 7 g/L and 14 g/L. The results of these experiments are shown below.

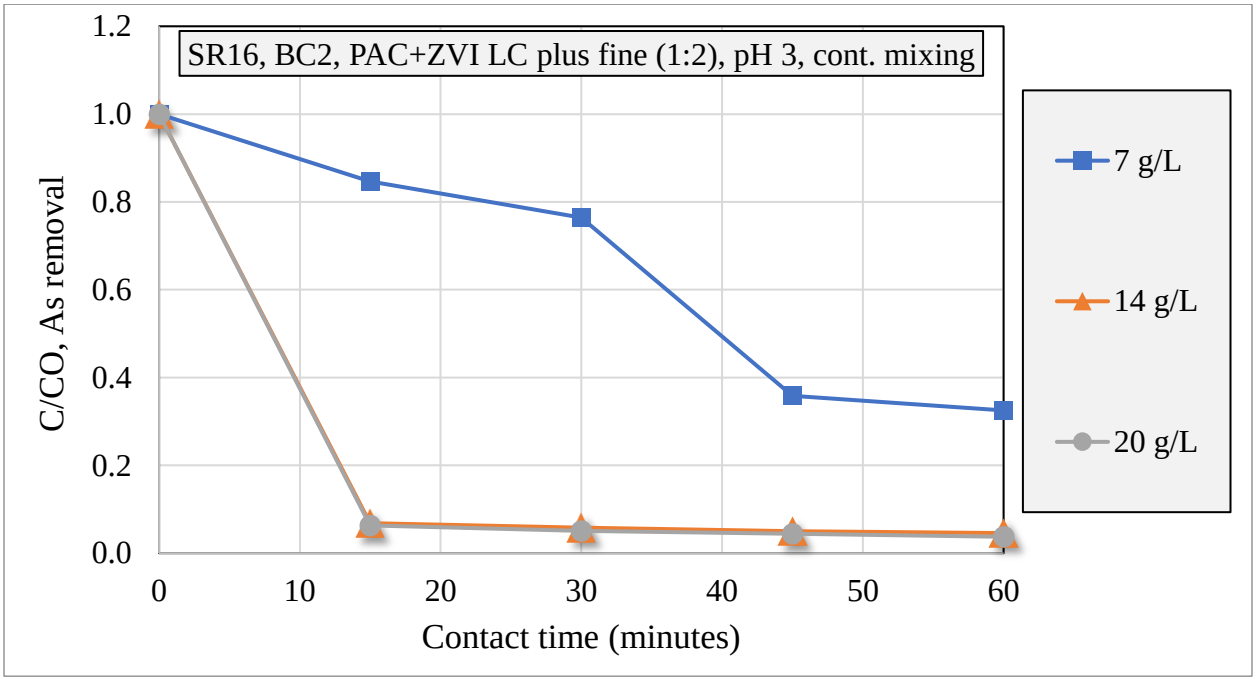

Figure 58 (As) - Comparison of ME treatment results for mechanical mixing with active media dosage variations: ME reactor using PAC and ZVI LC plus fine to treat 2 L of SR16 LFG condensate for active media dosing of 7, 14, and 20 g/L. Initial As concentration: 25 ppm

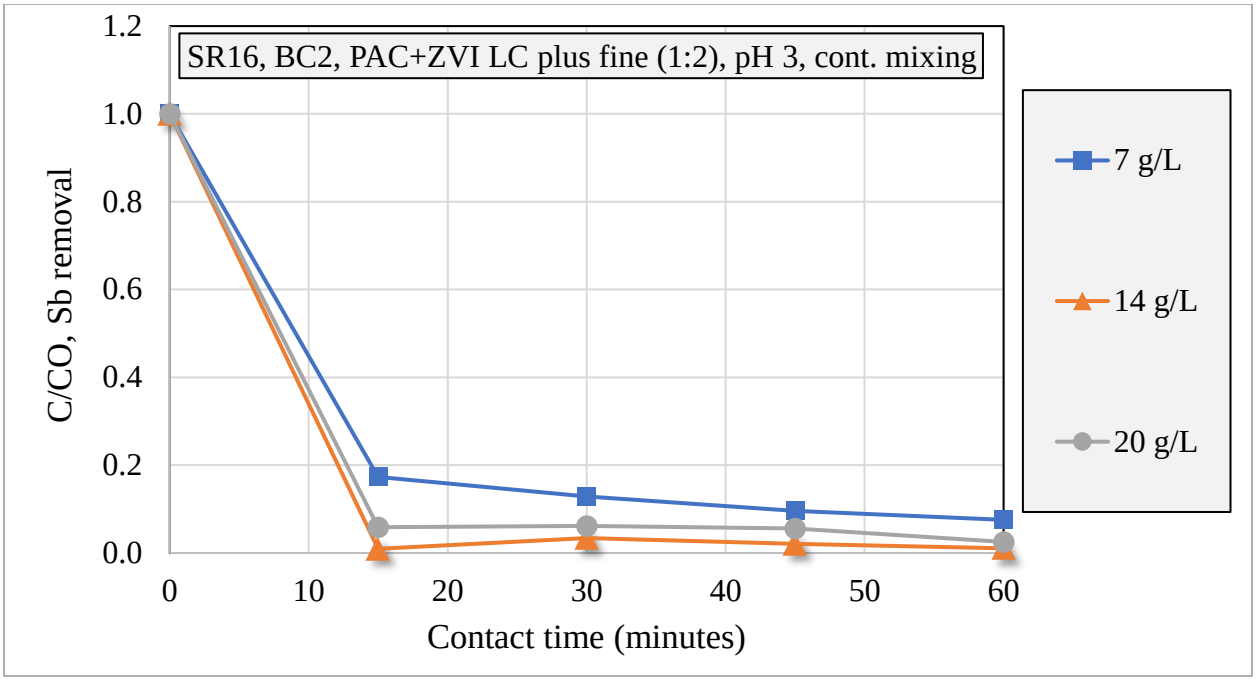

Figure 59 (Sb) - Comparison of ME treatment results for mechanical mixing with active media dosage variations: ME reactor using PAC and ZVI LC plus fine to treat 2 L of SR16 LFG condensate for active media dosing of 7, 14, and 20 g/L. Initial Sb concentration: 1.2 ppm

The use of a 14 g/L dose of mixed active media has demonstrated over 94% arsenic and antimony removal efficiency within 30 minutes of treatment, which is comparable to that achieved with 20 g/L. These results are encouraging in the context of the need to reduce the amount of active media required in ME treatment. However, further evaluation against active media reutilization experiments may be necessary to determine the optimal removal option with lower operational costs.

4.6.5. As removal in the presence of mechanical mixing: comparison of the data for different landfill gas condensate samples

Given the success and benefits of the mechanical mixing approach, it is necessary to demonstrate a high efficiency of arsenic and antimony removal for every sample available in the laboratory

using this process. The experiments involved a 1-hour mixing of 20 g/L PAC and fine ZVI without any gas injection or recirculation. The ensuing results are presented below.

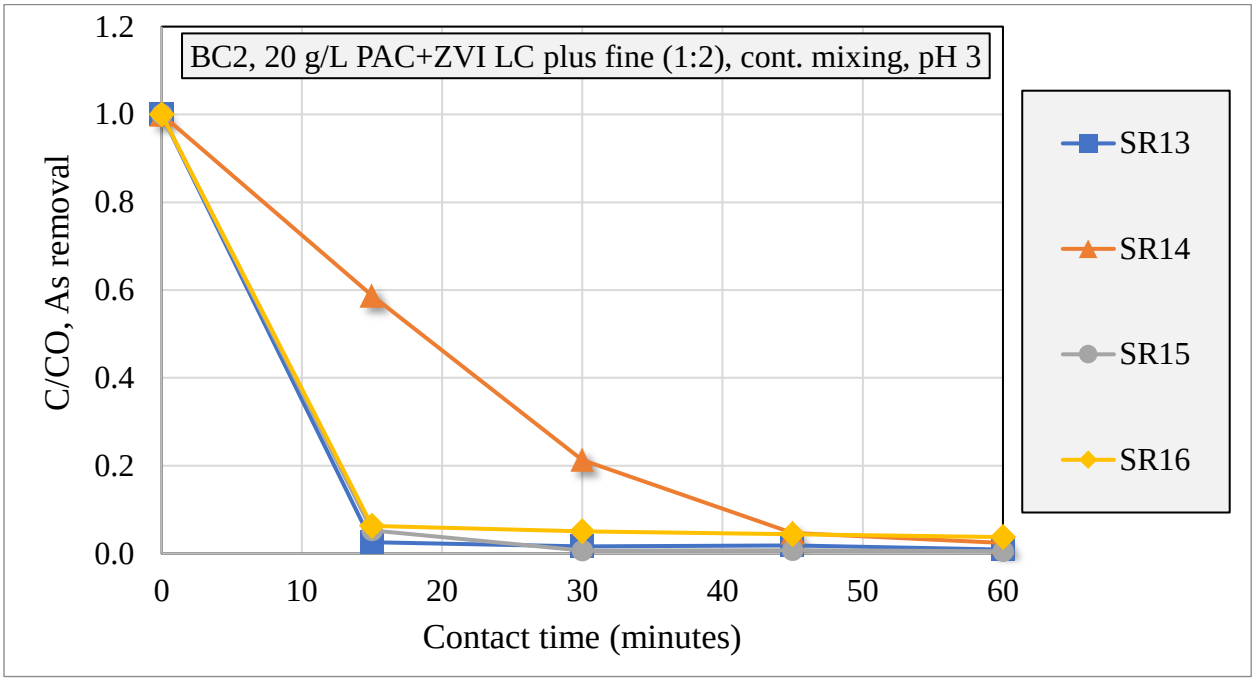

Figure 60 (As) - Comparison of ME treatment results for mechanical mixing with sample variations: ME reactor using 20 g/L of PAC and ZVI LC plus fine to treat 2 L of SR13, SR14, SR15, and SR16 LFG condensate. Initial As concentrations: SR13=8.1 ppm, SR14 =200 ppm, SR15=9.3 ppm, SR16=25 ppm

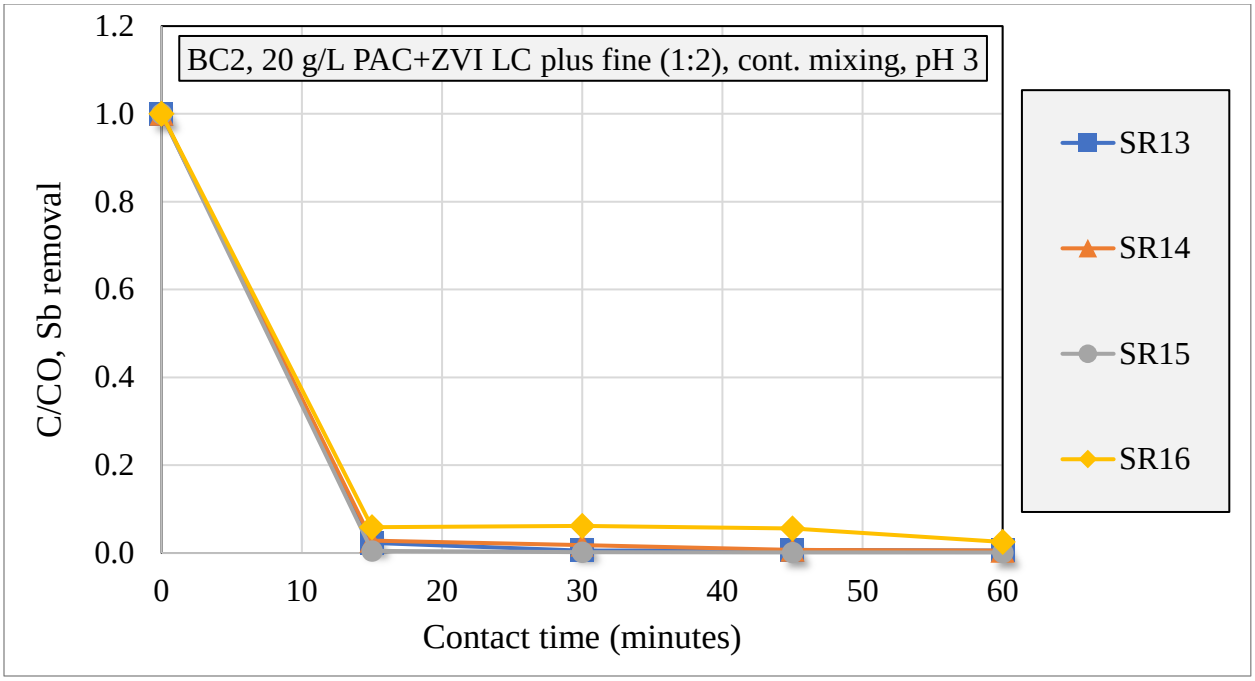

Figure 61 (Sb) - Comparison of ME treatment results for mechanical mixing with sample variations: ME reactor using 20 g/L of PAC and ZVI LC plus fine to treat 2 L of SR13, SR14, SR15, and SR16 LFG condensate. Initial Sb concentrations: SR13=0.4 ppm, SR14 =9.7 ppm, SR15=0.8 ppm, SR16=1.2 ppm

The findings are noteworthy, particularly given the challenges encountered with SR13 and SR14 in previous experiments (Initial As concentrations: SR13=8.1 ppm, SR14 =200 ppm; Initial Sb concentrations: SR13=0.4 ppm, SR14 =9.7 ppm). Within 30 minutes, the arsenic removal efficacy exceeded 95% for all samples, except for SR14, which achieved over 97% removal within 1 hour. Moreover, all samples displayed an antimony removal rate of >94% within 30 minutes. These outcomes are important, particularly when considering past experiments, as mechanical mixing appears to be the most effective approach for treating landfill gas condensate.

4.6.6. As removal in the presence of mechanical mixing: effects of active media particle size

Another operational parameter is the variation of the particle size of the active media when using mechanical mixing. It is worth highlighting that in previous experiments, specifically those

involving the effects of carrier gas flow, larger particle sizes active media had a very good As/Sb removal efficiency when utilizing higher dosages (as evidenced in Figure 38 and Figure 39).

To further investigate this phenomenon, increased dosages of GAC (mesh 12-40 - diameter between ~638 and ~1,700 µm, as shown in Figure *9*) and ZVI LC plus (53% of the particles have mesh 60 - diameter ~ 338 µm, as shown in Figure *7*) were employed, and their performance was compared to that of 20 g/L of PAC (mesh>500, diameter<50 µm) and ZVI LC plus fine (64% of the particles have mesh 140 - diameter ~ 157 µm, as shown in Figure *7*). The results are shown below.

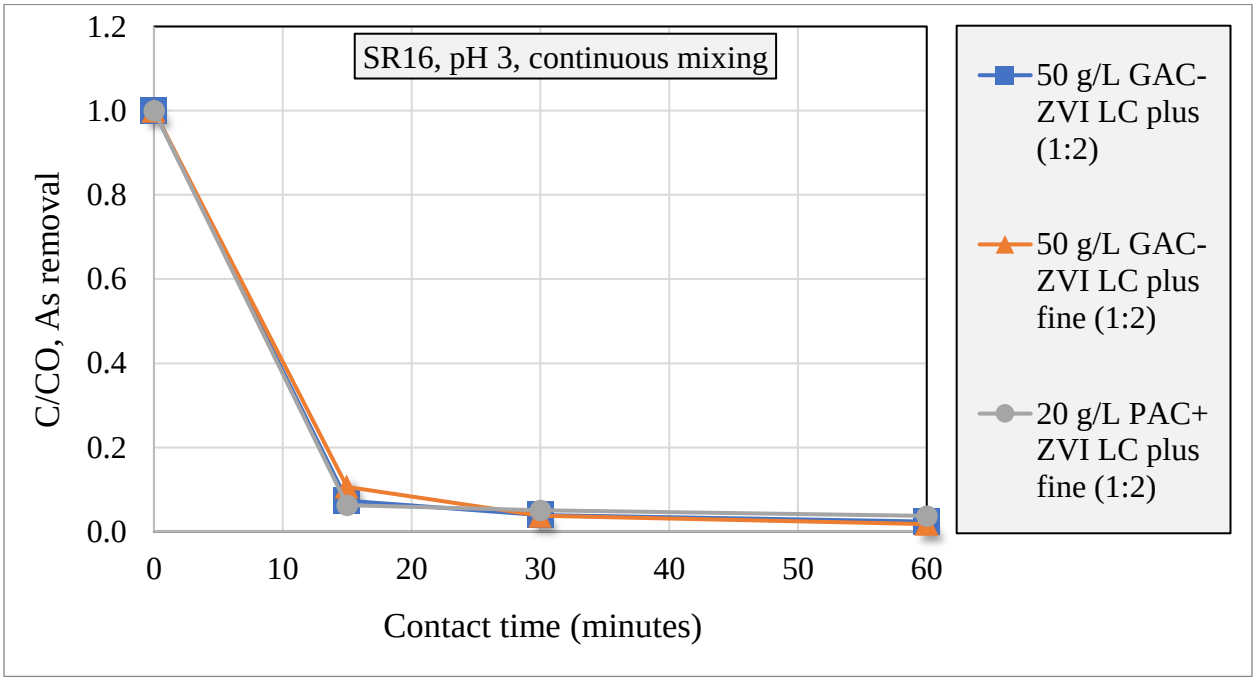

Figure 62 (As) - Comparison of ME treatment results for mechanical mixing with active media particle size variations: ME reactor using 20 and 50 g/L of active media to treat 2 L of SR16 LFG condensate, at pH 3 and with continuous mixing

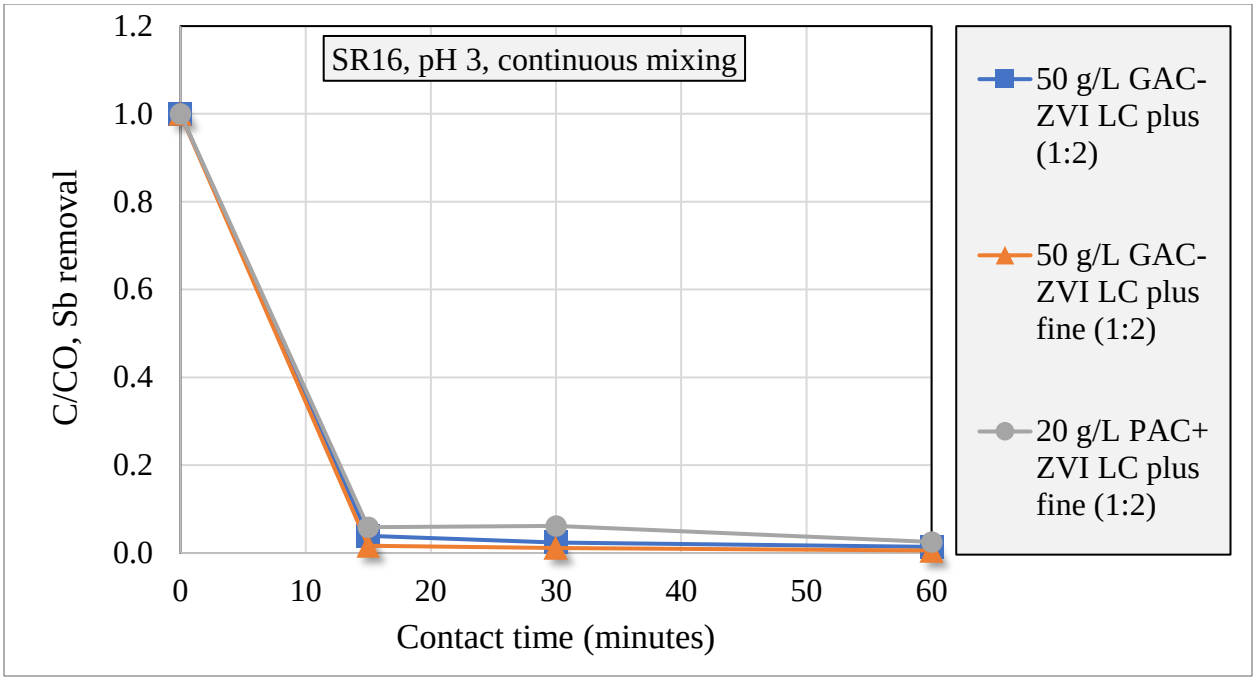

Figure 63 (Sb) - Comparison of ME treatment results for mechanical mixing with active media particle size variations: ME reactor using 20 and 50 g/L of active media to treat 2 L of SR16 LFG condensate

Based on the findings, the use of active media with larger particle sizes (e.g., GAC and ZVI LC plus) at a dosage of 50 g/L demonstrated comparable efficacy in the removal of arsenic and antimony, as contrasted to the use of small particle size active media at a dosage of 20 g/L. Notably, these results were obtained within a 30-minute timeframe and represent a significant finding that has implications for the operational and economic feasibility of the future practical applications. The use of larger particle size active media, such as GAC and ZVI LC plus, offers several operational advantages. Firstly, it simplifies the operation process as it requires less advanced filtration for the treated effluent. Additionally, the use of larger particles facilitates the reuse of the active media. Moreover, larger particle size active media is more cost-effective and practical in terms of storage and transportation. The reduced surface area-to-mass ratio results in less powder or fine particles, making it easier to handle. This can lower transportation costs and simplify storage arrangements.

4.6.7. As removal in the presence of mechanical mixing: Effects of repeated sample loading cycles (active media reuse)

Based on the successful outcome of the previous experiment in which the dose of 50 g/L of GAC-ZVI LC plus active media demonstrated exceptional performance within 30 minutes of treatment, the feasibility of the cycling of the active media in the presence of mechanical mixing was examined. In these experiments, four 30-minute cycles were carried out sequentially utilizing the same batch of the active media dosed using an initial dosage of 50 g/L GAC and ZVI LC plus. Additionally, four 30-minute cycles were tested with an initial dosage of 50 g/L GAC and ZVI LC plus (only for cycle 1), and 10 g/L of fresh GAC and ZVI LC plus (in a mass ratio of 1:2) were added from cycle 2 to 4. Both experiments allowed for 10 minutes of settling time between every cycle. The outcomes of the experiments are presented below:

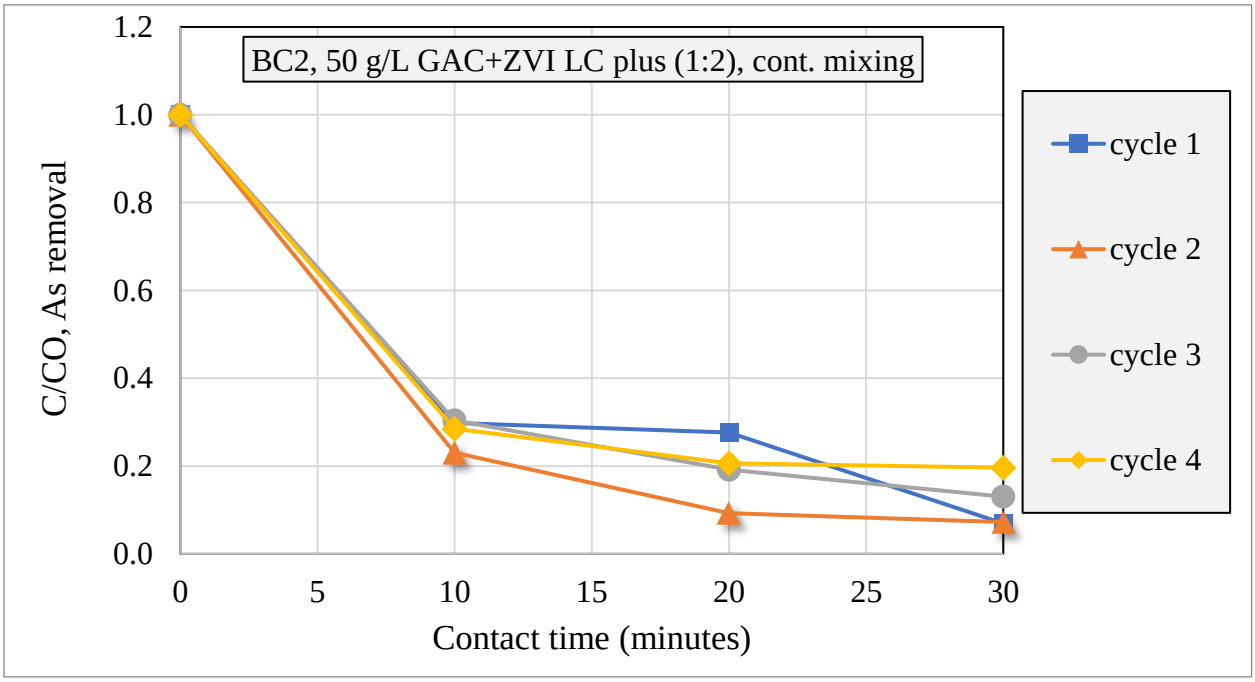

Figure 64 (As) – ME treatment results for repeated sample loading cycles in the presence of continuous mechanical mixing: 4 cycles using 50 g/L of GAC and ZVI LC plus to treat 4 loads of 500 mL SR16 LFG condensate. Initial As concentration: 25 ppm

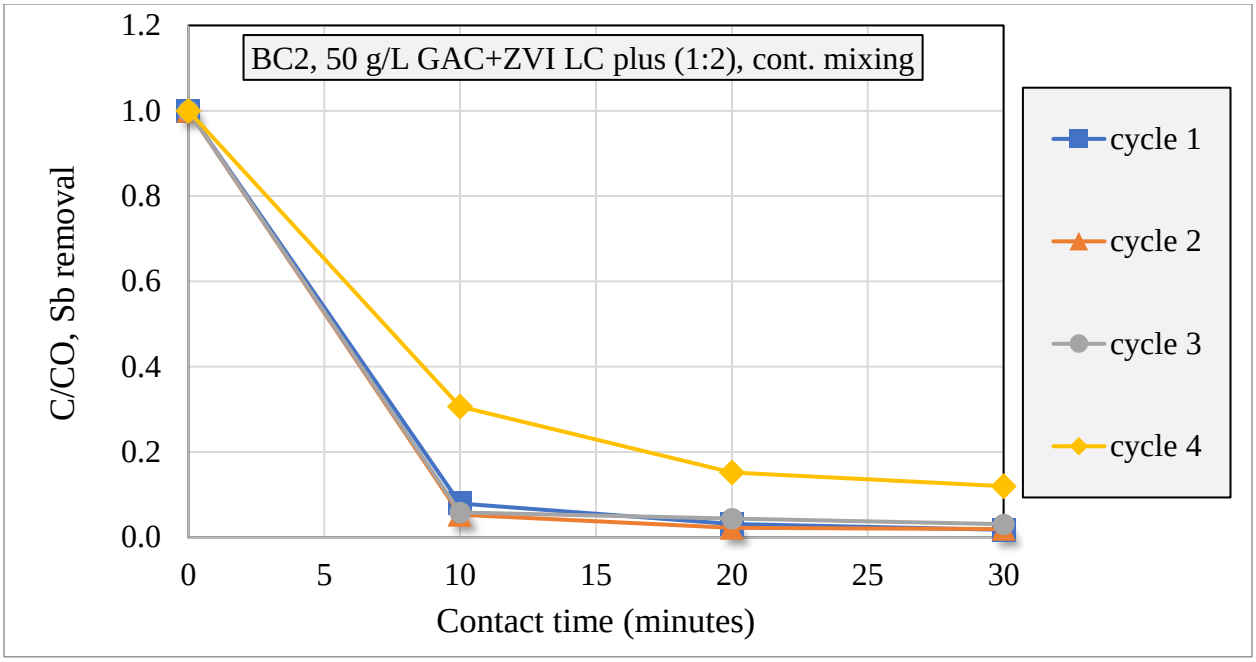

Figure 65 (Sb) – ME treatment results for repeated sample loading cycles in the presence of continuous mechanical mixing: 4 cycles using 50 g/L of GAC and ZVI LC plus to treat 4 loads of 500 mL SR16 LFG condensate. Initial Sb concentration: 1.2 ppm

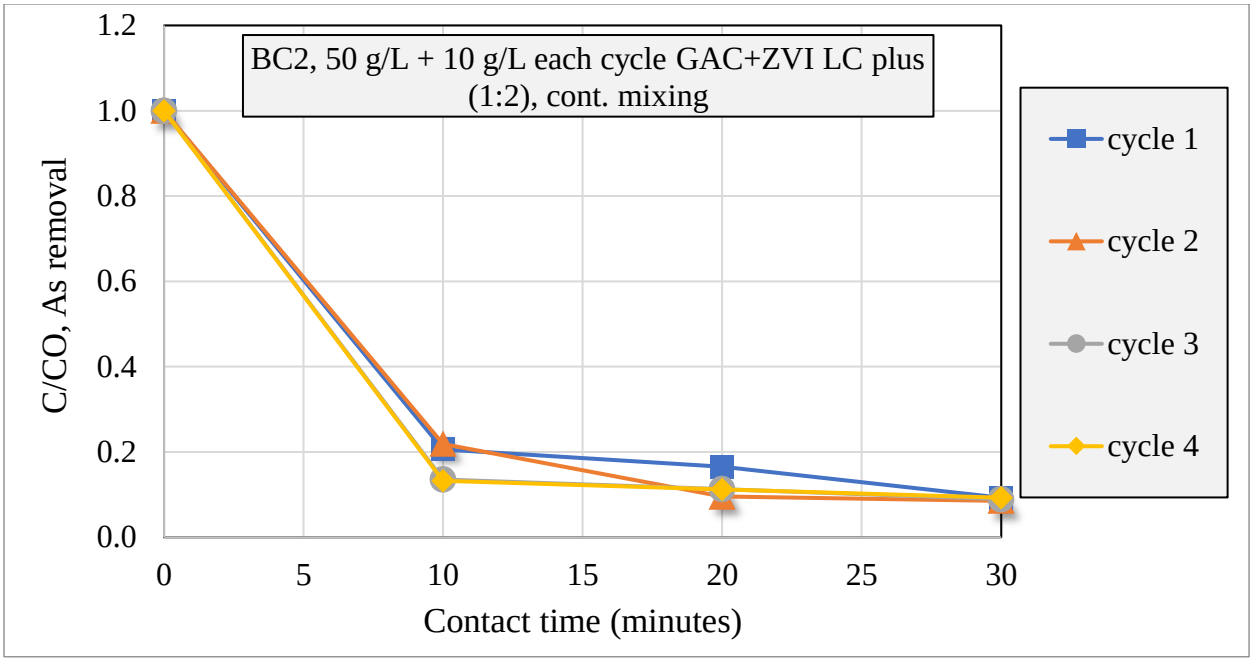

Figure 66 (As) – Comparison of ME treatment results for repeated influent loading cycles: 4 cycles using 50 g/L of GAC and ZVI LC plus and adding 10 g/L of fresh active media per cycle to treat 4 loads of 500 mL SR16 LFG condensate using continuous mechanical mixing. Initial As concentration: 25 ppm

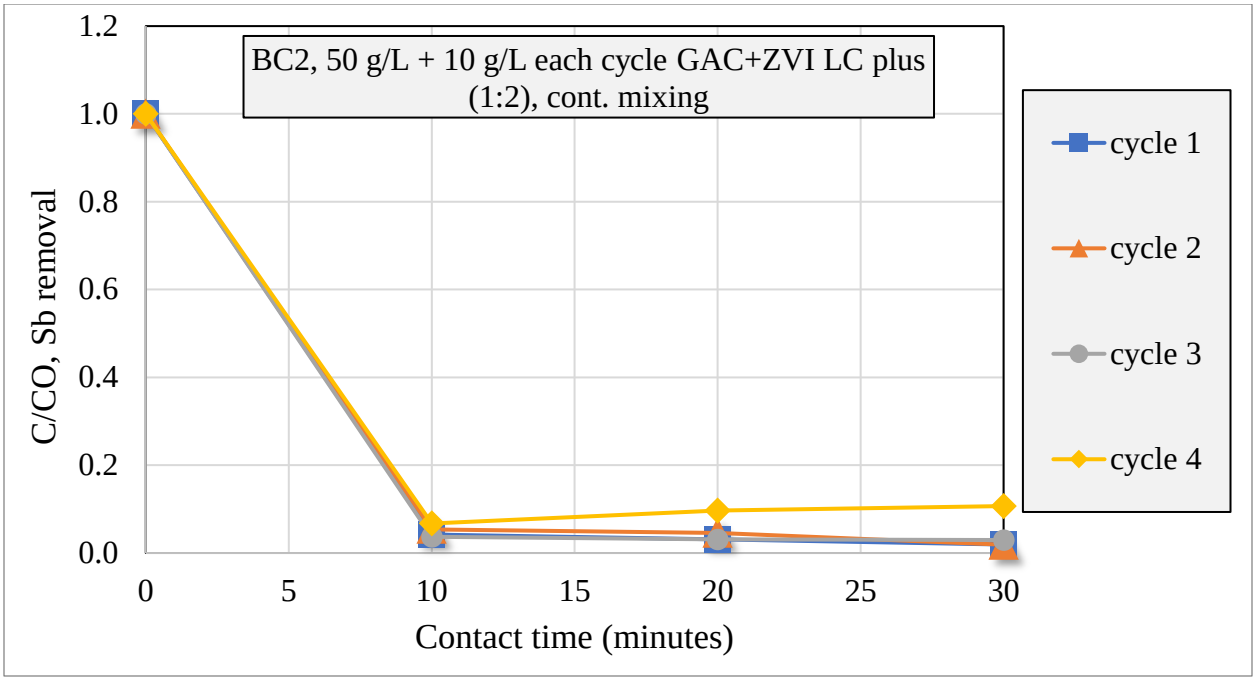

Figure 67 (Sb) – Comparison of ME treatment results for repeated influent loading cycles: 4 cycles using 50 g/L of GAC and ZVI LC plus and adding 10 g/L per cycle to treat 4 loads of 500 mL SR16 LFG condensate using continuous mixing. Initial Sb concentration: 1.2 ppm

The presented plots demonstrate that at an initial dosage of 50 g/L, all four treatment cycles achieved over 80% removal efficiency of arsenic within 30 minutes, and over 90% removal efficiency of antimony within the same time frame. Although there was a slight decrease in the arsenic removal efficiency observed in the subsequent cycles, the active media still exhibited sufficient capacity for remove arsenic. Further experiments were deemed necessary at this point to further explore the cycling capacity of the active media in ME treatment.

When analyzing the initial 50 g/L of large particle size active media (GAC and ZVI LC plus) with the addition of 10 g/L of fresh GAC and ZVI LC plus in a ratio of 1:2 from cycles 2 to 4, a less significant variation in removal efficiency was observed between the cycles for both arsenic and antimony, achieving over 88% removal efficiency for all four cycles. However, rapid accumulation of the active media at the bottom of the column reactor was observed during the experiments.

Further experiments with a higher number of loading cycles were then performed using smaller increments of the dosing of ZVI/GAC active media.

To evaluate the potential of the treatment process, the number of cycles was increased to ten using two options: 1) Initial dosage of 50 g/L of large particle size active media and no addition of active media per cycle; 2) Initial dosage of 50 g/L of large particle size active media and addition of 1 g/L of the active media in each cycle. Figure 68 to Figure 75 show the results of this extended loading cycle analysis.

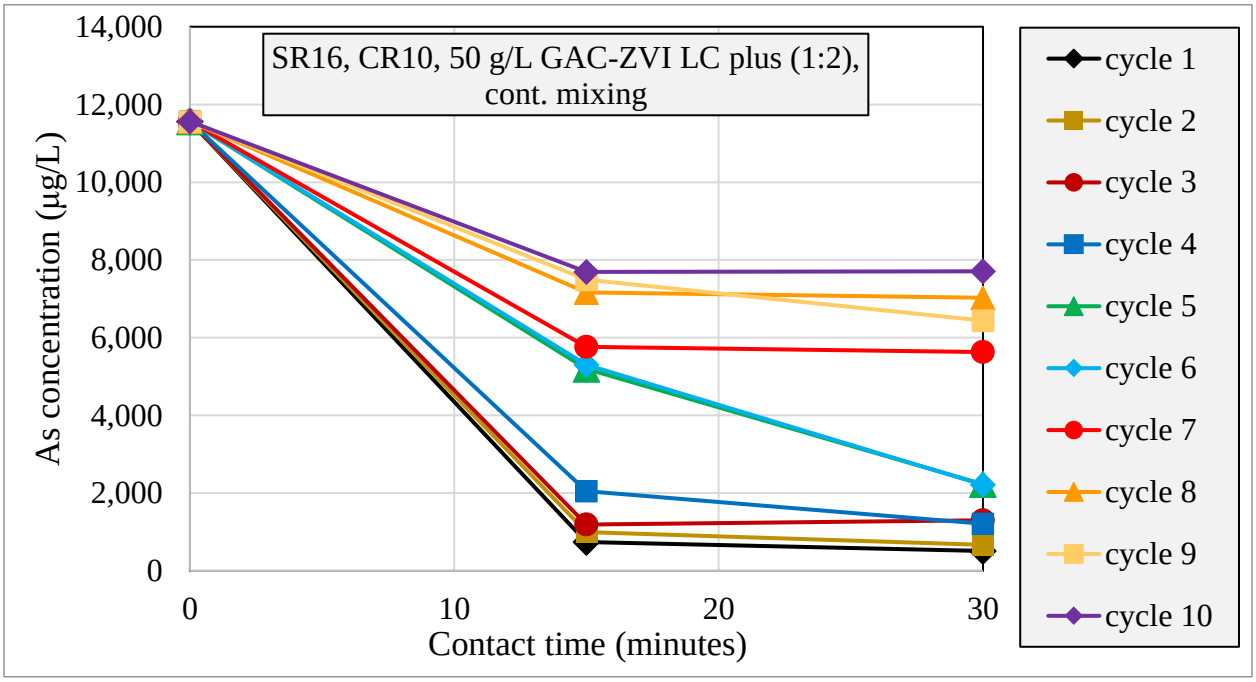

Figure 68 (As) - Comparison of ME treatment results for repeated sample loading cycles: 10 cycles using 50 g/L of GAC and ZVI LC plus to treat 10 loads of 500 mL SR16 LFG condensate

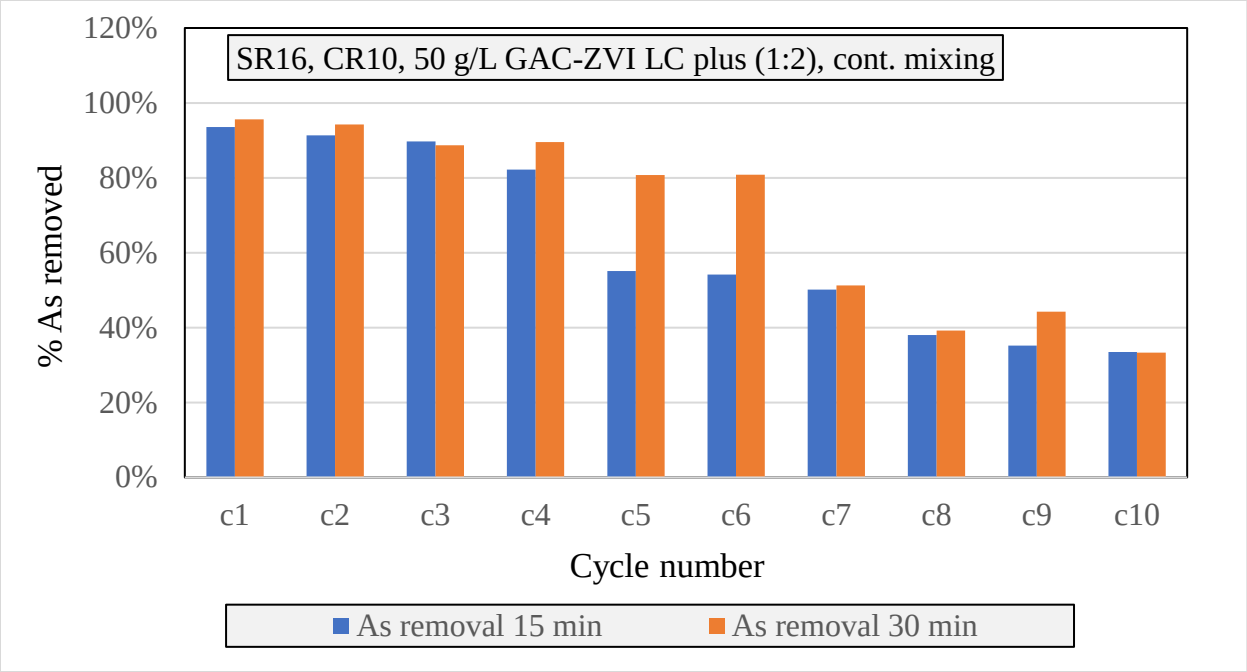

Figure 69 – As removal efficiency for repeated sample loading cycles: 10 cycles using 50 g/L of GAC and ZVI LC plus to treat 10 loads of 500 mL SR16 LFG condensate

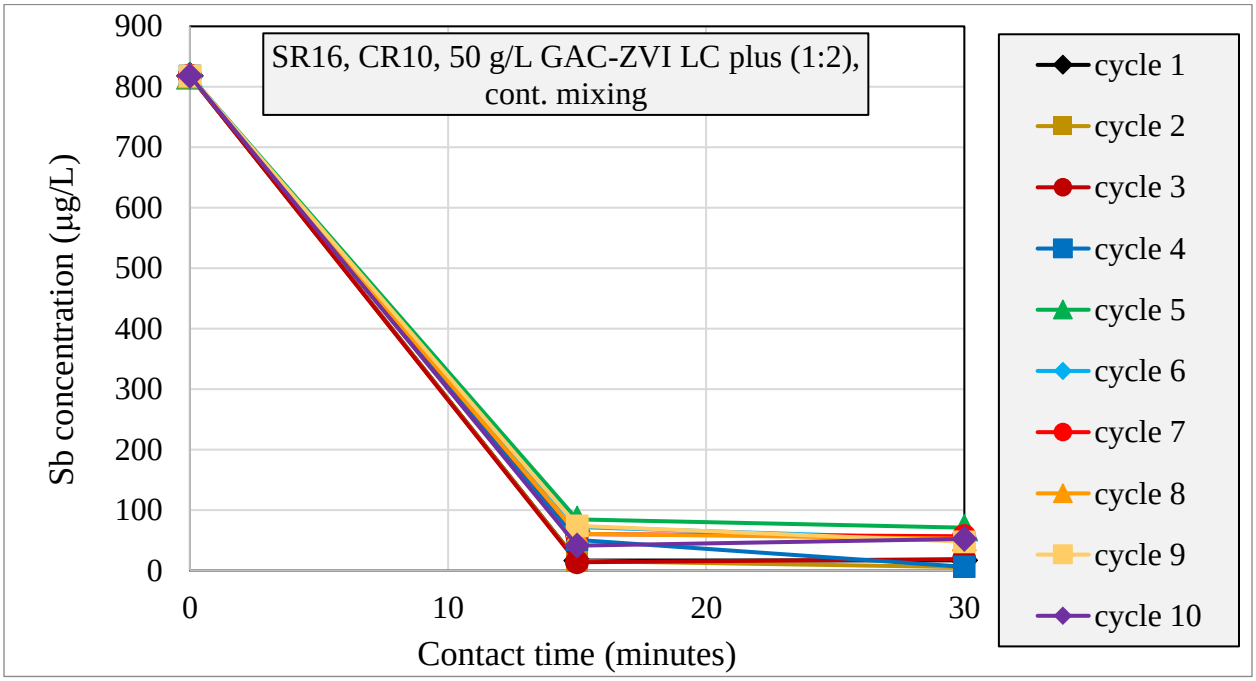

Figure 70 (Sb) - Comparison of ME treatment results for repeated sample loading cycles: 10 cycles using 50 g/L of GAC and ZVI LC plus to treat 10 loads of 500 mL SR16 LFG condensate

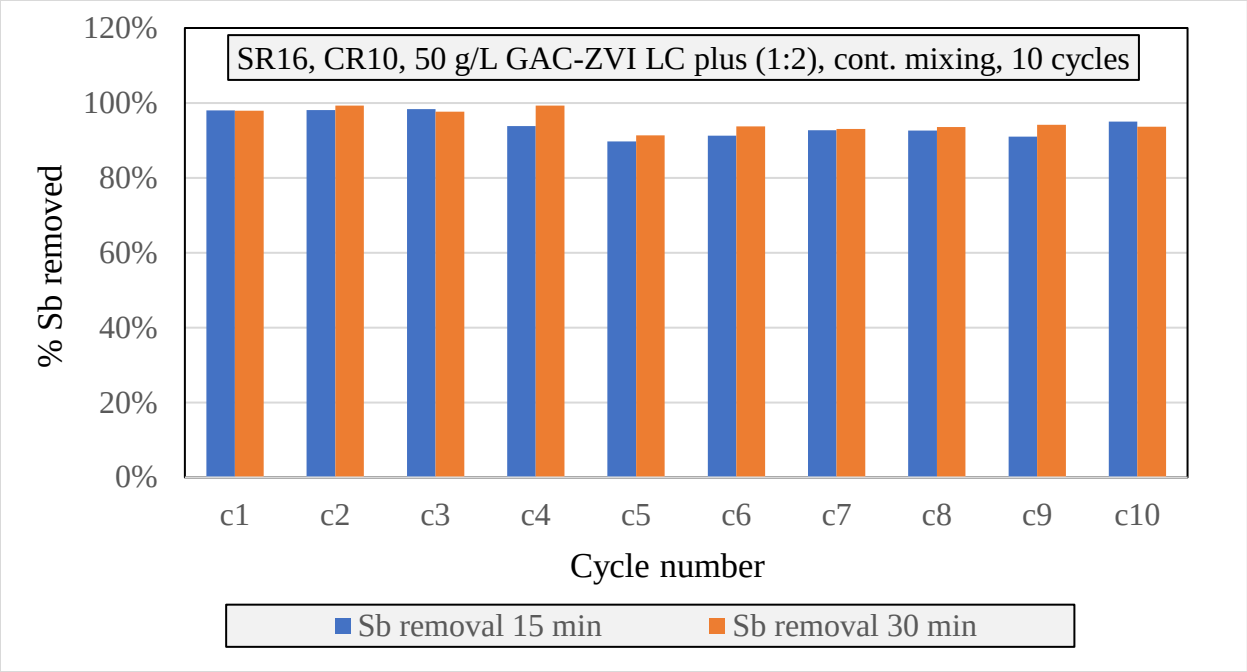

Figure 71 – Sb removal efficiency for repeated sample loading cycles: 10 cycles using 50 g/L of GAC and ZVI LC plus to treat 10 loads of 500 mL SR16 LFG condensate

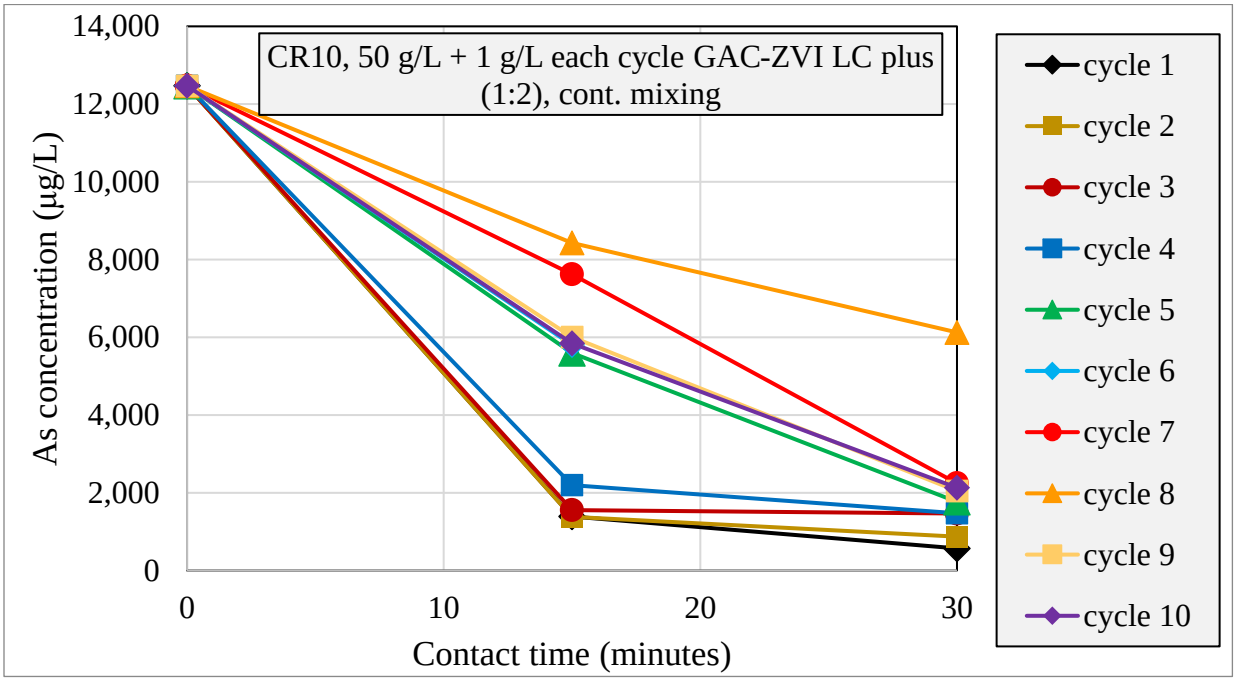

Figure 72 (As) - Comparison of ME treatment results for repeated sample loading cycles: 10 cycles using 50 g/L of GAC and ZVI LC plus and adding 1 g/L per cycle to treat 10 loads of 500 mL SR16 LFG condensate

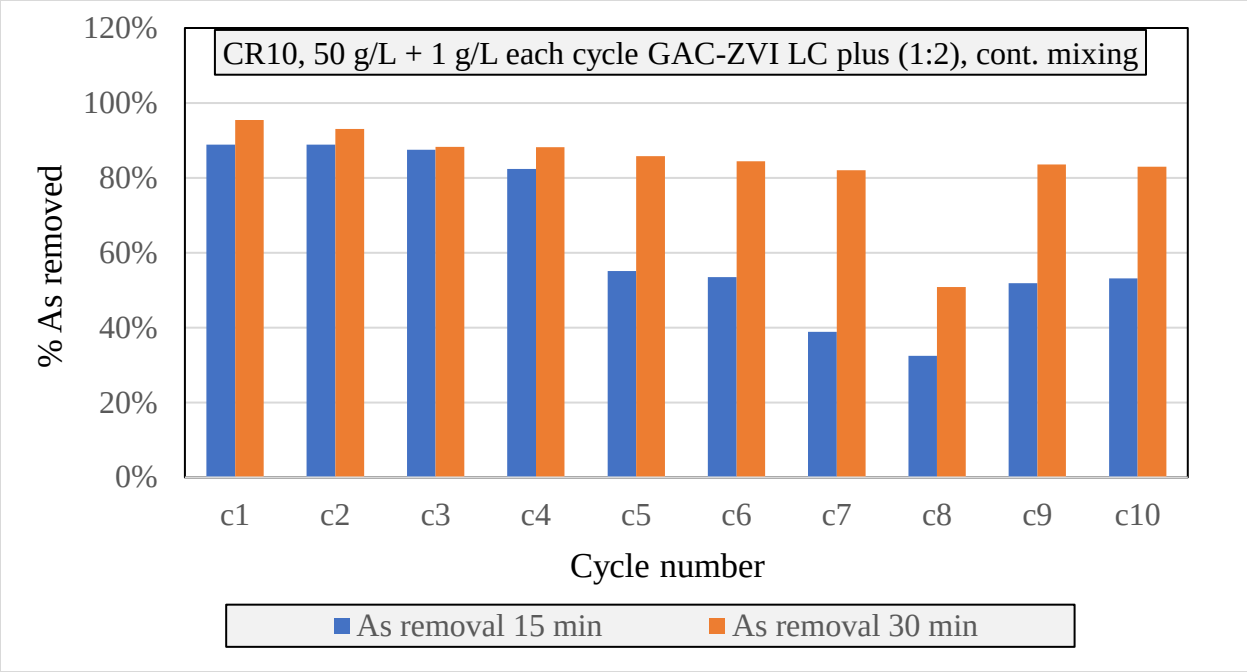

Figure 73 - As removal efficiency for repeated sample loading cycles: 10 cycles using 50 g/L of GAC and ZVI LC plus and adding 1 g/L per cycle to treat 10 loads of 500 mL SR16 LFG condensate

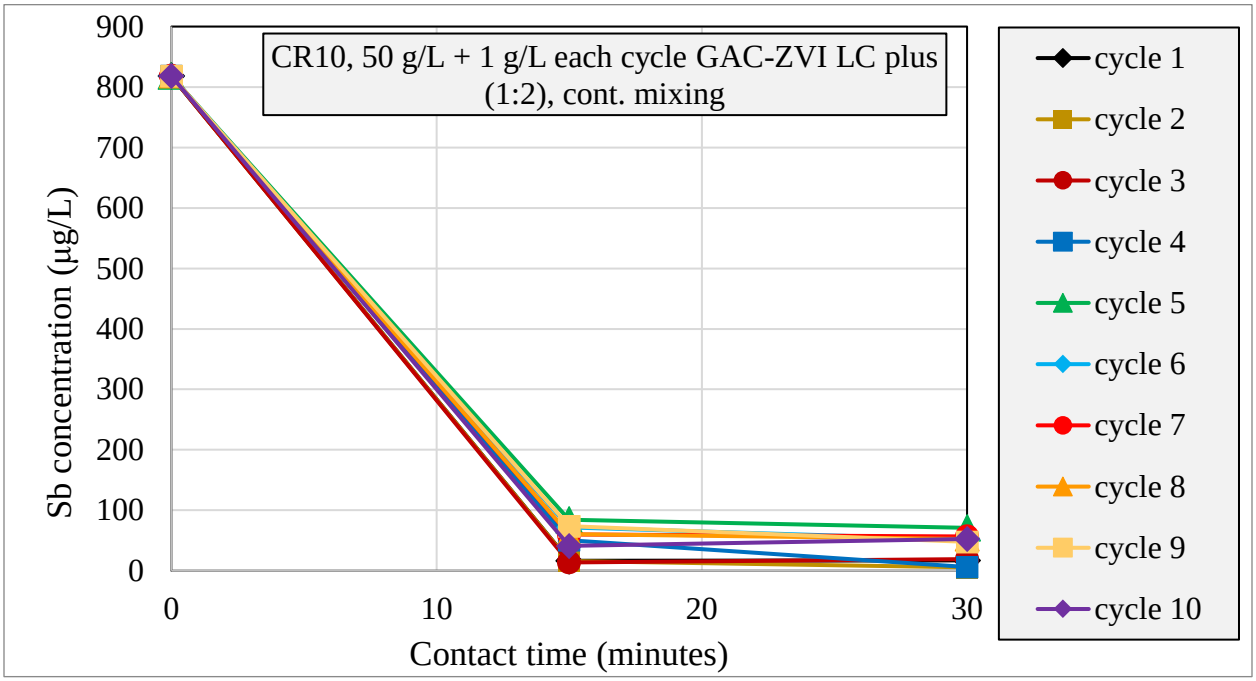

Figure 74 (Sb) - Comparison of ME treatment results for repeated sample loading cycles: 10 cycles using 50 g/L of GAC and ZVI LC plus and adding 1 g/L per cycle to treat 10 loads of 500 mL SR16 LFG condensate

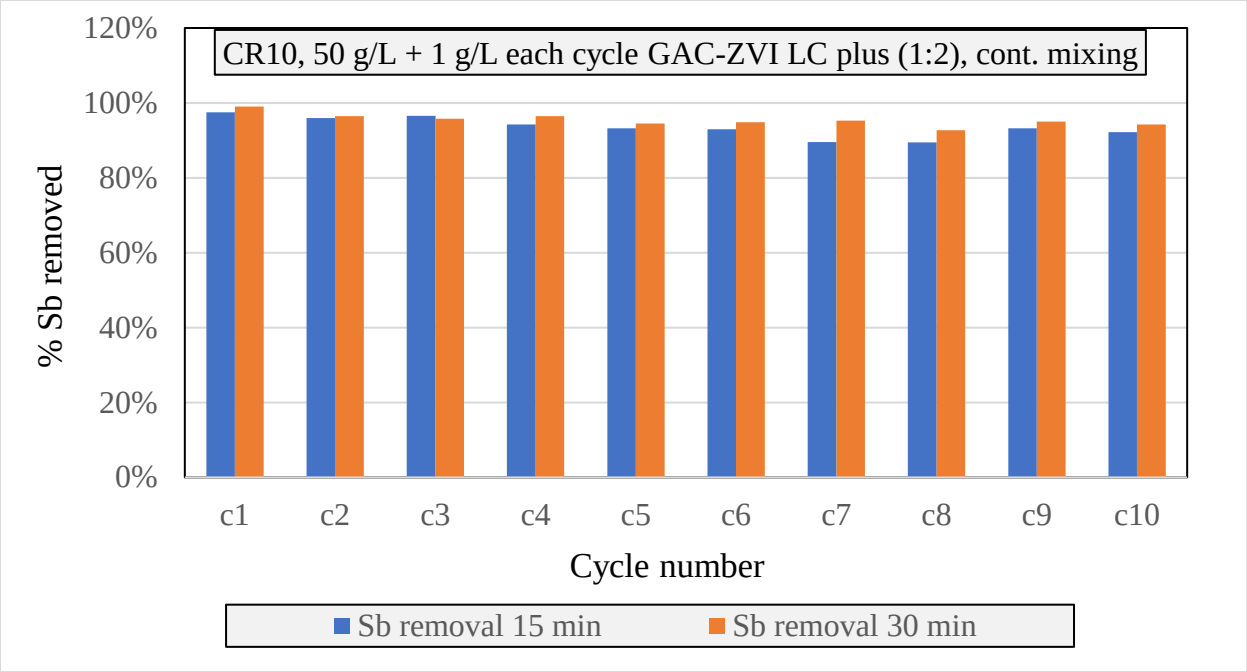

Figure 75 - Sb removal efficiency for repeated sample loading cycles: 10 cycles using 50 g/L of GAC and ZVI LC plus and adding 1 g/L per cycle to treat 10 loads of 500 mL SR16 LFG condensate

In the case of the 50 g/L initial dosage experiments, the first six cycles achieved an As removal efficiency of over 80%, while the subsequent four cycles resulted in decreasing active media performance each subsequent cycle. In contrast, when adding 1 g/L of the active media per cycle to the initial 50 g/L dosage, the As removal efficiency remained above 80% for all cycles, except for cycle eight, which may be attributed to an analytical error. However, for both cases, antimony removal efficiency exceeded 90% in every cycle.

These results suggest the possibility of reusing the active media for a longer period than originally anticipated. Further investigation is required to determine the maximum number of sample loadings that the active media can withstand.

Given the high removal efficiency observed in the previous experiment with ten cycles, a follow-up experiment was conducted to assess the impact of intermittent mixing on treatment

performance. In this experiment, the same conditions were maintained, but with a cycle of 2.5 minutes of mixing followed by 5 minutes of quiescence. The experiment was conducted over five cycles, and the results are presented in Figure 76 to Figure 79.

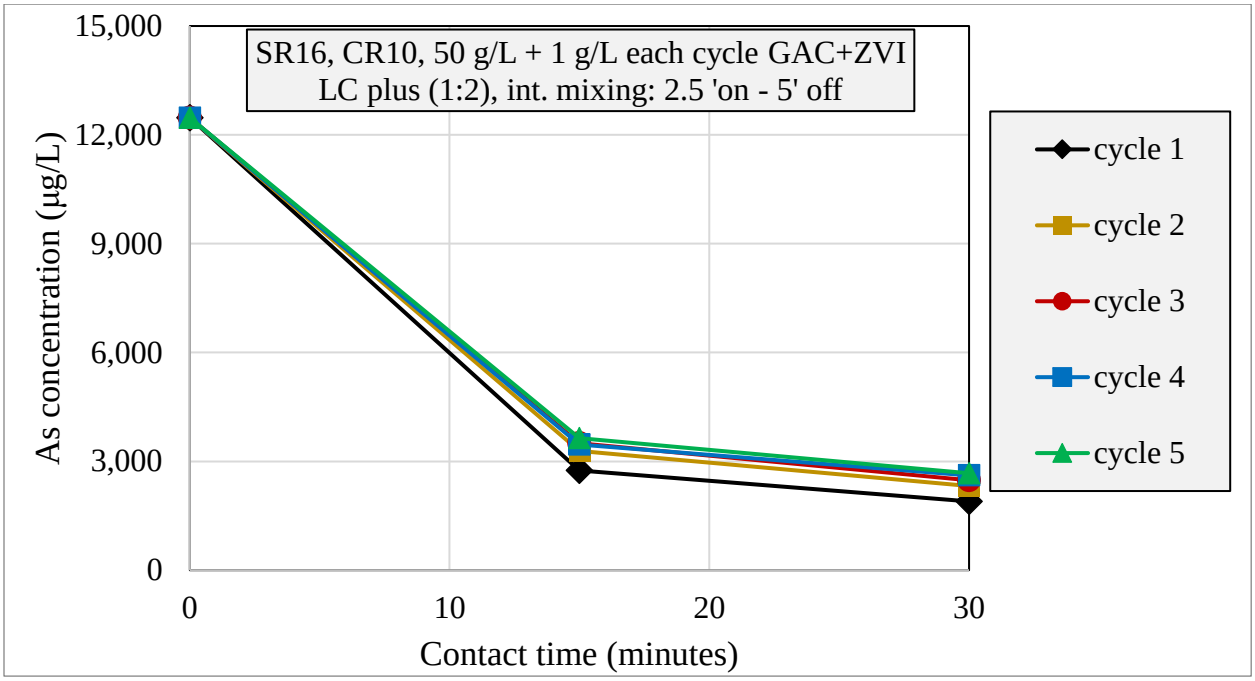

Figure 76 (As) - Comparison of ME treatment results for repeated sample loading cycles: 5 cycles using 50 g/L of GAC and ZVI LC plus and adding 1 g/L per cycle to treat 10 loads of 500 mL SR16 LFG condensate using an intermittent mixing configuration (2.5 minutes on - 5 minutes off)

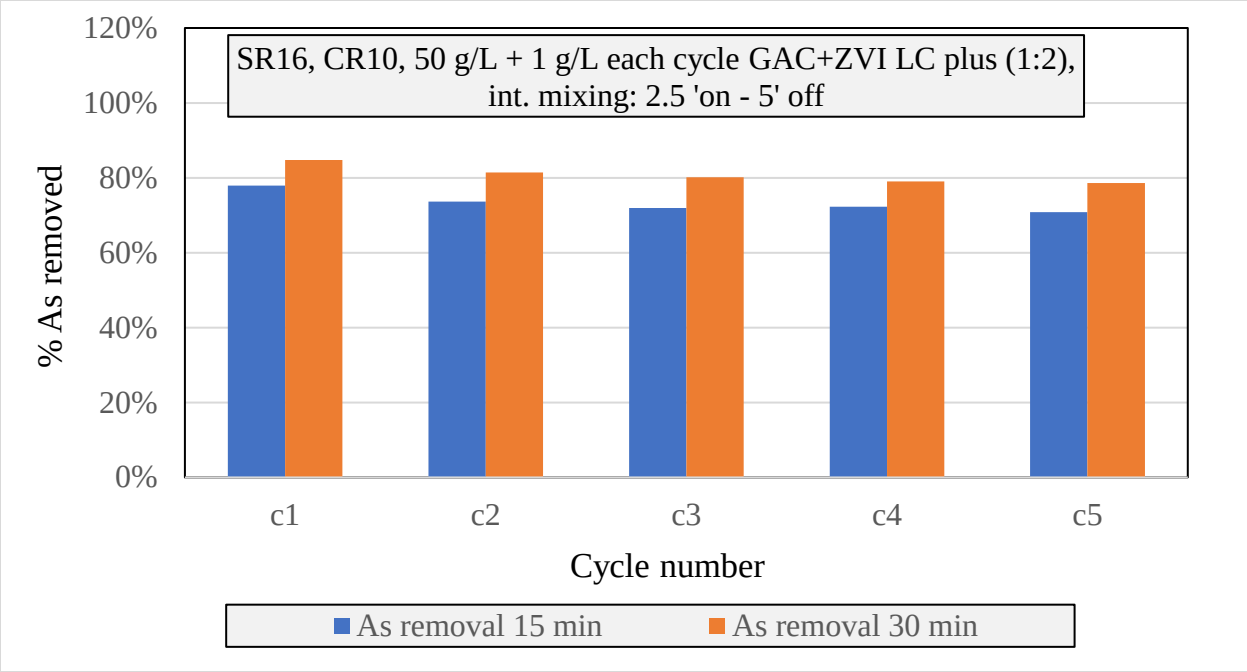

Figure 77 - As removal efficiency for repeated sample loading cycles: 5 cycles using 50 g/L of GAC and ZVI LC plus and adding 1 g/L per cycle to treat 10 loads of 500 mL SR16 LFG condensate using an intermittent mixing configuration (2.5 minutes on - 5 minutes off)

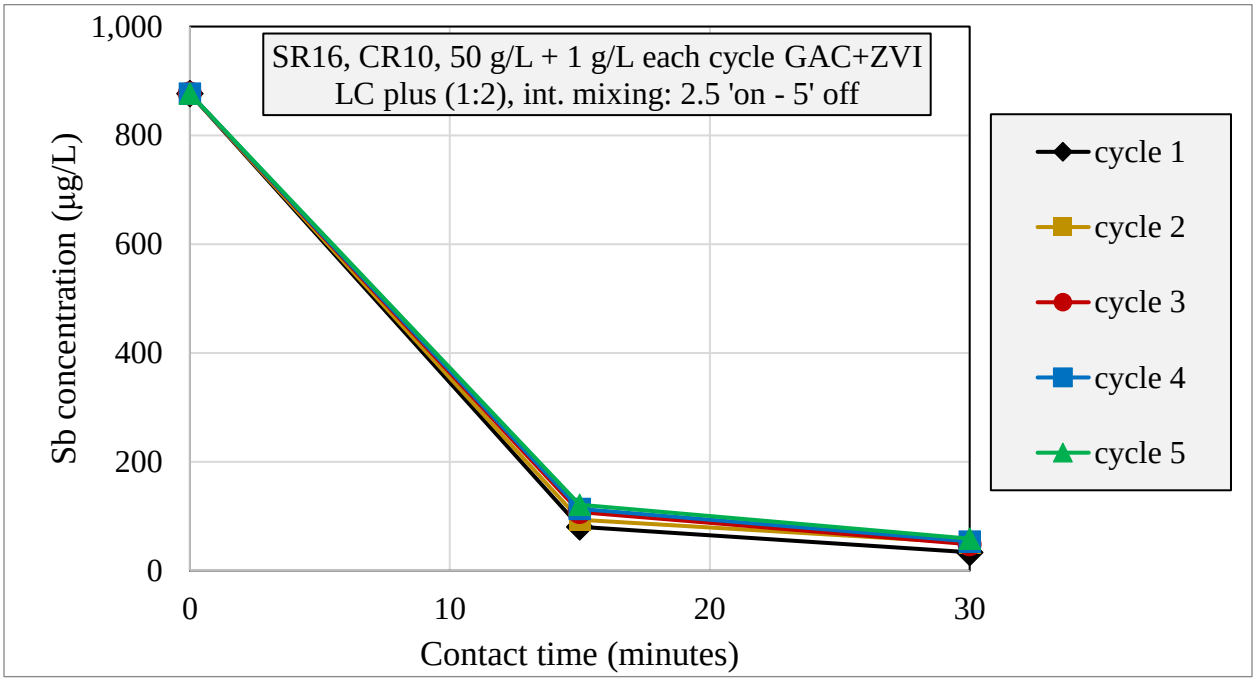

Figure 78 (Sb) - Comparison of ME treatment results for repeated sample loading cycles: 5 cycles using 50 g/L of GAC and ZVI LC plus and adding 1 g/L per cycle to treat 10 loads of 500 mL SR16 LFG condensate using an intermittent mixing configuration (2.5 minutes on - 5 minutes off)

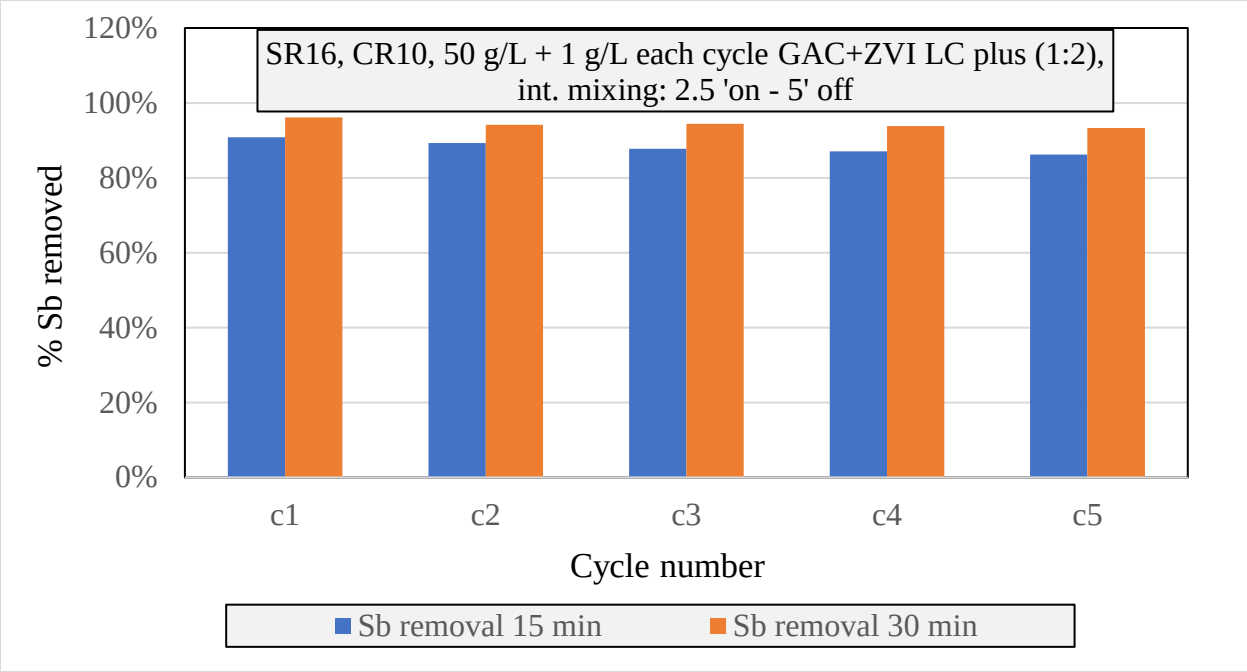

Figure 79 - Sb removal efficiency for repeated sample loading cycles: 5 cycles using 50 g/L of GAC and ZVI LC plus and adding 1 g/L per cycle to treat 10 loads of 500 mL SR16 LFG condensate using an intermittent mixing configuration (2.5 minutes on - 5 minutes off)

The data shown in the figures above indicate that intermittent mixing led to slightly lower removal efficiencies in comparison to continuous mixing for all cycles. Nonetheless, all cycles still exhibited >80% As removal efficiency and >90% Sb removal efficiency.

The findings of this experiment suggest that intermittent mixing can be successfully utilized when a small number of cycles are required. However, further investigation is needed to conduct a trade-off study to evaluate the cost and carbon footprint associated with energy usage between continuous and intermittent mixing, as well as the number of cycles required for efficient treatment.

To further investigate the potential of the treatment process, and considering the results obtained in Figure 44 to Figure 47, a final experiment was conducted using only zero-valent iron (ZVI) cycles with larger particle size ZVI and higher dosages. The experiment involved three cycles with

33.3 g/L of ZVI LC plus (which is equivalent to the mass of ZVI added in a 50 g/L dosage when using it together with GAC). The results of this experiment are presented in Figure 80 to Figure 83.

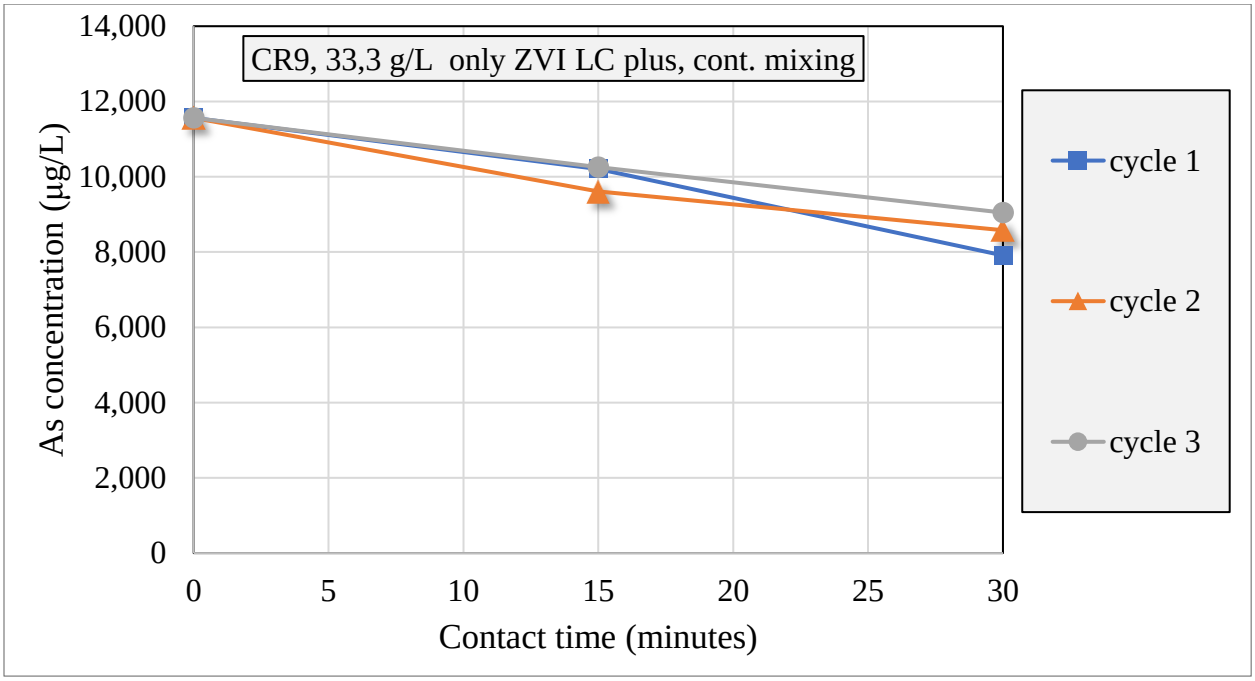

Figure 80 (As) - Comparison of ME treatment results for repeated sample loading cycles: 3 cycles using 33.3 g/L of ZVI LC plus only, to treat 3 loads of 500 mL SR16 LFG condensate using continuous mixing

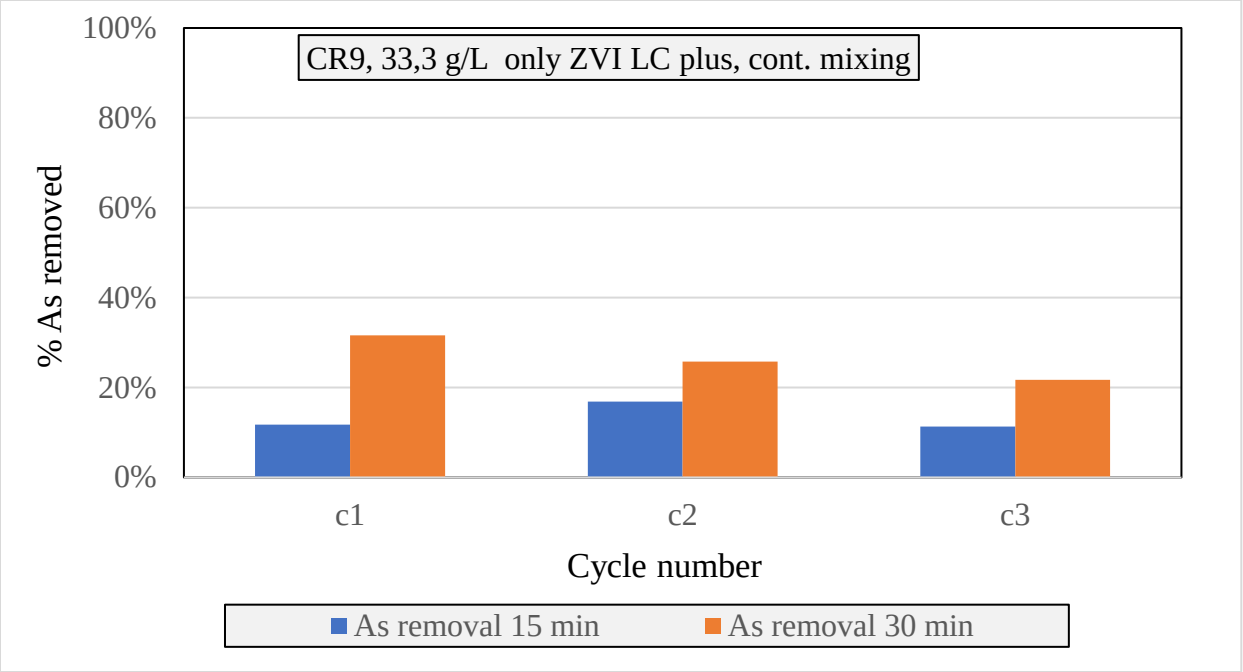

Figure 81 – As removal efficiency for repeated sample loading cycles: 3 cycles using 33.3 g/L of ZVI LC plus only, to treat 3 loads of 500 mL SR16 LFG condensate using continuous mixing

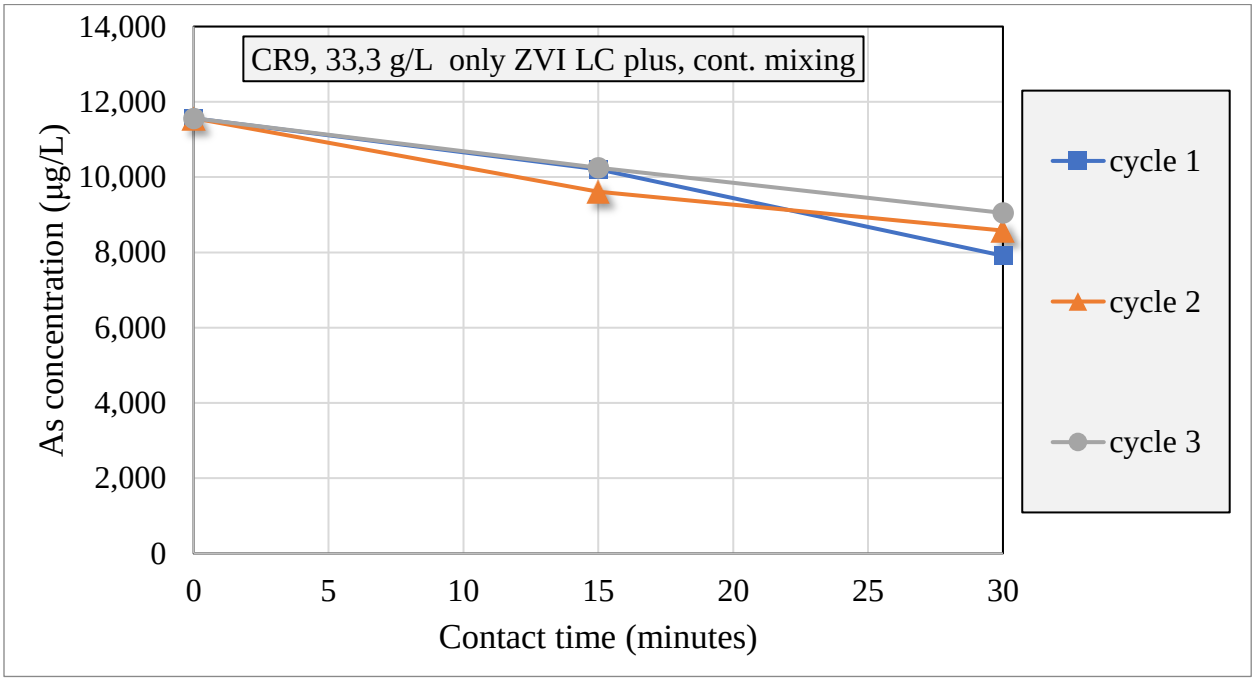

Figure 82 (Sb) - Comparison of ME treatment results for repeated sample loading cycles: 3 cycles using 33.3 g/L of ZVI LC plus only, to treat 3 loads of 500 mL SR16 LFG condensate using continuous mixing

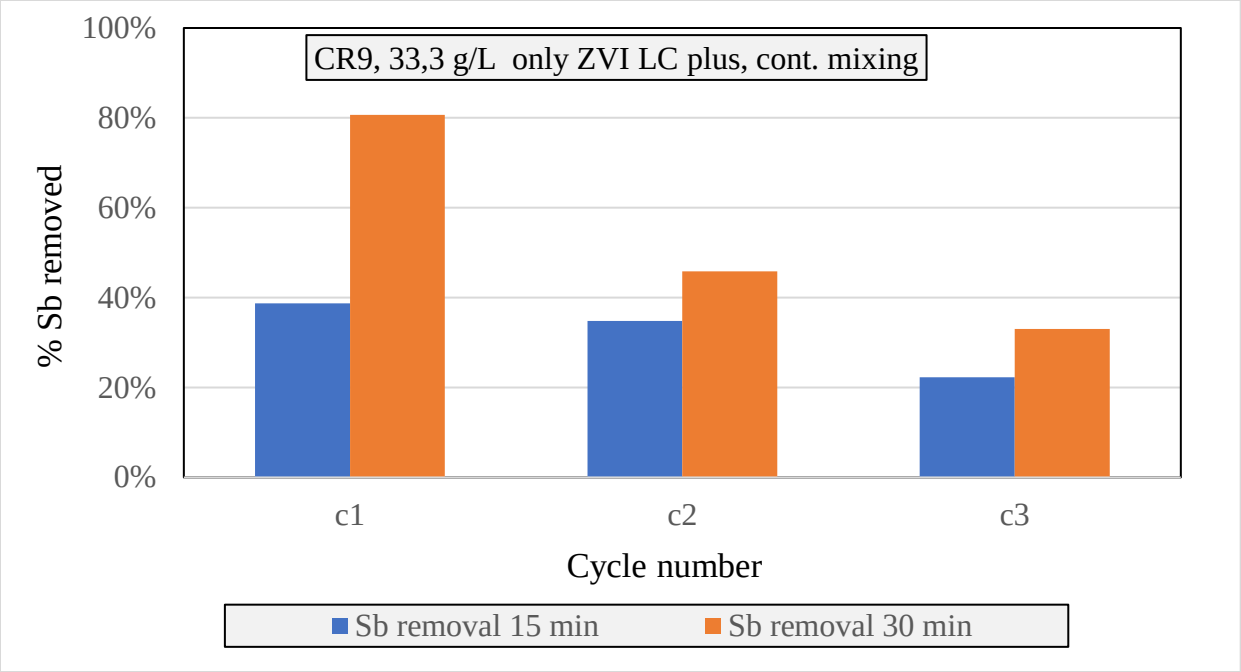

Figure 83 -Sb removal efficiency for repeated sample loading cycles: 3 cycles using 33.3 g/L of ZVI LC plus only, to treat 3 loads of 500 mL SR16 LFG condensate using continuous mixing

The results shown above indicate that all cycles achieved <40% As removal within the initial 30 minutes, with a reduction in efficiency observed in each subsequent cycle. Similarly, antimony removal efficiency exceeded 80% only in the first cycle, with a subsequent decrease in removal efficiency observed in the subsequent cycles.

These findings suggest that while ZVI can contribute to the removal of contaminants, the presence of activated carbon in the reactor is necessary because it significantly enhances the treatment efficiency.

4.7. Effects of temperature variations on As and Sb removal in ME reactors

Considering the variability of environmental conditions in field applications of ME treatment, it is important to ensure the efficacy of the process for temperatures ranging from low temperatures (e.g., 6 C: the reactor was placed outdoors on a winter day) to high temperatures (e.g., 34 C: the

reactor was placed on an environmental chamber). In light of this, experimental investigations were conducted at different temperatures. The results of these tests are illustrated below.

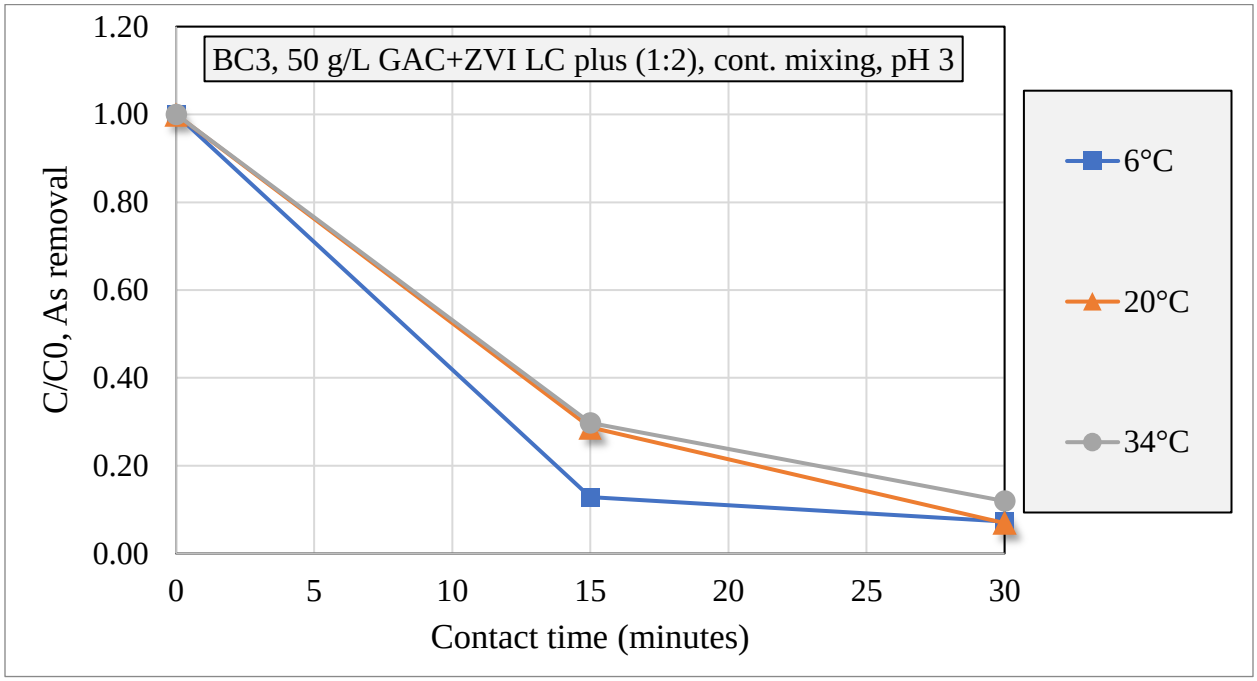

Figure 84 (As) - Comparison of ME treatment at varying temperatures: ME reactor at 6, 20, and 34 Celsius degrees using 50 g/L of GAC and ZVI LC plus, to treat 2 L of SR16 LFG condensate using continuous mixing. Initial As concentration: 25 ppm

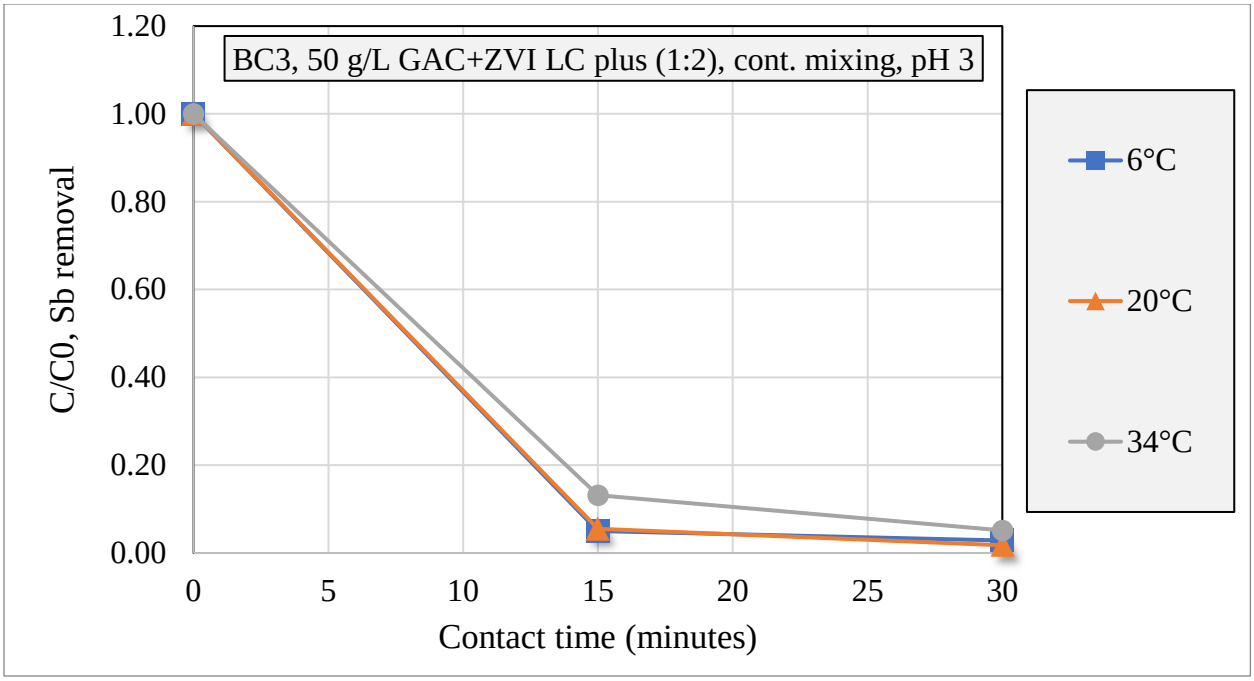

Figure 85 (Sb) - Comparison of ME treatment at varying temperatures: ME reactor at 6, 20, and 34 Celsius degrees using 50 g/L of GAC and ZVI LC plus, to treat 2 L of SR16 LFG condensate using continuous mixing. Initial Sb concentration: 1.2 ppm

The results indicate that while variations of ambient temperature did not result in pronounced changes of the rate of As/Sb removal, it was slightly better for lower temperatures. The findings suggest that the ME treatment method can effectively withstand temperature variations when treating landfill gas condensates and as such, the ME treatment can maintain excellent removal efficiency throughout the year.

4.8. Effects of reactor headspace on As/Sb removal in ME reactors

Based on the experimental results presented in the preceding sections of this thesis, the presence of oxygen in the system hinders the ME treatment process. Consequently, several experiments were conducted to evaluate the impact of residual oxygen on arsenic and antimony removal efficiency. The hypothesis was that the presence of residual oxygen in the system would be proportional to the size of the headspace in the ME column reactor.

The experiments were conducted using sample volumes of 3 L, 2 L, 1 L, 500 mL, and 250 mL in a large column reactor (BC3), under conditions of continuous mechanical mixing, no CO_2 gas flow, 50 g/L of GAC (mesh 12-40 - diameter between ~638 and ~1,700 µm, as shown in Figure *9*) and ZVI LC plus (53% of the particles have mesh 60 - diameter ~ 338 µm, as shown in Figure *7*), and pH 3. The figures below present the results.

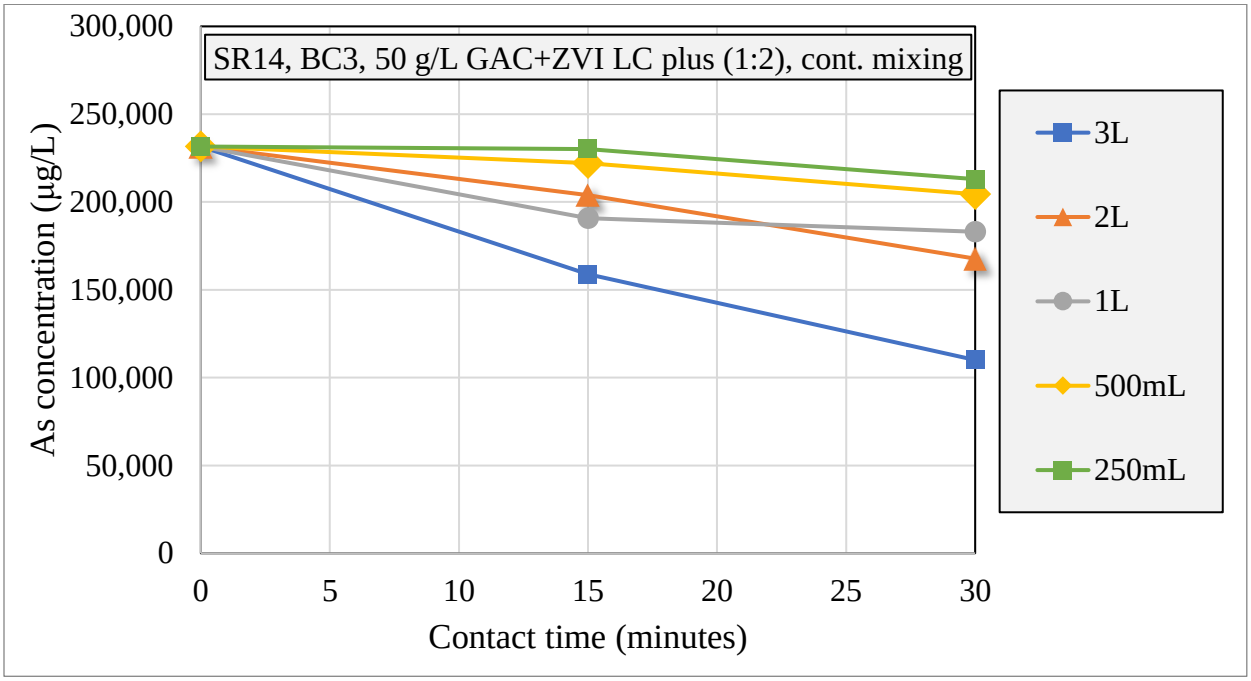

Figure 86 (As) - Comparison of ME treatment results for reactor headspace variations: ME reactor using 50 g/L of GAC and ZVI LC plus, to treat 3 L, 2 L, 1 L, 500 mL, and 250 mL of SR14 LFG condensate using continuous mixing

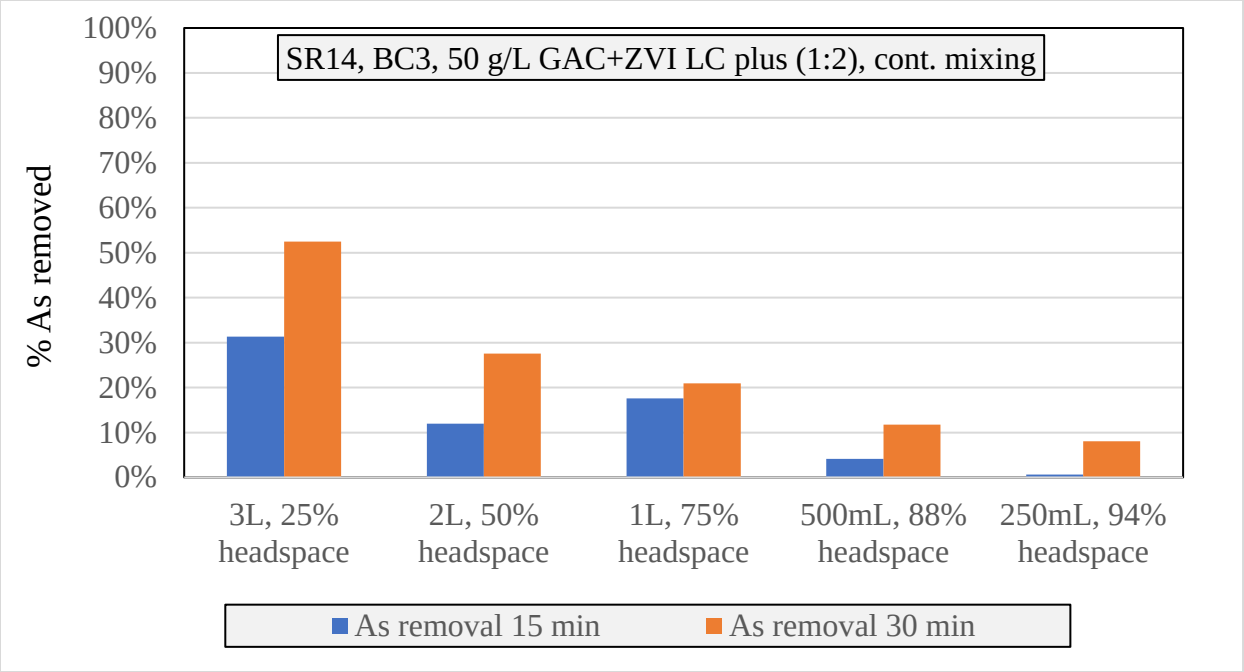

Figure 87 - As removal efficiency for different headspace in the reactor: ME reactor using 50 g/L of GAC and ZVI LC plus, to treat 3 L, 2 L, 1 L, 500 mL, and 250 mL of SR14 LFG condensate using continuous mixing

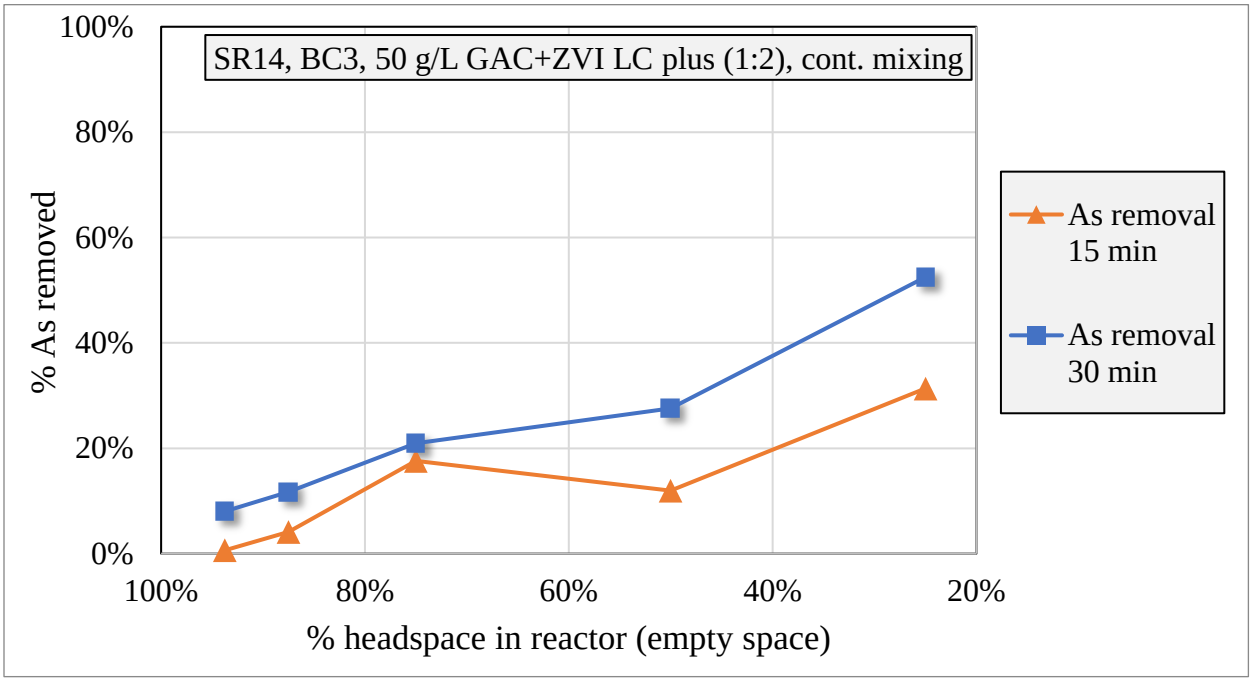

Figure 88 – As removal efficiency and headspace percentage in the reactor relation: ME reactor using 50 g/L of GAC and ZVI LC plus, to treat 3 L, 2 L, 1 L, 500 mL, and 250 mL of SR14 LFG condensate using continuous mixing

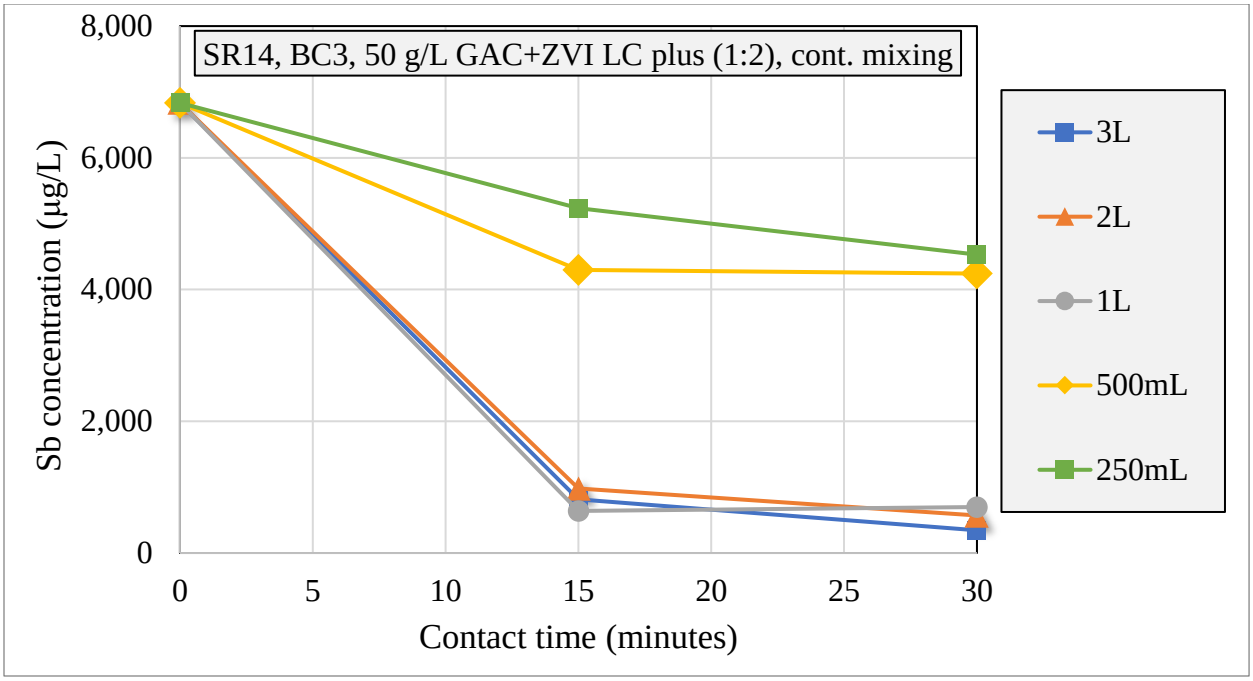

Figure 89 (Sb) - Comparison of ME treatment results for reactor headspace variations: ME reactor using 50 g/L of GAC and ZVI LC plus, to treat 3 L, 2 L, 1 L, 500 mL, and 250 mL of SR14 LFG condensate using continuous mixing

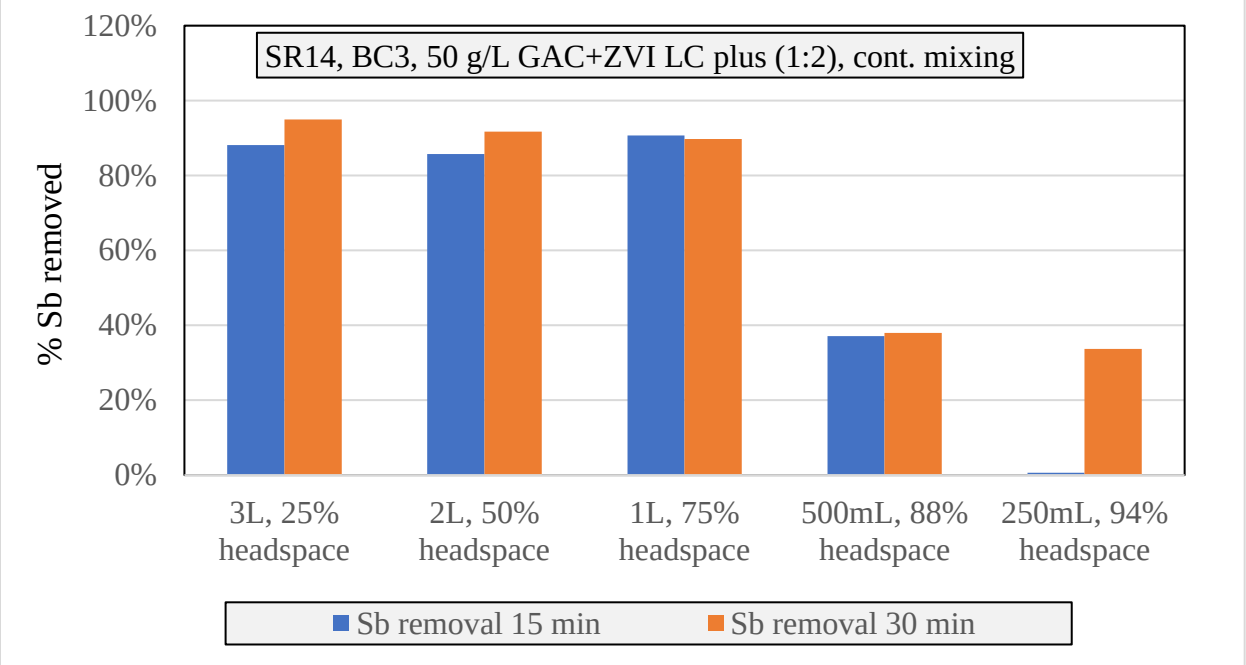

Figure 90 - Sb removal efficiency for different headspace in the reactor: ME reactor using 50 g/L of GAC and ZVI LC plus, to treat 3 L, 2 L, 1 L, 500 mL, and 250 mL of SR14 LFG condensate using continuous mixing

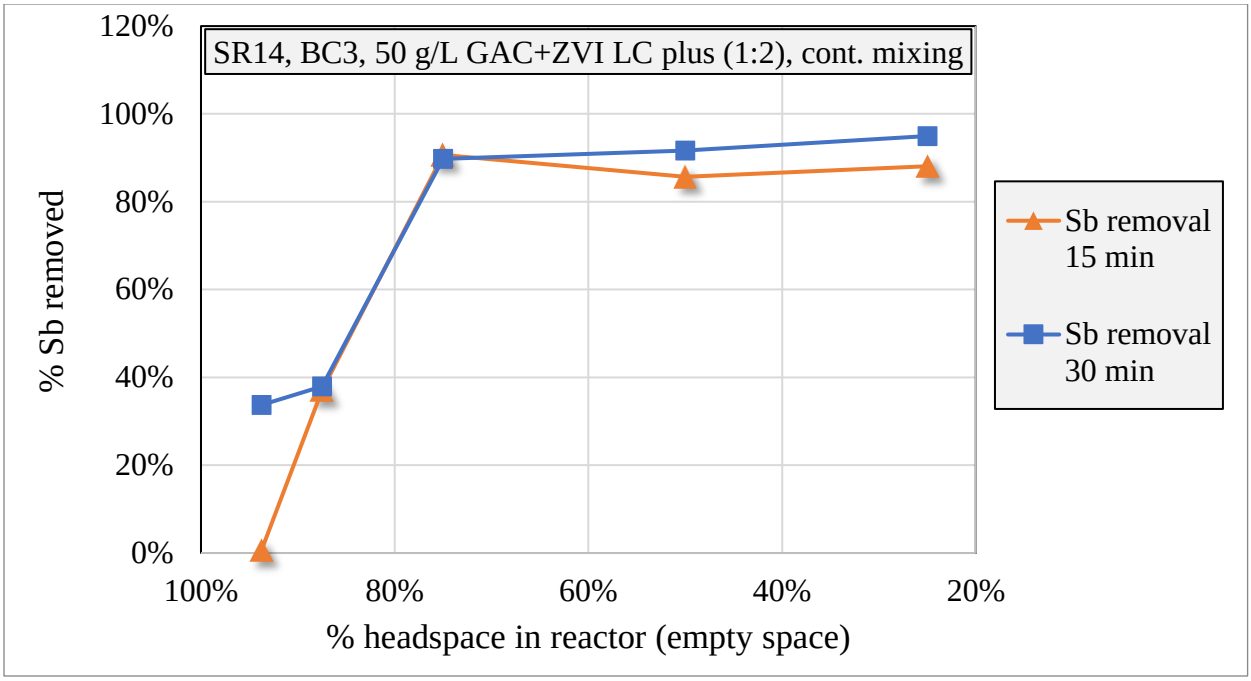

Figure 91 - Sb removal efficiency and headspace percentage in the reactor relation: ME reactor using 50 g/L of GAC and ZVI LC plus, to treat 3 L, 2 L, 1 L, 500 mL, and 250 mL of SR14 LFG condensate using continuous mixing

The experiments were conducted using sample SR14, which had exceptionally high As and Sb concentrations. The results suggest that for such challenging samples, longer treatment times may be required. However, in the 30-minute experiment analysis, the findings reveal that the arsenic removal efficiency exceeds 50% when treating 3 L of sample, but as the sample volume decreased, the treatment efficiency also decreased. Similarly, for antimony, the same trend is observable, but with higher removal efficiencies. These outcomes led to the hypothesis that a larger headspace in the column reactor results in more oxygen being present during the process, leading to reduced removal efficiency (as shown in Figure 11 and Figure 12). Alternatively, these results may be interpreted to indicate that a larger fraction of As/Sb may have volatilized into the headspace. In future research, an analysis will be conducted to assess the amount of As/Sb that might be volatilizing outside of the process. However, the results obtained in these experiments suggest that

a higher efficiency of As/Sb removal can be achieved by filling the reactor at its maximum capacity with LFG condensate.

The potential occurrence of these processes was investigated in the subsequent set of experiments, wherein the same setup was employed but the headspace was flushed with CO_2 at the start of every round to remove the oxygen in the column reactor. The results of these experiments are presented in Figure 92 to Figure 97.

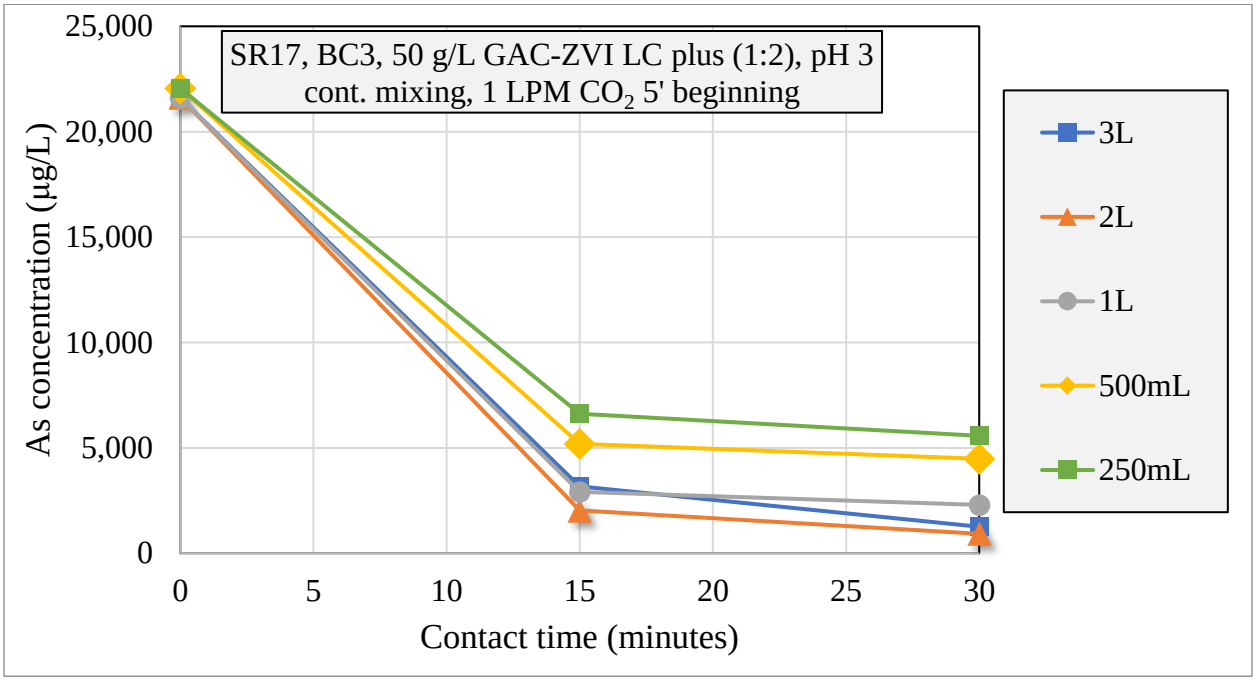

Figure 92 (As) - Comparison of ME treatment results for reactor headspace variations: ME reactor using 50 g/L of GAC and ZVI LC plus, to treat 3 L, 2 L, 1 L, 500 mL, and 250 mL of SR17 LFG condensate using continuous mixing and CO_2 flushing at the beginning of the experiment

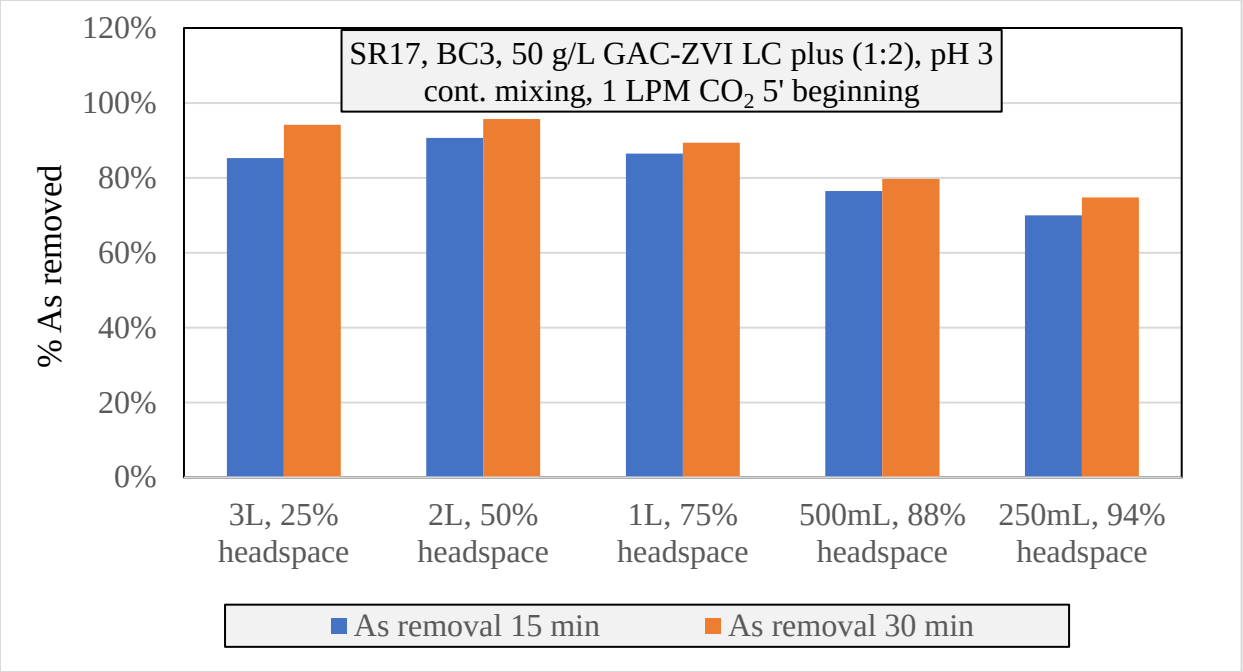

Figure 93 - As removal efficiency for different headspace in the reactor: ME reactor using 50 g/L of GAC and ZVI LC plus, to treat 3 L, 2 L, 1 L, 500 mL, and 250 mL of SR17 LFG condensate using continuous mixing and CO_2 flushing at the beginning of the experiment

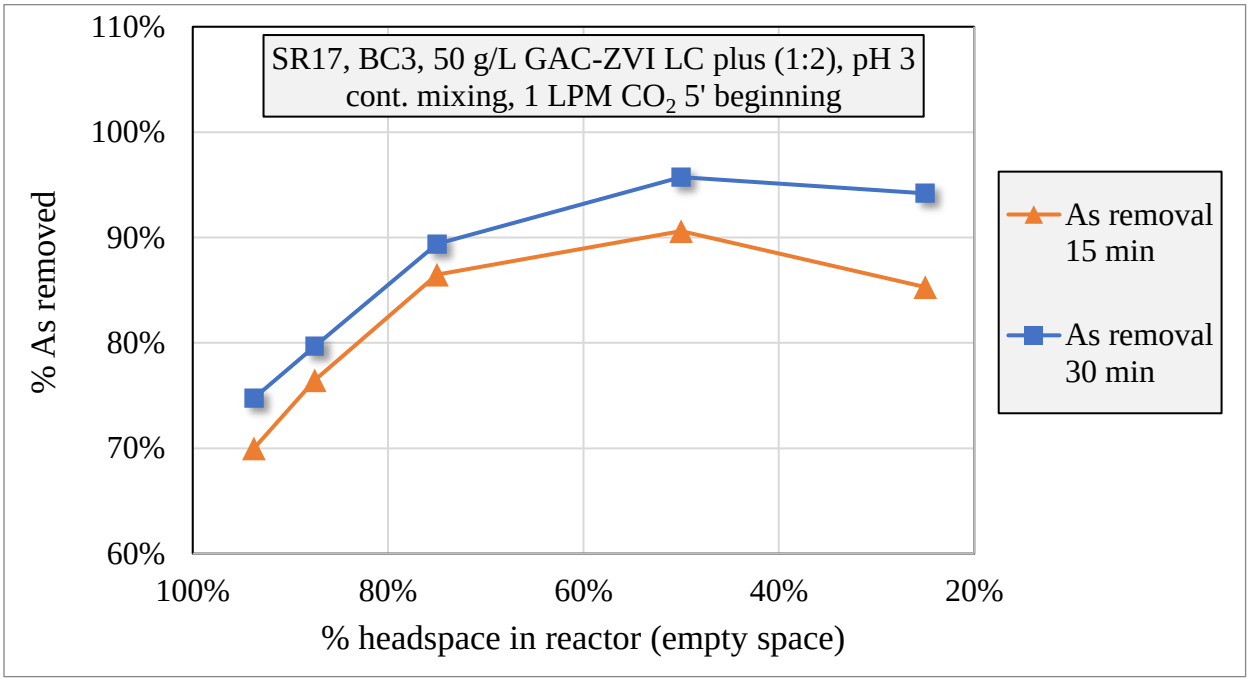

Figure 94 - As removal efficiency and headspace percentage in the reactor relation: ME reactor using 50 g/L of GAC and ZVI LC plus, to treat 3 L, 2 L, 1 L, 500 mL, and 250 mL of SR17 LFG condensate using continuous mixing and CO_2 flushing at the beginning of the experiment

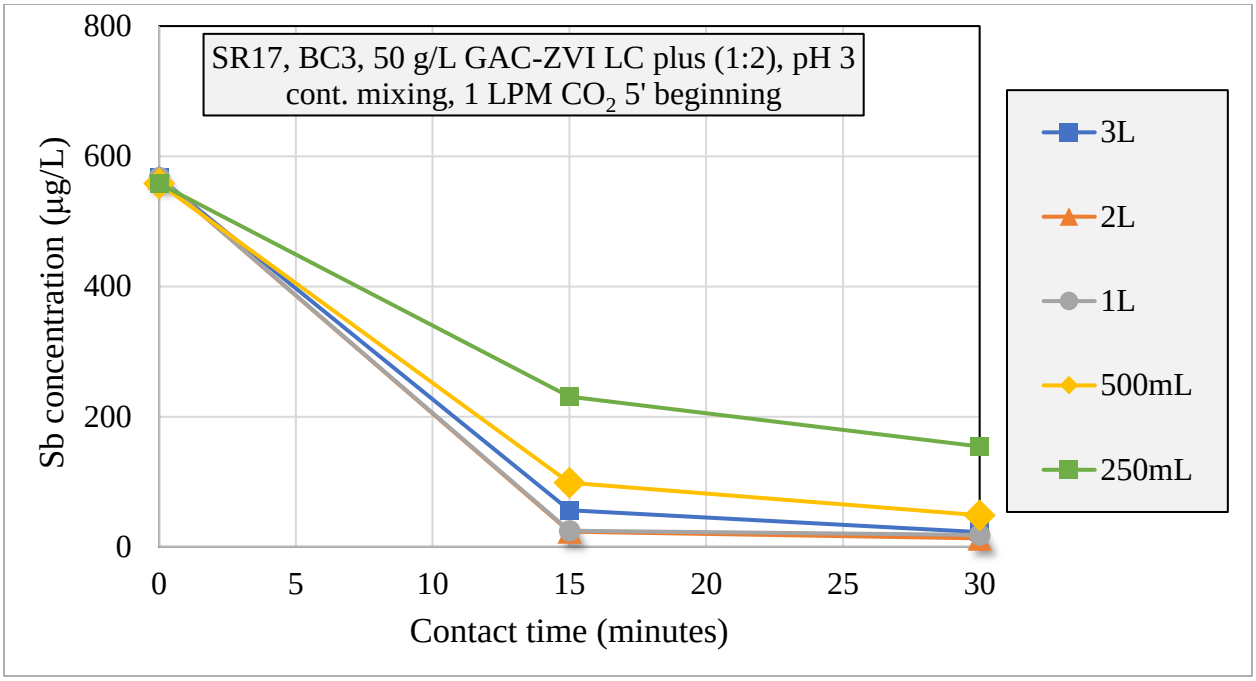

Figure 95 (Sb) - Comparison of ME treatment results for reactor headspace variations: ME reactor using 50 g/L of GAC and ZVI LC plus, to treat 3 L, 2 L, 1 L, 500 mL, and 250 mL of SR17 LFG condensate using continuous mixing and CO_2 flushing at the beginning of the experiment

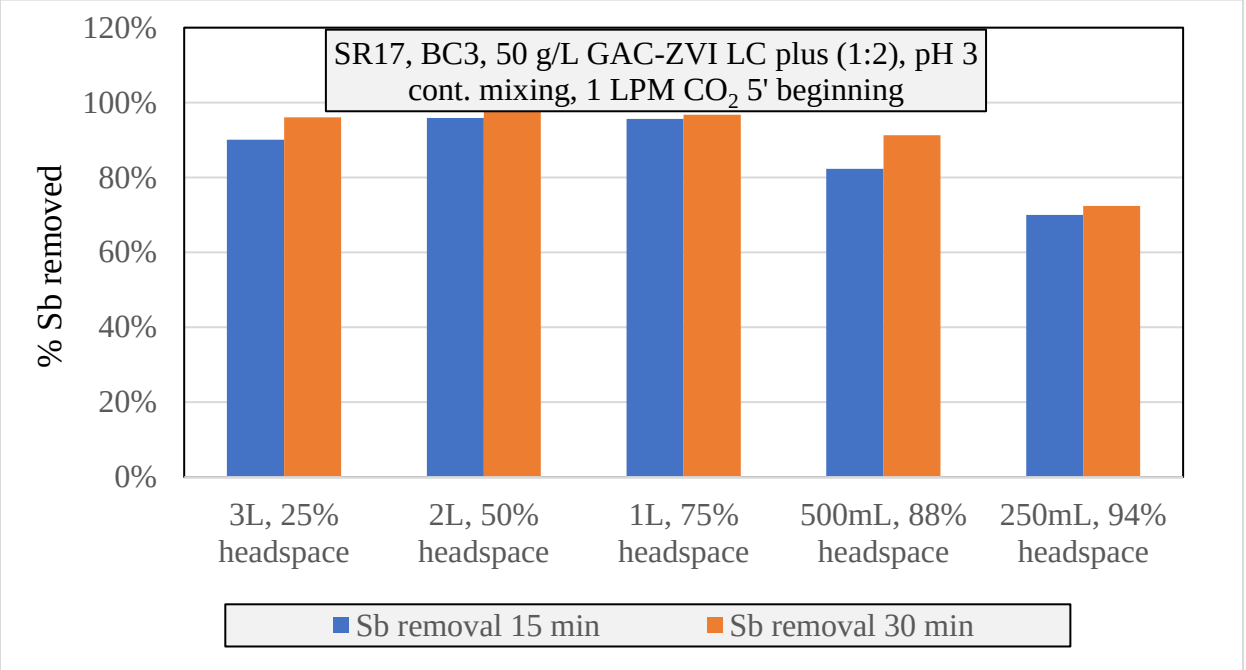

Figure 96 - Sb removal efficiency for different headspace in the reactor: ME reactor using 50 g/L of GAC and ZVI LC plus, to treat 3 L, 2 L, 1 L, 500 mL, and 250 mL of SR17 LFG condensate using continuous mixing and CO_2 flushing at the beginning of the experiment

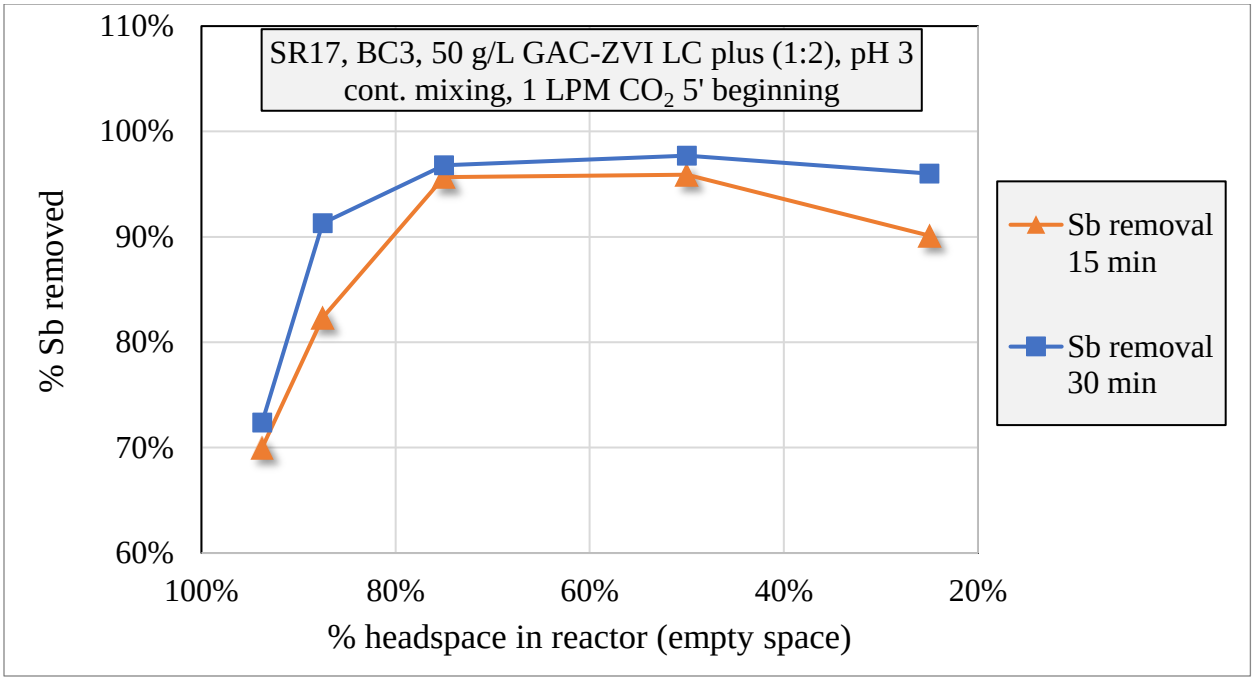

Figure 97 - Sb removal efficiency and headspace percentage in the reactor relation: ME reactor using 50 g/L of GAC and ZVI LC plus, to treat 3 L, 2 L, 1 L, 500 mL, and 250 mL of SR17 LFG condensate using continuous mixing and CO_2 flushing at the beginning of the experiment

The experiments were conducted using sample SR17, which differs from SR14 in that it has lower initial concentrations of arsenic and antimony (Initial As concentrations: SR14 =200 ppm, SR17=9.5 ppm; Initial Sb concentrations: SR14 =9.7 ppm, SR17=0.6 ppm). This is an important point to consider as the use of a different sample may introduce some variability in the results.

The findings of these experiments reveal that, similar to the headspace experiment without CO_2, the removal efficiency of both arsenic and antimony decreases somewhat as the sample volume decreases (or the headspace increases proportionally). However, the removal efficiency for both elements exceeded 70% across all five experiments. Because the removal efficiency was faster and more effective than in the previous experiments conducted using all volumes of sample, these results suggest that the presence of even traces of residual oxygen in the headspace reduces the efficiency of the microelectrolysis treatment. This also demonstrates that As/Sb volatilization is

unlikely to have a significant role in As/Sb removal in ME reactors that employ relatively high ZVI/GAC doses, short reaction times and mechanical mixing. These aspects of ME treatment were examined in more detail in the experiments concerned with the mass balance of As and Sb in ME treatment.

5. Arsenic mass balance experiments

The mass balance experiments were performed to determine the distribution of the retained arsenic in the solid ZVI/GAC active media. To achieve this objective, several rounds of measurements were carried out, with their conditions elaborated at each sequential round. These experiments are described henceforth in the order in which they were performed.

Sodium hydroxide (NaOH) was initially employed to extract and measure the concentrations of As in the active media (Cheney-Irgens, 2022). The effectiveness of the strong base in removing heavy metals from the active media was evaluated by creating a release profile of the active media in NaOH. The active media used in the base release profile was obtained from the experiments listed below:

1) 2 L of SR16 in a column reactor, with pH 4.5, continuous mixing, and 20 g/L of PAC and ZVI LC plus fine (Results of the removal in Figure 56 and Figure 57).
2) 2 L of SR16 in a column reactor, with pH 7, continuous mixing, and 20 g/L of PAC and ZVI LC plus fine (Results of the removal in Figure 56 and Figure 57).
3) 2 L of SR16 in a column reactor, with pH 3, continuous mixing, and 7 g/L of PAC and ZVI LC plus fine (Results of the removal in Figure 58 and Figure 59).
4) 2 L of SR16 in a column reactor, with pH 3, continuous mixing, and 14 g/L of PAC and ZVI LC plus fine (Results of the removal in Figure 58 and Figure 59).

The ZVI/PAC active media produced in the experiments listed above were separated from the treated effluent using a vacuum filter. Then, 1 g aliquot of the filtered active media was added to 100 mL of 0.1 M sodium hydroxide (NaOH) while still wet. The active media were suspended in the base and agitated for 24 hours. Samples of the supernatant were taken at predefined time intervals. The obtained results are presented in the figures below.

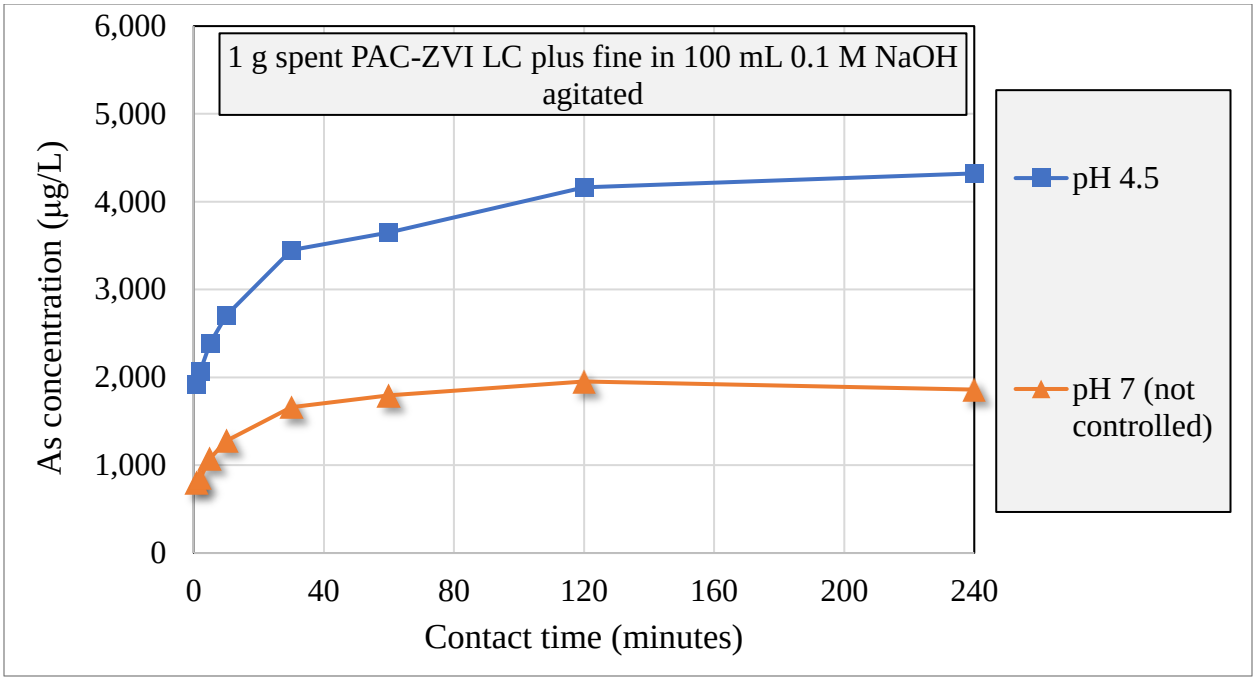

Figure 98 (As) - Release profile from spent PAC / ZVI LC plus fine active media suspended in 100 mL of 0.1 M NaOH agitated up to 24 hours: ME treatments using 2 L of SR16 in a column reactor, with 20 g/L PAC and ZVI LC plus fine, continuous mixing, and pH and 7 (not controlled)

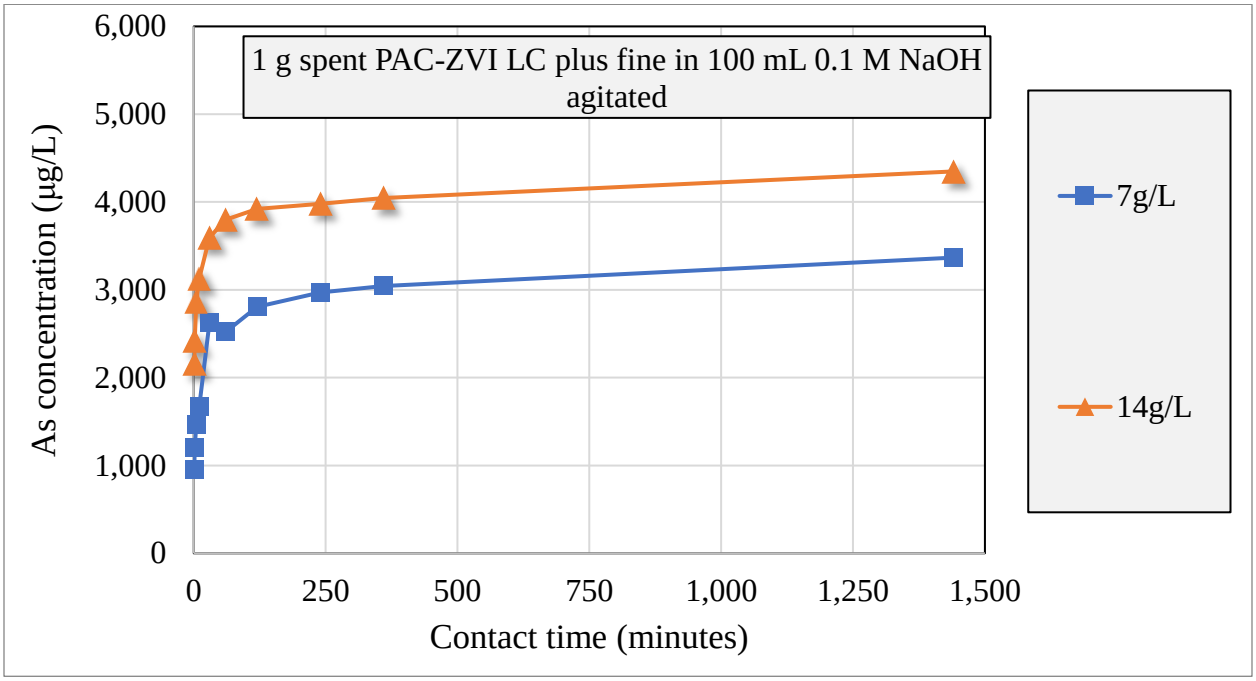

Figure 99 (As) - Release profile from spent PAC / ZVI LC plus fine active media suspended in 100 mL of 0.1 M NaOH agitated up to 24 hours: ME treatments using 2 L of SR16 in a column reactor, pH 3, continuous mixing, and active media dosing of 7 and 14 g/L

The figures above demonstrate that the release of arsenic in the sodium hydroxide reaches a significant percentage of its maximum within four hours.

The figures presented show that it is possible to determine the concentration of arsenic in the spent active media by suspending them in NaOH. The base reaches the peak of As release at 24 hours, but practically all As release takes place within the first four hours. Based on these results, NaOH was selected as the medium to measure the concentration of As in the active media for the subsequent experiments.

Multiple mass balance experiments were carried out using the aforementioned approach, and the most noteworthy outcomes are depicted below. The primary mass balance outcomes were obtained from a 2 L column experiment conducted with SR16 and 20 g/L PAC and ZVI LC plus fine (1:2), pH 3, and different mixing configurations (the As removal results in which the active media were obtained are shown in Figure 54). The mass balance was obtained from the calculation of the mass of arsenic removed from the LFG condensate and comparing that with the estimated mass found in the strong base. The results are shown in Figure 100 (Data in Table 4, Appendix 9.1).

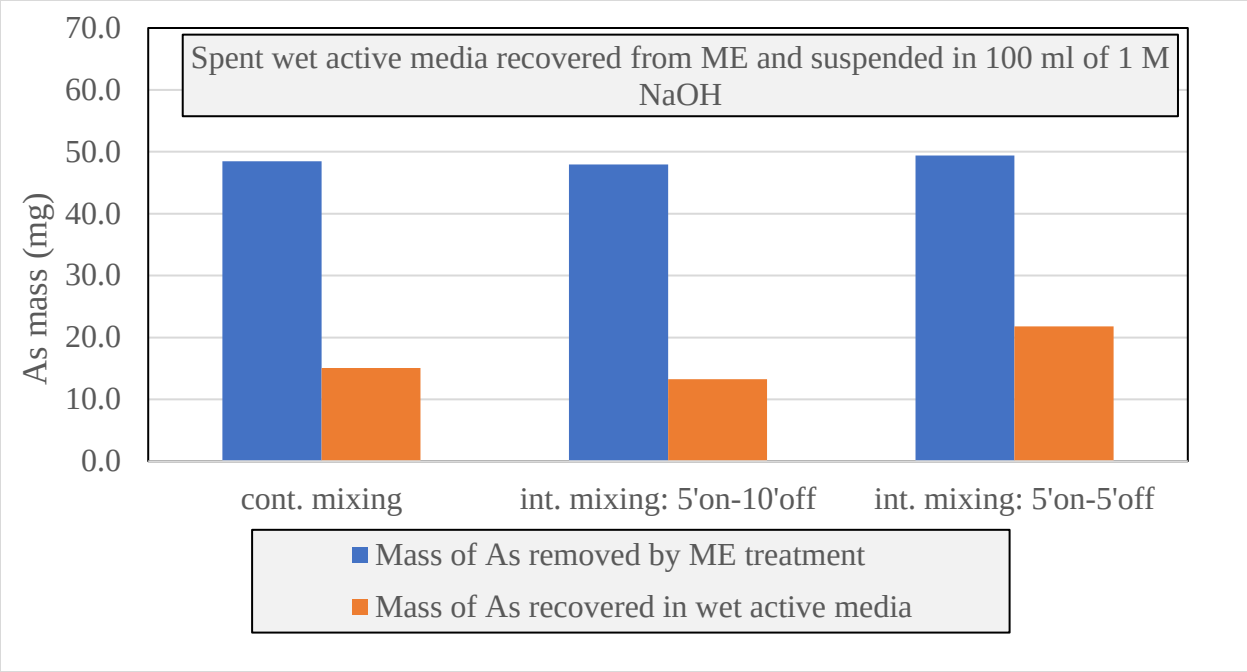

Figure 100 - Mass balance experiment results: Spent wet active media recovered from ME treatment suspended in 100 mL of 1 M NaOH. Experiment details: 2 L of SR16 treated with 20 g/L PAC- ZVI LC plus, and pH 3 (For As initial and final concentrations in the ME process, see Figure 54)

Figure 100 show that the mass of As recovered (orange bar) is less than 40% that the mass of As removed by ME (blue bar) for the three experiments. The outcomes presented in Figure 100 are indicative of multiple of the column reactor experiments, where typically <40% of the arsenic mass extracted during the treatment were recovered/released by the active media in NaOH.

Subsequently, a set of experiments dedicated exclusively to mass balance closure was carried out after obtaining similar results from repeated experiments. A few theories are proposed to explain why the arsenic eluted by the strong base did not account for 100% of the retained As. These theories included: 1) non-uniform distribution of arsenic in the active media. The sample taken after treatment (1 g out of 40 g) is not representative enough; 2) incomplete release of arsenic in NaOH; and 3) volatilization of arsenic from the column reactor and system.

To confirm the first point regarding the non-uniform distribution of arsenic in the active media, three experiments were performed by adding 200 mL of LFG condensate sample to an Erlenmeyer flask, and applying the same operational conditions used in the column reactor experiment: pH 3 controlled with 1 M sulfuric acid and 20 g/L of PAC and ZVI LC plus fine. The active media from each experiment were then retrieved and placed in three separate flasks: 1) 4g of active media in 100 mL of 0.1 M NaOH; 2) 4g of active media in 100 mL of 1 M NaOH; and 3) 1 M NaOH passed through 4g of active media while in the vacuum filter.

The outcomes of the mass balance experiment are presented in Figure 101 (Data in Table 5, Appendix 9.1).

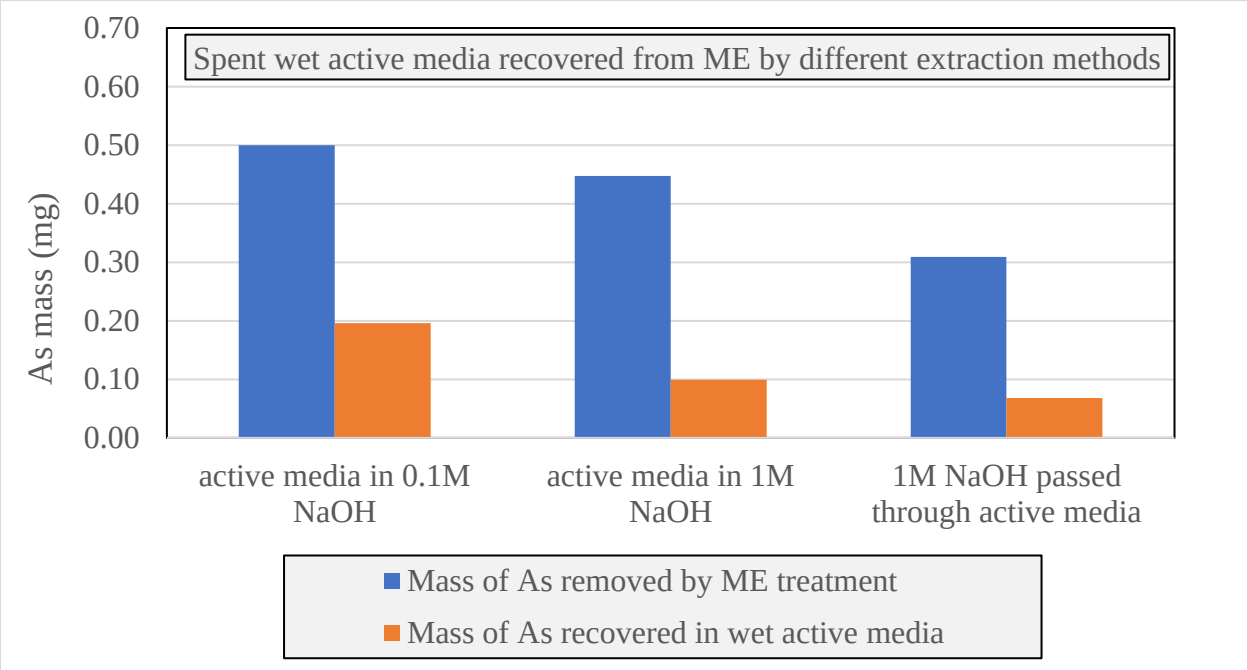

Figure 101 - Mass balance experiment results: Spent wet active media recovered from ME treatment suspended in 100 mL of 1 M NaOH, 0.1 M NaOH and passing 1 M NaOH over the spent active media. Experiment details: 200 mL of SR16 treated in a beaker with 20 g/L PAC- ZVI LC plus fine, pH 3, and continuous mixing

The results shown in Figure 101 did not demonstrate an appreciable improvement compared to those conducted in the column reactors shown in Figure 100. These results indicate a low efficiency in removing arsenic in the Erlenmeyer flask whose shape was not optimized for ME reactions. Nevertheless, a high removal efficiency is not necessary to calculate the mass balance.

The mass balance results indicate that, regardless of the extraction method used with NaOH, the retention/release of arsenic mass was < 40% for all experiments. These findings, along with other experiments performed, prompted the team to explore an alternative approach for measuring the amount of arsenic in the active media. Two crucial elements for mobilizing arsenic from the active media to a strong acid or base include an elevated temperature, and vigorous agitation. After considering various options, the team decided to utilize microwave digestion with a strong acid as extracting solvent.

To carry out the microwave digestion (MWD), an Anton Paar Microwave Reaction System was employed. The SR14 headspace experiment active media samples were used for the analysis (As removal results shown in Figure 86). To perform the digestion, 0.05g of wet active media were suspended in three tubes containing 10 mL of concentrated HNO_3 (S1, S2, and S3) and one tube containing 10 mL of concentrated HCl. The microwave digestion was performed with eight tubes per batch, at 800W of power, and for a duration of 30 minutes. The samples were extracted from each tube and subjected to ICP-MS analysis. The results are presented in Figure 103. (The corresponding data are summarized in Table 6 and Table 7, Appendix 9.1).

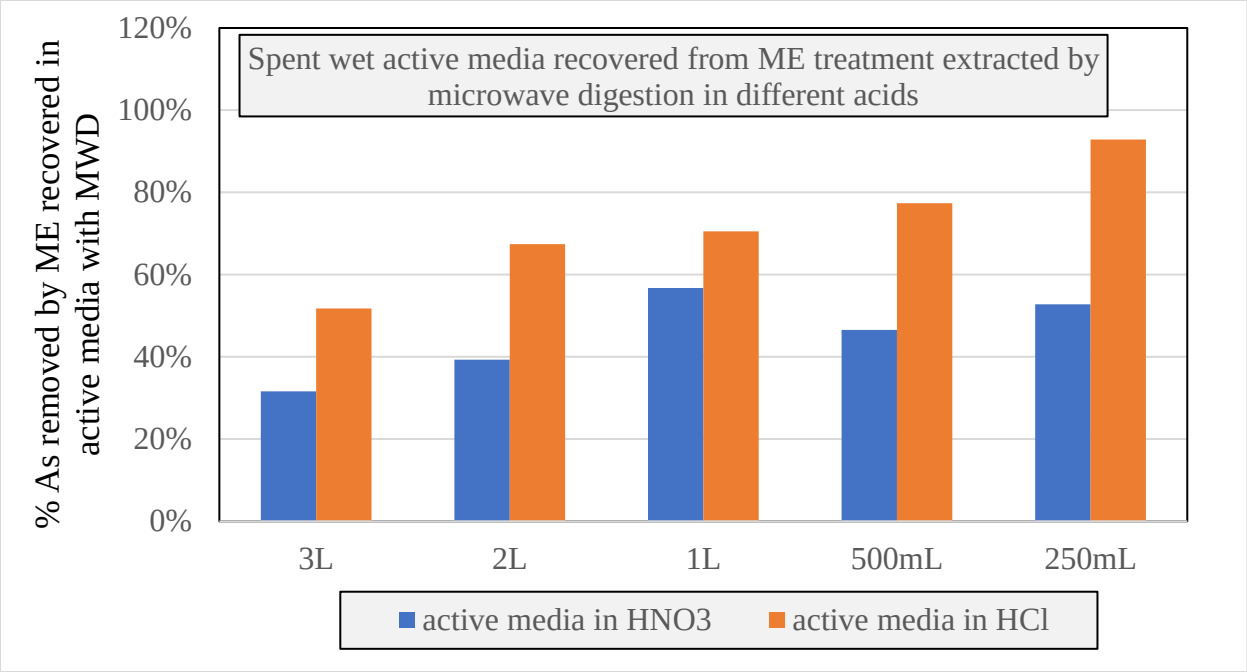

Figure 102 - Mass balance experiment results: Spent active media recovered from ME treatment suspended in 10 mL of concentrated HNO_3 and HCl and exposed to microwave digestion (MWD). Experiment details: Headspace experiments for SR14 treated with 50 g/L GAC- ZVI LC plus, pH 3, and continuous mixing (As removal results in Figure 86)

The results presented in Figure 102 indicate that the arsenic recovery through microwave digestion using HNO_3 are equally effective than agitating the active media in strong base for 24 hours. However, the results showed variation in the S1, S2, and S3 concentrations (see Table 6), which should be similar as they are part of the same process active media. This variability could be attributed to the lack of homogeneity in the active media, as discussed earlier, and is an issue that needs to be addressed in future experiments. On the other hand, the microwave digestion using HCl showed better results for the content of arsenic in the active media.

It is worth noting that the first round of microwave digestion was performed using only wet active media, and the calculation of arsenic concentration was done considering that the 0.05g used were dry and no correction for water content was made. This approach could generate a high probability

of error in the arsenic concentration calculation. To obtain a more accurate result for the next microwave digestion experiments, sufficient aliquots of the spent active media were dried and weighed, and a water correction was done to calculate the As concentration in the active media.

Based on the results presented in Figure 102, a new round of microwave digestion was conducted using only HCl. This time, three samples were used to examine the repeatability of these measurements and to explore the arsenic retention in the active media. The experiments were performed for both wet and dried active media in the headspace with CO_2 experiments to treat SR17 (experiments detailed in Figure 92). The results of these experiments are shown in Figure 103 (Data in Table 8 and Table 9, Appendix 9.1).

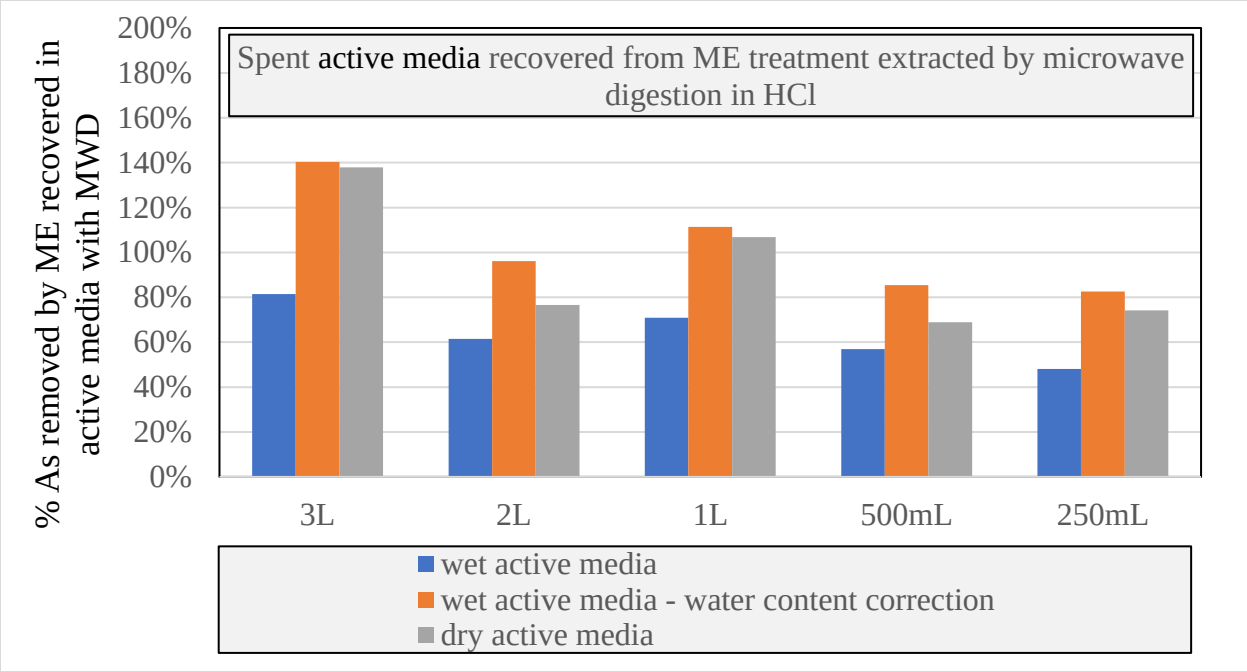

Figure 103 - Mass balance experiment results: Spent active media recovered from ME treatment suspended in 10 mL of concentrated HCl and exposed to microwave digestion. Experiment details: Headspace experiments for 3 L and 2 L of SR17 treated with 50 g/L GAC- ZVI LC plus, pH 3, continuous mixing, and CO_2 flushing at the beginning to push out the oxygen in the reactor (As removal results in Figure 92)

Figure 103 illustrates that the microwave digestion in HCl yields higher average concentrations of arsenic in the active media, and even higher recoveries when considering the corrected water content in the active media. The results presented for the dry active media (red bar in the figures above) are likely more accurate than any previous results as they use the actual amount of active media used in the arsenic release experiments. The percentage being over 100% may be attributed to the lack of homogeneity in the samples, as the 0.05g of active media selected may have had a higher-than-average concentration of As in the active media.

The results obtained when correcting the water content are comparable to the outcomes obtained when suspending 0.05g of pre-dried active media in the HCl microwave digestion (grey bar in the figures above).

These results demonstrate that microwave digestion using HCl is a more effective method for measuring the amount of arsenic in the active media compared to agitating the active media in strong NaOH for 24 hours. The better performance of HCl digestions, compared with the exposures in HNO_3 or NaOH, may be related to the passivation of As solids in the latter digestants, and formation of mobilizable As complexes with chloride ions. The hypothesis needed to be explored in future research, but the current digestion results are clearly indicative of essentially 100% recoveries of the retained As from the used ZVI/activated carbon media. Additionally, the use of dried active media and the correction of water content helped to reduce the error probability in the concentration calculation.

Further experiments are needed to ensure sample homogeneity and accurate mass balance calculations, and to ensure that all the arsenic is retained in the active media during the ME treatment.

6. Examination of changes of redox potential during ME treatment

One of the challenges of ME treatment in pilot-scale or full-scale applications is to find a way to determine changes of the concentration of As and Sb during the process without relying on laboratory tests.

During the experiments, a potential correlation between the redox potential and the removal of As/Sb was observed. It was noted that, for most of the experiments, the redox potential tended to decrease to very negative values when the ME process achieved high As/Sb removal efficiencies. To further investigate this relationship, over fifty ME experiments were analyzed, by measuring redox potential in the LFG condensate bulk at the same time a sample was taken for As/Sb concentration determination. The data was then categorized and examined using statistical tools to establish a mathematical correlation between redox potential and As/Sb concentrations.

This lays the groundwork for further research that will allow to enhance the understanding of the behavior of the redox potential during the ME treatment, and its connection with the extent of As/Sb removal. The potential outcomes of this further research would be highly valuable for operational purposes, as the redox potential can be measured in situ and instantaneously, while analyzing As/Sb concentrations by ICP-MS typically requires a couple of hours. If a correlation between redox potential and As/Sb concentrations is established, it would enable operators to predict the As/Sb concentration in the LFG condensate being treated by simply measuring the redox potential inside the reactor. This predictive capability would be advantageous for real-time monitoring and control of the treatment process. Operators would have a rapid and reliable indicator to assess the efficiency of As/Sb removal without waiting for the results of a time-consuming concentration analysis.

To examine the possible correlation between the concentrations of As/Sb and the redox potential, scatter plots were created using Python through JupyterHub. The scatter plots were prepared by adding data points taken from more than fifty ME experiments. The plots contain the redox potential data in the x-axis and the logarithm in base 10 of the concentration of As/Sb in μg/L in the y-axis. Figure 104 shows the scatter plot used for this analysis.

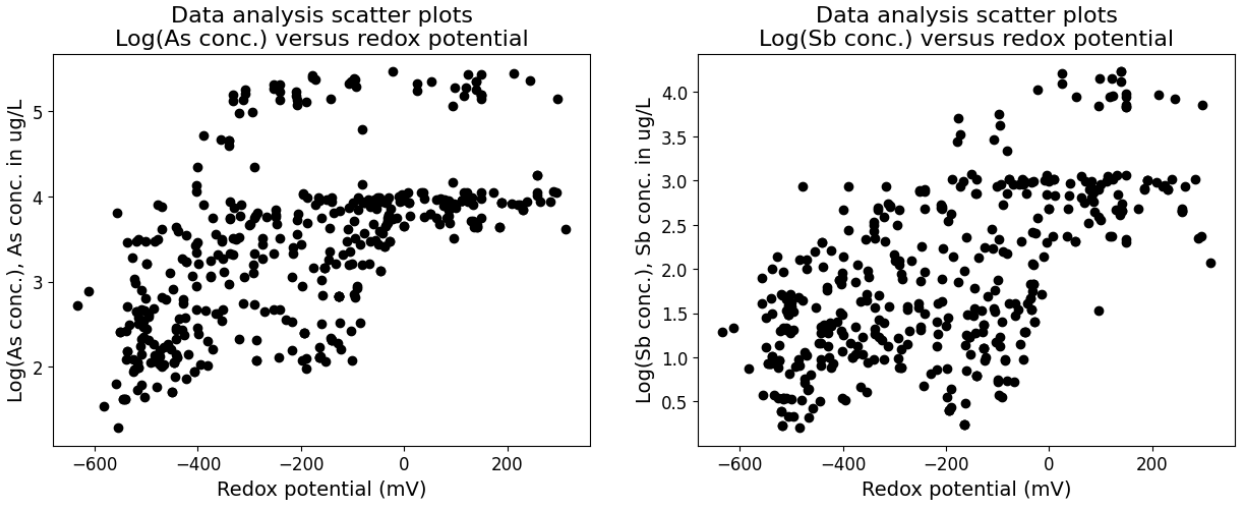

Figure 104 - Logarithm of As and Sb concentrations vs. redox potential scatter plots obtained from multiple ME treatment experiments developed with different samples and operational conditions

From the figure, it is evident that there is an order of magnitude differences between the data points. However, with knowledge of the data and its origin, it can be separated based on the type of sample: SR12, SR13, SR14, and SR15. The scatter plots for each sample can be viewed in Figure 105 to Figure 108.

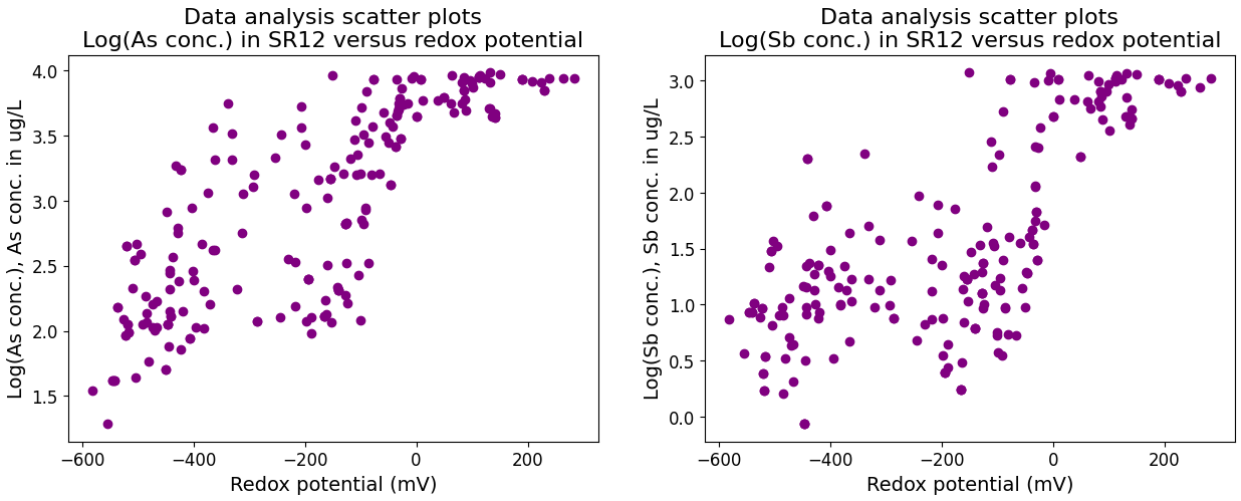

Figure 105 - Logarithm of As and Sb concentrations in SR12 vs. redox potential scatter plots obtained from multiple ME treatment experiments developed with different samples and operational conditions

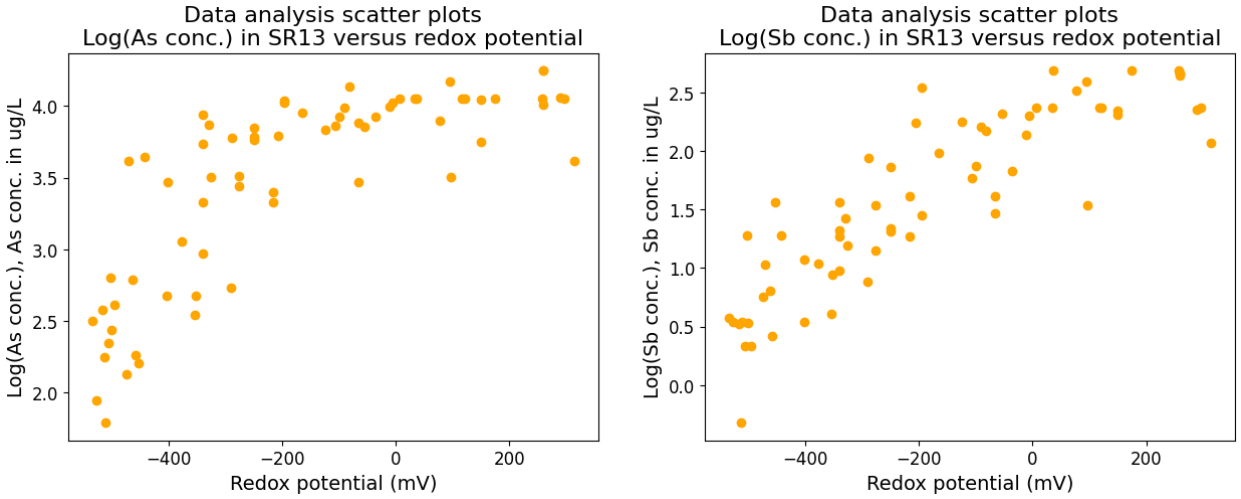

Figure 106 - Logarithm of As and Sb concentrations in SR13 vs. redox potential scatter plots obtained from multiple ME treatment experiments developed with different samples and operational conditions

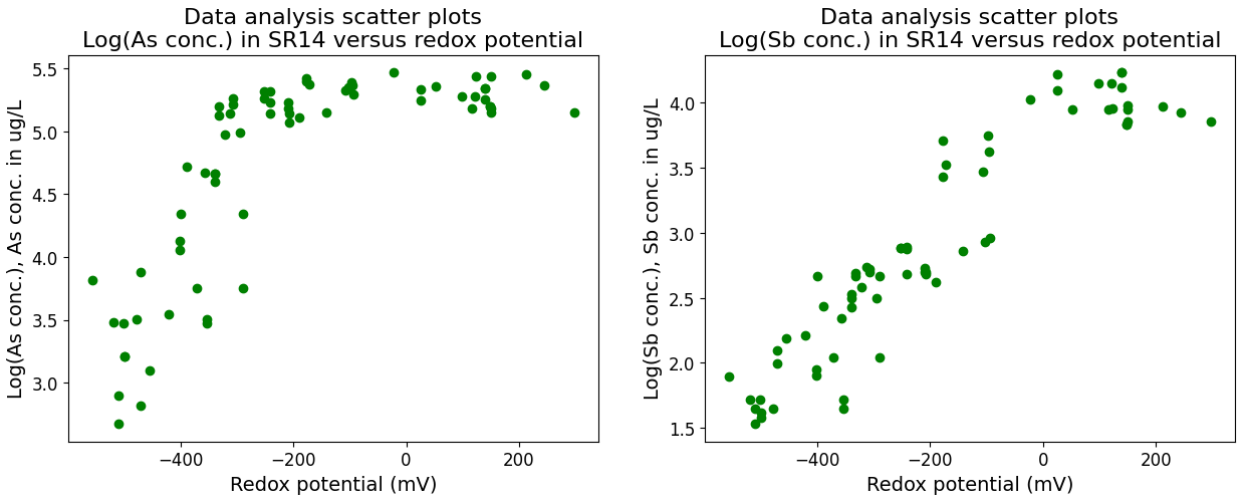

Figure 107 - Logarithm of As and Sb concentrations in SR14 vs. redox potential scatter plots obtained from multiple ME treatment experiments developed with different samples and operational conditions

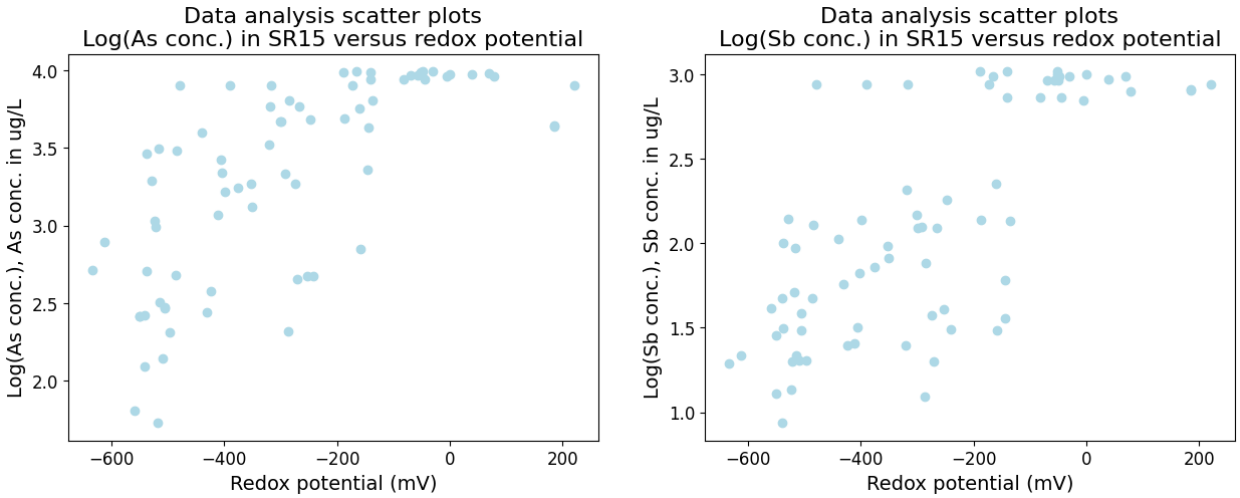

Figure 108 Logarithm of As and Sb concentrations in SR15 vs. redox potential scatter obtained from multiple ME treatment experiments developed with different samples and operational conditions

Once the data was organized based on initial concentration and separated into similar ranges by sample round, three statistical methods were applied to analyze it. These methods included linear regressions, quantile regressions, split-sample analysis, and zonal probability.

6.1. Regressions between As/Sb concentrations and redox potential changes

The first method was applied to test the hypothesis of a linear correlation between redox potential and As/Sb concentrations. To do this, a basic linear least squares regression was used.

For each linear regression, a typical least squares method was utilized, and basic outputs were calculated, including residuals between model-predicted and observed values, sum of squared errors (SSE), sum of squares total (SST), and standard deviation (s). A standard α value of 0.05 was used to establish 2-sided 95% confidence intervals for each regression to assess conformity with the null hypothesis: redox potential and As/Sb concentrations are uncorrelated. Two sample rounds were chosen for linear regression. Figure 109 below shows the results of the linear regressions performed on the data.

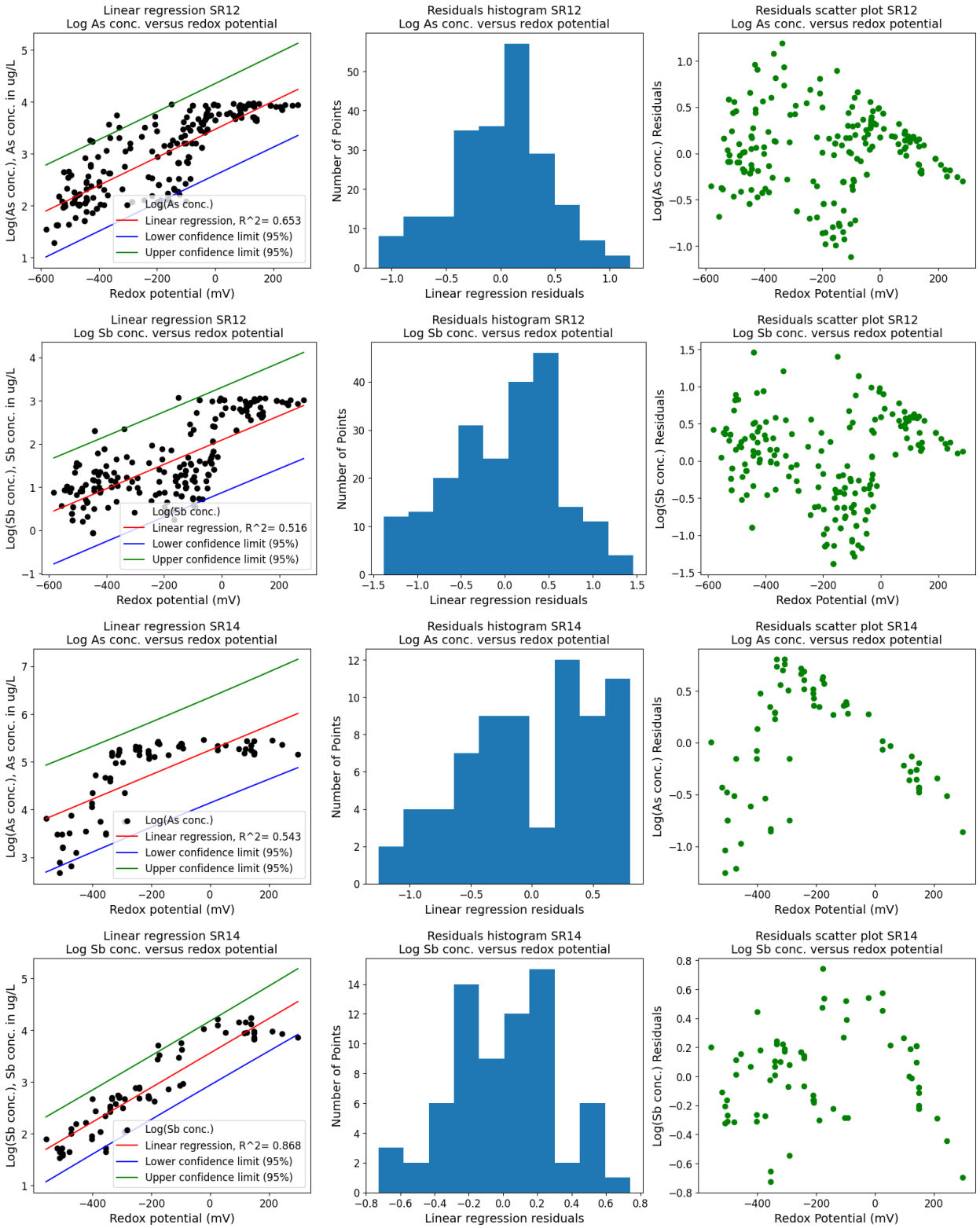

Figure 109 - SR12 and SR14 linear regressions and residuals results obtained from multiple ME treatment experiments developed with different samples and operational conditions

Although the R^2 values for the linear regression fall between 0.516 and 0.868, the heteroscedasticity observed in the residual plot suggests that a linear regression model is not the most appropriate fit. This is because the linear regression does not consider the logistic, stepwise curves that reach maximum concentration at positive redox values. As a result, the residuals exhibit a negative linear trend at the right-hand side of the plots. Moreover, the observed values fall outside the 95% confidence intervals estimated by the linear model, leading to a rejection of the null hypothesis that there is a statistically significant linear correlation with an α value of 0.05.

In an attempt to improve the accuracy of the linear model, a piecewise function was used to split the correlation into different redox potential intervals for SR14. The linear regressions were performed using the same methods as before, but this time the data was divided into three intervals: values < -200 mV, values > 0 mV, and values between 0 and -200 mV. This process is known as "segmenting" and was based on a visual evaluation of the data shape in order to increase the predictive power of the segmented models.

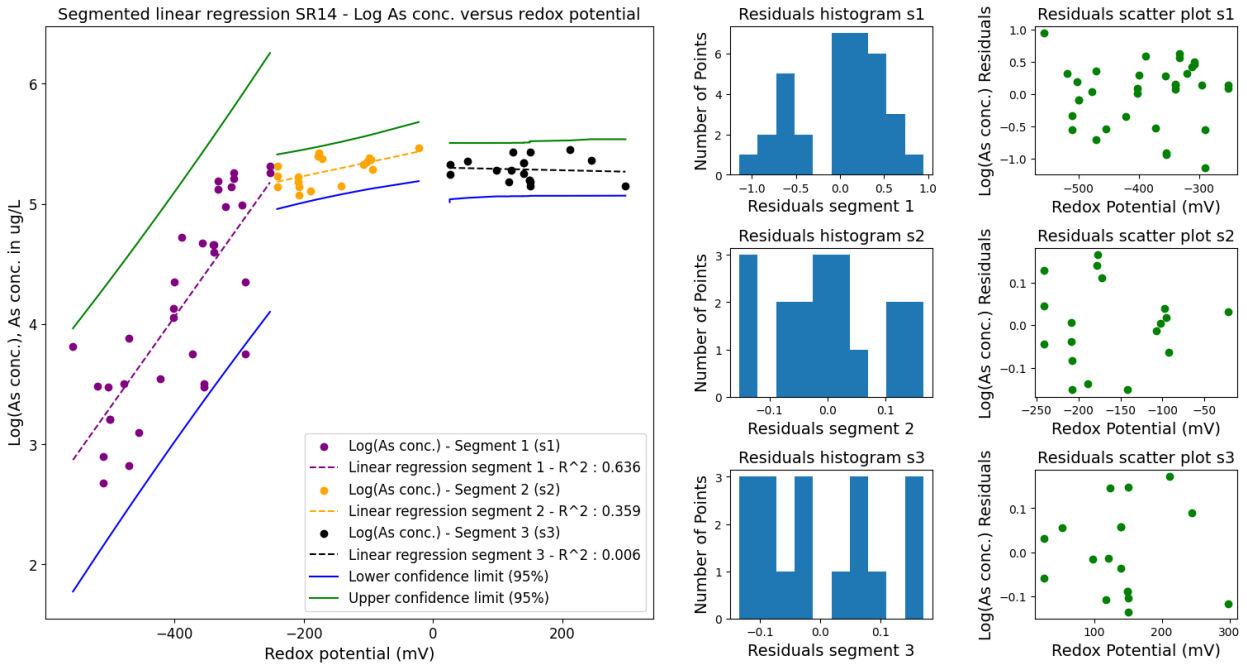

Figure 110 - SR14 segmented linear regressions and residuals results obtained from multiple ME treatment experiments developed with different samples and operational conditions: Log As concentrations

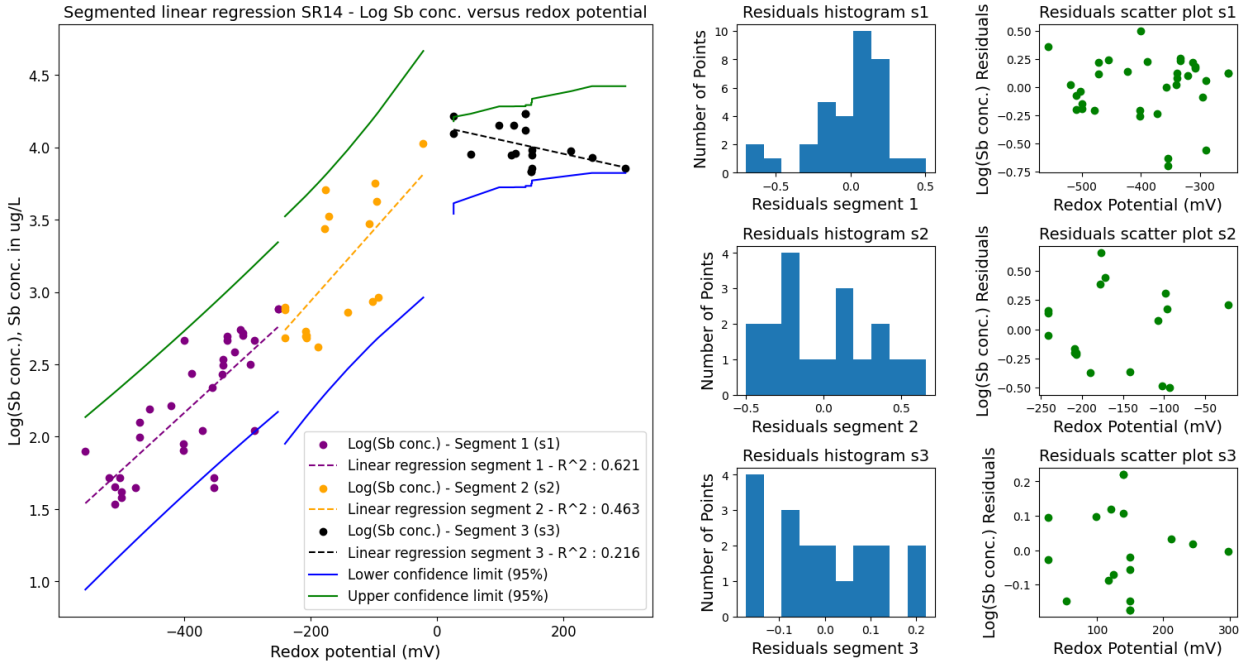

Figure 111 - SR14 segmented linear regressions and residuals results obtained from multiple ME treatment experiments developed with different samples and operational conditions: Log Sb concentrations

The linear regression models and segmented linear regression models were not effective in characterizing the data. These models failed the confidence interval test and had low R^2-values. In Figure 110 and Figure 111, the model also showed a practical concern for concentration predictions near -200 mV and 0 mV at the junctions of the segments. This would make it difficult to use as a predictive model because of the discontinuous functions.

After finding that linear regression models and segmented linear regression models were ineffective, a method based on quantile regressions and a probabilistic approach was performed.

6.2. Quantile Regressions and a Probabilistic Approach

In light of the presence of heteroscedasticity in the residuals, it was apparent that the underlying relationship between the variables was not linear. Consequently, an alternative approach was explored, which involved using quantile regressions to determine the trend empirically, taking into account the shape of the observed data. This approach allowed for more accurate predictions, as they were better able to reflect the non-linearity of the relationship.

Quantile regressions were performed using the Cunnane plotting position and the interp1d and mquantiles functions from Scipy library (Python).

The next step involved applying the segmentation process used in linear regressions to the quantiles. However, in this case, it was not applied to the quantile regressions themselves but to the empirical cumulative density functions (CDFs) created by plotting the values based on their quantiles. The resulting segmentation of the CDFs did not produce a predictive model, but instead represented the distinct populations of contaminant concentration values within different redox potential intervals. The results, which can be found in Figure 112 and Figure 113, illustrate this segmentation process.

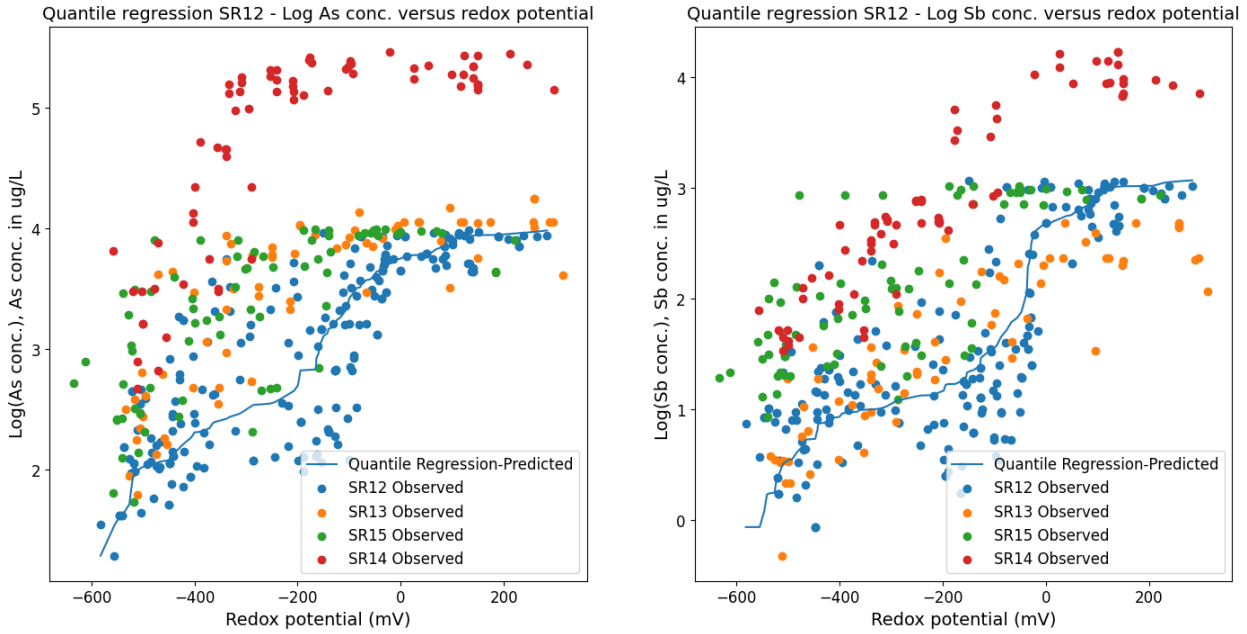

Figure 112 - SR12 Quantile Regressions of logarithms of As and Sb concentrations with split-sample analysis obtained from multiple ME treatment experiments developed with different samples and operational conditions

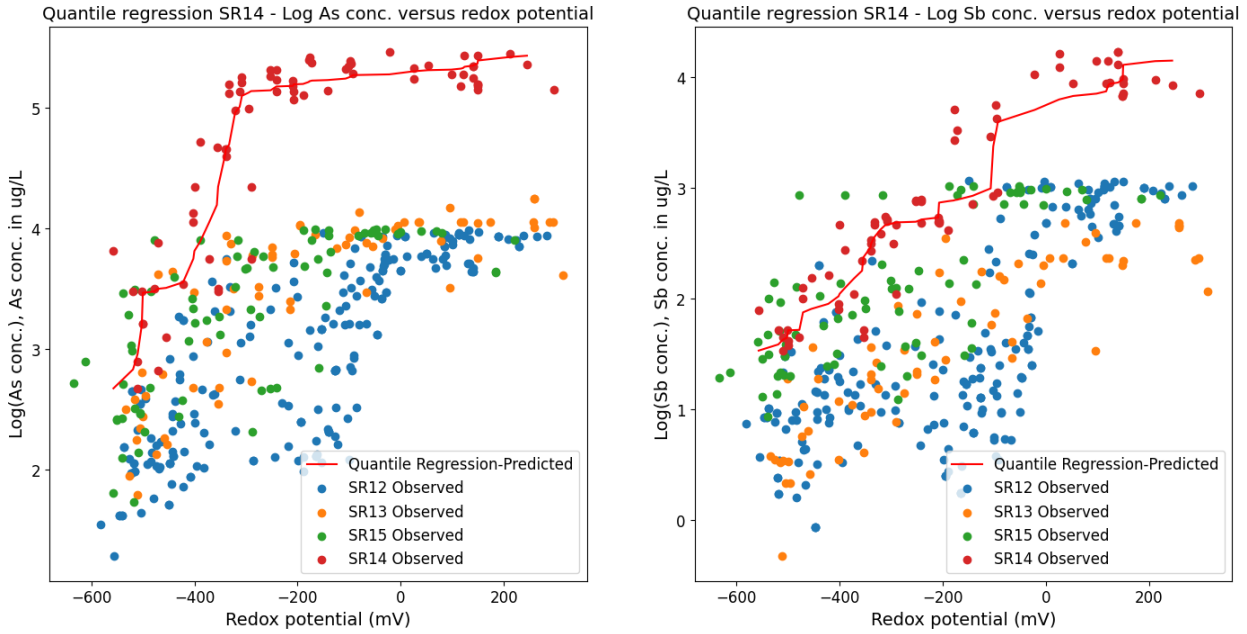

Figure 113 - SR14 Quantile regressions of logarithms of As and Sb concentrations with split-sample analysis obtained from multiple ME treatment experiments developed with different samples and operational conditions

Figure 112 and Figure 113 present the outcomes of the quantile regressions conducted on samples SR12 and SR14, encompassing all observed data. The plots indicate several noteworthy features, including the abnormally high concentrations evident in SR14 and the clear definition of the trend as a stepwise, logarithmic-shaped curve. The SR12 plots reveal a back-and-forth oscillation between preferentially positive and preferentially negative residuals before returning to positive residuals, owing solely to SR14's high values. Conversely, the high concentration of SR14 in the SR14 plots may be obstructing the same curve pattern, but this model may be beneficial in establishing a maximum value for contaminant concentration. However, due to its reliance on specific redox measurements, this empirical function cannot be used to compute exact split-sample residuals or to predict contaminant concentration effectively from redox potential. Despite the inability to develop a predictive model, a visual examination of the plots suggests that although these regressions might reflect the average shape of the trend, they cannot accurately anticipate contaminant concentration from redox potential.

The data variability around regressions led to the decision to move away from a predictive model and to focus on establishing a probabilistic sense of contaminant concentrations within intervals of redox potential. This analysis utilized segmented quantile regression, which splits the redox potential into three segments and compares the data in each segment, similar to segmented linear regression. The outcomes are presented in Figure 114.

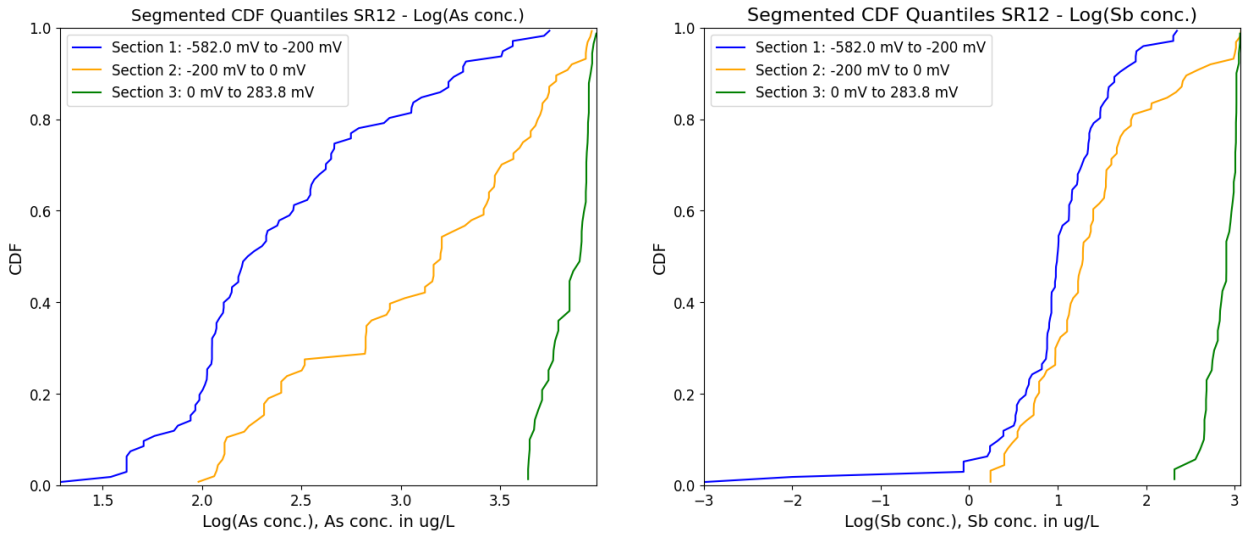

Figure 114 - SR12 segmented quantile regressions of logarithms of As and Sb obtained from multiple ME treatment experiments developed with different samples and operational conditions

As seen in Figure 114, with log (As), there is a difference in the populations of the concentration data between the three intervals. This is contrasted with the log (Sb) results which show that while there is a distinct and narrow range of concentrations for positive redox potentials, the negative redox intervals have nearly the same distribution and thus the probability of any log (Sb) value will be almost the same in either interval. This either means there are only two distinct intervals of log (Sb) probability or different intervals need to be chosen to see the probabilities diverge.

In the Figure 114, it can be observed that the lowest redox potential intervals (negative redox) have smaller cumulative concentrations compared to less negative and positive redox potential intervals. This observation can enhance our understanding of the data and facilitate the development of an in-situ measurable control variable. To improve the accuracy of the selected intervals, the next analysis used a partition of 5 intervals: x<-400 mV, -400<x<-200 mV, -200<x<0 mV, 0<x<200 mV, and x>200 mV, with x being the measured redox potential in mV. All observed data were used together to obtain a comprehensive picture of the probabilities of contaminant concentrations. For each redox potential interval, a PDF was calculated based on the corresponding contaminant

concentrations using a histogram function with 14 bins and "Density=True" to normalize the integral of the PDF to 1. Heatmaps were created using the matplotlib pyplot "imshow" function to visually represent the probabilities of concentration values for each redox interval.

The zonal probabilities, which are the probabilities of contaminant concentration values by interval of redox potential, were used to conduct a probabilistic analysis. The resulting zonal PDFs and corresponding heat maps provide a quantitative understanding of the data, which can assist in controlling the treatment process. This analysis represents a confident conclusion that can be drawn from the data and is shown in Figure 115.

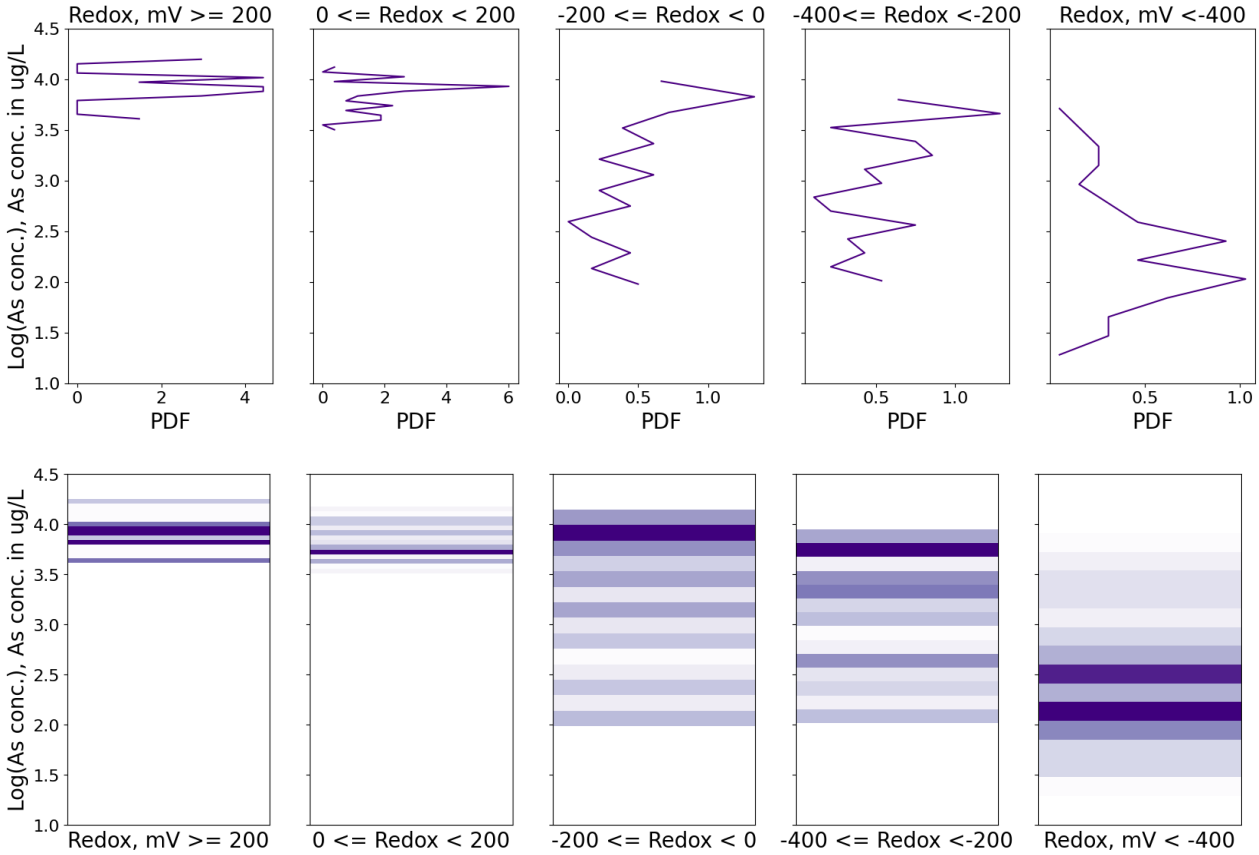

Figure 115 – Probability density function and heatmap of log10 As concentration in µg/L across 200 mV redox intervals obtained from multiple ME treatment experiments developed with different samples and operational conditions. Sample used for this analysis: SR12, SR13 and SR15

In Figure 115, a visual representation of the analysis is provided. The PDFs of arsenic concentrations within each redox range are displayed above the corresponding heatmaps, which are shown below. The heatmaps are created by using shades of purple on the matplotlib pyplot colorbar to represent the PDFs. The darker the shade of purple, the higher the probability of the contaminant concentration being at a particular value within the corresponding interval, and vice versa.

As a standalone result, Figure 115 can inform treatment operators about the quantified probability of little or no removal occurring if the redox potential remains above 0 mV. This suggests that they may need to extend the operation time or adjust other process variables until the redox potential values move into the negative zone.

The results of this analysis are beneficial for the treatment process and future pilot plant operations because they can aid in predicting the success of ME treatment. By analyzing the contaminant concentrations within discrete redox potential intervals, the more probable concentration can be determined. This information can be useful in optimizing the treatment process and ensuring the success of the pilot plant in the future.

The treatment experiments are continuing, and as new data is accumulated, further analysis should be conducted. This may involve more precise segmentation of redox intervals based on CDFs, investigating functions to potentially model the correlation observed in the quantile regressions, and applying other specialized tests to the data for further correlation.

From an operational standpoint, it's important to conduct more in-depth analysis concerning the placement of redox probes within the ME treatment reactors and determine the impact of active media mixing on redox readings, as well as the behavior of the redox potential in a full-scale setup.

Additional studies focused on the relationship between the redox potential and the efficiency of As/Sb removal are critical for advancing the pilot plant and should be given priority, as they can be utilized as a tool for automating the ME process.

7. Conclusions and future work

7.1. ME optimization conclusions

The successful exploration of the ME process in this study provides a promising solution for removing arsenic from LFG condensate and scaling it up to a pilot plant size.

As outlined in this thesis, multiple optimization experiments were carried out. The main variables studied involved varying operational parameters such as isolation of reactor from the atmosphere, CO_2 flow rates requirement and injection modes, gas recirculation, mechanical mixing, active media dosage, ratio, and particle size, active media reutilization, operating pH, headspace in the reactor, and operating temperature.

One of the key aspects found in this study is that the performance of ME treatment is strongly influenced by the ingress of atmospheric oxygen to the column reactor. The results of the isolation experiments indicated that after four hours, the reactor exposed to air achieved only 24% and 73% removal efficiency for As and Sb respectively, while the insulated reactor connected to potassium permanganate and sodium sulfite displayed over 95% and 99% respectively. These findings further emphasize the importance of minimizing the ingress of atmospheric oxygen to achieve optimal ME treatment performance.

Previous research has also established the importance of CO_2 as a carrier gas for ME treatment of LFG condensates. CO_2 optimization experiments conducted in this study demonstrated that flow rates between 0.2 and 0.6 LPM achieved >98% removal of arsenic and antimony after six hours of treatment, with higher flows attaining faster As/Sb removal than lower flows. Additionally, continuous CO_2 flow was found to achieve >99% of As/Sb removal after six hours, whereas intermittent flow only achieved 90% efficiency. Moreover, the gas recirculation experiments

showed that flushing the system with CO_2 for a few minutes, and subsequently recirculating the generated gas, yielded over 75% and 89% As and Sb removal efficiency after 30 minutes of treatment. This finding has the potential to minimize the use of CO_2 while also preventing As volatiles from escaping the system.

Although the use of CO_2 carrier gas was greatly optimized in this thesis, an alternative approach for ME involved using a mechanical mixer in the insulated (oxygen-free) batch column reactor instead of continuous CO_2 flushing. For these experiments, mechanical mixing with gas recirculation achieved removal efficiencies greater than 85% and 94% for As and Sb respectively, within a 30-minute timeframe for both scenarios. For experiments using mechanical mixing only, with no CO_2 injection, the removal efficiencies for both As and Sb exceeded 94% within 60 minutes of treatment. These experiments were carried out for multiple samples, including SR14 (high As/Sb concentration sample), with similar results for all of them. The possibility of removing CO_2 from the process presents great value, as it helps reduce the cost, facilitates the operation, and removes the uncertainties of possible As/Sb volatiles escaping to the atmosphere.

Furthermore, the experimental results indicate that using intermittent mixing modes may have similar results compared with continuous mixing, with As/Sb removal efficiencies consistently exceeding 90% within a 30-minute timeframe. These findings suggest that optimizing the mixing modes could result in energy savings and reduced operational costs. A treatment duration of 30 minutes is sufficient for sufficiently high AC/ZVI dosages, as the achieved As/Sb removal efficiency within this period is excellent.

On the other hand, this thesis studied the effects of active media activation, dosage, ratio, and reuse. The results indicate that non-activated ZVI demonstrated equal or superior performance in the removal of As/Sb compared to activated ZVI under the same experimental conditions. The

findings also suggest that a more acidic environment can enhance the efficiency of contaminant removal, as the ZVI self-activates within the reactor.

Regarding the impact of the ratio of weight of AC/ ZVI, the experiment conducted with 3 g/L of PAC and ZVI LC plus fine showed that the combination of AC/ ZVI always exhibited greater removal efficiency of arsenic and antimony than using only ZVI, even when using higher dosages of ZVI. Moreover, the performance of all other ratios analyzed was found to be relatively similar, with a slightly better performance for PAC/ ZVI LC plus fine weight ratios of 1:1 and 1:2.

When analyzing the effects of PAC/ZVI dosage, an increase in the active media dosage was shown to result in a corresponding enhancement in arsenic and antimony removal efficiency. Notably, for active media dosages exceeding 10 g/L of PAC and ZVI LC plus fine, the removal efficiency is markedly high within the initial 30 minutes. This outcome is significant as it translates to substantial design simplification or energy savings by reducing the treatment time from six hours to 30 minutes.

The particle size of active media is also a crucial factor in the operational convenience of any treatment processes. The experimental results indicated that smaller particle size active media (PAC and ZVI LC plus fine) demonstrate superior removal efficiency for both As and Sb compared to larger particle size active media (GAC and ZVI LC plus). However, large particle size media still exhibited significant, practically acceptable removal efficiency. These results led to testing higher doses of large particle size active media. The results suggested that using 20 g/L of GAC and ZVI LC plus instead of 3 g/L led to significantly improved and rapid removal of arsenic and antimony. Within 60 minutes, arsenic removal increased from 20% to 65%, and antimony removal from 45% to 97%.

When using an increased dosage of 50 g/L of GAC and ZVI LC plus, comparable efficacy in the removal of arsenic and antimony was obtained, as contrasted to the use of small particle size active media at a dosage of 20 g/L. Notably, these results were obtained within a 30-minute timeframe and represent a significant finding that has implications for the operational and economic feasibility of the future practical applications.

When a higher dosage of active media is used for the reaction, further optimization of active media dosing may be necessary. To address this issue, one approach explored in this study involves the reutilization of active media. The experiments were conducted using active media dosages of 10 and 20 g/L of PAC and ZVI LC plus fine for 3 cycles. The results showed that in the presence of CO_2 carrier gas, 3 consecutive cycles successfully removed over 92% of As/Sb in the LFG condensate within 30 minutes.

To evaluate the potential of the treatment process in a continuously mechanically mixed ME reactor, the number of cycles was increased to 10, using an initial dosage of 50 g/L of GAC and ZVI LC plus and comparing it to an initial dosage of 50 g/L of GAC and ZVI LC plus, adding 1 g/L of the active media combination in each cycle.

In the case of the 50 g/L initial dosage analysis, the first six cycles achieved an As removal efficiency of over 80% within 30 minutes, while the subsequent four cycles resulted in decreasing removal. In contrast, when adding 1 g/L of GAC per cycle to the initial 50 g/L dosage, the As removal efficiency remained above 80% for all cycles in the same timeframe. For both cases, antimony removal efficiency exceeded 90% in every cycle.

The results are equally as good when repeating the experiments using intermittent mixing, as all cycles still exhibited >80% As and Sb removal efficiency within 30 minutes. The findings of this

experiment suggest that intermittent mixing can be successfully utilized when a small number of cycles are required. However, further investigation is needed to conduct a trade-off study to evaluate the cost and carbon footprint associated with energy usage between continuous and intermittent mixing, as well as the number of cycles required for efficient treatment.

Another important optimization to ME treatment process is the amount of reagents used in the process while using mechanical mixing. In this thesis, additional experiments were conducted to compare the removal of As at different pH values. Specifically, the experiments were performed with a pH value of 3, a pH value of 4.5, and with no pH control. Based on the results, the efficacy of removing arsenic and antimony is generally comparable at pH 3 and pH 4.5, whereas the absence of pH control leads to minimal removal of arsenic.

Considering the variability of environmental conditions in field applications of ME treatment, it is important to ensure the efficacy of the process for temperatures ranging from low (e.g., 6 Celsius) to high (e.g., 34 Celsius) degrees. The results indicated that while variations of ambient temperature did not result in pronounced changes of the rate of As/Sb removal, it was slightly better for lower temperatures. The findings suggested that the ME treatment method can effectively withstand temperature variations when treating landfill gas condensates and as such, the ME treatment can maintain excellent removal efficiency throughout the year.

To establish the operational parameters that would avoid the presence of residual oxygen in the system, headspace variations experiments were performed, with CO_2 flushing at the start of every round to remove the oxygen in the column reactor. The findings of these experiments confirmed that the removal efficiency of both As and Sb decreases as the sample volume decreases in the column reactor. The results suggested that the presence of residual oxygen in the headspace reduces the efficiency of the microelectrolysis treatment. Considering these results, the

experiments developed with 3 L of sample, mechanical mixing and CO_2 flushing at the beginning attained the best As/Sb removal efficiency.

Overall, although there was variability in arsenic concentration across different sampling rounds, the ME treatment with sufficiently optimized operational parameters consistently showed its effectiveness in removing most of the arsenic and antimony contained in all samples, regardless of the initial concentration. These results highlight the reliability and efficiency of ME technology in removing arsenic from LFG condensate within a short operation time.

The project's future plans involve scaling up the treatment to a pilot scale and eventually a full-scale operation with the support and collaboration of CHRLF.

7.2. Mass balance conclusions

The mass balance experiments were performed to determine the distribution of the retained arsenic between the solid ZVI/AC active media and their levels that potentially can be ascribed to their transfer to the gas phase.

To extract and measure the concentration of As in the active media, sodium hydroxide was utilized. The results showed that NaOH suspensions could be used to determine the concentration of As in the active media. The base exhibited the highest As release within 24 hours, but it had good performance in the first 4 hours. Using this approach, multiple mass balance experiments were conducted, but generally, less than 40% of arsenic extracted during treatment were released by the active media in strong base. These findings, along with other experiments, led the team to investigate the use of microwave digestion.

According to the findings, microwave digestion using HNO_3 was as effective as agitating the active media in strong base for 24 hours in terms of arsenic recovery, with an average recovery rate of

35% for arsenic from the active media. However, there was some variability in the results of the three repetitions for the same solid sample, which could be due to the non-uniformity in the active media and the absence of water content correction in the wet spent active media.

In contrast, using HCl for microwave digestion resulted in higher average concentrations of arsenic in the active media, with even higher concentrations when considering the corrected water content in the active media. The results have an average of 118% recovery for arsenic from the active media. The percentage being over 100% may be attributed to the lack of homogeneity in the samples. These results suggest that microwave digestion using HCl is a more effective method for measuring the amount of As in the active media.

The findings indicated that the active media effectively retained all of the As extracted from the LFG condensate during the ME treatment, and none of it was released into the atmosphere due to the reactor isolation. Nevertheless, additional experiments are required to guarantee the uniformity of the samples and precise mass balance computations, as well as to verify that all the arsenic is retained in the active media during the ME treatment.

7.3. Redox potential and As/Sb removal correlation conclusions

In the course of the experiments, a potential correlation between the redox potential and the removal of As/Sb was observed. To test this hypothesis, more than fifty sets of experimental results were analyzed using statistical methods to establish a mathematical relationship between the two variables.

The analysis of redox potential involved testing the hypothesis of a linear correlation between arsenic/antimony concentrations and redox potential. However, the linear regressions conducted

failed to establish a significant relationship. As a result, quantile regressions were performed, but these also failed due to high variability and heteroscedastic residuals.

As a result, the data was segmented into discrete redox potential intervals, and the CDF and PDF for each interval were analyzed. The results showed that the concentration of arsenic and antimony varies in different intervals of redox potential, with lower concentrations observed in more negative intervals and higher concentrations in more positive intervals.

These results are valuable as a preliminary analysis when it comes to determining the most probable contaminant concentrations within a given redox potential interval. However, future research regarding the optimal position of the redox probes, the effect of solid particles suspension in the redox potential, and a more detailed correlation between redox and removal needs to be done.

7.4. Recommendations for future work: Engineering aspects of ME treatment

The project has presented promising results on the ME batch column reactor's effectiveness in treating LFG condensate contaminated with arsenic and antimony. However, there are several areas where further investigation is required. The following are the recommended future works for this project:

- Scaling-up: The future work for the project will focus on scaling up the ME batch column reactor to pilot plant-scale and full-scale operations, with the cooperation and help from CHRLF.
- Redox potential analysis: Future research should focus on the behavior of redox probes in different positions in the reactor to select the best location to monitor the process, a correlation between redox potential and active media particle suspension, and a detailed correlation between the absolute redox potential and the arsenic and antimony removal efficiency.
- Standardization: Certain process parameters need to be standardized, such as evaluating the optimal energy consumption operation principles for the system and estimating the costs of constructing and operating the pilot plant. An example of this would be to select the dosage and size of active media, together with the number of active media reutilization cycles, and the mixing mode to minimize the cost and the environmental impacts without affecting the quality of the ME removal.
- Active media feeding: Further investigation is required to optimize the feeding of active media into the ME reactor, ensuring the isolation of the active media and sample from the atmosphere, and a clean addition of the active media into the reactor.

- Active media particle suspension analysis: Further investigation is required to understand the trajectory of the particles inside the conical base column reactor, and an optimization of the mixing parameters such as the blades size and position to ensure a top draw-off moderate uniformity of the particles in the reactor.
- Active media reuse investigation: Further investigation is required to determine the maximum number of sample loadings that the active media can withstand.
- Mass balance investigation: Further study is necessary to ensure the analysis of As/Sb concentration in a whole batch of spent active media. The main goal of this recommendation is to close the mass balance with concentrations closer to 100% for As and Sb.
- Acid consumption: Future work should focus on calculating the optimal amount of acid required for efficient treatment during pH control of ME treatment.
- GAC and ZVI regeneration research: A further study required for ME treatment is the regeneration/reuse of treatment media. This is highly relevant to the process's applicability at a larger scale and the disposal of the active media.
- Speciation of As volatiles: Further experiments need to be performed to determine the speciation of As volatiles, if such are formed in the ME treatment and the likelihood of volatiles being released to the atmosphere.

In summary, the project has demonstrated the effectiveness of the ME batch column reactor in treating LFG condensate contaminated with arsenic and antimony. However, several areas require further investigation to ensure the scalability and applicability of the process to a larger scale.

8. References

1. Sahoo, P. K., & Kim, K. (2013). A review of the arsenic concentration in paddy rice from the perspective of geoscience. Geosciences Journal, 17, 107-122.]
2. De Oliveira, F. D., Robey, N. M., Smallwood, T. J., Spreadbury, C. J., & Townsend, T. G. (2022). Landfill gas as a source of anthropogenic antimony and arsenic release. Chemosphere, 307, 135739.
3. Smedley, P. L., & Kinniburgh, D. G. (2002). A review of the source, behavior and distribution of arsenic in natural waters. Applied geochemistry, 17(5), 517-568.
4. Huang, J. H., Ilgen, G., Vogel, D., Michalzik, B., Hantsch, S., Tennhardt, L., & Bilitewski, B. (2009). Emissions of inorganic and organic arsenic compounds via the leachate pathway from pretreated municipal waste materials: a landfill reactor study. Environmental science & technology, 43(18), 7092-7097.
5. Bolan, N., Kumar, M., Singh, E., Kumar, A., Singh, L., Kumar, S., ... & Siddique, K. H. (2022). Antimony contamination and its risk management in complex environmental settings: a review. Environment International, 158, 106908.
6. Zhao, R., Novak, J. T., & Goldsmith, C. D. (2013). Treatment of organic matter and methylated arsenic in landfill biogas condensate. Waste management, 33(5), 1207-1214.
7. Chen, P. A., Wang, H. P., Kuznetsov, A. M., Masliy, A. N., Liu, S., Chiang, C. L., & Korshin, G. V. (2023). XANES/EXAFS and quantum chemical study of the speciation of arsenic in the condensate formed in landfill gas processing: Evidence of the dominance of As-S species. Journal of Hazardous Materials, 445, 130522.
8. Sundar, S., & Chakravarty, J. (2010). Antimony toxicity. International journal of environmental research and public health, 7(12), 4267-4277.
9. Ying, D., Peng, J., Xu, X., Li, K., Wang, Y., & Jia, J. (2012). Treatment of mature landfill leachate by internal micro-electrolysis integrated with coagulation: a comparative study on a novel sequencing batch reactor based on zero valent iron. Journal of hazardous materials, 229, 426-433.
10. Vaverková, M. D. (2019). Landfill impacts on the environment. Geosciences, 9(10), 431.
11. Brown, K. A., & Maunder, D. H. (1994). Using landfill gas: A UK perspective. Renewable Energy, 5(5-8), 774-781.

12. Zhao, R. (2012). Management strategy of landfill leachate and landfill gas condensate (Doctoral dissertation, Virginia Tech).
13. Konkol, I., Cebula, J., Świerczek, L., Piechaczek-Wereszczyńska, M., & Cenian, A. (2022). Biogas Pollution and Mineral Deposits Formed on the Elements of Landfill Gas Engines. Materials, 15(7), 2408.
14. Intrakamhaeng, V., Clavier, K. A., Liu, Y., & Townsend, T. G. (2020). Antimony mobility from E-waste plastic in simulated municipal solid waste landfills. Chemosphere, 241, 125042.
15. Masuda, H. (2018). Arsenic cycling in the Earth's crust and hydrosphere: interaction between naturally occurring arsenic and human activities. Progress in Earth and Planetary Science, 5(1), 1-11.
16. Cheney-Irgens, A. (2022). Mass Balance of Arsenic in Microelectrolysis Treatment of Arsenic-Containing Landfill Gas Condensate and Initial Study of Formation of Volatile Arsenic Species (Doctoral dissertation).
17. Walters, S. (2022). A Study of Removal Techniques for Arsenic Species in Landfill Gas Condensate (Doctoral dissertation).
18. Rifkin, G. (2021). Arsenic in Landfill Gas Condensates and Gas Treatment Solids: a Study of Removal by Alternative Treatment Approaches and Mobilization. University of Washington.
19. Malik, S. (2020). Comparison of Physicochemical Methods to Remove Arsenic from Landfill Leachate and Gas Condensate. University of Washington.
20. Raju, N. J. (2022). Arsenic in the geo-environment: A review of sources, geochemical processes, toxicity and removal technologies. Environmental research, 203, 111782.
21. Yann, R. A., Armando, G. A., Irene, C. R., Moisés, G. V., & Raúl, M. A. (2017). Arsenic liberation from mine wastes derived of skarn deposits at Sierra Madre Oriental, México. Procedia Earth and Planetary Science, 17, 833-836.
22. Buddhawong, S., Kuschk, P., Mattusch, J., Wiessner, A., & Stottmeister, U. (2005). Removal of arsenic and zinc using different laboratory model wetland systems. Engineering in Life Sciences, 5(3), 247-252.
23. Valles-Aragón, M. C., Olmos-Márquez, M. A., Llorens, E., & Alarcón-Herrera, M. T. (2014). Redox potential and pH behavior effect on arsenic removal from water in a constructed wetland mesocosm. Environmental Progress & Sustainable Energy, 33(4), 1332-1339.

Biterna, M., Antonoglou, L., Lazou, E., & Voutsa, D. (2010). Arsenite removal from waters by zero valent iron: batch and column tests. Chemosphere, 78(1), 7-12.

24. Nikolaidis, N. P., Dobbs, G. M., & Lackovic, J. A. (2003). Arsenic removal by zero-valent iron: field, laboratory and modeling studies. Water research, 37(6), 1417-1425.
25. Yan, W., Vasic, R., Frenkel, A. I., & Koel, B. E. (2012). Intraparticle reduction of arsenite (As (III)) by nanoscale zerovalent iron (nZVI) investigated with in situ X-ray absorption spectroscopy. Environmental Science & Technology, 46(13), 7018-7026.
26. Sarkar, A., & Paul, B. (2016). The global menace of arsenic and its conventional remediation-A critical review. Chemosphere, 158, 37-49.
27. Su, F., Zhou, H., Zhang, Y., & Wang, G. (2016). Three-dimensional honeycomb-like structured zero-valent iron/chitosan composite foams for effective removal of inorganic arsenic in water. Journal of colloid and interface science, 478, 421-429.
28. O'Carroll, D., Sleep, B., Krol, M., Boparai, H., & Kocur, C. (2013). Nanoscale zero valent iron and bimetallic particles for contaminated site remediation. Advances in Water Resources, 51, 104-122.
29. Peng, C. Y., & Korshin, G. V. (2011). Speciation of trace inorganic contaminants in corrosion scales and deposits formed in drinking water distribution systems. Water research, 45(17), 5553-5563.
30. Van Genuchten, C. M., Etmannski, T. R., Jessen, S., & Breunig, H. M. (2022). LCA of disposal practices for arsenic-bearing iron oxides reveals the need for advanced arsenic recovery. Environmental Science & Technology, 56(19), 14109-14119.
31. Li, S., Wang, W., Liu, Y., & Zhang, W. X. (2014). Zero-valent iron nanoparticles (nZVI) for the treatment of smelting wastewater: A pilot-scale demonstration. Chemical Engineering Journal, 254, 115-123.
32. Tucek, J., Prucek, R., Kolarik, J., Zoppellaro, G., Petr, M., Filip, J., ... & Zbořil, R. (2017). Zero-valent iron nanoparticles reduce arsenites and arsenates to As (0) firmly embedded in Core-Shell superstructure: Challenging strategy of arsenic treatment under anoxic conditions. ACS Sustainable Chemistry & Engineering, 5(4), 3027-3038.
33. Briggs, J. (1988). Municipal landfill gas condensate. US Environmental Protection Agency, Hazardous Waste Engineering Research Laboratory.

34. Korshin, G. (2021). "Redox transitions. pe, pH predominance diagrams for Fe3+/Fe2+ and As5+/As3+ transitions". Lecture.
35. Cedar Hills Regional Landfill. King County. Available at: https://kingcounty.gov/depts/dnrp/solid-waste/facilities/landfills/cedar-hills.aspx (Accessed: March 17, 2023).
36. Aziz, H. A., Abu Amr, S. S., Vesilind, P. A., Wang, L. K., & Hung, Y. T. (2021). Introduction to solid waste management. Solid Waste Engineering and Management: Volume 1, 1-84.
37. Raven, K. P., Jain, A., & Loeppert, R. H. (1998). Arsenite and arsenate adsorption on ferrihydrite: kinetics, equilibrium, and adsorption envelopes. Environmental science & technology, 32(3), 344-349.
38. Liu, S., Kuznetsov, A. M., Han, W., Masliy, A. N., & Korshin, G. V. (2022). Removal of dimethylarsinic acid (DMA) in the Fe/C system: roles of Fe (II) release, DMA/Fe (II) and DMA/Fe (III) complexation. Water Research, 213, 118093.
39. Khodabakhshi, A., Amin, M., & Mozaffari, M. (2011). Synthesis of magnetite nanoparticles and evaluation of its efficiency for arsenic removal from simulated industrial wastewater. Journal of Environmental Health Science & Engineering, 8(3), 189-200.
40. Mohan, D., & Pittman Jr, C. U. (2007). Arsenic removal from water/wastewater using adsorbents—a critical review. Journal of hazardous materials, 142(1-2), 1-53.
41. Shih, M. C. (2005). An overview of arsenic removal by pressure-driven membrane processes. Desalination, 172(1), 85-97.
42. Zaw, M., & Emett, M. T. (2002). Arsenic removal from water using advanced oxidation processes. Toxicology letters, 133(1), 113-118.
43. Babu, D. S., Srivastava, V., Nidheesh, P. V., & Kumar, M. S. (2019). Detoxification of water and wastewater by advanced oxidation processes. Science of the Total Environment, 696, 133961.
44. Crecelius, E. A. (1975). The geochemical cycle of arsenic in Lake Washington and its relation to other elements 1. Limnology and Oceanography, 20(3), 441-451.
45. Nazari, A. M., Radzinski, R., & Ghahreman, A. (2017). Review of arsenic metallurgy: Treatment of arsenical minerals and the immobilization of arsenic. Hydrometallurgy, 174, 258-281.

9. Appendices

9.1. Additional Tables

Table 4 - Mass balance experiment results: Spent wet active media recovered from ME treatment suspended in 100 mL of 1 M NaOH. Experiment details: 2 L of SR16 treated with 20 g/L PAC-ZVI LC plus fine (1:2), and pH 3 (Experiment results: Figure 54, Mass balance chart: Figure 100)

As removed by ME treatment	cont. mixing	int. mixing: 5'on-10'off	int. mixing: 5'on-5'off
Concentration SR15 0' (µg/L)	25,184	25,184	25,184
Concentration SR15 60' (µg/L)	942	1,209	488
Volume of sample (L)	2.0	2.0	2.0
Total mass removed 60' (mg)	48.5	48.0	49.4

As in the active media	cont. mixing	int. mixing: 5'on-10'off	int. mixing: 5'on-5'off
PAC/ZVI in NaOH (µg/L)	3,761	3,312	5,440
Mass of active media in treatment (g)	40.0	40.0	40.0
Mass of active media in NaOH (g)	1.0	1.0	1.0
Volume of NaOH (L)	0.1	0.1	0.1
As mass captured by active media (mg)	15.0	13.2	21.8
% removed As captured by active media	31.0%	27.6%	44.1%

Table 5 - Mass balance experiment results: Spent wet active media recovered from ME treatment suspended in 100 mL of 1 M NaOH. Experiment details: 200 mL of SR16 treated in a beaker with 20 g/L PAC- ZVI LC plus, pH 3, and continuous mixing (Mass balance chart: Figure 101)

As removed by ME treatment	active media in 0.1 M NaOH	active media in 1 M NaOH	1 M NaOH passed through active media
Concentration SR16 0' (µg/L)	14274	13653	13503
Concentration SR16 30' (µg/L)	11774	11417	11957
Volume of sample (L)	0.2	0.2	0.2
Total mass removed 60' (mg)	0.50	0.45	0.31

As in the active media	Active media in 0.1 M NaOH	Active media in 1 M NaOH	1 M NaOH passed through active media
PAC/ZVI in NaOH (µg/L)	1962	994	679
Mass of active media in treatment (g)	4.0	4.0	4.0
Mass of active media in NaOH (g)	4.0	4.0	4.0
Volume of NaOH (L)	0.1	0.1	0.1
As mass captured by active media (mg)	0.20	0.10	0.07
% removed As captured by active media	39.2%	22.2%	21.9%

Table 6 - Mass balance experiment results: Spent active media recovered from ME treatment suspended in 10 mL of concentrated HNO_3 and exposed to microwave digestion. Experiment details: Headspace experiments for SR14 treated with 50 g/L GAC- ZVI LC plus, pH 3, and continuous mixing (Experiment results: Figure 86, Mass balance chart: Figure 102)

As removed by ME treatment	3 L	2 L	1 L	500 mL	250 mL
Concentration SR14 0' (µg/L)	231,602	231,602	231,602	231,602	231,602
Concentration SR14 30' (µg/L)	110,053	167,758	183,073	204,420	213,025
Volume of sample (L)	3	2	1	0.5	0.25
Total mass removed 30' (mg)	365	128	49	14	4.6

As in the active media	3 L	2 L	1 L	500 mL	250 mL
GAC/ZVI in HNO_3 - MWD 1 (µg/L)	11,995	2,342	3,224	1,396	508
GAC/ZVI in HNO_3 - MWD 2 (µg/L)	5,136	2,695	2,646	1,429	1,512
GAC/ZVI in HNO_3 - MWD 3 (µg/L)	2,586	3,148	3,318	1,313	1,323
Mass of active media in treatment (g)	150	100	50	25	13
Mass of active media in MWD (g)	0.05	0.05	0.05	0.05	0.05
Volume of acid recovered - MWD 1 (L)	0.004	0.009	0.010	0.009	0.009
Volume of acid recovered - MWD 2 (L)	0.010	0.009	0.009	0.010	0.009
Volume of acid recovered - MWD 3 (L)	0.010	0.010	0.009	0.009	0.009
As mass captured by active media - MWD 1 (mg)	126	42	31	6.3	1.1
As mass captured by active media - MWD 2 (mg)	146	49	24	6.8	3.4
As mass captured by active media - MWD 3 (mg)	74	60	28	5.9	2.8
% removed As captured by active media - MWD 1	35%	33%	63%	46%	25%
% removed As captured by active media - MWD 2	40%	38%	49%	50%	73%
% removed As captured by active media - MWD 3	20%	47%	58%	43%	61%
% removed As captured by active media - Average	32%	39%	57%	47%	53%

Table 7 - Mass balance experiment results: Spent active media recovered from ME treatment suspended in 10 mL of concentrated HCl and exposed to microwave digestion. Experiment details: Headspace experiments for SR14 treated with 50 g/L GAC- ZVI LC plus, pH 3, and continuous mixing (Experiment results: Figure 86, Mass balance chart: Figure 102)

As in the active media	3 L	2 L	1 L	500 mL	250 mL
GAC/ZVI in HCl- MWD (μg/L)	7,408	4,784	4,028	2,215	2,156
Mass of active media in treatment (g)	150	100	50	25	13
Mass of active media in MWD (g)	0.05	0.05	0.05	0.05	0.05
Volume of acid recovered - MWD (L)	0.009	0.009	0.009	0.010	0.008
As mass captured by active media - MWD (mg)	189	86	34	11	4.3
% removed As captured by active media	52%	67%	71%	77%	93%

Table 8 - Mass balance experiment results: Spent active media recovered from ME treatment suspended in 10 mL of concentrated HCl and exposed to microwave digestion. Experiment details: Headspace experiments for SR17, with 50 g/L GAC- ZVI LC plus, pH 3, continuous mixing, and CO_2 flushing at the beginning (Experiment results: Figure 92, Mass balance chart: Figure 103)

As removed by ME treatment	3 L	2 L	1 L	500 mL	250 mL
Concentration SR17 0' (µg/L)	21,605	21,605	21,605	22,058	22,058
Concentration SR17 30' (µg/L)	1,256	923	2,293	4,481	5,571
Volume of sample (L)	3	2	1	0.5	0.25
Total mass removed 30' (mg)	61	41	19	9	4.1

As in wet active media	3 L	2 L	1 L	500 mL	250 mL
GAC/ZVI in HCl - MWD 1 (µg/L)	2,202	1,601	1,855	1,287	892
GAC/ZVI in HCl - MWD 2 (µg/L)	2,058	1,646	1,529	1,129	886
GAC/ZVI in HCl - MWD 3 (µg/L)	1,823	1,528	1,472	1,048	1,077
Mass of active media in treatment (g)	150	100	50	25	13
Mass of active media in MWD (g)	0.05	0.05	0.05	0.05	0.05
Volume of acid recovered - MWD 1 (L)	0.008	0.007	0.008	0.009	0.008
Volume of acid recovered - MWD 2 (L)	0.009	0.009	0.009	0.008	0.009
Volume of acid recovered - MWD 3 (L)	0.008	0.009	0.009	0.009	0.009
As mass captured by active media - MWD 1 (mg)	53	22	15	5.8	1.8
As mass captured by active media - MWD 2 (mg)	52	28	13	4.5	1.9
As mass captured by active media - MWD 3 (mg)	44	26	13	4.7	2.3
% removed As captured by active media - MWD 1	87%	54%	77%	66%	43%
% removed As captured by active media - MWD 2	86%	68%	67%	51%	46%
% removed As captured by active media - MWD 3	72%	63%	69%	54%	56%
% removed As captured by active media - Average	81%	62%	71%	57%	48%

As in the active media - water content correction	3 L	2 L	1 L	500 mL	250 mL
Water content estimation (%)	42%	36%	36%	33%	42%
Estimated mass of active media used (g)	0.029	0.032	0.032	0.033	0.029
As mass captured by active media - MWD 1 (mg)	91	35	23	8.7	3.1
As mass captured by active media - MWD 2 (mg)	90	44	20	6.8	3.2
As mass captured by active media - MWD 3 (mg)	75	41	21	7.1	3.9
% removed As captured by active media - MWD 1	149%	85%	121%	99%	74%
% removed As captured by active media - MWD 2	148%	106%	106%	77%	78%
% removed As captured by active media - MWD 3	124%	98%	108%	81%	95%
% removed As captured by active media - Average	140%	96%	111%	85%	83%

Table 9 - Mass balance experiment results: Spent active media recovered from ME treatment dried and suspended in 10 mL of concentrated HCl and exposed to microwave digestion. Experiment details: Headspace experiments for SR17 treated with 50 g/L GAC- ZVI LC plus, pH 3, continuous mixing, and CO_2 flushing at the beginning to push out the oxygen in the reactor (Experiment results: Figure 92, Mass balance chart: Figure 103

As in dry active media	3 L	2 L	1 L	500 mL	250 mL
GAC/ZVI in HCl - MWD (µg/L)	4,007	5,277	2,949	1,730	1,631
Mass of active media in treatment (g)	150	100	50	25	13
Mass of active media in MWD (g)	0.05	0.05	0.05	0.05	0.05
Volume of acid recovered - MWD (L)	0.007	0.003	0.007	0.007	0.008
As mass captured by active media - MWD (mg)	84	32	21	6.1	3.1
% removed As captured by active media - MWD	138%	77%	107%	69%	74%

9.2. P&ID of the treatment process